INVESTIGATIONS OF PREFERENTIAL AND MATRIX FLOW IN A MOLE DRAINED SOIL BLOCK.

by

LYNDA KAREN DEEKS

A thesis submitted to the university of Plymouth in partial fulfilment for the degree of

DOCTOR OF PHILOSOPHY

Department of Geographical Science Faculty of Science

In collaboration with The Institute of Grassland and Environmental Research

June 1995

To Peter

ABSTRACT.

INVESTIGATIONS OF PREFERENTIAL AND MATRIX FLOW IN A MOLE DRAINED SOIL BLOCK.

LYNDA KAREN DEEKS.

An innovative research study was established at IGER, North Wyke, Devon, to investigate preferential flow through a poorly structured relatively impermeable soil. Macropore channels were added by a mole plough in order to investigate soil water pathways and chemical transport in a soil in which preferential flow was guaranteed. The investigation focused on water and solute movement through specific flowpaths, namely macropores and mesopores, and the interaction between mobile and immobile zones within the soil.

Two large soil blocks (1 m^2 by 0.85 m) of the Hallsworth series were removed from the field and placed on sand tables so that a suction could be induced at the base of the soil block. The edge was sealed using paraffin wax. Eight tensiometers and suction cup lysimeters were installed in each block together with fifteen pairs of time-domain reflectometry wave guides. A regular spacing pattern was employed so that spatial variations could be easily identified. Samples were collected from suction cup lysimeters every 4 hours. Soil water status was observed from the TDR probes daily and from tensiometers every 10 minutes.

Five tracer experiments were conducted; three involved the miscible displacement of chloride at concentrations of 100 and 250 mg l^{-1} and two used nitrate (500 mg l^{-1}) and chloride (2500 mg l^{-1}) applied as a pulse. Tracer and irrigation water was applied through a misting system at an irrigation rate of 2.76 mm h^{-1}.

Three techniques were used to examine soil structure in the macropore and mesopore pore size range to investigate potential flowpaths in more detail. The profile tracing method (PTM), binary transect method (BTM) and resinated core section method (RCSM) provided useful quantitative structural information.

Soil water status averaged over a large sampling volume (TDR, 1540000 mm^3) was considered to be stable through time. Detailed observations of soil water suction using tensiometers showed that soil water conditions remained unsaturated, at approximately 10 to 20 cm H_2O, and varied by 3 cm H_2O throughout the experiment. Suction varied depending on the location of each tensiometer with respect to position within or between aggregates.

Results based on Poiseuille's law and suction data showed that the flowpaths were predominantly mesopores. This result was supported by breakthrough curve analysis for the bulk of the soil although macropore flow was observed towards the mole drain. Flow rates observed from tracer movement varied throughout the soil regardless of depth. Chloride moved quickly towards the mole drain and the arrival of tracer was recorded within 4 hours. Time to breakthrough monitored at the suction cups varied from 4 to 76 hours. When the concentration gradient between applied solute and antecedent solute was large, reduced time to attain peak concentration was noted. As the concentration gradient reduced, speed of rise to peak concentration increased. An advection-dispersion model (CLEARY) fitted change in observed solute concentration through time at the suction cup lysimeters well. The study concluded that although water moved rapidly through the soil, the tortuous nature and increased contact with soil particles encountered as water moved through the mesopores resulted in water with matrix flow solute characteristics.

CONTENTS.

CHAPTER 2.
CHARACTERISATION OF SOIL AT LANDSCAPE AND DETAILED SCALE.

CHAPTER 3.
THE SOIL BLOCKS AND EXPERIMENTAL DESIGN.

CHAPTER 4.
SOIL BLOCK MONITORING TECHNIQUES.

TABLES.

CHAPTER 1.

CHAPTER 2.

CHAPTER 3.

CHAPTER 4.

CHAPTER 5.

CHAPTER 6.

CHAPTER 7.

CHAPTER 8.

FIGURES.

CHAPTER 1.

CHAPTER 2.

CHAPTER 3.

CHAPTER 4.

CHAPTER 5.

CHAPTER 6.

CHAPTER 7.

CHAPTER 8.

APPENDIX D

PLATES.

CHAPTER 2.

CHAPTER 3.

CHAPTER 4.

CHAPTER 5.

ACKNOWLEDGEMENTS.

I wish to thank Dr. Andrew Williams for his support and advice during this research. The supervision of Dr. John Down (University of Georgia) and Dr. David Scholefield (Institute of Grassland and Environmental Research) is also gratefully acknowledged.

I am indebted to Mr Kevin Solman, Miss Ann Kelly and Mrs Pat Bloomfield, at the University of Plymouth, for their technical support and advice.

The assistance of the following people is also gratefully acknowledged:
Andy Stone for technical support at IGER. Dave Simmons for so skilfully lifting the soil blocks. Maria Penn for assisting in field work. Adrian Holmes for computer advice. Tim Absalom for producing some of the diagrams used in this Thesis. My parents for proof reading Chapter 1 and 2.

Finally, I wish to thank Peter Rustage for his unreserved support, assistance and encouragement throughout this research project.

AUTHOR'S DECLARATION

At no time during the registration for the degree of Doctor of Philosophy has the author been registered for any other University award.

This study was financed with the aid of a studentship from the Ministry of Agriculture, Fisheries and Food, and carried out in collaboration with the Institute of Grassland and Environmental Research.

The training programme consisted of an involvement in setting up a surface water hydrology research experiment (Lizard, Cornwall) as well as a short course at the University of Georgia, USA. The following meetings were attended, South West Soils at Bristol University, Royal Agricultural College and European Geographical union, Edinburgh.

signed.....Lynda Deeks.....

date.....22-9-95.....

CHAPTER 1.

GENERAL INTRODUCTION.

1.1. BACKGROUND INTRODUCTION.

An understanding of field scale hydrological and solute transport processes is important, from both an economic and environmental point of view (Biggar and Nielsen, 1976; Russo *et al.*, 1989; Jensen and Refsgaard, 1991a; Ahuja *et al.*, 1993). However, these processes cannot be monitored easily unless the focus of study is at a detailed scale (Nielsen *et al.*, 1973; Russo and Bresler, 1981). This research explores the use of a small-scale soil block to investigate and monitor hydrological processes and mechanisms which operate naturally at the field scale in a heterogeneous soil. A series of experiments were designed to observe water movement and chemical transport through a naturally structured soil, with artificially manufactured preferential flowpaths created by a mole drain. The techniques of analysis developed in this research demonstrate how detailed micro-scale investigations can shed light on key environmental issues, such as nitrate pollution and natural leaching processes. The processes and mechanisms with which the research is principally concerned are those of water movement and chemical transport as controlled by soil structure. This investigation therefore addresses the influence of variable soil structural properties including pore size distribution, porosity, suction, soil water content and hydraulic conductivity on variations of soil water and solute movement.

1.2. CONTEXT OF EXPERIMENT: FIELD DRAINAGE.

Drainage has been used in lowland Britain, since the nineteenth century, to increase productivity and the intensity of landuse. Two innovations in particular led to the large-scale development of field drainage in Britain. The first was the use of permanent pipe drains buried in trenches up to 80 cm deep. The second was the introduction of mole drains

which required no excavation and were self supporting, unlined, channels (Davies *et al.*, 1972). Mole drains are used in finer-textured soils of low porosity and therefore tend to be shallower and more closely spaced (2 to 3 m separation) than pipe drains (20 to 30 m separation). The spacing of drains in a field affects the rate at which the water table rises and falls being faster with a closer spacing. The final water content of the field is not, however, affected by drain spacing (Findlay *et al.*, 1984). Installation of mole drains tends to be more economically viable for grassland agriculture where low economic returns prohibit the use of expensive drainage systems. The success of a mole drainage system is gauged by its rapid response to a rainfall event (Jarvis and Leeds-Harrison, 1987; Scotter *et al.*, 1990). At the field scale, the rapid movement of fertilisers through the soil along macro fissures and the mole drains has important implications in terms of nitrate pollution and the environment (Harris *et al.*, 1984; Addiscott *et al.*, 1991). Furthermore, the impact of drainage has wider hydrological implications than the field scale alone (Robinson and Beven, 1983) and therefore a better understanding of the processes and mechanisms controlling solute movement in a drained soil is required.

Mole drains are installed using a mole plough pulled behind a tractor. The 'mole' is a pointed cylindrical steel core, shaped like a bullet, of 5 to 8 cm length and 7.5 cm diameter, attached to a horizontal beam by the leg (Figure 1.1). As the mole is drawn through the soil at a constant depth of between 45 to 55 cm it creates a number of stress fractures. The cylindrical foot causes major soil failure planes from the side of the foot at 45° to the vertical which extend to the soil surface if ploughing occurs above critical depth. A loosening type failure (subsoil failure) may occur if the wedge of soil above the foot is isolated (Godwin *et al.*, 1981). The foot may also cause local soil reworking around the edge of the channel (Spoor and Ford, 1987). While the mole leg creates vertical leg cracks which run from the surface to the mole channel, inclined at 45° to the direction of travel.

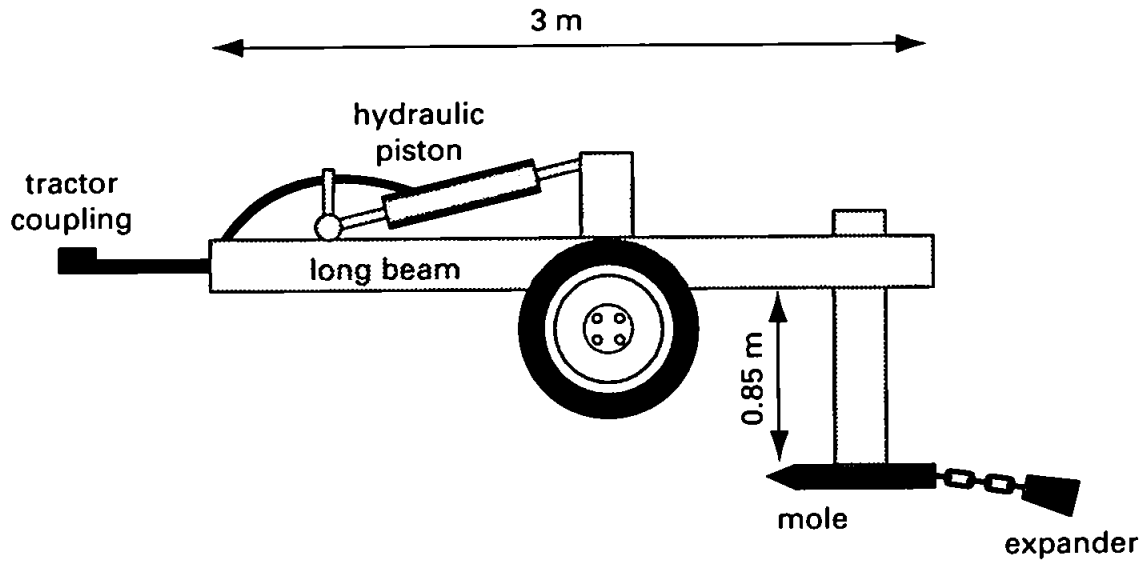

Figure 1.1 - Mole plough.

An expander, of approximately 10 cm diameter, attached to the mole by a short chain smooths, cleans and enlarges the channel created by the mole inducing further fissuring and reducing the leg slot in the top of the channel (Godwin *et al.*, 1981). Mole drains are spaced at 2 to 3 m intervals with a gradient of between 2 and 5 per cent (Findlay *et al.*, 1984). The mole drains convey the water to deeper tile drains which run almost at right angles to the mole drain. The tile drains are spaced at 20 to 30 m normal to the slope and are connected to the mole drain via permeable gravel. Successful fissuring of the soil above the mole drain is dependent upon prevailing soil conditions at the time of installation. A 'wet' soil has a more plastic consistency and is less successfully fissured by the mole plough. However, the soil must be at a water content sufficiently large for the mole channel to remain stable and have a long life. Stability of a mole system varies but typically remoling is necessary at three to five year intervals. The time of the year when mole drains

can be successfully pulled is limited. Ideally mole ploughing should be conducted when the surface soil is sufficiently dry to allow brittle fracturing while the soil at moling depth is still plastic and will therefore support the mole channel. The best time of the year for moling is May to June, and September to October when there is a soil water deficit of about 50 mm (Findlay *et al.*, 1984).

1.2.1. Hydrological Impact of Field Drainage.

Soil types that are acceptable for mole drainage include medium to heavy soil which typically have a clay content of not less than 30 per cent and a bulk density greater than 1.3 g cm^{-3} at moling depth (Spoor *et al.*, 1982). These soils are unsuitable for deeper soil pipe drains because of limited surface water movement (Hallard, 1988). The soils of the Culm Measures, specifically of the Hallsworth series are suited to mole drainage. Hydrologically the subsoil of the Hallsworth series has a slow permeable nature due to a high clay content and poor soil structure at depths below 30 cm which gives rise to a surface water gley. Excess winter rainfall leads to rapid lateral flow predominantly as surface water flow as well as shallow subsurface flow.

Deep drainage techniques have been used on the soils of the Hallsworth series, however, wetness due to high rainfall or impermeable subsoils were not satisfactorily relieved by this method (Hallard, 1988). Mole drainage schemes have been found to be effective in controlling surface water problems (Trafford, 1971) as they permit the rapid removal of water from the upper soil layers (Leeds-Harrison *et al.*, 1982).

Although at depth the soil may be relatively impermeable the importance of naturally occurring soil structure in the upper horizons of the soil profile determines the affectiveness of the mole drainage system. Hallard (1988) demonstrated that the hydrological response

of a reseeded mole drained field was similar to that of an undrained permanent pasture field. During the process of reseeding the natural soil structure was disrupted which affected the flowpaths from the soil towards cracks and fissures created when the mole was pulled. Even though moling creates a system of fissures and cracks that provide a direct pathway for water and solutes to move directly to the mole drain without the natural soil structure water is less likely to move through the soil and intercept drainage cracks and therefore drainage becomes less efficient.

Observations made by Leeds-Harrison *et al.* (1982) have shown the disturbance created by the mole plough leg to be confined almost totally to the area above the drain, and the cracks generated to extend only 30 cm on either side of the leg slot, resulting in the fastest infiltration occurring directly above the mole. These mechanically generated macropores increase the porosity of clay rich soils common to grassland agriculture resulting in increased productivity and a prolonged grazing season (Tyson *et al.*, 1992).

The introduction of macropores in a soil causes substantial spatial (Leeds-Harrison *et al.*, 1982; Ogden *et al.*, 1992) and temporal (Reid and Parkinson, 1984; Watson and Luxmoore, 1986; Kluitenberg and Horton, 1990; Jarvis *et al.*, 1991) changes in soil water movement and therefore the hydrological characteristics. Observations between mole drained and undrained plots has shown that drainage increases the amount of precipitation moving via subsurface pathways by 60% (Addison, 1995). These changes directly affect the transport of chemicals and pollutants through the soil. Garwood *et al.* (1986) found that the proportion of soluble nitrate lost under drained field conditions increased by two or three times compared to undrained fields. The difference in proportion of available nitrate was linked to a reduction of denitrification due to improved soil water conditions. The extent to which macropores, mesopores and micropores (Luxmoore, 1981) influence chemical

movement through a drained soil is a central concern of this investigation.

1.3. NITRATE LEACHING.

There has been a notable increase in nitrate concentration over the last two decades in many lowland river catchments of Britain. This increase has been associated with an intensification of agricultural practices (Burt and Haycock, 1992). Intensification of agriculture, with increasing reliance on nitrogen fertilizer, has significantly contributed to the problem of increasing nitrate leaching (Ryden *et al.*, 1984). However, drainage practices have also been shown to have a significant impact on the amount of nitrate leached from the soil (Harris *et al.*, 1984; Scholefield *et al.*, 1993; Scholefield and Jarvis 1995). It was not until the beginning of the 1980s that concerns about the impact this practice was having on public health and the environment were really considered.

Agriculture is now recognised as the most important source of nitrate pollution in rural catchments although other sources include urban effluent and the atmosphere (Burt and Haycock, 1992). Nitrate (NO_3^-) is an inorganic species of nitrogen and is readily absorbed into solution. Once in solution nitrate is relatively unreactive and can only be transformed biologically (Meybeck *et al.*, 1989). Although nitrate is the main form in which nitrogen is found in water it may also be present in the form of ammonium (NH_4^+), nitrite (NO_2^-), nitrogen (N_2) and as nitrous oxide (N_2O) (Burt and Haycock, 1992).

Nitrogen in soil is present in both mobile and immobile forms, but is capable of moving from one state to another as a result of the activities of plants and micro-organisms. A simplified version of the changing form of nitrogen in the nitrogen cycle is shown in Figure 1.2. Nitrate may be lost from the soil by two processes, denitrification and leaching. Denitrification creates an environmental problem because of the release of the

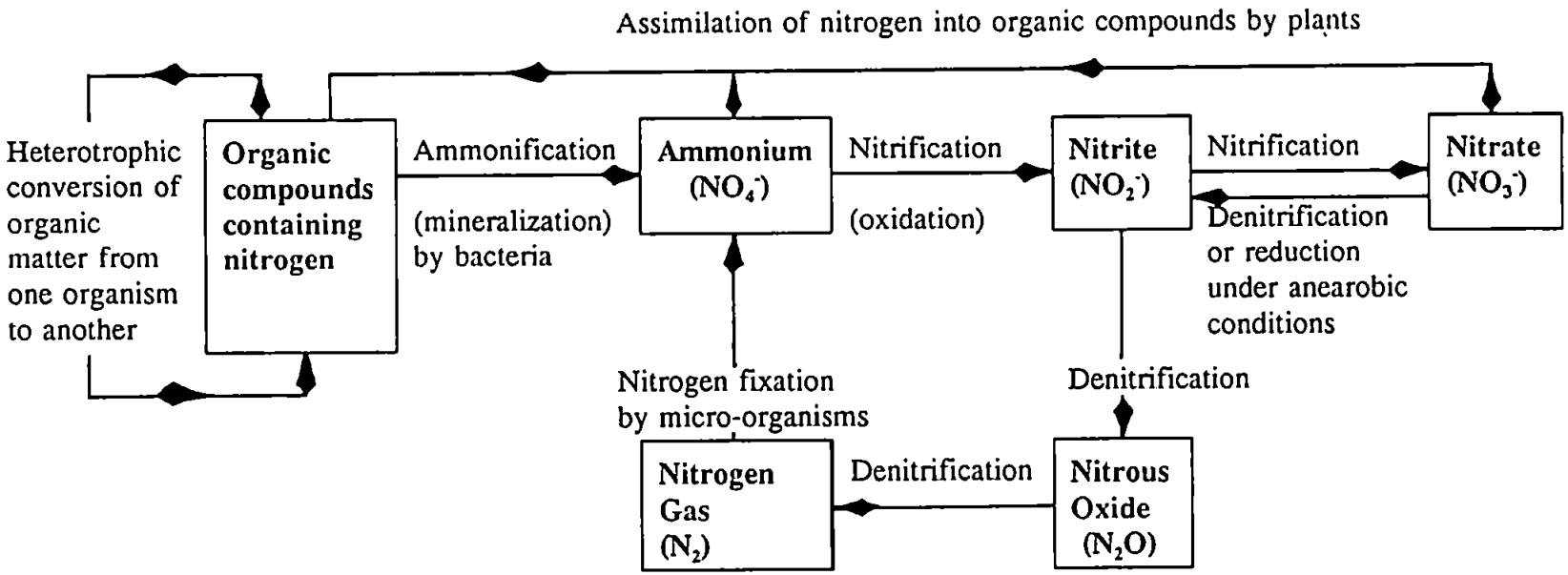

Figure 1.2 - The nitrogen cycle showing some of the biological reactions (Burt and Haycock, 1992).

greenhouse gas and ozone depletor nitrous oxide.

Nitrate leaching is the loss of nitrate from a soil in drainage water. Losses of nitrate from grassland farming tend to be smaller than losses under arable farming as more nitrate is taken up in the autumn under grassland (Burt and Haycock, 1992; Powlson, 1993). Sources of leached nitrate come from fertilizer not taken up by crops, as well as from the mineralization of organic matter especially in autumn when the soil is warm and moist. The mineralization and nitrification of nitrogen in animal excreta can increase levels of nitrate leaching from grazed grassland (Jarvis, 1993). Losses of nitrate from grassland are smaller when fertilizer applications are modest < 250 kg ha^{-1} a^{-1} (Burt and Haycock, 1992), increasing as application increases. However, no direct link has yet been established between proportion leached and amount of fertilizer applied.

Soil drainage has significant implications for nitrogen leaching (Harris *et al.*, 1984; Armstrong and Garwood, 1990). Field drainage of a clay rich soil alters the pathway of water movement. In a clay rich soil without artificial drainage the soil remains saturated throughout the winter and as the water table remains high any additional rainfall tends to travel predominantly by overland flow. Nitrate is lost from the soil by denitrification to the atmosphere under anaerobic conditions. Under a drained clay soil the winter water table is reduced and rainfall predominantly enters the soil resulting in very little overland flow but rapid subsoil flow. Subsequently overall volume and timing of water leaving the site is altered only slightly. However, significant changes in pathways exist between drained and undrained sites as a result of which nitrate leaching is increased through the drained soil (Scholefield *et al.*, 1993). Drainage of the soil increases mineralization under aerobic conditions and allows movement of water through the profile increasing leaching potential. Harris *et al.* (1984) found an increase of 85% loss in nitrate by leaching from a mole

drained plot compared to an undrained plot. Drainage of a soil may also lead to a more intensive landuse for grazing, or landuse may be changed to arable production, in either case the potential loss of nitrate from the land is liable to be increased as a result. Artificial drainage in soil, therefore, allows the rapid movement of solute, which minimises residence time, and reduces the potential of uptake by the soil and loss by denitrification. Conventional wisdom assumes that the implication of such rapid movement leads to an increased concentration of nitrate reaching the water course than would be experienced through an undrained soil. However, Scholefield *et al.* (1993) have shown that peak concentration is lower because of the larger amount of mixing which takes place between rapid moving water in the peds and the relatively immobile water of the soil matrix. The examination of preferential flow through both natural and artificially created structural pathways is therefore important in explaining nitrate loss from a soil. For this reason the experiment in this thesis was established with artificially manufactured pathways and drainage created by a mole drain.

1.3.1. Nitrate Sensitive Areas.

In response to concerns over growing nitrate levels in many lowland river catchments and restrictions placed on levels of nitrate in drinking water by the EC, the government in 1988 announced the introduction of its Nitrate Sensitive Areas scheme. In 1988 the Department of the Environment concluded that landuse control could provide a cheaper option than water treatment alone in limiting nitrate in water. On the 1 July 1994 the government announced details of its new Nitrate Sensitive Areas for regions where water sources exceed or were predicted to exceed the EC limit of 50 mg l^{-1} (equivalent to 11.3 mg NO_3-Nl^{-1}). The new scheme extends the original 10 catchment areas established in 1990 by a further 22 catchments. The Nitrate Sensitive Areas scheme (NSA) is an EC assisted environmental scheme proposed by the Ministry of Agriculture Fisheries and Food (MAFF)

as a consequence of the Common Agricultural Policy reform agreed in 1992. NSA are at present voluntary but given present over production levels and grants, have proven to be thus far successful. The voluntary restrictions include the avoidance of fertilizer, manure or slurry application in autumn, recommended maximum rates of fertilizer application, for example, reducing nitrogen fertiliser inputs for grassland from 250 kg N ha^{-1} to 150 kg N ha^{-1}, planting of a winter cover or cash crop in autumn, and avoidance of grassland ploughing in autumn which can increase mineralisation processes.

1.3.2. Soil Structure and Buffer Zones.

An understanding of the importance that soil structural properties play in the movement and storage of chemicals such as nitrate, together with management policies is needed to help reduce the amount of nitrate loss to catchment streams. Artificially created structure, such as mole drains, can significantly increase the movement of water and therefore chemicals from the soil surface to drainage water (Shuford *et al.*, 1977). The study of water and solute movement and the interaction within the soil is needed to provide a basis for the establishment of management policies, such as buffer zones, to reduce nitrate loss.

Properties of soil such as texture and structure can affect water and chemical transport (Quisenberry *et al.*, 1993). As the percentage clay content increases aggregation increases, flow of water and solutes become less uniform, and water and chemicals have greater potential to move rapidly through the soil with minimal displacement. The presence of preferential or bypass flowpaths greatly influence the amount of nitrate (chemical) leaching though a soil (Scholefield *et al.*, 1993). The importance of soil structure to the concentration of leachate lost from fields to river courses can be used to provide a solution to the problem.

Buffer zones have been proposed by Burt *et al.* (1993) as a method for reducing agricultural pollution of river systems by fertilizers such as nitrate. The soil structure of a buffer zone is of importance in reducing nitrate leaching. Rate of solute movement must be slowed down to allow time for reaction with the soil, as discussed later, as well as assimilation by plants and microorganisms. A supply of carbon to microorganisms if vital in this process. Burt *et al.* (1993) proposed the use of low conductivity land with homogeneous soil properties, such that no preferential flow pathways exist within the soil, as a method for reducing agricultural pollution of nitrates into river systems. Initial investigations focused on undrained flood plains which were shown to act efficiently as a nutrient retention zone through denitrification and in summer by assimilation. The slow hydraulic conductivity of these soils allows for a long residence time for subsurface flow and thus sufficient time for nutrient reaction. Such zones, referred to as buffer zones, down slope of agricultural land may reduce nitrate leaching loss, by subsurface flow, to below recommended EC levels even if the land is intensively farmed.

Increased residence time of nitrate rich water will lead to an increase in denitrification and a subsequent reduction in nitrate lost to streams. However, buffer zones also have their draw backs; an increased residence time will also lead to a subsequent increase in the release of nitrogen (N_2) and nitrous oxide (N_2O) through denitrification. Nitrous oxide is recognised as a harmful greenhouse gas which is 150 times more effective at increasing warming than carbon dioxide (CO_2) and is also believed to be linked to ozone depletion in the stratosphere (Powlson, 1993).

An understanding of the mechanisms involved in water and chemical transport through soil is therefore needed not only to understand field scale movement of solutes but also the potential implications to the wider scale catchment area. This experiment was designed with

the intention of examining in detail the importance of soil properties such as soil structure, to solute movement through the soil. The following section outlines the objectives of this work.

1.4. RESEARCH OBJECTIVES.

The concept of 'classical' bypass macropore flow suggests that pathways through the soil are discrete and that little interaction occurs between soil matrix solution and irrigation water. The discussion above has highlighted the necessity to investigate in greater detail the hydrological importance of different flowpaths, including macropore, mesopore and micropore (Luxmoore, 1981), to the movement of water and solutes through the soil (Luxmoore *et al.*, 1990; Harvey, 1993). To achieve this objective a detailed soil block experiment was conducted under steady state conditions to investigate the following:

Aim 1:

The primary aim of this experiment was to conduct a detailed investigation into the variability of soil water movement and to determine the mechanisms which influenced water and solute movement through a small scale soil block (0.85 m^3). Sub-aims of this major objective were:

1. To monitor soil suction through the profile and around the mole drain, and to establish the hydraulic gradient or water movement driving force.
2. To measure the soil water content at a number of locations in the soil block, to determine its variability and to verify whether steady state conditions had been achieved.
3. To calculate the unsaturated hydraulic conductivity at various points in the soil profile using Darcy's law.

4. To compare predicted unsaturated hydraulic conductivity, as determined for selected points, with saturated hydraulic conductivity calculated for the soil to give an indication of the degree of saturation within the soil and also to highlight the problems of sampling scale within a heterogeneous soil.
5. To make a detailed investigation of the structural properties and to integrate this information with the soil water movement measurements and details of tracer experiment observations.

Aim 2:

A second aim was to investigate the interaction between rapid preferential or bypass flow routes and matrix water. Sub-aims of this second objective were:

1. To observe the behaviour of conservative (chloride) and non-conservative/biological (nitrate) tracers, spatially and temporally, through the blocks to see if any discernable changes in tracer concentration occur, and to integrate these findings to porosity and hydraulic conductivity to link speed of movement to concentration loss from mobile paths.
2. To make comparisons between tracer experiments to see what effect residual (immobile) solute concentration had on peak concentration discharge.
3. To compare the various levels of residual nitrate in the soil to hydraulic soil properties.
4. To interpret breakthrough curves to determine diffusion and dispersion characteristics within the soil.
5. To analyse the observed relationships using mathematical models to predict dispersivity.

(Sub-aims 1,2 and 3 can be used to suggest potential interaction between mobile and immobile zones. Sub aims 4 and 5, can be used to calculate rate of interaction between different pathways).

1.5. THESIS STRUCTURE.

The structure of the thesis is outlined in Table 1.1. There are five major sections namely introduction, soil structure, hydrology and solute transport, synthesis and the conclusion.

The introduction sets out the aims of the investigation, including the experimental approach adopted and reviews the literature covering soil structure, water retention and movement, pathways, solute movement and interpretation of solute and water movement using breakthrough curves and models (Chapter 1). Included in the overall introduction is a wide scale description of soil type and typical landuse of such soils, combined with qualitative and quantitative descriptions on a smaller scale of soil properties including structure, texture, bulk density, porosity, soil water retention capacity, soil water and saturated hydraulic conductivity (Chapter 2). The overall design of the experiment is outlined in Chapter 3. A description of the major instrumentation used to monitor soil water conditions including tensiometers and time domain reflectometry and solute movement using suction cup lysimeters is made in Chapter 4.

The section detailing soil structure focuses on quantitative measurements of soil structure relating to pore space. Three methods were used: profile tracing method, binary transect method and resinated core section method (Chapter 5).

The section on hydrology and solute transport investigates patterns of: soil water movement (Chapter 6) based on suction, hydraulic gradient, hydraulic conductivity and soil

Table 1.1 - Structure and organisation of the thesis.

Section	Chapter	Contents
1. Introduction and Aims	1.	Introduction: aims, experimental approach, background research and literature review.
	2.	Wide scale soil description, land use and small scale soil characteristics: qualitative and quantitative description of soil and land use.
	3.	Experimental design: methodology and research techniques.
	4.	Instrumentation: description of design and function of tensiometers, TDR and suction cup lysimeters.
2. Soil Structure	5.	Soil structure: quantitative measurement of soil structure (macropore and mesopore) using profile tracing method, binary transect method and resinated core section method.
3. Hydrology and Solute Transport	6.	Soil water movement: measurement of soil water content using TDR and soil suction using tensiometer responses.
	7.	Solute movement: interpretation of changes in solute concentration through time, breakthrough curves and modelling, using chloride and nitrate tracers.
4. Synthesis	8.	Soil structure, soil water movement and solute transport: integration of soil property variabilities to explain solute movement.
5. Conclusions	9.	Conclusion and future work.

water content, and solute transport (Chapter 7) based on the interpretation of change in solute concentration through time, breakthrough curves and modelling.

The interdependency of soil structure, soil water movement and solute movement are drawn together in Chapter 8 to interpret how soil properties and mechanisms affect solute and water variability both spatially and temporally in the soil. The final chapter (Chapter 9) draws conclusions from the main findings, including implications, to field scale investigations and makes suggestions on how to improve the investigation in the future.

1.6. EXPERIMENTAL APPROACH.

1.6.1. Scale.

Three distinct scales of observation have been used to investigate solute transport through the soil; field (large scale), plot (intermediate scale) and intact soil cores (small scale). The scale of investigation needs to be appropriate to the phenomena being observed. At the field scale the complex structuring of a heterogeneous soil encourages spatial variability (Nielsen *et al.*, 1973; Curtis *et al.*, 1987; Sassner *et al.*, 1994)) which limits the viability of detailed hydrological investigations (Holden *et al.*, 1995a). To interpret the processes and mechanisms at work within the soil a more focused approach is therefore needed. Experimentation on plots of land, isolated but not removed from the field are favoured because of the minimal effect on the observed volume of soil and because of the relative ease and inexpense of isolating a plot of land from the field. Table 1.2 gives examples of some plot scale experiments. However, very detailed observations about mechanisms and processes of water movement and chemical transport are still not feasible even at an intermediate scale. Although as scale reduces the nature of the soil becomes increasingly heterogeneous (Beven and Germann, 1981; Miyazaki, 1993) and therefore more complex. Small scale investigations allow a more intense monitoring programme to be established

Table 1.2 - Examples of isolated *in situ* plot scale experiments.

Author(s)	Aim	Comments
Shuford *et al.*, 1977	To investigate the importance of large pores as major pathways. An undisturbed *in situ* isolated plot 0.915 m by 0.915 m was used.	Large pores will increase tracer movement when the soil is near field capacity.
Jardine *et al.*, 1990	To observe the movement of bromide tracer through an *in situ* isolated plot 2 m by 3 m.	Rapid response was observed in the larger pores while smaller pores increased in concentration more slowly but to a higher concentration.
Holden *et al.*, 1995a	To investigate preferential flow in a well structured soil at a high spatial and temporal resolution. The experiment was conducted on an *in situ* isolated plot 5.4 m by 3.4 m by 1.2 m.	Automation combined with large isolated soil block have been able to provide useful data for advancing the knowledge of the mechanisms of transport at a larger scale.
Addison, 1995	To investigate the concept of new water replacing old water on an isolated *in situ* soil block 8 m by 3 m.	Rapid interaction between bypass flow and water held in soil matrix.

and also reduce the complexity of the soil by reducing the number of variables. Only at the small scale can an intensive monitoring program be established. Table 1.3 gives examples of some small scale soil experiments.

The main limitation of a plot experiment occurs at the artificially created boundary which would not be found in the natural field. The boundary represents a potential pathway for rapid loss of water and solute due to the edge effect. Pressure gradients may also be altered by the removal of the surrounding soil influencing the movement of water close to the boundary of the plot.

The advantages of observing tracer movement at a smaller scale than in the field include the ability to observe in greater detail the phenomena that effect solute movement in the soil profile. The main disadvantage of making observations at a small scale, in a heterogeneous soil, is the problem of how representative the findings are of what is

Table 1.3 - Examples of small scale laboratory column experiments.

Author(s)	Aim	Comments
Booltink and Bouma, 1991	To characterize the processes of bypass flow on solute movement in a well-structured clay soil. Soil cores 20 cm diam. by 10 cm length.	Experiment showed flow of water in a structured soil to be more complex than is suggested by the concept of mobile/immobile water.
Singh and Kanwar, 1991	To investigate preferential solute transport through macropores using 6 undisturbed soil columns (15 cm diam. by 61 cm length)	Shape of breakthrough cure showed presence of macropore flow through the undisturbed columns.
Cameron *et al.*, 1992	An improved design and sampling procedure for large (80 cm diam. by 120 cm length) undisturbed monolith lysimeters to prevent edge flow.	The modified design was successful in preventing edge effect.
Ela *et al.*, 1992	To examine the effect of simulated rainfall on water infiltration into soils with earthworm and artificial macropores.	Surface seal decreased macro-flux, not all macropores will flow due to blockages or insufficient water content.
Tindall *et al.*, 1992	To improve the method of field extraction of large, undisturbed soil cores (30 cm diam. by 38 cm length) and laboratory analysis.	Results showed their suggested method to be a reliable, efficient and economic way of conducting saturated and unsaturated solute transport experiments.
Marshall, 1994	To determine the effect of preferential flow paths, in a structured soil, to the movement of contaminants. Tracer experiments conducted on both intacked and repacked cores (30 cm diam. by 38 cm length).	This work highlights the importance of preferential flow paths, as a result of natural soil structure, to the rapid movement and minimal reaction of a tracer in the soil.
Poletika and Jury, 1994	To investigate the effects of cultivation and irrigation methods on uniformity of water flow and dispersion of solute. Undisturbed field soil (80 cm by 80 cm by 30 cm) used.	Shallow cultivation lowered the hydrodynamic dispersion leading to a decrease in spreading of the leached solute pulse.
Quisenberry *et al.*, 1994	To measure the effect of application rate on the magnitude and spatial distribution of macropore flow. An undisturbed column of soil (32.5 cm by 32.5 cm by 32.5 cm)was used.	The significance of macropore flow is dependent on irrigation rate, reducing as irrigation rate reduces. The pore system within the soil controls the rapid macropore flow within the soil.
Buchter *et al.*, 1995	To assess the effect of flow heterogeneity on solute transport in a stony subsoil using miscible displacement experiments on a large undisturbed gravel monolith (30 cm diam. by 75 cm length)	Under steady state water flow conditions flow paths remained constant between consecutive runs. Implying flow paths to be an intrinsic property of a soil medium for a given water content.

actually happening at the field scale. A compromise must therefore be reached between scale of investigation and the field scale problem.

To investigate solute movement at a fine scale but also be able to predict field scale movements from the observations, experiments have been conducted at a fine scale using a dense sampling pattern and the combined observations averaged to predict what is happening at the larger scale. Sassner *et al.* (1994) used 29 undisturbed soil monoliths (20 cm in diameter and 100 cm long) from a field plot of 15 × 175 m^2. Breakthrough curves were predicted for each of the 29 monoliths. The breakthrough curve for the plot was then estimated by spatially averaging the small scale breakthrough curves. However, using a small scale and estimating up to a larger scale may neglect some large scale variability. The constraints of the column walls imposes a restriction on flow that does not apply to the same extent at the block scale (Luxmoore *et al.*, 1990), and which do not occur at the field scale.

Work by Beven and Germann (1982) and Bouma (1989) has referred to the representative elementary volume (REV) of a sample. The REV is the smallest volume of soil which can be used to define the heterogeneity of soil properties, including spatial variability of bulk density, soil water content and suction. Implying that a detailed experiment can be set up that would represent the larger scale drainage problem. Scale must take into account the representative elementary volume (REV) of the observed phenomena, for example the REV for investigating macropore flow may need to be much larger than for micropore flow (Beven and Germann, 1982; Bouma, 1989). Bouma (1989) recommended that a REV should contain at least 30 peds in a cross section. Beven and Germann (1981) suggested that a REV for a combined micropore and macropore system may need to be in the order of 1 to 10 m^2 in area, with a depth related to changes in the distribution of macropores in

the soil profile, to obtain a spatial average that is statistically characteristic of the soil around a point. The macropores may still only represent 1 to 5 % of the total volume at this scale (1 to 10 m^2).

1.6.2. Block Experiment.

To achieve the objectives of the investigation a small scale block experiment was established. The scale of the block, 1 m^2 (cross-sectional area) by 0.85 m depth, fulfilled the suggested order of magnitude for representative elementary volume, made by Beven and Germann (1981), of a combined macropore and micropore system.

The soil block was removed from the natural environment and placed under controllable laboratory conditions. The advantage of this procedure was that all boundary conditions were known, as with the field scale. Furthermore, the irrigation input could be controlled and therefore steady state conditions could be established and maintained. The removal of the soil block and subsequent sealing and instrumentation are described in detail in Chapter 3. A second soil block was obtained from a site adjacent to the first and instrumented so that a spatial comparison could be made between REVs of the same soil.

1.6.3. Structure.

The structural properties of the soil were of primary interest in this investigation because of the influence soil structure has over other soil properties including; porosity, suction, soil water content, pore size distribution and hydraulic conductivity and the effect these properties have on soil water movement and solute transport.

Prior to the removal of the soil blocks from the field a mole drain was drawn through the soil. The purpose of the mole drain was to generate a wider range of structural pathways

in the soil and to enable rapid drainage, as explained above. The creation of larger structural pathways including macropore and mesopore channels through a naturally poorly draining soil enabled two domain flow to be observed. Two domain flow is a division of flow between rapid flowing pathways and slower or stagnant flow pathways, discussed in Section 1.10. The existence of two such distinctive pathways was fundamental in satisfying the two main objectives presented in this thesis (Section 1.4.).

1.6.4. Water Movement.

Central to this experiment and the fulfilment of aim 1 was an understanding of subsurface flow processes. Unfortunately flow cannot be monitored directly. Many of the intellectual problems considered in this thesis revolve around the twin difficulties of conceptualising how subsurface water moves and in trying to monitor it using equipment which monitors at a point or over a small soil volume. The use of tensiometers to monitor at a point suction (matric potential) and TDR to monitor soil water conditions over an averaged area are discussed in Chapter 4. The matric potential at a point can be measured using tensiometers but direction and magnitude of flow from such point measurements can only be inferred. TDR values can be used to suggest whether steady state conditions were achieved throughout the soil block.

1.6.5. Solute Transport.

As an alternative method to examining soil water movement (aim 1), the study of the movement of naturally occurring tracers has some advantages since the behaviour of a tracer at a point represents the integration of a number of flow routes followed prior to the monitoring location. In this study conservative (chloride) and biological (nitrate) tracers were applied to the top of the isolated block and were observed both spatially throughout the block, using suction cup lysimeters (describe in Chapter 4) and temporally throughout

each experiment and between experiments (Chapter 5). Methods of application (miscible displacement or pulse) and concentration of tracers used are cited in Chapters 3 and 5.

1.6.6. Breakthrough Curves and Modelling.

Although the movement of both soil water and solute can be perceived from the observations above, the interaction between different pathways, mobile and immobile zones, within the soil is not easily monitored. An interpretation of the interaction within different areas of the soil can be made from the interpretation of solute breakthrough curves and predictions based on mathematical formulation.

The interpretation of the shape of breakthrough curves with reference to active flowpaths is well documented (Bouma and Wösten, 1979; Walker and Trudgill, 1983; Kluitenberg and Horton, 1990; Singh and Kanwar, 1991) and is examined in Chapter 7. A rapid initial rise in concentration has been linked to bypass flow while a slower increase in concentration closer to the peak concentration is associated with the movement of solutes through the matrix. The amount of mixing experienced by the solute can be related to relative concentration at one pore volume of applied tracer.

A model [CLEARY (Cleary and Ungs, 1979)] based on a one-dimensional advection and dispersion flow equation was used to predict diffusion and dispersion rates of solute to sample location. Chapter 7 outlines the model used in this investigation.

1.7. SOIL STRUCTURE.

Soil structure is defined as the interconnecting framework formed by the arrangement of solid particles and the size, shape and distribution of solid particles and voids both between and within the particles (Bouma and Anderson, 1971; Marshall and Holmes, 1979; Rowell,

1994). The solid particles that form the skeleton of the soil are linked by fine-textured materials (clays, iron oxides and organic material) to form units, known as peds or aggregates. Voids, referred to as pore spaces, exist between particles as well as between individual peds. Two distinct zones of water movement can be defined within the soil structure; intrapedal (pore spaces between particles) and interpedal (pore spaces between peds). The importance of these two zones to water movement is discussed later.

Structure until recently was only described qualitatively. A qualitative description of soil structure is limited to the shape, size and distribution of soil aggregates. Such a qualitative description of soil structure is given in Chapter 2. A quantitative description of soil structure can also include observations of the size, shape and distribution of pore spaces within the soil. The ability to quantify soil structure is important to the description of solute distribution through a soil (Lawrence, 1977). The quantification of soil structure is not easy because of the complex nature of soil (Newman and Thomasson, 1979). However, quantitative descriptions of soil structure have been attempted (Jongerius *et al.*, 1972; Murphy *et al.*, 1977; Moran *et al.*, 1989; Moran, 1990; Bullock and Thomasson, 1979; Walker and Trudgill, 1983; Ringrose-Voase and Bullock, 1984; Ringrose-Voase, 1987). Quantitative descriptions of the soil are detailed in Chapter 5.

Water and tracer movement through a soil is governed by the size, shape, distribution and continuity of the soil pores present (Bouma and Anderson, 1971; Harvey, 1993) these are all properties of soil structure. The structure of a soil governs the availability of water and oxygen to soil fauna and flora. The stability of the soil structure will determine temporal porosity. An understanding of soil structure is therefore important as it regulates the movement of water and solute through the soil (Booltink, 1993). Heterogeneity effects the movement of water and solutes leading to highly variable water content and solute

concentration. The two basic parameters of soil structure which determine unsaturated flow are water retention and hydraulic conductivity (Jensen and Refsgaard, 1991a).

1.8. WATER RETENTION.

The ability of a soil to store or conduct water is dependent on pore size distribution (linked to soil structure) within the soil. In 1897 Briggs stated that water exists in the soil in one of three states; hygroscopic, capillary and gravitational, as shown in Table 1.4 (Towner, 1989). Although these divisions of water status were made arbitrarily their validity is still generally accepted. Several soil water states are recognised including: drainage water, available water and unavailable or structural water (Birkeland, 1984; Rowell, 1994). In an

Table 1.4 - Soil water status as defined by Briggs, 1897 (cited by Towner, 1989).

Hygroscopic:	water absorbed onto the surface of particles, moving mainly by evaporation and condensation.
Capillary:	water held by surface tension around particles moving by capillary action from wetter to drier regions in any direction.
Gravitational:	water that occupies pore spaces and moves under gravitational or hydrostatic pressure gradients.

initially saturated soil water that exists between pores is held under lower surface tension. This loosely held water is the first to drain under the influence of gravity alone and is referred to as gravimetric water. When the soil drains it is the water in the centre of the macropore that exits first as it has the most potential energy, and least resistance to move, and thus is the most mobile. Water drains from the soil under gravity until a point is reached where water is held in the soil by a force equivalent to gravitational pull. The water in the soil at this point is then said to be at field capacity and is constant for a given soil. Further drainage of the soil, below field capacity, can occur by evaporation and

transpiration. Once the force holding the water equals the drainage force of evapotranspiration drainage ceases again. The soil water content under these conditions is described as the permanent wilting point and is unavailable to plants. The difference in water content between field capacity and permanent wilting point is described as the available water. The relationship between the three soil water states (drainage, available and unavailable water) to pore size is defined in Table 1.5 (Rowell, 1994).

Water in a soil is held in a variety of mobile and immobile states (De Smedt and Wierenga, 1979). Around the perimeter of a single soil particle where negatively charged oxygen atoms are exposed, water molecules are strongly attracted and there exists a resilient adhesive force. Adhesion water is the most immobile water in a soil having the

Table 1.5 - Soil water classification as a function of pore size (Rowell, 1994).

Soil Water Classification	Pore Size / Definition	Drainage
Drainage water	>50 μm - Transmission pores	Drained by gravity
Available water	50 - 0.2 μm - Storage pores	Drained by evaporation and transpiration
Unavailable/structural water	<0.2 μm - Residual pores	Water held so strongly that it is not available to plants

lowest energy level. As distance away from the soil particle increases its potential attractive force decreases. Beyond this sphere of strong attraction, cohesive forces operate, whereby water molecules attract each other by hydrogen bonding. Adhesion water and cohesion water together form the water film surrounding a soil particle after gravimetric drainage. The water molecules on the outer edge of this film have the greatest potential energy and the greater tendency to move.

Within a soil where individual particles are close to or touch each other, water films surrounding the particles overlap. Interstices and pores become water filled. Pore spaces that are sufficiently small to retain water after soil wetting and downward drainage (due to gravity) are defined as capillary or micropores. At the point where only adhesion plus cohesion water remains (water held against gravity) the soil is considered to be at field capacity. At field capacity the aeration or macropores are airfilled. The size of these macropores is discussed below.

The proportion of different pore sizes (pore size distribution) in a given sample and the force required to drain them (critical suction) can be calculated using a soil water characteristic curve (Chapter 2). Critical suction is the suction required to empty pores of a known size, Table 1.6 shows the relationship between different pore sizes and suction. Pore size is calculated as effective pore size drained equivalent to a cylindrical pore or circular neck which would empty at a given suction to simplify the calculation. Work by Luxmoore (1981) has specified boundaries to distinguish different pore size classes based on capillary tensions. The volume of water lost for a given suction is used to calculate the proportion of pores of a given radius drained at each suction and can therefore be used to calculate pore size distribution.

1.9. WATER MOVEMENT.

Three forces act on water to cause it to move or be retained in the soil: matric potential, gravity and osmosis. Combined, these forces are termed soil water potential (ψ). Matric potential (ψ_m) is a measurement of attraction between soil and water and causes water to move from wet areas where suction is low (pressure is high) to dry areas where suction is high (pressure is low), regardless of spatial direction. The influence that gravitational potential (ψ_g) has on water movement increases with height above an arbitrary datum:

Table 1.6 - The relationships between pore size and critical suction required to drain the pore (cited in Rowell, 1994).

Pore size, diameter (μm)	Critical soil water suction (kPa)	Equivalent hydraulic head, h_w (m H_2O)	Comments
20 000	0.015	0.002 (2 mm)	A 2 cm crack
4 000	0.075	0.008 (8 mm)	An earthworm channel
300	1.0	0.10 (10 cm)	The diameter of a cereal root
60 - 30	5 - 10	0.5 - 1.0	Soil water suction at field capacity. Transmission pores are >50 μm
2	150	15	Size of a bacterial cell. Limit of 'readily available' water. Upper size limit of a clay-sized particle. Storage pores are 50 - 0.2 μm
0.2	1500 (1.5 MPa)	150	Water suction at the wilting point. Residual pores are <0.2 μm
0.003	100 000 (100 MPa)	10 000	Water suction in air-dry soil. The pore size is approximately 10 × the size of a water molecule

gravity potential dominates in a saturated soil. Osmotic potential (ψ_o) is a measurement of attraction between ions and water. This force is usually regarded as negligible in most soils of low salinity except around plant roots. Total potential (ψ_t) which determines the direction that water moves, therefore, is dependent mainly on gravity (ψ_g) and matric potential (ψ_m) (Rowell, 1994):

$$\psi_t = \psi_g + \psi_m \qquad (1.1)$$

Water will move in the direction of the most dominant force. A dry top soil may have sufficient suction to over come gravitational force resulting in a net upward migration of water.

Water moves in soil from regions of higher-energy water to regions of lower-energy water, in the direction of decreasing energy status, along a gradient known as the water potential gradient (F) (Foth, 1990).

$$F = \frac{\psi_A - \psi_B}{L} \qquad (1.2)$$

Where, ψ is the water potential at points A and B; and L is the distance between points A and B.

Velocity of water is dependent on the total water potential gradient (ψ_t) (i.e. the driving force) and hydraulic conductivity (K) (i.e. the ease with which water moves through the

soil). The saturated conductivity of water is greater in soils composed of larger pores because less energy is lost due to frictional resistance. Velocity of flow (V), or water flux, is equal to water potential gradient times the hydraulic conductivity (Foth, 1990) and is expressed by Darcy's Law:

$$V = KF \qquad (1.3)$$

Water flux equals the volume of water passing through a unit cross-sectional area of soil per unit of time ($m^3\ m^{-3}\ s^{-1}$). However, average pore water velocity is faster than the water flux velocity because only a fraction of the total area is conducting water: as the other part is occupied by soil particles.

Hydraulic conductivity is the ability of a soil to transmit water and is dependent on water content, tortuosity of the pore system and size of water filled pores (Marshall and Holmes, 1979; Rowell, 1994). The size of pores through which water moves is related to the water content of the soil. Under saturated conditions, when all pores are assumed to be filled with water, there is rapid flow through the larger pores while in smaller pores water movement is slow to nonexistent (stagnant). As the soil water drains, water moves through decreasing pore sizes because larger pores empty first. Hydraulic conductivity (K) therefore decreases with decreasing soil water content, as conductivity is dependent on pore size to the fourth power of pore radius, according to Poiseuille's flow equation (Section 8.2., Equation 8.1). The more tortuous the route water has to travel through the further it has to travel compared with the actual increase in depth in the profile. Tortuosity increases as water content decreases and therefore conductivity also decreases. Several of these aspects of soil structure, conductivity and water movement are discussed at length in Chapters 5, 6 and

8.

The theory of soil water transport was developed from classical laws of physics that applied to heat and electrical transport. The following section discusses the background to water movement in the soil and Darcy's Law.

1.9.1. Darcy's Law and Richards' Equation.

In 1856 Darcy demonstrated that the rate of flow of water through a column of saturated sand was proportional to the velocity of flow, potential difference between the ends, cross-sectional area and time, and inversely proportional to the length of the column (Darcy, 1856):

$$Q = K \times F \times A \times t \qquad (1.4)$$

Where, Q is the volume of water, K is the hydraulic conductivity, F is the water potential gradient, A is the cross-sectional area and t the time of flow.

Darcy's equation concerns itself only with the velocity of water entering and leaving the column. Therefore, little is actually known about the velocity of the water once it enters the labyrinth of pore space of the sand. However, for the water to equal the same volume per second of water entering and leaving the column the water in the soil, on average, must be travelling in excess of this velocity. The effective velocity or velocity of flow is the hypothetical velocity at which water would flow through a given cross-section, unobstructed by solid particles, in a direction opposite to that which the potential is increasing. Velocity of flow in a porous material is different at different points, being lower where the cross-

section of flow is of greater area. Potential difference also varies at different parts of a porous body. Darcy's law can only therefore be stated under these circumstances for each sub-element of the total volume, treating the sub-element as a column of soil.

Darcy's law has three statements to it:

1. Rate of flow is proportional to the potential difference between the two points provided that the flow is laminar and not turbulent.

2. Darcy assumes that the body is sufficiently large, in comparison with the size of its pores, for it to be regarded as a uniform body, capable of division into identical subsamples (RESs). This important concept was discussed in Section 1.6.1.

3. For vertical flow in soil, rate of flow is independent of path length. For horizontal flow soil water movement is proportional to the length of the column.

Darcy's law has several limitations: firstly the rate of flow is averaged over a large soil volume (REV) as discussed above. Therefore, Darcy's law holds for observations made at a macroscopic scale but the analysis of tracer movement at the microscopic scale is not adequately explained (Beven and Germann, 1981). Secondly the equation cannot be solved directly where unsaturated conditions exist. Water velocity is not even throughout a heterogeneous soil (Andreini and Steenhuis, 1990). Although Darcy's Law can be used to explain flow in a homogenous soil, it does not explain flow well when there is rapid flow through one part of the soil and a more sluggish flow elsewhere. In particular Darcy's law can not adequately explain infiltration and redistribution of water where the soil contains macropores and micropores. Darcy's law may be used to explain matrix flow but a separate concept is needed to explain the macropore flow.

Equation 1.4, cannot be used to solve transient conditions found in unsaturated soils because hydraulic conductivity is a function of soil water content. As explained previously, hydraulic conductivity is a function of pore size, it is also a function of water content which depends on flux, because of this Equation 1.4 has two unknowns in it for unsaturated conditions and therefore cannot be solved.

Richards' (1931) equation combines Darcy's Law with the equation of continuity (principle of conservation of mass) to solve the soil water equation for transient vertical flow under steady state conditions. Steady state conditions apply when inputs equal outputs from a known volume of soil. Assuming no sources or sinks Richards' equation states (Miyazaki, 1993):

$$\frac{\delta\theta}{\delta t} = \frac{\delta}{\delta x}\left[K\frac{\delta\psi_m}{\delta x}\right] \qquad (1.5)$$

Where, θ equals volumetric water content ($m^3\ m^{-3}$); ψ_m is matric head (mm); K equals hydraulic conductivity (mm d^{-1}); t equals time (d); and x equals depth (mm).

Differential water capacity equals:

$$C(\theta) = \delta\theta / \delta\psi_m \qquad (1.6)$$

Therefore substituting Equation 1.6 into 1.5 Equation 1.5 can be rewritten as:

$$\frac{\delta \psi_m}{\delta t} = \frac{\delta}{\delta x}\left[K \frac{\delta \psi_m}{\delta x}\right] \qquad (1.7)$$

In which matric head is the only dependent variable, and K is dependent on water content (Wagenet, 1992).

Darcy's Law and the Richards' equation used to describe water flow have a number of limitations (Hutson and Wagenet, 1992):

1. Data needed to calculate the equations, especially hydraulic conductivity data, is not easily obtainable.

2. The equations are complex and therefore time-consuming to calculate

3. Richards' equation assumes the soil to be homogeneous horizontally with no vertical preferential flowpaths.

Matrix flow may be modeled using Richards' equation based on Darcy's Law (Richards, 1931). Although Darcy's Law has many limiting factors its basic concepts have been well proven in the past (Beven and Germann, 1981). The limitations of using Darcy's law to consider water movement through large pores are discussed in the next section.

1.10. MACROPORE, MESOPORE AND MICROPORE FLOW.

Porosity or pore size distribution of a soil refers to the amount and distribution of space through which water and air can migrate and is primarily determined by soil structure. A pore is the space left between aggregates, of irregular shape, on packing (Marshall and Holmes, 1979). The three-dimensional lattice structure that results from the packing of aggregates is built up of particles of various shapes and sizes, determined by parent material. How closely these particles are packed together is dependent on size, shape and stability of the aggregate. Through this lattice structure biological channels and mechanically formed cracks also penetrate and function as hydraulic pathways. Towner (1989) suggested that soil was

> "...a very complex medium, consisting of mineral and organic particles of irregular and varied shapes, arranged in intricate undefinable geometric patterns, generating a network of pores of varying dimensions in which soil water can reside or through which it can flow."

As stated above pore size can directly influence the rate of flow of water through the soil, and as examined later influence the speed, mixing and diffusion rate of solutes transported through the soil. An understanding of the distribution and function of different sized pores is therefore of importance to this investigation. Although, pore sizes, in a heterogeneous soil, may vary continuously for convenience of classification they are divided into group classifications according to size. Many researchers simplify changing pore sizes by defining a soil as a dual porous system (Beven and Germann, 1982; Chen *et al.*, 1993). A dual porous system divides pores into two categories, macropores (mobile zones) and micropores (immobile zones) (Germann and Beven, 1981a; Beven and Germann, 1982; Van Genuchten and Dalton, 1986), although other researchers have gone further and suggested a three domain split into macropores, mesopores and micropores (Jongerius, 1957; Luxmoore, 1981). In reality these boundaries are arbitrary. Work by Germann and Beven (1981) also

suggested the presence of a secondary soil matrix, where water was held at high capillary potentials, possibly macropores loosely filled with eroded material. They believed this matrix allowed preferential movement of water but with a lower hydraulic conductivity than macropores. There is no agreed standard definition of scale at which a pore ceases to be a micropore and becomes a macropore. Definitions that have been used to determine the point at which micropores become macropores include; the measurement of the volume of pores drained at field capacity (Luxmoore, 1981), and pore radius corresponding to a capillary potential (ψ) of ψ equal to -1.0 (Germann and Beven, 1981a). Luxmoore *et al.* (1990) provide a more detailed list of different delineations for determining macropores, mesopores and micropores. The most common method used to define pore size is with reference to soil water retention curves, where a measure of effective pore size is related to capillary potential through the Laplace equation for capillary pressure (Beven and Germann, 1982; Harvey, 1993). Harvey's (1993) two domain criterion of pore sizes were defined as:

- macropores: = > 70 μm (diameter)
- micropores: = < 70 μm (diameter)

For a three domain split Luxmoore (1981) used capillary tension to define pore size as:

- macropores: pores subject to a capillary tension of $\psi < 0.3$ kPa (≡ > 1000 μm or 1 mm diameter)
- mesopores: pores subject to a capillary tension of $0.3 < \psi < 30$ kPa (≡ 10 - 1000 μm or 0.1 - 1 mm diameter)
- micropores: pores subject to capillary tension of $\psi > 30$ kPa (for clayey soils) (≡ < 10 μm or 0.1 mm diameter)

The definitions of macro-, meso- and micro- pores made by Luxmoore (1981) will be used in this thesis.

Researchers such as Skopp (1981) have argued that the actual classification of pore size is unimportant, rather the function of different pores in the soil is more important. Skopp (1981) used the functions described in Table 1.7 to define soil porosity terms.

Table 1.7 - A functional classification of pores (Skopp, 1981).

Macroporosity - designates the pore space which provide preferential paths of flow so that mixing and transfer between pores is limited.
Matrix porosity - designates the pore space which transmits water and solutes at a rate slow enough to result in extensive mixing and relative rapid transfer of molecules between different pores.

The relationship between pore size and water retention was discussed in Section 1.8. (Table 1.6). Macropores and mesopores hold water at low tensions within the soil and allow the rapid transmission of water through the soil profile under suitable conditions. Micropores hold water at higher tensions in the soil matrix and therefore only transmit water slowly through the profile.

The rate of flow of water through a larger pore depends on the saturation state of the channel morphology, surrounding matrix and entrapped air. From Poiseuille's flow Equation (8.1) it is known that the size of a pore directly affects the rate of flow (flow rate is controlled by the smallest pore neck in any continuous channel). Water movement through the soil matrix or micropores is very slow compared to potential flow through a macropore. Because of the difference in flow rate between macropores and micropores, water within the soil matrix is sometimes regarded as being stagnant. Although macropores may only

account for a small proportion of a soil's total porosity their contribution to hydraulic conductivity may be considerable (Beven and Germann, 1982). Peterson and Dixon (1971) (reviewed by Beven and Germann, 1982)

> "Reported that the opening of a single macropore increased the infiltration capacity of a particular 1.35 m^2 plot from 1.7 to 2.8 $10^{-5} m\ s^{-1}$, for an increased pore space of 0.002%."

Work by Brűlhart (1969), Aubertin (1971), Germann (1976), Anderson and Bouma (1977), Schuh and Cline (1990), Harvey (1993) and Setiawan and Nakano (1993), all observed a rapid reduction in hydraulic conductivity from a fully saturated soil where water was moving through both macropores and soil matrix, to an unsaturated soil where water only moved through the soil matrix. Entrapped air within the soil can reduce infiltration rates by a factor of three (Linden and Dixon, 1973). However, macropores may also provide an important pathway for escaping air.

Rapid movement of water and solute around aggregates in the soil has been associated with the occurrence of fast flowing routeways which circumvent areas of slower or stagnant flow (Germann and Beven, 1981a; White, 1985; Radulovich, 1992). The more rapid flow has been referred to as preferential flow (Steenhuis, 1990; Singh and Kanwar, 1991), bypass flow (Singh and Kanwar, 1991; Radulovich, 1992), Short circuiting (Beven and Germann, 1982; Singh and Kanwar, 1991), macropore flow (Germann and Beven, 1981a; Watson and Luxmoore, 1986) and mobile/immobile flow (Smedt and Wierenga, 1979). There is still no agreed definition and classification of preferential flow paths (Miyazaki, 1993). However, three classifications of preferential flow were advocated by Kung (1990):

1. Bypass flow.
2. Fingering flow.

3. Funnelled flow.

The definitions of these three classifications of flow are given in Table 1.8.

Table 1.8 - Definition of three classifications of preferential flow (Kung, 1990).

Bypass flow also referred to as short circuiting.	Flow that occurs through macropores and cracks through the soil. Flow occurring in these channels when irrigation exceeds infiltration into finer pores (Beven and Germann, 1982).
Fingering flow.	Flow that occurs in coarse layers overlain by finer soils due to an instability in the wetting front (Glass *et al.*, 1989; Selker, 1992a and b).
Funnelled flow.	Concentration of flow into a column of saturated flow due to lateral flow on top of a coarse sand layer or densely packed fine layer, which act as funnel walls (Kung, 1990b).

Bypass flow is the vertical movement of free water along non-capillary pores including both macropores and mesopores (Stiphout *et al.*, 1987; Radulovich *et al.*, 1992). For a number of years it was widely believed that bypass flow would only occur if the soil was fully saturated (Bouma, 1981; Seyfried and Rao, 1987). However, there is growing evidence to support the theory that bypass flow may not require full saturation of the soil (Stiphout *et al.*, 1987; Luxmoore *et al.*, 1990; Radulovich *et al.*, 1992). Work by Phillips *et al.* (1989) showed water to enter simulated macropores in unsaturated conditions. Additional work by Russell and Ewel (1985) and Radulovich and Sollins (1987) using zero-tension lysimeters and by Sollins and Radulovich (1988) using studies of dye penetration showed water to move along preferential paths without surface ponding, in a microaggregated soil. Radulovich *et al.* (1992) suggest that water will flow in all non-capillary pores (i.e. macropores), regardless of size, once hydraulic conductivity of the microaggregates is exceeded, although rate of flow is limited by pore size. Other field and laboratory evidence supports the assertion that bypass flow in unsaturated conditions is of vital significance: for

example Parlange *et al.* (1988) found measured rates of water and solute transport through macropores in unsaturated soils to be comparable to transport rates under saturated conditions. Germann and Beven (1981a) and Jardine *et al.* (1990) both observed that water may be transmitted to depth in a soil profile via macropores and/or preferential flow even when the soil matrix, through which it passed, was unsaturated, providing the supply to the macropore exceeded lateral flow into the matrix. Macropores may conduct a considerable quantity of water without being saturated as 'rivulets' along the walls of the pores (Beven and Germann, 1982). Water may bypass the majority of the soil to a lower horizon in the soil profile. Where the pore terminates, the water will be absorbed into the surrounding soil and may result in an irregular water content with depth. The point at which the pore terminates can be referred to as an 'internal catchment' (Stiphout *et al.*, 1987).

The route through which water enters and moves through the soil is determined by the intensity and duration of precipitation and the infiltration capacity of the soil matrix. Infiltration capacity is determined by the hydraulic conductivity of the soil. Infiltration at the soil surface can be divided into three stages (Beven and Germann, 1982). Stage 1: precipitation is less than infiltration rate, water arriving at the soil surface is absorbed into the soil matrix (micropores). Stage 2: precipitation exceeds infiltration rate into the soil matrix but is less than the combined infiltration into the matrix plus seepage into macropores. Water is taken up simultaneously by macropores and micropores. Lateral flow from the macropore walls into the soil matrix also occurs reducing macropore flow and penetration. As the soil matrix becomes more saturated less lateral flow will take place from the macropores and hence macropore flow will penetrate deeper into the profile. An initially moist soil may allow deeper penetration of water due to a reduction in lateral loss (Quisenberry and Phillips, 1976 cited in Beven and Germann, 1982). Stage 3: precipitation exceeds infiltration and seepage into macropores and micropores. Water begins to pond on

the soil surface and overland flow starts. A rainfall intensity of 1 - 10 cm hr^{-1} may be sufficient to initiate macropore flow (Topp and Davis, 1981; Beven and Germann, 1982).

Trying to quantify macropore flow in a soil is extremely difficult because of the irregular morphology and tortuosity of channels through the soil. Not all large pores are macropores in the sense that not all large pores have a structure that permits non-equilibrium channelling flow. Macroporosity was measured in this experiment by three techniques profile tracing method, binary transect method and resinated core section method (Chapter 5). Although impregnation and thin section give no indication of channel connectivity. The connectivity of macropores through a soil may be inferred using suction methods which effectively only measure pore pathways that are connected to the suction interface. The different methods and their results are discussed in more detail in Chapters 2 and 5.

1.11. TRACER MOVEMENT AND CHANGE IN SOLUTE CONCENTRATION THROUGH TIME.

The objective of this research was to investigate the movement of water and solute. The preceding sections have discussed the ability and potential for water to flow through the soil. The following sections examine: the movement of solute in comparison to water flow; the importance of change in solute concentration through time to the interpretation of active pathways through the soil, including the use of breakthrough curves and mathematical models; and a brief review of how the aforementioned movement and interpretation can be used in conjunction with 'tracers' to perform experiments to examine both the movement and interaction of solutes within the soil.

1.11.1. Pathways.

Soil profile drainage consists of two distinctly different modes of flow: highly mobile

regions of water and solute transport which bypass the majority of the soil profile (Bouma, 1981; Beven and Germann, 1982), and zones of slower matrix flow (Smedt and Wierenga, 1979). The longer the residence time of the solute in the soil the greater the potential that diffusion and advection processes will occur between mobile and immobile regions (Kluitenberg and Horton, 1990). The rapid pathways as a result have minimal contact time with soil aggregates reducing the potential chemical reactions and mixing of new water with old (resident) soil water (Beven and Germann, 1982; Luxmoore *et al.*, 1990). Solutes will be retained in micropores for a longer period of time than in larger pores (Beven and Germann, 1982; Jardine *et al.*, 1990). The difference in tensions of different pore sizes cause the solute concentration to vary among pore classes because of various physical and chemical processes (Litaor, 1988). The presence of macropores provide pathways for surface applied chemicals to move rapidly through a soil profile. Preferential or bypass flow may be the most important controlling factor of peak concentration of leaching from a soil. A need therefore exists to investigate the relative importance of bypass flow compared with matrix and/or preferential routes. The distinctions between these different types of flow were discussed above. It is important to note that the measurements required to investigate these flow mechanisms require extremely detailed measurements of soil water movement and hence the soil profile must be monitored in great detail.

1.11.2. Mechanisms.

The movement of solute through a soil and retention within is not only governed by the forces acting on the water, as described above, but also comes under the influence of advective (in both liquid and gaseous form) and diffusive (in both liquid and gaseous form) processes (Hutson and Wagenet, 1992). Advection is a process by which solutes are transported by the mass flow of soil water (Freeze and Cherry, 1979). However, due to the non-uniformity of flow within the soil the movement of solute tends to deviate from the

suggested pathway described by mass flow. The 'spreading out' of the solute along the advective path, due to the movement of fluid, is referred to as hydrodynamic dispersion. Hydrodynamic dispersion is both a function of mechanical mixing during fluid movement and molecular diffusion. In this thesis both mechanical dispersion and molecular diffusion will be considered (Chapters 7 and 8).

Mechanical dispersion results in a change in concentration of a solute by the mixing of solutes of different concentration along the interface between the two solutions. The mechanism by which dispersion achieves mixing differs from diffusion in that it is the result of non-uniformity of soil water flow velocity. The rate of dispersion is expressed as:

$$Q_d = -D_h \, \delta\theta / \delta x \qquad (1.8)$$

Where, Q_d is dispersive flux per unit cross-sectional area of the soil, D_h is the dispersion coefficient, $\delta\theta C/\delta x$ is concentration gradient influenced by volumetric wetness Θ.

Diffusion occurs between two solutes of different concentrations. Diffusion of a solute occurs as the result of Brownian Motion in a direction from a stronger to a weaker concentration (Greenland and Hayes, 1981). The rate of diffusion is directly dependent on the difference in concentration between the two solutes, and the temperature and velocity of the molecules (as temperature increases velocity increases and diffusion occurs faster). Diffusion is, however, inversely related to the distance between the two solutes. Rate of diffusion can be described by Fick's first law:

$$Q_s = -D_o \, \delta C / \delta x \qquad (1.9)$$

Where, Q_s is the quantity of diffusing substance transferred in unit time across unit area (mass flux), D_o is the diffusion coefficient, $\delta C/\delta x$ is the concentration gradient.

Diffusion mainly occurs near plant roots as a result of nutrient uptake by the plant, but it can also occur at the front of a solute layer moving through the soil or in regions of slow solute flow.

Dispersion and diffusion are difficult to distinguish although dispersion tends to be the more dominant process and always occurs as a solute moves down through a profile. Dispersion of a liquid is known as hydrodynamic dispersion. There are four main causes of hydrodynamic dispersion in a soil (Greenland and Hayes, 1981):

1. Frictional resistance on water molecules adjacent to soil particle reduces the speed of flow of these molecules while water molecules closer to the centre of the pore experience less frictional resistance and therefore have a faster rate of flow, resulting in a non-uniform flow of water molecules across the pore channel.
2. Difference in velocity: flow through larger pores is quicker than flow through smaller pores because of the first statement.
3. Tortuosity: the water has to move around particles in the soil, not every pathway will be of the same length, surface area or roughness, therefore different rates of flow per unit length of soil exist in a profile.
4. Density difference of solution. Denser solution fingering down in an uneven front.

As pore water velocity increases (>1 cm h^{-1}) hydrodynamic dispersion becomes increasingly

the more dominant form of dispersion. At pore water velocities below 0.1 cm h^{-1} diffusion becomes more significant (Hu and Brusseau, 1994).

An uneven distribution of solute movement though a soil, as observed by Brusseau and Rao (1990), Kluitenberg and Horton (1990) and Singh and Kanwar (1991), can be related to specific pathways travelled by the solute:

1. Mixing or dispersion is always observed. Dispersion causes the solute layer to become less concentrated. The amount of mixing increases as pathways become more tortuous.
2. Anion exclusion where repulsion near negatively charged surfaces results in an effective reduction in pore volume for anions and therefore anions travel faster than predicted flow rate for the pore volume.
3. Not all pores conduct because they are not open at both ends therefore effective pore volume is less than measured. Some solute will move into the soil matrix or into slower pathways (mesopores) resulting in a delay of output of this solution. This delayed flow of solute effects the shape of the solute output curve (breakthrough curve) discussed in Section 1.13.
4. Preferential flow paths permit the rapid movement of solution to depth while matric flow occurs at a slower rate. Faster movement reduces the potential for diffusion, more direct pathways tend to be less tortuous and therefore result in a quick initial observation of solute in output followed by a rapid rise in concentration. The shape and interpretation of breakthrough curves will be discussed later.

These aforementioned characteristics can be used to infer the pathways travelled by solute from a measurement of solute concentration through time. This is considered in the following section as it is of fundamental importance to this investigation in answering aim

2 (Section 1.4.).

1.12. CHANGE IN SOLUTE CONCENTRATION THROUGH TIME.

Mass Flow:

The pathway and speed at which the solute travels will affect the physical and chemical processes that the solute is exposed to. Solutes moving through larger than average pores may enter the soil matrix either by diffusion or advection (adsorption of solute into the soil matrix). The speed at which the solute moves through the soil directly affects the amount of diffusion and advection. Observations, made by Kluitenberg and Horton (1990), of rapid transport of solute through the soil showed that minimum contact time for diffusion and advection resulted in effluent leaving the system undiluted as a result of which a quick, peaked, response was recorded. Soils with smaller average pore sizes were shown to allow more contact time with the soil matrix and to increase the amount of spreading of the solute and suppress the peak response concentration.

Diffusion:

Assuming that larger average pore sizes conduct much of the flow, solutes may move from large to small pore regions by advective transport, resulting in a concentration gradient between the bulk solution and solution held in smaller pores (Jardine *et al.*, 1990). Diffusion may then occur between the bulk solution and the smaller pores to adjust equilibrium concentrations. The movement of solute from large to small pore regions may at best result in a concentration in the micropores that is equal to the concentration of the solution in the macropores. Experimental results have shown high concentration peaks, delayed in appearance compared to predicted macropore pathways, which can only be attributed to vertically mobile solute from small pores (Jardine *et al.*, 1990). Once concentrations in small pores exceeds that of large pores, convection and diffusion may

occur from small to large pores. Smaller pores retain solute longer and therefore become a source of solute transport in large pores by convection and diffusion during later rain events.

Pathway-Supply Hypothesis:

One way to consider the relative importance of the different pathways is the 'pathway-supply hypothesis' (Luxmoore *et al.*, 1990). Path length increases with continuing rainfall and decreases when rainfall ceases, the water travelling along the longer paths has more time to interact with soil particles. At peak flow water moving along the longest path lengths mix with and contribute to the outflow along the shorter paths.

1.13. BREAKTHROUGH CURVES.

The rate of movement and loss, from and to, different pathways as a process of hydrodynamic dispersion and diffusion can be inferred from the shape of a 'breakthrough curves'. A breakthrough curve is a plot of relative concentration against relative pore volume (defined in Section 7.7.), and shows the variation of solution concentration with time and the volume of water required to displace a tracer through a column of soil. The shape of a breakthrough curve is influenced by:

1. How the tracer is initially applied, as a pulse or spike or as a miscible displacement (Kluitenberg and Horton, 1990).
2. The pathways the solute moves through, for example immobile and mobile, micropore or preferential (Walker and Trudgill, 1983; Brusseau and Rao, 1990).

The shape of the breakthrough curve can therefore be used as a means to interpret pathways and mechanisms at work in the soil (Kluitenberg and Horton, 1990; Singh and Kanwar, 1991; Radulovich *et al.*, 1992). A steep initial rise within one pore volume indicates the presence of a faster velocity pathway than calculated by Darcy's law of the volume passing

through unit cross-sectional area alone. A rapid breakthrough is due to effective pore volume being less than water filled pore space which results in a higher mean pore water velocity. Anion exclusion may also result in some tracers being transported faster than the bulk water flow. Laboratory measurements of breakthrough curves made by Singh and Kanwar (1991) have shown that a few large pores occupying a small proportion of the total volume can influence the shape of a breakthrough curve, resulting in a quick initial breakthrough and steep rise to peak concentration. While a sustained reduction from peak indicates the presence of slower moving solute pathways. The peak concentration of a spike of tracer gives an indication of the amount of dispersion and diffusion. As dispersion and diffusion processes increase, the shape of the breakthrough curve becomes more negatively skewed, and will result in peak irrigation concentration not being reached in a pulse experiment or being delayed in a miscible displacement experiment (Reeves and Beven, 1990). Dual peaks have been linked to transport of solutes in at least two pore size classes (Hornberger *et al.*, 1991). Work by Hornberger *et al.* (1991) has suggested that the expected pattern for a pulse input to a dispersive system would be a breakthrough curve with a rapid rise to a peak concentration followed by a gradual decline back down (an extended tail). The resulting positive skewness in the breakthrough curve with the extended tail is indicative of a dual porosity soil with preferential flowpaths where incomplete mixing occurs (Walker and Trudgill, 1983; Kluitenberg and Horton, 1990; Singh and Kanwar, 1991; Hornberger *et al.*, 1991). The shape therefore of the breakthrough curve is determined by the distribution of different velocities through the soil, referred to as 'hold-back' by Danckwerts (1953). The resulting shapes of the curve expected under different flow conditions are illustrated in Figure 1.3 (a-d) for miscible (frontal) displacement of solutes, and in Figure 1.4 (a-d) for a pulse (injection) input (where the x-axis represents volume of water and the y-axis concentration). The piston type flow illustrates the result

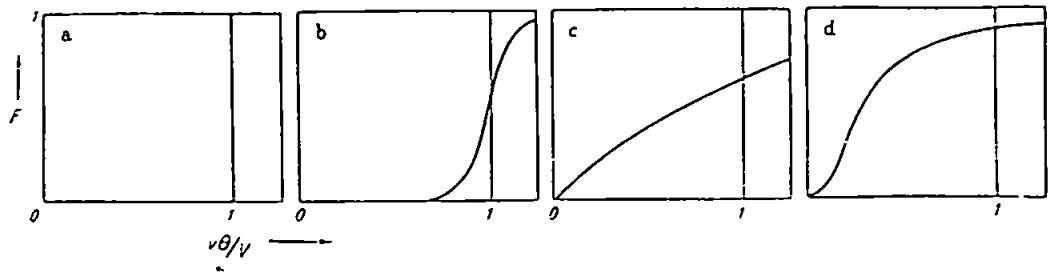

(*a*) Piston flow; (*b*) Piston flow with some longitudinal mixing; (*c*) Complete mixing; (*d*) Dead water.

Figure 1.3 - Shape of curve resulting from different flow conditions through a soil after miscible displacement of solute (Danckwerts, 1953).

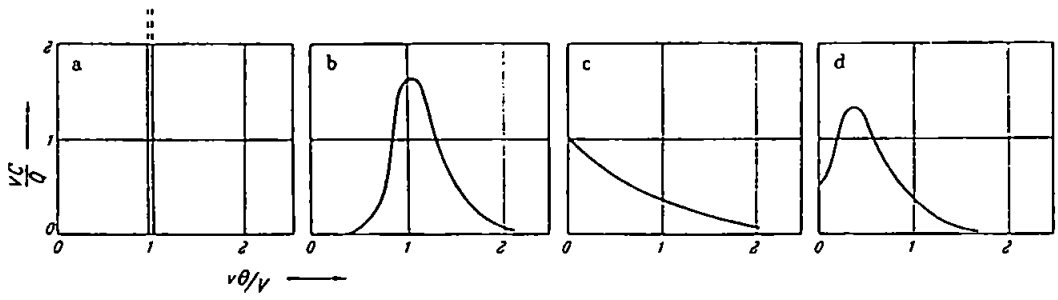

(*a*) Piston flow (*b*) Piston flow with some longitudinal mixing (*c*) Complete mixing (*d*) Dead water.

Figure 1.4 - Shape of curve resulting from different flow conditions through a soil after a pulse injection of solute (Danckwerts, 1953).

obtained if the solute moves through the soil in accordance to Darcian theory (Figures 1.3 and 1.4 (a)) where velocity is equal across the unit area. Piston type flow will never occur as diffusion will always take place and therefore the curve will exhibit characteristics of either longitudinal mixing (Figure 1.3 and 1.4 (b)), complete mixing (Figure 1.3 and 1.4 (c)) or dead water (Figure 1.3 and 1.4 (d)). If there is 'dead water' in the system it means that the majority of flow is occurring through restricted channels while a high proportion of the solute is trapped in eddies or by 'dead-end' channels and thus spends more than the average estimated length of time in the soil.

Examples of the use of breakthrough curve analysis in experimental observations of flowpath are given later under tracer experiments (Table 1.9). The following section looks at the mathematical simulation or modelling of observed data and its use in predicting field scale events from small laboratory column samples.

1.14. MATHEMATICAL MODELS.

The use of mathematical modelling to predict complex spatial and temporal changes in solute movement through the soil is today widely accepted. In soil science there are three types of model deterministic, stochastic and mechanistic. The complexity of soil property variability makes field scale observations limited in terms of spatial and temporal resolution. Detailed observations are therefore conducted at a finer resolution on representative soil volumes (Saleh *et al.*, 1990). The small scale column is regarded as a model which simulates field conditions as closely as possible (Saleh *et al.*, 1990). An understanding of soil transport processes has developed from experimental investigations conducted on simple uniform porous materials (Youngs and Leeds-Harrison, 1990). Models are based on the observation of the movement of non-sorptive chemicals such as chloride through a soil column. The movement of such a non-sorptive chemical through a porous

media such as soil is generally assumed to occur by advection and dispersion (Bear, 1972; Leij and Dane, 1989). These experiments have led to the development of dispersion equations. Sometimes referred to as the convection-dispersion equation (model)

but more accurately named advection-dispersion equation (model), one dimensional steady-state fluid flow is described as:

$$R \frac{\delta C}{\delta t} = D \frac{\delta^2 C}{\delta x^2} - v \frac{\delta C}{\delta x} \qquad (1.10)$$

Where, C is solute concentration (ML^{-3}), x is distance from where solute is introduced (L), t is time (T), D is hydrodynamic dispersion coefficient (L^2T^{-1}), υ is average pore-water velocity (LT^{-1}), and R is retardation factor (dimensionless) (Singh and Kanwar, 1991).

Advection refers to the mass flow of solute, while dispersion can be subdivided into longitudinal dispersion (dispersion due to flow rate) and transverse dispersion (dispersion due to diffusion), as discussed earlier. The main assumption and limitation of advection-dispersion flow is that the porous material through which flow occurs is homogeneous and velocity of flow is even throughout. The model adequately describes macroscopic flow through a uniform soil. However, as flow becomes more complex due to an increasing heterogeneity of soil physical properties, the model is less able to explain divisions of flow into mobile and less mobile regions (Singh and Kanwar, 1991). Despite this advection-dispersion models have been used to predict flow (Kluitenberg and Horton, 1990; Singh and Kanwar, 1991). The advection-dispersion equation was used to predict dispersion in this experiment (Chapter 7). The predicted values made by the model compared to actual

observations are compared and criticised in Chapters 7 and 8. Conclusions will be drawn as to its suitability in describing the observed flowpaths.

The following section looks at the application of chemical tracer experiments to the interpretation of solute movement through the soil.

1.15. TRACERS.

Davis *et al.* (1980) defined a hydrological tracer as:

> "matter or energy carried by water which will give information concerning the direction and/or velocity of the water as well as potential contaminants which would be transported by the water"

To understand the fate of added fertilizers, pesticides and chemical contaminants to a soil, a better understanding and interpretation of the processes and mechanisms at work on them in the soil is needed. The fate of solutes moving through a soil can be determined by observing a known chemical input or tracer as it moves down through a profile through time.

The interaction between water moving down macropores and the water residing within the matrix has been studied using tracers (Dowd *et al.*, 1991). The heterogenous mix of pore sizes throughout a soil may result in the incomplete mixing of soil water between macropores and micropores. Work by Biggar and Nielsen (1976), Jardine *et al.* (1990) and Harvey (1993) has shown that although the majority of water, labelled by a tracer, is rapidly transported through a soil, a significant proportion of the water lags behind. The generally accepted explanation for this being a non-uniformed mix between the faster moving water of the macropores and stagnate or slow moving water of the surrounding soil

matrix. The proportion of old water versus new water contributing to subsurface flow and the speed at which new water acquires old water characteristics are still not fully understood (Luxmoore *et al.*, 1990).

The change in concentration through time can be used to infer which pathways are active in the soil and the amount of dispersion and diffusion that has occurred on route, through the interpretation of breakthrough curves and mathematical models (Section 1.13. and 1.14.). The scale at which the experiment is conducted determines the detail of information about water movement that can be defined.

At a large scale, for example in a field, tracer observation is mainly limited to mass input and output budget calculations because of the heterogeneous nature of soil. A lot of tracer work has therefore been carried out at a smaller scale using columns of soil or large blocks. Although this scale also has limitations as previously discussed it provides a useful working scale to observe the movement and dilution of tracers such as chloride, nitrate, bromide, ^{18}O -labelled water and dyes.

Reeves and Beven (1990) suggested that tracers should fulfil a number of requirements:

1. A tracer should not be able to be filtered or sorbed by the medium through which it passes.
2. Its concentration should exceed any residual concentration level present in the pre-existing soil water.
3. It should be conservative in nature in that it will not be broken-down either chemically or biologically (unless there is a need for such a specific characteristic).
4. A tracer should have a low toxicity.
5. It should be inexpensive.

6. It should be easily detectable. Dilution and dispersion may reduce tracer concentration below detectable levels.

7. It should not have any hydrological influence. Differences in densities between the tracer and the soil water can lead to an alteration of flow characteristic. Ion exchange and chemical precipitation can alter permeability.

Chloride (Cl^-), bromide (Br^-), iodide (I^-) and nitrate (NO_3^{-1}) are all anionic tracers. Anion tracers are widely used in soil water experiments because their potential adsorption or ion-exchange is minimal (Davis *et al.*, 1980). Nitrate is regarded as a non-conservative tracer because of its vulnerability to transformation by chemical and biological reactions under both aerobic and anaerobic conditions (Section 1.3.). Immobilization of nitrate by plants and denitrification under anaerobic conditions both reduce the proportion of nitrate in soluble form and therefore need to be taken into account when considering change in concentration of leachate through time. Chloride is a conservative tracer in that it is not readily broken-down in the soil or adsorbed by soil particles. The use of dyes is also widely used as they can provide useful information about actual active pathways. Dyes have some limitations, molecular size may increase the viscosity of the solution and so alter active pathways and dyes are also usually charged, by definition they 'stick to things'. For the experiment in this thesis potassium chloride was the primary tracer used in all 5 experiments, although potassium nitrate was also used but only in runs 4 and 5 (Section 7.5.1. and 7.5.2.).

The way in which a tracer is applied will directly influence how it moves through the soil. Solutes introduced into relatively immobile soil water will be displaced differently by solute-free water than a solute introduced into relatively mobile soil water (Kluitenberg and Horton, 1990). Work by Kluitenberg and Horton (1990) has highlighted the importance of

precise clarification of how solute tracers are applied to a soil, with macropores, as the method used has been observed to directly affect the pathway through which solutes move through the soil. Tracer experiments can be divided into two categories depending on how the tracer is applied:

1. Miscible displacement experiments.
2. Pulse experiments.

In a miscible displacement experiment tracer labelled solution is continually applied over an extended period of time until collected solute samples have obtained an equivalent concentration to the irrigated solution. The observed change in concentration through time and the shape of the resultant curve produced can be used to infer speed of movement of tracer pathway, mixing and losses, from the analysis of breakthrough curves (White, 1985). In a pulse experiment a tracer is added to the top of the soil in solution or as a powder and is subsequently flushed through with water which contains smaller concentration levels of the applied tracer. Pulse experiments simulate field type application of fertilizer followed by a rainfall event. Table 1.9 lists some examples of laboratory soil column tracer experiments used to identify flowpaths.

1.16. SUMMARY.

This initial chapter has outlined the most important properties of soil that control water and solute movement, as well as physical processes that influence the direction of travel and mixing between different pathways through the soil. A consideration of relevant research has been presented and the experimental design used in this investigation has been briefly outlined. In the succeeding chapters techniques and ideas will be built upon to examine how successful as well as how appropriate the chosen scale and design of the experiment were in achieving the aims of the investigation (Section 1.4).

Table 1.9 - Examples of laboratory column tracer experiments.

Author(s)	Aim	Conclusions
Tyler and Thomas, 1981	Potassium chloride applied as a pulse through an undisturbed soil column (15 cm diam. by 30 cm length) - To determine when rapid flow through larger pores is likely to be important.	Results of breakthrough curves suggested channelling of water through well-defined soil structure.
Andreini and Steenhuis, 1990	Bromide and dye tracers applied as a pulse through an undisturbed soil column (35 cm by 35 cm by 34-46 cm) - To investigate preferential solute movement through conservative and conventional tillage soil profiles.	Showed preferential flow to be highly spatially variable from the interpretation of breakthrough curves.
Kluitenberg and Horton, 1990	Calcium chloride and calcium sulphate applied as a miscible displacement and pulse experiment through undisturbed soil columns (18 cm diam. by 33-35 cm length) - To assess the effect of solute application method on resultant preferential transport of solutes in soil.	Method of application and initial soil conditions effected the movement of solute through the soil as interpreted using breakthrough curves.
Booltink and Bouma, 1991	Methylene blue dye through undisturbed soil columns (20 cm diam. by 20 cm length) - to study flow processes including vertical and lateral infiltration and internal catchments, during bypass flow.	Shows water movement to be more complex than mobile/immobile concept suggests.
Singh and Kanwar, 1991	Chloride applied as a miscible displacement experiment through 6 soil columns (15 cm diam. by 61 cm length) - To examine preferential solute transport through macropores, using breakthrough curve analysis.	The shape of the breakthrough curves clearly showed preferential flow along macropore pathways to be active. Convection-dispersion equation fitted observed breakthrough curve results well. As the range of pore water velocity increased the fit was less accurate.
Booltink *et al.*, 1993	Methylene blue dye through undisturbed soil columns (20 cm diam by 20 cm length) - To develop a method that could measure bypass flow, provide a morphological analysis of the water-conducting macropore system, and combine a physical and morphological data in a simulation model for prediction purposes.	A simple and effective method of rapidly assessing bypass flow was achieved.
Brusseau, 1993	Tritiated water and pentafluorobenzonate tracers through soil columns (2.5 cm diam. by 5-10 cm length) - To investigate the effect of solute size, pore water velocity and intraparticle porosity on dispersion.	Non-ideal transport is indicated by breakthrough curve of different tracers being dissimilar. Also diffusion was shown to be important at low pore water velocities.
Harvey, 1993	Potassium bromide through soil columns (10 cm diam. by 5 cm length) - To measure variation in soil solute tracer concentration across a range of pore sizes relating concentration to retention and conductance characteristics of soil.	A two-porosity characterisation of the soil was supported by the findings. Although concentration varied continually with pore size therefore only a broad classification.
Buchter *et al.*, 1995	Miscible displacement of chloride through an undisturbed soil column (30 cm diam. by 75 cm length) - To assess the effects of flow heterogeneity on solute transport.	Using breakthrough curve analysis consistency of results between successive experiments suggested flow paths remained constant through time, and may be an intrinsic property of a soil medium for a given water content.

In Chapter 2 an examination of the wider scale landuse as well as specific soil characteristics of the Hallsworth series is considered.

CHAPTER 2.

CHARACTERISATION OF SOIL AT LANDSCAPE AND DETAILED SCALE.

2.1. INTRODUCTION

The purpose of this investigation was to examine in detail the mechanisms involved in water and solute movement through a small soil block which represented a unit of soil in the wider landscape. This study of soil water pathways, at a detailed scale, forms part of a long established research effort at the Institute of Grassland and Environmental Research (IGER), North Wyke, Devon (Figure 2.1), to examine water movement and nitrate leaching. Previous research investigations considered water movement and solute transport

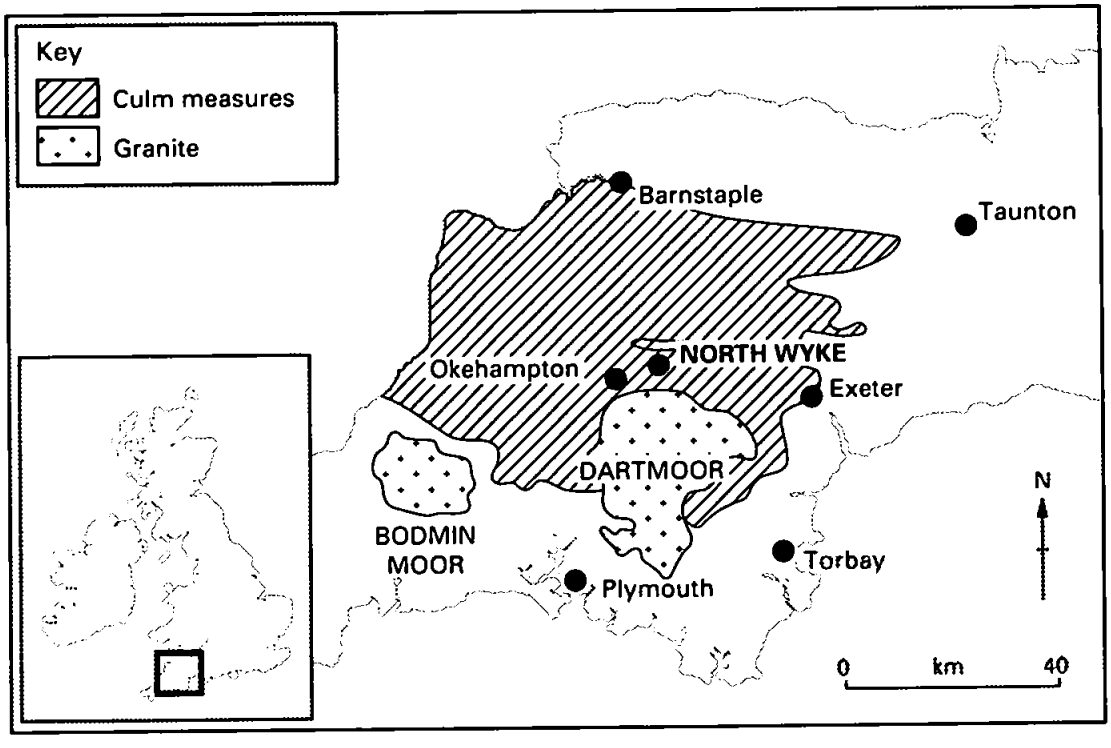

Figure 2.1 - Location of site - regional setting.

in ten one hectare drained and undrained, improved and unimproved grassland plots at Rowden Moor (Armstrong *et al.*, 1984, Hallard, 1988; Scholefield *et al.*, 1993; Addison, 1995). The grassland nitrate leaching experiment had been conducted on the IGER drainage plots since 1982 and therefore constitutes the longest running experiment of its kind. Hydrologically nitrate losses on the Rowden Moor site have been monitored at the field scale by Scholefield *et al.* (1995), Hallard (1988) has analysed outflow hydrographs from experimental plots and examined hydrological response characteristics, while Addison (1995) used small scale isolated plots within drained and undrained fields to monitor soil water status and to examine water movement, and small soil block lysimeters taken from the Rowden site have also been set up under laboratory conditions to study nitrate leaching (Scholefield, pers. comm.). For this present experiment large soil blocks, 0.85 m^3, were extracted from the Rowden field to conduct the detailed water and solute transport experiments. This chapter describes the site from which the blocks were excavated (the methodology will be detailed in Chapter 3), together with the soil's physical characteristics, as determined in the laboratory and the laboratory procedures used to characterise the soils in more detail.

2.2. SITE DESCRIPTION.

The soil blocks were collected from the Rowden Moor experimental site, IGER (Figure 2.1) located 10 km north east of Okehampton, mid-Devon. Before describing the soil characteristics within the blocks, the physical geography of the area, including geology, landuse and a generalized soil profile description will be will be given in order to set the characteristics of the soil block within a wider field and landscape context.

The particular site that the soil blocks were extracted from was chosen for the following reasons:

1. The field site had previously been subjected to detailed scientific investigations (Armstrong *et al.*, 1984; Hallard, 1988; Addison, 1995). There is a considerable body of literature on the soil variability, hydrological behaviour, nutrient cycling and soil macro and micro fauna.
2. The soil characteristics of this particular soil were conducive to undisturbed sampling, i.e. not particularly stony.
3. The soil type was sufficiently clay rich (clay or clay loam soil) to support a mole drain which was a fundamental part of the experiment (aim 1, Section 1.4.).
4. The site was accessible to the machinery necessary to lift and transport the soil blocks causing minimal disturbance.
5. Removal of such large scale blocks of soil from the chosen location did not interfere with any other experiments or landuse.
6. The soil was representative of the local soil.

2.2.1. Geology.

The underlying geology of North Wyke and Rowden Moor forms part of the 'Culm Measures' which underlies approximately 100,000 ha of land in South West Britain. The soil formation on the gentle, lower slopes of Rowden is dominated by hydrological conditions. The dark grey Carboniferous clay shale or 'shillet' of this formation readily break down to illitic (micaceaous) clay minerals, which have a small cation exchange capacity relative to clay content and negligible shrink-swell potential. The small cation exchange capacity of the soil therefore leaves the majority of soil solutes vulnerable to leaching. The intense release of clay from the Carboniferous shale in this location has produced coarsely structured and impermeable subsoils (Harrod, 1981), which combined with a high local rainfall has culminated in a surface water gley.

2.2.2. Landuse.

The clay texture and slow permeability, on the Rowden site, present a number of management difficulties. The site is predominantly used as pastoral land to raise beef stock. Mean rainfall at the site is 1035 mm per year based on a 30 year average (Tyson *et al.*, 1993), and there is typically 465 mm of precipitation from October to December (Harrod, 1981). High rainfall combined with low evapotranspiration restricts the number of grazing days per year to approximately 180 days.

Climatically the area has a potential for a large yield of grass but climate also restricts the ease of utilisation. Utilisation of a crop is influenced by trafficability and susceptibility to poaching of the ground. Wet soil conditions create many problems with respect to poaching, causing smearing and compaction by grazing stock leading to difficulties in harvesting and sowing grass seed, leaving part of the potential yield unrealised.

To improve the land and extend the grazing season the Culm grassland sites, such as those at Rowden Moor, are often drained. Improved drainage allows the soil to dry out more efficiently so that field capacity is reached before that of undrained soil (Addison, 1995). Low economic returns in stock rearing require cheap methods of drainage. Therefore, most grassland farmers favour widely spaced field drains combined with an intensive system of mole drains, as described in Section 1.2. Mole drains act as sinks in the soil and remove water by gravity when the soil is at or in excess of field capacity.

Work by Leeds-Harrison *et al.* (1982), Goss *et al.* (1983) and Scotter *et al.* (1990) have all focused on the hydrological effects mole drains have on discharge. Their work has shown that peak discharge increased from mole drained compared to undrained fields and lag time to peak discharge was reduced. Further work is needed on interpreting the movement of

solutes, such as nitrate, to a mole drain and part of this experiment therefore focuses on the movement of chloride and nitrate.

2.2.3. Profile Description.

The soils of Rowden were described by Harrod (1981) following the standard procedure outlined by Hodgson *et al.* (1976) of the Soil Survey and Land Research Centre. The soil where the blocks were extracted from was formally known as the Tedburn series but has subsequently been renamed as the Hallsworth series.

Harrod (1981) described the Hallsworth series as a clayey pelostagnogley soil which was gleyed throughout the profile. The top horizon being grey or grey-brown, strongly mottled clay loam, silty clay loam or clay, which overlies a strongly gleyed, grey and rusty mottled clay subsoils, with a coarse or very coarse prismatic structure (Table 2.1). The profile descriptions of the experimental blocks, presented in Table 2.2, indicate the presence of gleying in the lower horizon below 35 cm (from soil surface) but not throughout the entire profile as suggested by Harrod (1981; Table 2.1). Similar textural characteristics were, however, observed between the two different profile descriptions (Tables 2.1 and 2.1). It may, therefore, be confidently assumed that the soil blocks were representative of the wider scale Hallsworth field soil.

2.3. SOIL CHARACTERISTICS.

The following soil properties were measured in the laboratory:

1. Soil texture.
2. Structure.
3. Bulk density.
4. Porosity.

Table 2.1 - Soil profile of the Hallsworth series as described by Harrod (1981).

0 - 20 cm -- Ahg Dark grey, slightly mottled, slightly stony clay loam or clay.
20 - 50 cm -- Bg Grey with many ochreous mottles, slightly stony clay or silty clay; strong coarse prismatic structure.
50 - 100 cm -- BCg or Cr Grey with many ochreous mottles, very stony clay; weak coarse angular blocky or massive structure or shale *in situ*.

Table 2.2 - Description of block A and B soil profile.

0 -35 cm Strong brown (7.5YR 5/6, moist), sub-angular blocky coarse breaking down to medium/fine sub-angular blocky (Plate 2.1), silty clay loam or silty clay, few medium stones.
35 - 80 cm Brownish yellow (10YR 6/6, moist), mottled white (10YR 8/1) and red (10YR 4/6; 2.5YR 5/8), very coarse prismatic (plate 2.2), silty clayey or clay, large sub-rounded platey stones becoming more common with depth.

Plate 2.1 - Example of sub-angular blocky structure in top 0 to 35 cm of soil.

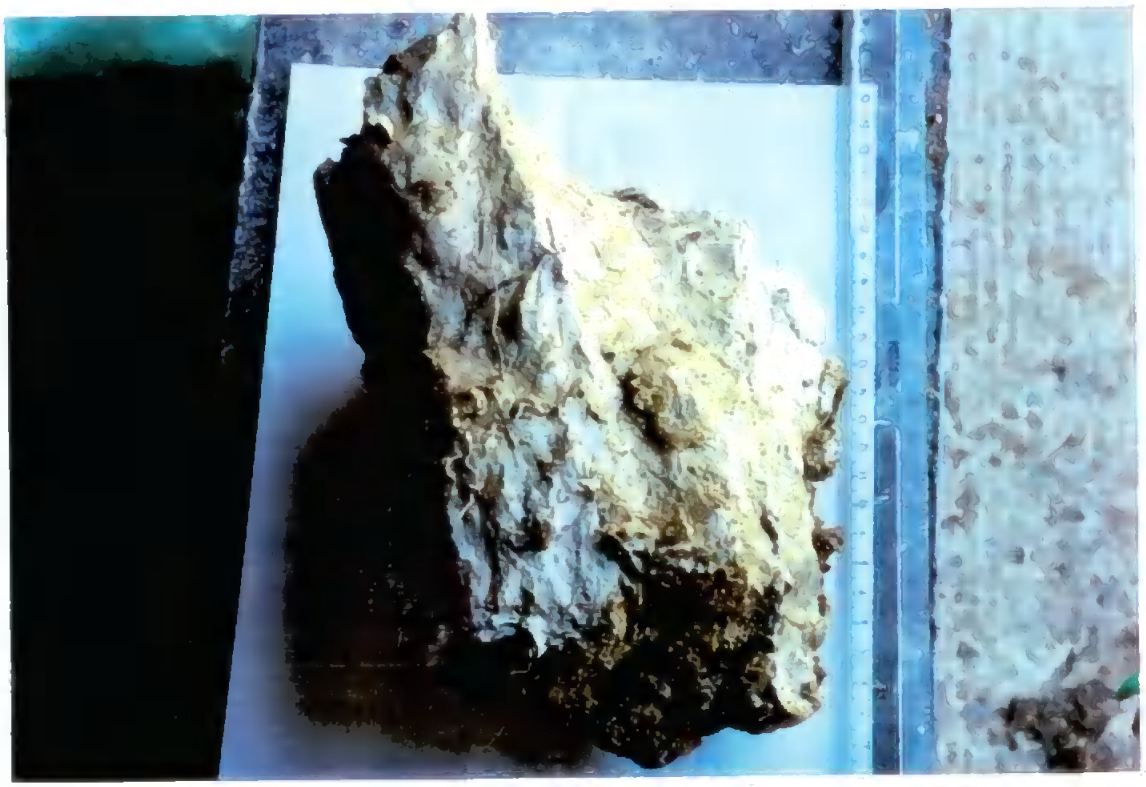

Plate 2.2 - Example of very coarse prismatic structure below 35 cm.

5. Soil water characteristic curves and pore volume.

6. Volumetric water content.

7. Saturated hydraulic conductivity.

On completion of the experiments, the soil blocks were destructively sampled, and analysed for the properties as set out above. The heterogeneous nature of the soil properties in the blocks as determined in the laboratory at the detailed scale will be discussed in this chapter as well as in Chapters 5 and 8.

2.3.1. Soil Texture.

A total of 30 samples of soil were collected from the area around where the blocks were extracted at 10 cm, 20 cm, and 50 cm depth. Soil texture of the block was not analysed. Samples were then divided up into representative sub-samples for textural analysis. Textural analysis of the coarser fraction of the soil (>63 μm) was carried out using the method of wet sieving. The sample was first air dried, the aggregates broken down and then soaked in dilute calgon (4% w/v sodium hexa-metaphosphate and sodium carbonate) to disperse the particles before being washed through a series of sieves (2 mm, 500 μm, 250 μm and 63 μm). The amount retained on each sieve represented the mass of grains whose maximum diameter lay between the diameter of the preceding sieve through which it passed and the lower sieve on which it rested. The weight retained on each sieve (the fraction) was calculated and converted into a percentage of total weight of sample.

The finer fraction (<63 μm) was calculated using the Analysette 20 Scanning-photo-sedimentograph (Model No. A20). Approximately 2 g of the <63 μm fraction was pretreated with 6% hydrogen peroxide to remove any vegetable matter and the particles were dispersed in 4% calgon. The sedimentograph was used to calculate the percentage silt

(63 -2 μm) and clay (≤2 μm) according to Stokes Law of sedimentation which states that spherical particles of a known density in a medium of known density and viscosity will descend at a rate proportional to the radius squared. The sedimentograph measures the change in optical density over time to calculate particle size distribution. A sample rich in clay maintains a higher optical density because the fine particles remain in suspension.

Results:

Table 2.3 - Average textural composition of the soil (percentage by weight retained).

Depth	Sand % 2000 - 63 μm	Silt % 63 - 2 μm	Clay % ≤2 μm	Soil textural class (UK system)
10 - 15 cm	15.7	51.0	33.3	Silty clay loam
20 - 25 cm	13.0	52.2	34.8	Silty clay or silty clay loam
50 - 55 cm	6.1	43.9	50.0	Clay or silty clay

The results of the textural analysis (Table 2.3) classify the soil as a silty clay loam from 10 cm down to 15 cm, a silty clayey or silty clay loam between 20 and 50 cm, and a clay or silty clay below 50 cm. The percentage clay content increases down the profile. These findings are similar to the ones made by Harrod (1981) as described earlier in this chapter. The high silt content would imply that the soil could be prone to erosion, compaction and capping.

2.3.2. Soil Structure.

Soil structure is a good indicator of soil pore space (Soil Survey Staff, 1975). Quantitative analysis of soil structure is important as it provides information as to the potential mobility of solutes through a profile. A number of techniques were used to investigate the structural properties of the soil in a qualitative and quantitative manner. These methods included a

visual description of soil structure (as used to produce Table 2.2), profile sketches of major cracks and pores, profile transects of pore spaces and resination of soil core samples. Results of the experiment to quantify soil structure will be discussed in greater detail in Chapter 5.

2.3.3. Bulk Density.

Bulk density results combined with soil textural information are often used as a surrogate for soil structure. When a soil is damaged by cultivation or trafficking, bulk density increases as the porosity decreases.

Dry bulk density (BD) is the ratio of the mass of dry solids to the bulk volume (Rowell, 1994), expressed as:

$$BD = M_d / V \qquad (2.1)$$

Where, M_d is the total mass of dry soil (g) and V is total volume of soil sample (cm^3). The mass of the dry solids being calculated by subtracting the weight of the soil that had been dried at 105 °C for 24 hours, from the original ('wet') sample weight.

Using a Soil Moisture Corporation Pitman Corer soil samples with a volume of 60 cm^3 were collected, at the end of the experiment, from blocks A and B as part of the characterisation of the relationship between soil water content and suction (Section 2.3.5). Dry bulk density was calculated using the 60 cm^3 samples as well as samples collected from block B alone to estimate volumetric soil water content (Section 2.3.6). Each of the volumetric samples represented a 200 cm^3 volume of soil.

Results:

The soil profile was equally divided into five columns across an 80 cm, horizontal profile, which was sub-divided into sections, as listed in each table. The variability of bulk density values for the 60 cm^3 samples both across the soil blocks and with increasing depth are illustrated in Tables 2.4 and 2.5.

Block A had a mean profile bulk density of 1.276 compared to 1.267 (g cm^3) for block B. Block A showed an increasing bulk density with depth in the profile, with the greatest bulk density being recorded directly underneath the mole drain (Table 2.4). Block B showed a similar increase in bulk density with depth (Table 2.5), however, bulk density readings were marginally smaller than those observed in block A. In block B two of the largest values were recorded in the top horizon (10 cm), these results may be linked to a clay rich band approximately 2 cm in diameter, running across the width of the block at this location. The band of clay was also observed in block A but discrepancy due to size of sample may account for lower bulk density values being recorded in block A compared to block B.

Bulk density values for block B based on a larger sample volumes (200 cm^3) showed a general trend of increasing bulk density with depth down to 40 cm (above the mole drain) (Table 2.6). Below 40 cm bulk density decreases again (Table 2.6). The larger bulk densities above 40 cm may be the result of compaction caused under grazing while the smaller bulk density with depth may be the result of soil disturbance caused by the mole plough.

The bulk density values calculated during sampling for soil water characteristic curve data (Table 2.5) were approximately 10% larger than those calculated from the larger sample volume (Table 2.6). This discrepancy is most probably due to the larger samples being

Table 2.4 - Bulk density values (g cm^{-3}) calculated from soil water release samples for block A. O represents location of the mole drain.

1.013	1.153		1.048	1.173	10 cm
1.228	1.255		1.133	1.217	25 cm
1.447	1.321	O	1.438	1.372	45 cm
1.392		1.543		1.364	60 cm

Table 2.5 - Bulk density values (g cm^{-3}) calculated from soil water release samples for block B. O represents location of the mole drain.

0.974	1.154		1.403	1.393	10 cm
1.234	1.203		1.204	1.039	25 cm
1.366	1.363	O	1.301	1.366	45 cm
1.298		1.396		1.280	60 cm

Table 2.6 - Dry bulk density values for block B (values in g cm^{-3}). O represents location of the mole drain.

0.91	0.82	0.86	1.11	0.94	10 cm
0.93	1.02	1.10	1.14	1.03	20 cm
1.08	0.97	1.09	1.08	0.96	30 cm
1.18	1.19	1.05 O	1.13	1.10	40 cm
0.97	1.09	0.93	1.26	1.05	50 cm
1.06	1.01	0.996	1.02	0.90	60 cm

more representative of the heterogeneous properties of the soil structure including the less prevalent larger structural features including macropores and cracks.

2.3.4. Porosity.

Porosity is a measurement of pore space within a soil and is closely linked to bulk density. Percentage porosity (n) can be calculated from bulk density (BD) using the formula below (Rowell, 1994):

$$n = \left(1 - \frac{BD}{2.65}\right) \times 100 \qquad (2.2)$$

Where, 2.65 is the particle density of soil.

Results:

The calculated porosity values determined from dry bulk density values in general show that porosity decreased with depth in the soil profile in both block A and B (Tables 2.7 and 2.8 respectively). However, the values of porosity calculated from dry bulk density samples collected for soil water content analysis (Table 2.9) showed a different distribution of porosity compared with Tables 2.7 and 2.8. The difference between the porosity values of the two sampling techniques may again be linked to volume of sample. The larger sample volume showed a larger porosity which can be associated with the presence of macropores in the sample.

Table 2.7 - Porosity values (%) from bulk density samples for block A. Showing location within the soil around the mole drain (●).

61.8	56.5		60.5	55.7	10 cm
53.7	52.7		57.3	54.1	25 cm
45.4	50.2	●	45.8	48.2	45 cm
47.5		41.8		48.6	60 cm

Table 2.8 - Porosity values (%) from bulk density samples for block B. Showing location within the soil around the mole drain (●).

63.2	56.5		47.1	47.4	10 cm
53.4	54.6		54.6	60.8	25 cm
48.5	48.6	●	51.0	48.5	45 cm
51.0		47.4		51.7	60 cm

Table 2.9 - Percentage porosity calculated from dry bulk density values for block B.

66	69	68	58	65	10 cm
65	62	58	57	61	20 cm
59	63	59	59	64	30 cm
55	55	60 ●	57	58	40 cm
63	59	65	52	60	50 cm
60	62	62	62	66	60 cm

2.3.5. Soil Water Characteristic Curves.

On completion of the experiment, 23 soil cores were taken from each block (Table 2.10) using the Pitman corer (Soil Moisture Corporation). These samples were used to determine the relationship between volumetric soil water content and soil water tension. From this data the distribution of pore space was calculated using the equation:

$$\rho g h = (2\gamma \cos\alpha) / r \qquad (2.3)$$

Where, ρ is the density of water (998.2 Kg m^{-3} at 20°C); g is the acceleration due to gravity (9.8 m s^{-2}); h is suction (m H_2O); γ is surface tension of water (72.75 × 10 J m^{-2} at 20°C); α is the angle of contact here assumed to be zero; r is the tube or pore radius (m).

Which can be expressed as:

$$r = 1.5/h \qquad (2.4)$$

Where, r is pore radius (mm) and h is the suction (cm H_2O)

The technique involved placing pre wetted (capillary saturation) cores of known weight and volume on a suction sand table (Hall *et al.*, 1977). The loss in weight of the cores was measured as suction was increased. The minimum radius of pore from which water was pulled from, for a given suction, was found from the water release curve.

Table 2.10 - Location of water release samples within the soil block with respect to the mole drain (●).

1	2A 2B		3A 3B	4	10 cm
5	6A 6B		7A 7B	8	25 cm
9	10A 10B	●	11A 11B	12	45 cm
13		14A 14B		15A 15B	60 cm

Results:

Tables 2.11 and 2.12 summarise the results obtained from the water release curves for blocks A and B. These tables present the recorded value of sample weights at suctions of 0 cm, 60 cm and 15000 cm (H_2O), from which the proportion of soil occupied by transient pores or macropores (saturation to 60 cm (H_2O), suction) and storage pore space or mesopores (60 cm to 15000 cm (H_2O), suction) was calculated. The location of these samples in the block is indicated in Table 2.10. The range of pores represented in the range 0 to 60 and 60 to 1500 cm H_2O are equivalent to the pore space in which water was considered to have been mobile and therefore contributing to solute movement within the soil. The pore size range between 0 and 60 cm H_2O represent potentially fast flow regions (i.e. macropores) while the pore size range between 60 and 1500 cm H_2O represent slower flow regions.

From Tables 2.11 and 2.12 it can be seen that the proportion of transient pores compared to storage pores decreases with depth in the soil. Although total pore space also decreased with depth in the soil, below 45 cm (middle of the mole) there were fewer transient pores compared with storage pores. This would imply that the soil above 45 cm was more porous than the soil below this depth. This data also suggest that block A (Table 2.11) had more

Table 2.11 - Water release characteristics for block A. Missing data represents cores that were disrupted by active fauna within the sample.

Sample	Saturation (0 cm)	60 cm H_2O	15000 cm H_2O	Transient $cm^3/100cm^3$	Storage $cm^3/100cm^3$	Total cm^3/cm^3
1	70.80	59.86	42.10	10.94	17.76	0.287
2A	65.81	57.42	40.33	8.39	17.09	0.255
2B	67.47	56.63	-	10.84	-	-
3A	70.31	64.83	-	5.48	-	-
3B	63.41	55.10	-	8.31	-	-
4	58.87	51.47	37.17	7.4	14.3	0.217
5	57.12	47.22	35.15	9.9	12.07	0.220
6A	60.40	48.78	35.69	11.62	13.09	0.247
6B	62.70	51.92	35.83	10.78	16.09	0.269
7A	60.03	49.64	34.71	10.39	14.93	0.253
7B	62.71	50.37	35.09	12.34	15.28	0.276
8	60.62	53.56	34.64	7.06	18.92	0.260
9	51.54	45.46	34.86	6.08	10.6	0.167
10A	50.33	39.01	28.77	11.32	10.24	0.216
10B	56.47	49.05	35.29	7.42	13.76	0.212
11A	53.19	43.93	30.87	9.26	13.06	0.223
11B	50.09	43.39	31.97	6.7	11.42	0.181
12	53.94	46.24	31.47	7.74	14.77	0.225
13	59.98	58.26	42.13	1.72	16.13	0.179
14A	50.62	41.96	31.52	8.66	10.44	0.191
14B	52.16	48.18	34.03	3.98	14.15	0.181
15A	61.05	56.49	39.67	4.56	16.82	0.214
15B	61.26	56.91	40.02	4.35	16.89	0.212

Table 2.12 - Water release characteristics of block B. Soil sample for location 3B was damaged during analysis.

Sample	Saturation (0 cm)	60 cm H_2O	15000 cm H_2O	Transient $cm^3/100cm^3$	Storage $cm^3/100cm^3$	Total cm^3/cm^3
1	65.16	57.1	40.95	8.06	16.15	0.242
2A	50.76	44.0	29.72	6.76	14.28	0.210
2B	65.96	57.5	39.59	8.46	17.91	0.264
3A	50.47	48.6	35.44	1.87	13.16	0.150
4	53.57	50.4	36.50	3.17	13.9	0.171
5	55.22	45.2	31.86	10.02	13.34	0.234
6A	56.89	48.3	35.00	8.59	13.3	0.219
6B	57.39	47.5	32.41	9.89	15.09	0.250
7A	62.70	54.1	37.61	8.6	16.49	0.251
7B	58.30	48.5	33.40	9.8	15.1	0.249
8	62.19	51.8	34.43	10.39	17.37	0.278
9	56.44	55.7	38.64	0.74	17.06	0.178
10A	56.43	55.0	40.95	1.43	14.05	0.155
10B	56.32	55.0	40.27	1.32	14.73	0.161
11A	52.76	51.9	37.32	0.86	14.58	0.154
11B	57.75	56.0	41.16	1.75	14.84	0.166
12	51.83	47.8	35.82	4.03	11.98	0.160
13	58.04	54.0	39.12	4.04	14.88	0.189
14A	58.67	57.0	41.20	1.67	15.8	0.175
14B	55.48	54.2	38.83	1.28	15.37	0.167
15A	59.48	57.4	41.55	2.08	15.85	0.179
15B	59.60	58.5	42.95	1.1	15.55	0.167

total pore space throughout the block than block B (Table 2.12) although the porosity results (Section 2.3.4.) indicated that the two blocks were not dissimilar. The differences between block A and B may be attributed to the natural heterogeneity of the soil.

Although porosity data, calculated from bulk density, provides an indication of potential space in which water may be held or transmitted, the values do not discriminate between different pore sizes. As stated in Section 1.8. pore space can be divided into three distinct categories, transient (macropore/mesopore), storage (mesopore) and stagnant (micropore). For the purpose of explaining water and solute movement, only transient and storage space within the soil are of interest. From results of transient plus storage pore space (=total) Tables 2.11 and 2.12, compared to porosity calculated from bulk density, Tables 2.8 and 2.7, it can be seen that porosity values are substantially different when calculated from bulk density values rather than when transient and storage pores, alone, are considered.

2.3.6. Volumetric Soil Water Content.

Soil samples of known volume and weight were collected from block B the day after the final experiment (run 5). Thirty samples were collected across the soil block the locations of which are illustrated in Table 2.13. One sample was collected per location. These samples were used to calculate the percentage of water held in the soil expressed volumetrically (θ_g) using the equation below:

$$\theta_g = \left(\frac{m_w - m_d}{V_d} \right) \times 100 \qquad (2.5)$$

Where, m_w is the mass of wet soil; m_d is the mass of dry soil; V_d is the volume of dry soil.

The volumetric water content was used to calculate the dilution factor of total oxygenated nitrogen (T.O.N. Section 4.5.1.) extracted from the soil, and to give an indication of residual T.O.N. in immobile parts of the soil, as discussed in Chapter 7.

Results:

The results for soil water content during the experiment, for blocks A and B, are discussed in greater detail in Chapter 6. Results for block B alone at the termination of the experiment are outlined briefly below. The percentage water content decreased from 10 to 20 cm (depth), 20 to 30 cm (depth) (except column 4) and from 30 to 40 cm (depth) by an average of 8%, 2% and 2% respectively (Table 2.13). From 40 to 50 cm water content increased (except in column 4) most notably in column 3 from 38.04% to 49.18%, which was directly under the mole drain (Table 2.13). Soil water content in column 4 was consistently dryer than other locations within the soil (Table 2.13 and Figure 2.2).

2.3.7. Hydraulic Conductivity.

Six soil core samples (80.12 cm^2 by 12.7 cm) were collected, in the field, from the two distinct soil horizons A (0 - 30 cm) and B (50 - 80 cm) to determine saturated hydraulic conductivity. The saturated hydraulic conductivity was determined in the laboratory using the Falling Head Permeameter, immersed cell method. This method ensures total saturation of the sample and should guarantee that no air bubbles are present. Saturated hydraulic conductivity was calculated from:

$$K_{sat} = \frac{2.302 A_m l}{A_s} \left[\frac{\log H_o - \log H_1}{t} \right] \qquad (2.6)$$

Table 2.13 - Percentage soil water content of block B with location of sample in profile.

1	2	3	4	5	Column
47.16	50.73	53.34	42.12	45.48	10 cm
40.85	38.75	41.73	36.99	41.67	20 cm
37.49	38.61	38.15	37.14	40.78	30 cm
36.59	35.08	38.04	35.52	35.63	40 cm
43.89	39.95	49.18	32.94	39.38	50 cm
41.09	41.58	40.95	40.13	45.47	60 cm

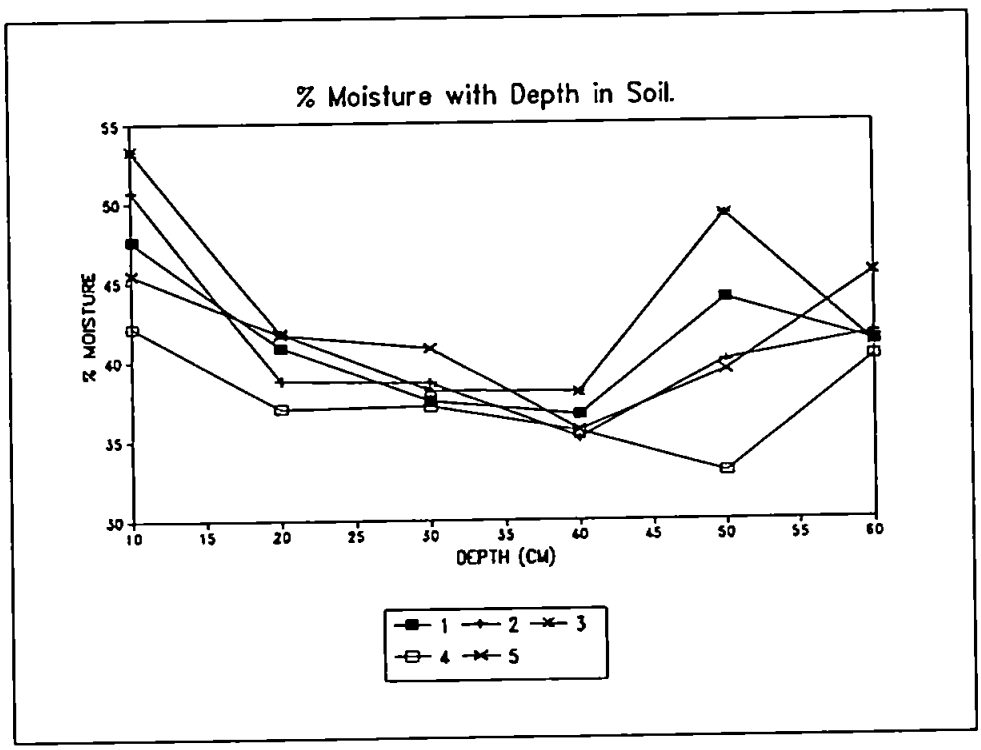

Figure 2.2 - Percentage of volumetric soil water plotted against depth in soil for block B.

Where, K_{sat} is the hydraulic conductivity (cm s^{-1}); A_m is the cross-sectional area of the manometer tube (0.4 cm diameter tube used in experiment) (cm^2); l is the sample length (cm); A_s is the cross-sectional area of the sample (cm^2); H_0 is the initial height of water in the manometer tube (cm); H_1 is the height of water in the manometer tube at the end (cm); and t is the time taken for H_0 to reach H_1 (s).

Results:

The hydraulic conductivity was 829.44 cm d^{-1} for the top 0 - 10 cm of soil and 0.376 cm d^{-1} at 50 - 60 cm. The smaller hydraulic conductivity reading at 50 - 60 cm (depth) may not accurately reflect the potential rate of water movement which may occur along ped interfaces owing to the discrepancy between size of sample and the size of the peds in this horizon. The peds in the lower horizon below 35 cm were described as very coarse prismatic with an average small axis (between ped walls) of 20 cm. The importance of using a representative scale when considering water movement was discussed in Chapter 1. Unsaturated hydraulic conductivity (K) results are considered in Chapters 6 and 8.

CHAPTER 3.

THE SOIL BLOCKS AND EXPERIMENTAL DESIGN.

3.1. INTRODUCTION.

The objectives of this investigation were to study flow and transport processes that occur along preferential pathways and the interaction between preferential pathways and the soil matrix, by monitoring water and tracer movement spatially and temporally. Water and solute movement within a soil have previously been investigated using a variety of experimental techniques. A number of limiting factors need to be considered within the experimental design. Experimental limitations will be outlined below with examples of previous work. This literature review acts as a basis from which the experimental design for this research was set. A description of the methods and technologies utilised in this research will be made after the review.

The design of the experimental set up is of primary importance as it can determine the type of observations that can be made and therefore data that can be collected. For this research the experimental design was subdivided into five principle areas of consideration:

1. Soil structure.
2. Scale of investigation.
3. Laboratory verses field experiment.
4. Soil water status.
5. Method of observing phenomena.

3.1.1. Soil Structure.

Physical laws, such as Darcy's law and Richards' equation, developed to explain the transport processes of water and chemicals through soil, have evolved from experiments

conducted on homogeneous materials with no diversity of structure (Youngs and Leeds-Harrison, 1990; Quisenberry *et al.*, 1993). The transport of solutes through a naturally structured soil can, however, be more complex than considered by these physical laws. Undisturbed field soil is not usually homogeneous in character, instead it tends to possess varying structural properties which lead to fluctuations in solute movement and concentrations throughout the soil (Biggar and Nielsen, 1976; Saleh *et al.*, 1990; Singh and Kanwar, 1991; Ogden *et al.*, 1992). For simplicity the varying structural properties of undisturbed soil has been classified as either bi-modal (macropore and micropore) or tri-modal (macropore, mesopore and micropore), as described in Chapter 1.

Observations of solute transport have been conducted using both disturbed (repacked soil with an unnatural structure) and undisturbed (natural soil structure) soil. The process of producing a repacked soil by drying and sieving destroys the soil structure (Buchter *et al.*, 1995). Natural undisturbed soils provide a more realistic medium in which to observe field type solute transport processes. Andreini and Steenhuis (1990) observed that in a tilled soil homogeneous flow occurred through the plough layer, which was unstructured, while short-circuiting was observed in the lower structured layer. Marshall (1994) conducted solute transport experiments on both repacked and undisturbed core samples. This research clearly demonstrated the importance of soil structure to the rapid movement of tracer through the soil via preferential flow paths.

The presence of structure in a soil is therefore an important concept to the experimental design as it will affect the way in which solute is transported through the soil. For an experiment to investigate preferential movement and the interaction between different pathways, as may exist in a field soil, the soil through which the movement is observed must possess variable soil structure properties.

3.1.2. Scale of Investigation.

The scale at which an experiment is conducted affects the scale of the phenomena that can be observed and how representative the observations made are to the wider field scale conditions. As the scale at which observations are made increases, the achievable resolution of spatial and temporal changes decreases, due to the limitations of practical manual sample collection (Holden *et al.*, 1995a). Preferential flowpaths operate at a scale of some few centimetres, such a small scale immediately limits the spatial sensitivity required to observe them. Improvements in temporal resolution of sampling have been made by the introduction of automated sampling systems (Booltink *et al.*, 1993; Marshall, 1994; Holden *et al.*, 1995a & b). However, the feasibility of such technology is limited by available technology and cost. The sensitivity of the instruments being used also limits the observations that are possible. Other limitations of instrumentation include the area over which samples are drawn, the speed at which samples can be collected and the disturbance to transport processes caused by the installation of instruments. These limitations will be examined in more detail in Chapter 4.

The experimental scale therefore depends on the objectives of the experiment. However, a limiting factor is the need for the block or column to be representative of the wider scale medium. In Chapter 1 this representative scale was referred to as the representative elementary volume (REV) (Beven and Germann, 1981). A REV represents the smallest volume of soil that is considered to be representative of the wider field scale heterogeneous soil properties. A representative volume is considered to be; in the order of 1 to 10 m^2 for a combined micropore and macropore system (Beven and Germann, 1981), or a sample containing 30 peds in a cross section (Bouma, 1990). Bouma's (1990) definition could in theory reduce the size of sample, for example, to 11 cm diameter for 2 cm peds, although for larger ped sizes the scale of the sample needed to achieve one REV may become

restrictive. The validity of some experiments may be brought into question because of the size of column used. Soil columns used for laboratory observations of flow range in size from small soil columns [35 cm by 35 cm by 34-46 cm (Andreini and Steenhuis, 1990); 20 cm diameter by 20 cm length (Booltink and Bouma, 1991); 30 cm diameter by 38 cm length (Tindall *et al.*, 1992); 32.5 cm by 32.5 cm by 32.5 cm (Quisenberry *et al.*, 1994)] to larger soil columns [3300 cm^2 by 50 cm length (Ogden *et al.*, 1992); 80 cm by 80 cm by 30 cm (Poletika and Jury, 1994); 30 cm diameter by 75 cm length (Buchter *et al.*, 1995)]. The advantages of working with small soil columns is that they are easier to extract, transport and handle as well as being more economically viable for restricted budgets. Sample sizes greater than one REV do not further reduce variability of measurements or increase potential information yield (Hendrickx *et al.* , 1994). Methods for the removal and transport of soil columns have been suggested by Singh and Kanwar (1991) and Tindall *et al.* (1992), using a metal core that is hydraulically rammed over a block of soil. The corer is later removed once the soil is positioned in the laboratory.

3.1.3. Laboratory Verses Field Experiment.

Experiments to investigate solute transport through the soil have been conducted on large isolated blocks left *in situ* in the field (Hornberger *et al.*, 1990; Hornberger *et al.*, 1991; Addison, 1995; Holden *et al.*, 1995a & b). The advantages of such experiments are the ability to observe flow processes through a larger area and therefore represents a better comparison to the wider field system, as explained above. Such experiments are relatively inexpensive to set up and only minimal disturbance to soil conditions is incurred, primarily at the boundaries. However, as stated above, spatial and temporal sampling resolution is limited by an increase in scale. The observation of solute transport which requires fine spatial and temporal resolution, at present is accommodated more satisfactorily by small soil columns removed from the field and placed under laboratory conditions.

In situ block experiments and laboratory soil columns both experience the disadvantage of edge effect. Edge effect can result in artificially rapid transfer of solute along the interface of the isolated soil, such conditions do not exist in the natural field. Artificial edges also incur other hydrological changes including truncation of flowpaths and change in pressure gradients. As the size of the column or block increases, edge effect becomes less important as instrumentation can be located deeper in the soil away from the edges and therefore be less influenced by the boundary. The problem of sealing the edges of small scale soil column experiments has to some extent been successfully over come, for example, Singh and Kanwar (1991) used a combination of liquid rubber and molten wax to seal their columns walls while Tindal *et al.* (1992) used molten paraffin wax effectively.

3.1.4. Soil Water Status.

Water movement through soil has been investigated in both saturated and unsaturated conditions. Soil water conditions have been observed to effect active solute pathways (Kluitenberg and Horton, 1990; Youngs and Leeds-Harrison, 1990; Marshall, 1994). Some research points to the possibility of active pathways remaining constant through time at a given water content (Quisenberry *et al.*, 1994; Buchter *et al.*, 1995). In a saturated soil solute potentially flows through the whole soil volume, however, as soil water content decreases flow becomes more restricted as structural variability results in spatial disruptions to flow (Quisenberry *et al.*, 1993). Only under exceptional circumstances do saturated conditions exist in field systems, therefore for the majority of the time unsaturated conditions of flow persist.

Until recently rapid movement of water and solute via preferential paths was only believed to occur under saturated conditions. However, subsequent work has proven this not to be entirely accurate. Preferential flow has been observed to occur under unsaturated conditions

also (Section 1.10.). Over the past few years research has begun to focus on the transport of water and solute through unsaturated soil (Andreini and Steenhuis, 1990; Radulovich *et al.*, 1992; Poletika and Jury, 1994; Buchter *et al.*, 1995).

The application of water and solute to soil columns have included ponding the water on the soil surface (Kluitenberg and Horton, 1990; Singh and Kanwar, 1991), drip application (Kluitenberg and Horton, 1990; Tindall *et al.*, 1992),rainfall simulation (Andreini and Steenhuis, 1990; Booltink and Bouma, 1991; Ela *et al.*, 1992) and misting (Dirksen and Matula, 1994; Marshall, 1994). The method by which water and/or solute is applied to the soil influences subsequent transport processes (Kluitenberg and Horton, 1990). Rainfall simulation and drip application mimic more idealistically natural field conditions while misting systems have been found useful in applying a more even distribution of tracer across the soil surface.

In the laboratory unlike in the field the conditions at the base of the soil column can be controlled and monitored to allow free drainage as well as spatial observation of solute variability. Previous work has employed free drainage experiments as well as positive suction at the base of the soil column. Free drainage experiments have been conducted by Radulovich *et al.* (1992);Booltink and Bouma (1991), Singh and Kanwar (1991), Booltink *et al.* (1993) through perforated disks; Tyler and Thomas (1981) using glass tubing at the base; and by Ela *et al.* (1992) using sand at the base of the column. Positive suction drainage experiments have been conducted using porous ceramic plates on which the soil column is seated (Tindall *et al.* (1992); Marshall (1994); Buchter *et al.* (1995)).

Spatial variability of solute samples at the base of soil column experiments have been observed using a variety of techniques: support containing nineteen isolated porous ceramic

plates (Buchter *et al.*, 1995); free draining grid lysimeters (Andreini and Steenhuis, 1990; Ogden *et al.*, 1992); and wick samplers (Poletika and Jury, 1994).

3.1.5. Methods of Observing Phenomena:

Movement of water through the soil only partially reflects solute movement through the soil because of different forces involved (Section 1.11.). Soil water content can be observed using TDR while potential water movement can be inferred from suction measurements made by tensiometers. The processes and mechanisms by which these instruments work is discussed in detail in Chapter 4. The movement and redistribution of solute through the soil can be simulated using conservative tracers, such as chloride. Observations of spatial and temporal changes in tracer concentration in the soil column and at the base can be used to infer the amount of mixing and active pathways by the interpretation of the shape of the breakthrough curves (Section 1.13. and 7.7.). Observed results can also be compared to mathematical model predictions of dispersivity from which active pathways can be implied (Section 1.14. and 7.8.).

Breakthrough curve analysis is widely used in the interpretation of preferential flow and solute movement (Tyler and Thomas, 1981; Andreini and Steenhuis, 1990; Kluitenberg and Horton, 1990; Steenhuis *et al.*, 1990; Singh and Kanwar, 1991; Tindall *et al.*, 1992). Mathematical models are also an increasingly used and accepted technique, especially when trying to predict field scale movement from column sized observations (Andreini and Steenhuis, 1990; Brusseau and Rao, 1990; Kluitenberg and Horton, 1990; Saleh *et al.*, 1990; Steenhuis *et al.*, 1990; Sudicky, 1990; Jarvis *et al.*, 1991a; Singh and Kanwar, 1991; Hayot and Lafolie, 1993).

The way in which a tracer is applied to a soil will affect the way in which the tracer moves

through the soil (Kluitenberg and Horton, 1990). Both miscible and pulse experiments have previously been employed to observe solute movement and preferential flowpaths (Section 1.15.). The type of tracer used will also affect its subsequent movement through the soil. A conservative tracer (chloride) will not chemically react or be broken down as it travels through the soil, while a biological tracer, such as nitrate, may be absorbed and chemically broken down by microbial action.

In summary the following factors were taken into account when considering the experimental design (Table 3.1).

Table 3.1 - Summary of considerations that need to be addressed in determining experimental design.

Areas of consideration	Limitations of observations	
Soil structure	disturbed	undisturbed
Scale of investigation	plot	column
Laboratory verses field experiment	*in situ* soil block	laboratory soil column
Soil water status	saturated/no drainage	unsaturated/drained
Method of observing phenomena	water movement	solute dispersion

3.2. EXPERIMENTAL DESIGN.

The discussion above outlined the decisions made in establishing an experimental design for the research used in this investigation.

An artificially, as well as, naturally structured soil was chosen so that variabilities due to structural heterogeneity in the soil could be observed. The presence of soil structure was fundamental to answering both primary aims of the research (outlined in Section 1.4). A

block of 1 m^2 by 0.85 m depth centred on the mole was chosen as it fulfilled the minimal requirements of REV set by Beven and Germann (1981) for a dual porous system. This size of block also represented the maximum dimension which could be feasibly removed, transported and handled. A laboratory experiment was established as it allowed a controllable environment in which to observe detailed water and solute transport. Included in the design was an ability to control drainage at the base of the block using a sand table. Water and solute movement were monitored using instrumentation, including some automated as well as manual systems. Both conservative (chloride) and biological (nitrate) tracers were employed using a combination of miscible displacement (applied using a misting system) and pulse application. A detailed description of these components in the experimental design for this research is given below. The timetable for the different components of the experiment is presented in Appendix A.

3.3. PREFERENTIAL FLOW ROUTES AND INSTALLATION OF A MOLE DRAIN.

The primary objectives of this experiment were to monitor solute movement along preferential flowpaths at a detailed scale but at a scale that was still representative of the wider field scale system. A mole drained soil block provided the opportunity to monitor the affects of artificially created macropores through a naturally structured but poorly drained soil. The process of installing a mole drain creates a number of fissures that radiate from the mole as was discussed in Section 1.2. The fissures created by the mole plough provide preferential pathways along which water and solute can, potentially, be rapidly transported to depth. The size of the cracks generated by the mole being dependent on the soil moisture content at the time of moling.

A mole drain was specially drawn on the 11th June 1992 for this experiment. At the time of moling the soil water deficit was calculated to be 43.4 mm (North Wyke records

Unpubd., 1992). The soil layer above 50 cm became progressively dryer to the touch towards the surface while the soil below 40 cm was still moist and malleable. The soil moisture content was therefore deemed to be suitable for successful fissuring of the soil by the mole plough as described by Leeds-Harrison *et al.* (1982) and Findlay *et al.* (1984). A new mole drain was pulled so that its exact location, orientation and depth were known, and because mole drains have a limited life span (Spoor and Ford, 1987). The channel created by the mole plough had an approximate diameter of 10 cm at a depth of between 40 and 50 cm in the soil profile. Other mole drains on the Rowden Moor site have been drawn at a similar depth which represents the 'critical depth' at this location (Hallard, 1988)

The mole drain was positioned in the subsequent soil blocks so that it was orientated along a central axis, at a depth of 50 cm (depth from surface to base of mole drain). As the normal interval between mole drains is 2 to 3 m the limited dimensions of the extracted soil blocks (1 m^2) meant that a mid-mole to mid-mole was not practically possible. The depth, location and orientation of the mole drain in the two blocks were identical. Instrumentation was organised in the soil blocks by locating them with reference to the mole drain.

3.4. SIZE AND EXTRACTION OF SOIL BLOCK.

Part of the project involved the design of the technique to remove and transport large soil blocks without causing structural disturbance within the soil. A JCB digger was used to excavate a trench, 1 m wide and 1.5 m deep on three sides and 2 m by 1.5 m on the fourth side, around a central soil monolith of dimensions 1.2 m × 1.2 m × 1.5 m. A wooden former had been built (internal dimensions 1 m × 1 m × 0.85 m) to support the soil block during transport. The wooden frame was placed over the centre of the soil monolith and

the excess soil was cut away from the edges of the wooden framework as it was gently tapped down over the soil. This process was continued until the soil surface had reached the top of the wooden frame work. The block was then excavated underneath to assist in fracturing as the block was lifted. Six steel scaffold poles were mechanically rammed underneath the base of the block and lashed together with separate poles to provide a support to the base of the block and to aid in lifting. The JCB lifted, from the scaffold poles (i.e. from the base of the block), one side then the other in a rocking motion to fracture the soil at the base of the block and finally lifted the soil block out of the field. The boxed soil was left berried in the field until September (Appendix A) when the sand tables were ready to receive them. The soil blocks were transported back to the laboratory supported by the scaffold frame work at the base and the wooden frame work around the sides. The size and weight (1.5 tons) of the soil block required that strict safety procedures were followed at all times. Restrictions included the use of trained staff being present, the use of an industrial lifting rig and the prohibition of personnel standing directly under the raised block.

Before being placed on the prepared sand tables, excess soil at the base of the blocks was carefully removed by plucking away at the soil. This pretreatment was required to ensure that an even contact was made between the base of the soil block and the sand table to reduce air entrapment. Although the base of the block was not perfectly flat the weight of the soil block aided in a good contact being achieved.

A combination of, three sets of, fabric strops (2.5 cm width) and wire mesh (10 cm by 100 cm) were used to remove the scaffold poles that had supported the base of the soil block during transport. The strops and wire mesh had to remain *in situ* once the soil blocks had been lifted off of the scaffold support frame and onto the sand tables, therefore, the area

occupied by the strops and wire mesh was kept to a minimum, to maintain a good contact between the soil and sand interface, while maintaining a generous safety margin for lifting. Wire mesh was used in conjunction with the fabric strops to distribute the weight of the load and thus prevent the strops from cutting into the block when the full weight of the soil was lifted. A fork lift truck was used to lift the blocks over the sand tables, still supported at the base by the scaffold framework. The strops were attached to the fork lift and the block was lifted off of the scaffold framework, which was then quickly removed, and lowered down onto the sand table. The final lift was done as swiftly as possible to prevent excess stress being placed on the internal soil structure of the blocks. No slumping was observed during this procedure.

3.5. SEALING EDGES TO PREVENT EDGE EFFECT.

Water and solute flowing down the sides of the block or column without infiltrating the soil, of small scale experiments, lead to breakthrough curves which could be attributed to the flow of water down the sides of the column alone. Uncertainty about the contribution of edge effect to the shape of the breakthrough curve can result in the misinterpretation as to the actual active processes occurring in the soil. To prevent water and chemicals by-passing the block at the sides, the edges of the block were sealed using paraffin wax, as described by Tindall *et al.* (1992). The wooden framework was cut away, from the soil block, in increments of 0.2 m and a cardboard former was placed around the exposed soil. Molten paraffin wax was then poured between the cardboard and the soil. This procedure was repeated until the whole of the sides of the block had been waxed. A prior experiment in the laboratory on a smaller soil core (0.3 m diameter by 0.3 m depth) of the same soil type was used to identify any potential problems that may be encountered when applying the molten wax. The small scale experiment showed the molten wax would only slightly penetrate the soil, by about 4 mm, such a penetration was sufficient to provide a good seal

between the soil and the wax and hence would not allow water to bypass the soil block at the edge. On the larger scale, experimental, block a problem occurred along one particular side of the block. On the side of the block closest to the more extreme changes of temperature the wax and soil began to separate, and remedial action had to be taken to prevent edge effect as a consequence of this. A 2 cm (width) horizontal band of wax was removed from around the block, 20 cm from the top of the soil. The subsequent exposed soil was sealed using puddling clay and a fine layer of wax to prevent the clay from drying out. The band of puddling clay prevented any vertical movement of water or solute along the edges of the soil block below this layer. On completion of the experiment destructive analysis of the soil blocks revealed that a good contact had been achieved between the wax and soil on three sides of the block (Plate 3.1). The separation of wax and soil on the fourth side was put down to extremes of temperature and/or slight instability of the block due to its size. Subsequent work may incorporate a tensioning device to help prevent this.

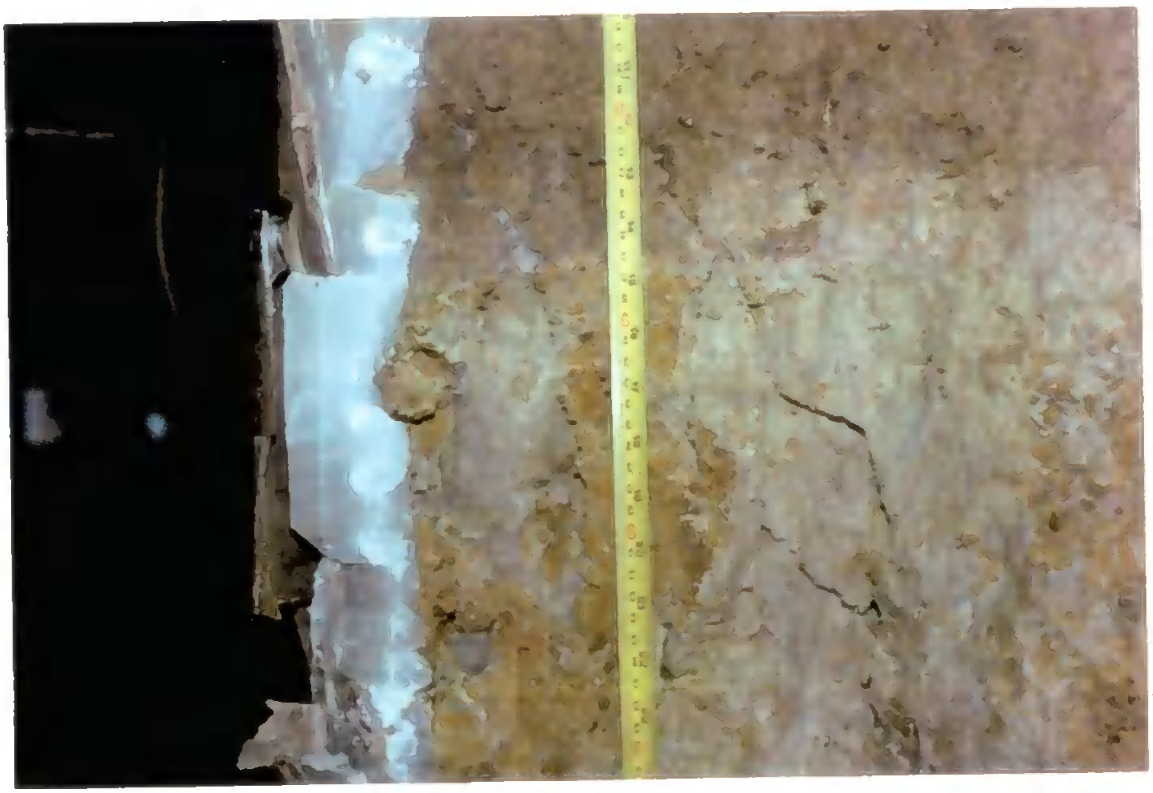

Plate 3.1 - Soil and wax interface at edge of soil block.

3.6. SUCTION SAND TABLES.

Two sand tables were custom built for this experiment, at a scale of 1.2 m × 1.2 m × 0.4 m, using the method described in Hall (1977) which used a combination of Chelford 60 and Redhill HH sand. The construction of the sand tables was a crucial and time consuming part of the experiment. Extreme care was taken with the construction of the sand tables so that a suction could be induced at the base of the soil block. The ability to vary suction at the base of the soil block would have allowed a variety of drainage conditions to be simulated and observations of solute movement under different drainage conditions to be made.

The two sand types used, Chelford 60 and Redhill HH, were initially tested to determine their particular air entry characteristics, using a Haines Apparatus (Rowell, 1994). The coarser sand, Chelford 60, held a suction of approximately 60 cm H_2O (0.06 bar). The air entry characteristics of the Chelford 60 sand made it suitable for the coarse sand layer at the base of the sand table that surrounds the drainage network of the sand table (Figure 3.1). The second sand, Redhill HH, had a finer texture than the Chelford 60 sand and subsequently held a suction in excess of 100 cm H_2O (0.1 bar). The finer Redhill HH sand was therefore suitable for the main volume of sand in the sand table (Figure 3.1), where a high suction potential may be necessary to draw water out of micropores.

The large scale of the sand tables was such that the boxes holding the sand were constructed out of marine ply, and sealed to ensure that they were water tight. The drainage system was sealed into the base of the table. The table was then flooded through the drainage system using a pressure head system. Particular care was taken when saturating the sand table to ensure that water was only added from below to allow trapped air in the sand to escape and thus prevent an air lock occurring. This process required a head of 3

m of water to develop sufficient pressure in order to force water through the sand. Progress was therefore slow and the water table rose at approximately 1 cm per day (15 litre of water per sand table).

The sand tables were placed on benches 0.8 m above the ground (Figure 3.1). This height provided a potential range of suction of between 0 m (0 bar) and 1.2 m (0.12 bar) to be induced at the base of the soil block. However, the suction in the tables was not maintained when the blocks were emplaced. There are three possible reasons why the sand tables failed to hold a suction:

1. The weight of the block may have compressed the drainage network.
2. The drainage network was not sufficient to drain the size of sand table.
3. Stress fractures caused by overburden causing joints in the sand table to leak.

Subsequent investigation showed that the most likely cause of failure was due to the overburden causing stress fractures in the wood, the system could not be sealed as a result. Air entered into the sand table and suction was lost. The drainage network had not been compressed by the overburden and was working satisfactorily.

Although drainage could not be varied at the base of the block a positive connection was achieved between the soil and the sand. Water within the sand table could be varied by pumping out water which allowed a low soil water content to be maintained in the sand table. Observations of free drainage due to gravity within the soil block, to a depth below the level of the mole drain were possible. A simulation of summer time soil conditions could therefore be achieved. Winter/spring conditions could also be simulated by allowing water to accumulate within the sand table and soil, by restricting drainage from the base of the block.

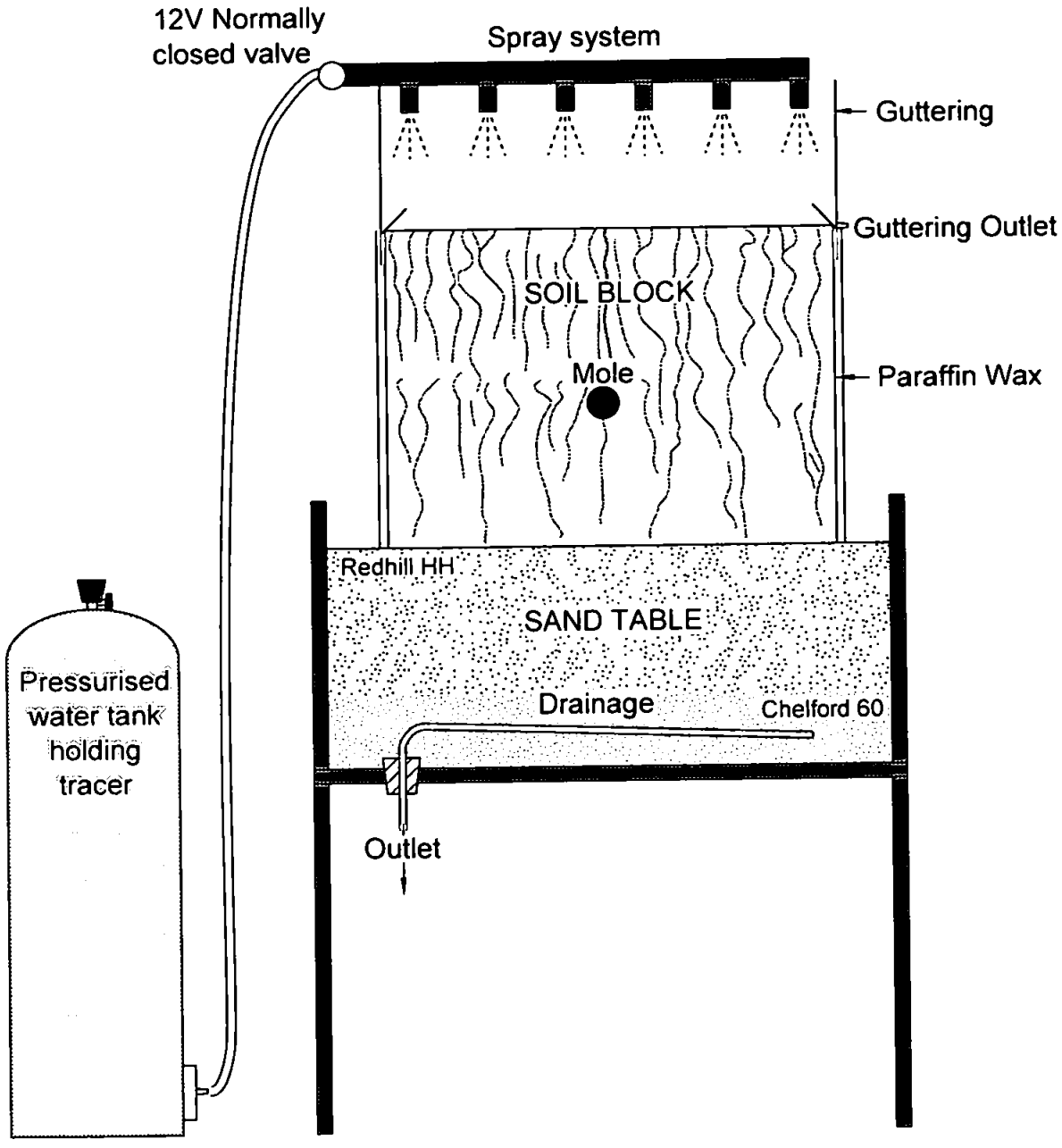

Figure 3.1 - Location of soil block within the irrigation and sand table system.

3.7. IRRIGATION.

As part of this experimental investigation preferential flow was analysed using breakthrough curves in order to determine which pathways solute had travelled through (Chapters 1 and 7). To ensure that observed flowpaths were due to soil properties and not to discontinuity of tracer application it was important that the tracer was applied evenly over the whole surface of the soil. In order to achieve an even application of tracer to the surface of the soil block an automated misting system was modified from a design of Marshall (1994). A spray rig constructed from poultry spray nozzles (part #M-2, Gold Kist Farm Supply, Commerce Ga.) was used to apply a fine mist to the surface of the block. The misting system was suspended 0.5 m above the surface of each soil block (Figure 3.1). Each irrigation system consisted of 18 nozzles organized in a grid system with sufficient overlap to ensure that an even application of solution was applied to the entire surface. The irrigation system was controlled via a pressure pump (pressure ranged from 2.76 - 3.45 bar) through a pressurised water reservoir (Figure 3.1). Rate of application was controlled by a Campbell 21X data logger, which operated a normally closed 12 V valve (Campbell 21X program presented in Appendix B). The controllable misting system enabled a variety of application rates and storm events to be considered. In the five experiments, however, rate of irrigation was kept constant (at 2.76 mm h^{-1}) so that a steady state condition was maintained within the blocks. The rate of irrigation, 2.76 mm h^{-1}, represented a 30 second spray every 15 minutes. The five experiments presented within this thesis therefore represent restricted irrigation and hydrological scenarios. A single irrigation scenario was not considered to be inappropriate as pathways actively involved in transmitting solution are dependent on many factors and may not necessarily be turned on and off under different irrigation rates.

The main constituent of the irrigation solution was tap water which had tracers dissolved

into it for parts of the experiments. Four sources of irrigation water had been identified: collected rainwater, drainage water, distilled water and tap water. Due to the quantity of water required each day (in excess of 60 l) tap water was chosen. Tap water also had the advantage of being less variable with regard to ionic strength than either rain or drainage water. The higher ionic strength of the tap water compared to deionised water also meant clay dispersion within the block was minimised.

To prevent loss of water by evaporation a cover was placed over the top of the spray rig. The system was sealed so that the only loss of water would be from the base of the block and sample collection points. The grass cover died off before the start of the experiment therefore no loss by transpiration occurred.

3.8. DRAINAGE WATER.

Drainage output was measured at the mole drain using a tipping bucket system to collect water of known volume for each tip (25 ml). Calibrated for a flow rate of up to 30 l h^{-1}. Each tip of the bucket was recorded by a magnetic counter and an electrical read switch attached to a Campbell 21X data logger which recorded the time of each tip (Campbell 21X program given in Appendix B). Using both methods meant both total number of tips and flow rate could be calculated. All the water that drained from the mole drain was collected as a double check for volume of water lost via the mole drain.

3.9. MONITORING TECHNIQUES.

The importance of monitoring techniques used in the experimental design is of such significance to the overall achievement of the research that it is discussed separately in Chapter 4.

3.10. EXPERIMENTAL PROGRAM.

In total five separate experiments were carried out during this research. The relative timings of the experiments within the overall experiment are presented in Appendix A. Experiments on blocks A and B were conducted separately because of limitations in manual sampling and equipment restrictions. Two experiments were conducted on block A (runs 1 and 2) and three experiments on block B (runs 3, 4 and 5). The duration and concentration of tracer applied in each of these experiments is listed in Table 3.2. The first three experiments (run 1, 2 and 3) utilise a technique involving the miscible displacement of the solute in the soil block with a solution of stronger chemical concentration, in which the tracer was continuously applied for an extended period of time exceeding one pore volume of the soil column. In these experiments the miscible displacement experiment was conducted over 12 days after which the more concentrated solution was replaced with background water (tap water) and the block was flushed for a further 12 days (Table 3.2). The final two experiments involved the application of a concentrated spike or pulse of, conservative, potassium chloride and non-conservative potassium nitrate flushed through by background water (Table 3.2). The pulse of chloride and nitrate was used to monitor dispersion and absorption from the mobile water.

It was not possible, because of safety restrictions, to keep the grass cover that had been present in the field alive. The grass on top of the blocks died off in February 1993 nine months prior to the nitrate experiments (runs 4 and 5, Section 7.5.1. and 7.5.2.). There was therefore no effect on the nitrate tracer due to vegetation. It is also considered that sufficient time had elapsed between the loss of vegetation and start of experiment for any nitrate produced by the dyeing vegetation to have been leached through the soil.

The two nitrate tracer experiments (runs 4 and 5) were conducted in November and

Table 3.2 - Tracer application program for experiment.

Sampling Run	Method	Number of days applied and sampled for.
1	miscible displacement flush miscible displacement flush	12 days irrigation with 100 mg l^{-1} Cl. 12 days irrigation at background, 10 mg l^{-1} Cl. 12 days irrigation with 250 mg l^{-1} Cl. 24 days irrigation at background
2	miscible displacement flush	12 days irrigation with 250 mg l^{-1} Cl. 12 days irrigation at background.
3	miscible displacement flush.	12 days irrigation with 250 mg l^{-1} Cl. 12 days irrigation at background.
4	slug of Cl (2500 mg l^{-1}) and NO_3 (500 mg l^{-1}).	Day 1 applied tracer and flushed through with background water for 12 days.
5	slug of Cl (2500 mg l^{-1}) and NO_3 (500 mg l^{-1}).	Day 1 applied tracer and flushed through with background water for 12 days.

December 1993 (Appendix A). The mean external air temperature range during this time was 5.6 °C and 4.6 °C respectively (North Wyke Meterological Records, Unpubd., 1993). Mineralization processes and biological activity would therefore have been limited at this time.

The aims of each of the five experiments are outlined in Table 3.3.

The following chapter (Chapter 4) describes in detail the instrumentation and analysis used to monitor soil water status and chemical movement through the soil.

Table 3.3 - Aims of individual experiments.

Sampling run.	Soil conditions and aims.
Run 1	Free drainage from base of block allowing the simulation of spring type conditions. Aims: To establish a suitable concentration for applied tracer. To observe the effect of tracer concentration to the appearance and variation in concentration throughout the soil block. To distinguish different active pathways throughout the soil, and observe spatial and temporal changes.
Run 2	Raised water table simulating autumn/winter conditions. Aims: To observe any changes in pathway from run 1 (low water table) to run 2 (high water table) as a result of raising the water table to the base of the mole. To observe any spatial and temporal changes in pathway between run 1 and run 2.
Run 3	Raised water table simulating autumn/winter conditions, similar to run 2. Aim: To compare solute variability between identical (REV) soil blocks to identify how variable soil properties are even over a short distance.
Run 4	Low water table simulating spring time conditions. Simulating chemical application followed by rainfall event. Aims: To observe any differences in solute movement between a pulse of conservative (chloride) and non-conservative (nitrate) tracer.
Run 5	Low water table simulating spring time conditions. Aims: To observe differences in the reaction time and variability in solute movement in an initially gravimetrically drained soil compared to an initially 'wet' soil (run 4). To observe temporal and spatial changes in concentration due to resident chemical conditions.

CHAPTER 4.

SOIL BLOCK MONITORING TECHNIQUES.

4.1. INTRODUCTION.

To observe in detail the movement of water and solute through a soil along specific pathways a number of factors must be considered:

1. The features that are to be observed.
2. The scale of observation (spatial).
3. The time interval between observations (temporal).

4.1.1. Features to be Observed.

The movement of water through the soil can be observed by taking measurements of soil water content, suction and drainage. Instrumentation used to monitor these soil conditions include: tensiometers, which measure soil suction from which potential soil water movement can be inferred; TDR, which have been used over the past few years to monitor *in situ* soil water content; and tipping buckets, that can be used to monitor both rate of flow and volume of water leaving the drainage network. The movement of solute through the soil may be observed directly via the monitoring of tracer movement as a change in concentration through time. Solute samples can be collected using *In situ* suction cup lysimeters which can be located at different vertical depths and horizontal separations so that the change in solute concentration can be observed both spatially and temporally.

4.1.2. Spatial Scale.

Scale of observation required depends on the spatial scale at which the phenomena to be observed changes. As explained in Sections 1.6.1. and 3.1.2. the sample volume required

to fulfil a meaningful statistical average of the soil property has been referred to as the representative elementary volume (REV). The closer the sampling volume of an instrument is to the REV of the observed phenomena the less variable the results will be, also an increase in size of sampler reduces the number of sampling locations required to determine the soil property (Hendrickx *et al.*, 1994).

4.1.3. Temporal Scale.

The interval between samples will be dependent on the speed of change of the phenomena observed, for example, in a steady state soil experiment average soil water conditions will be expected to alter very little therefore observations need not be taken at a fine temporal resolution, once a day is adequate. However, microscopic variations of solute transport may be occurring continuously, in this instance the finer the temporal sampling resolution the more detailed the results will be. The limitation to temporal resolution will be the practical limitation of the sampling procedure used (Holden *et al.*, 1995a). A manual sampling system will be less sensitive to temporal changes than an automated system because of the physical time it takes to collect samples manually and the financial restrictions which limit number of personnel (and therefore speed of collection, analysis and interpretation). An automated system is not only capable of handling larger quantities of data in a given time span, it is also potentially more accurate and because data may be directly interpreted analytically the format of the results is in a more readily usable form. Subsequent analysis and interpretation of data collected by an automated system may as a result be more rapid than a manual system. Automated systems, however, are restricted by technological availability, practicality of using an automated system in a particular environment and cost restrictions.

The following section will consider the use of tensiometers, TDR and suction cup lysimeter

samplers to the monitoring of water and solute movement through the soil. Each section will consist of a brief definition, followed by an explanation of how the system works and will be concluded by a description of how it was used in this research.

4.2. TENSIOMETERS.

Tensiometers have been defined as a porous medium interface, between a sealed unit and soil, for measuring the energy status or matric potential of the soil (Gardner *et al.*, 1922). Tensiometers consist of a porous ceramic cup sealed to a non-porous tube which is stoppered with an air-tight cap. The tensiometer system only allows the movement of fluids across the saturated porous cup at pressures below the bubbling pressure (defined below). A pressure reading device such as a pressure gauge, mercury manometer or an electrical pressure transducer is located within the system so that the internal pressure of the tensiometer can be monitored. Electrical pressure transducers offer many advantages including the ability to be able to continuously measure pressure change using an automatic logging system (Dowd and Williams, 1989), good reproducibility and high precision. De-aired water is used to fill the tensiometer system as the use of non de-aired water may result in the release, by degassing, of unwanted gasses leading to a reduced efficiency in the response of the system.

When tensiometers are installed a good contact is required between the soil and the porous cup. Contact with the soil is important for a number of reasons: if a good contact does not exist at the porous cup end there is a possibility that the cup may dry out and thus allow gas to enter the system. A space around the cup would result in a false reading of matric potential that would not be equivalent to the actual surrounding soil. Spaces along the sides of the tensiometer may act as bypass flow paths for fluid to travel along, resulting in a false increase in the movement of water towards the ceramic cup end. To avoid artificially

induced flow along the sides of the tensiometer a number of techniques have been used including; back filling the space surrounding the tube with either soil or bentonite (Cassel and Klute, 1986), installing the instrument at an angle of 30° (Lord and Shepherd, 1993) or even installing the instrument horizontally.

4.2.1. Principle of Operation.

The fluid inside the tensiometer reaches a hydraulic equilibrium with the surrounding soil water across the porous interface. Fluid migrates across the interface along an energy gradient, moving from an area of high to lower energy. As the soil surrounding the tensiometer drains, its energy potential decreases with respect to the fluid in the tensiometer, fluid therefore moves out of the tensiometer into the soil until a balance is regained. Outward migration of fluid from the tensiometer results in a suction in the system. Conversely as the surrounding soil becomes saturated its energy potential with respect to the energy level in the tensiometer increases and fluid migrates into the tensiometer from the surrounding soil, increasing the pressure inside the system (i.e. decreasing suction). The energy status of the fluid inside the tensiometer reflects the changing energy status of the surrounding soil water once hydraulic equilibrium is reached.

The conditions required for hydraulic equilibrium can be described as a potential (Cassel and Klute, 1986). A number of factors influence the hydraulic potential: two forces act on the fluid in a tensiometer, gravity and pressure, of which pressure can be subdivided into pneumatic and matric. Of these forces the gravitational potential in the tensiometer and in the soil water adjacent to the tensiometer are equal. The only forces that may effect the pressure in the tensiometer are adsorptive forces and an inequality between gaseous soil pressure and external atmospheric pressure. In a swelling soil a fourth pressure can be identified, that of external load or overburden load.

4.2.2. Spatial Sensitivity.

The suction recorded by a tensiometer is an average of a range of suctions to which the cup is exposed (Cassel and Klute, 1986). The size of the cup will effectively limit what is recorded by the tensiometer (Bouma *et al.*, 1982; Hendrickx *et al.*, 1994). Bouma *et al.* (1982) found that large cup tensiometers responded quickly to irrigation water while smaller cups displayed a delayed response. The rapid response of the larger cups was linked to the influence of macropore channels that they intersected. A single macropore may represent a large proportion of an intersected area and will bias the result in favour of the suction present in the macropore. The smaller cups because of their size tended to be located in the soil matrix between macropores. As the size of cup is increased it has been shown that the variability of soil water tension measurements decreases (Hendrickx *et al.*, 1994). The most widely used tensiometer has a reactive surface area of 42.3 cm^2. Hendrickx *et al.* (1994) suggest that this size (42.3 cm^2) is well below the REV and therefore will result in a high level of variance.

4.2.3. Response Time

The response time of the tensiometer system determines the temporal sensitivity of the system. The response of the tensiometer is a measurement of the soil water potential (matric potential) including the effects of pneumatic forces, adsorptive forces and overburden load. This measurement is used to determine direction and rate of flow as detailed in Chapter 6.

The porous cup of the tensiometer has two important characteristics, bubbling pressure (point) and cup conductivity. Both of which are limiting factors in the system. The bubbling pressure is the point at which gas is able to move through a wet porous cup, and is a function of the largest pore in the cup. The cup conductance, K, has been defined

(Towner, 1980) as the volume of liquid crossing the porous interface per unit time across a pressure or energy gradient. Cup conductance is the primary determinant of the rate at which soil water and tensiometer fluid equilibrate.

The measurement of soil matric potential in the tensiometer is not instantaneous. The speed at which the system equilibrates with the matric potential of the surrounding soil is known as the response time of the system. The response time of the system is inversely related to cup conductivity and gauge sensitivity, the conductivity of the soil in which the tensiometer is placed also has an effect on the systems response time (Klute and Gardner, 1962). The rigidity of the materials that the tensiometer is constructed from and the compressibility of the fluid inside the system, effects the gauge sensitivity.

The porous interface between the soil and the tensiometer induces a disturbance to flow of fluid across the interface. For the tensiometer to record the 'true' soil suction the soil must be capable of storing and transmitting water with sufficient speed to smooth out the disturbance.

There are a number of factors which influence the response of the system. These include, soil hydraulic conductivity, unwanted gas entry into the system, altitude and diurnal temperature fluctuations.

4.2.4. Automated Tensiometer System.

The use of an automated tensiometer system increases both the spatial and temporal resolution that can be achieved. Automation increases the number of observations that can be made in a fraction of the time it takes a manual sampling system (Dowd and Williams, 1989; Nyham and Drennon, 1990). An improvement in spatial resolution can be achieved

either by increasing the size of the cup used or by increasing the number of observations made (Hendrickx *et al.*, 1994). Increasing the number of observations has been restricted by practicality in collecting large quantities of data manually and the expense of electrical equipment. Systems have been developed that have overcome both of these problems. A single transducer may be linked to a number of tensiometers via a scanivalve fluid switch (Chappell, 1990) thus increasing the number of observations at a minimal cost. The use of electrical pressure transducers either singularly or as part of a scanivalve system can improve the temporal resolution. An electrical pressure transducer such as the solid-state sensor used by Nyham and Drennon (1990) senses changes in pressure within the tensiometer by a diaphragm that flexes as pressure changes which results in a voltage out put that is proportional to pressure. For detailed observations of hydrological soil events which may change constantly a sampling interval must be sensitive to rapid changes. By using transducers in conjunction with electrical scanning and data storage systems the temporal resolution of tensiometer data can be vastly improved (Dowd and Williams, 1989). In manual sampling tensiometers may only be practically read once or twice a day while automated collection can read tensiometer response continuously. The only delay in an automated system is the response time of the tensiometer system (as explained above) and the time it may take to complete a scan of all tensiometers within the system. The other main advantage of an automated system that includes data acquisition is that data is collected in a digital format that is ready for processing.

4.2.5. Tensiometer System Design used in this Experiment.

Matric potential was determined using eight tensiometers, which were installed in the soil block from the side, so that there was no direct pathway from the top horizon to lower horizons. An access channel was augered which was the same width as the tensiometer. Before installing the tensiometers a slurry of silt was injected into the channel as

recommended by Lord and Shepherd (1993). The silt was used to create a tight contact between the tensiometer and the surrounding soil, as discussed in Section 4.2. Plates 4.1 and 4.2 illustrate the quality of the contact made between tensiometers and soil in this experiment. The tensiometers were installed at an angle of 10° above horizontal to ensure that the porous cup would remain flooded at all times.

The tensiometers were located in the soil profile at depths of 10 cm, 25 cm, 45 cm and 60 cm (from the soil surface). The positioning of the tensiometers (Figure 4.1) (as well as the suction cup lysimeters, Figure 4.5) represented locations within areas of both artificial fracturing due to the mole plough (tensiometers 1, 2, 5 and 6, Figure 4.1) as defined by Leeds-Harrison *et al.*(1982) (Section 1.2.1.), as well as locations where only natural channels would occur (tensiometers 3, 4, 7 and 8, Figure 4.1). Tensiometers 1, 2, 5 and 6 were approximately 20 cm away from the major 'leg' fissure. There were two tensiometers installed at each depth, one either side of the mole drain so that spatial variability at similar levels could be observed. The tensiometers were installed in excess of one month prior to the start of the first experiment so that they had time to settle in the soil.

The construction of the tensiometer (Figure 4.2) consisted of porous ceramic cups attached to various lengths of PVC tubing using Araldite adhesive. A 90° bend was attached to the external end of the tensiometer so that it could be filled with de-aired water and more importantly so water would not be lost from the system. A neoprene bung was used to seal the external end of the tensiometer. Each tensiometer was fitted with a Honeywell transducer (150PC series flow-thru pressure sensor), through the neoprene bung. The transducers were monitored by a Campbell 21X data logger, using a configuration similar to the one described by Dowd and Williams (1989). The millivolt response of the tensiometer was converted to equivalent cm head of suction (H_2O) using calibration curves.

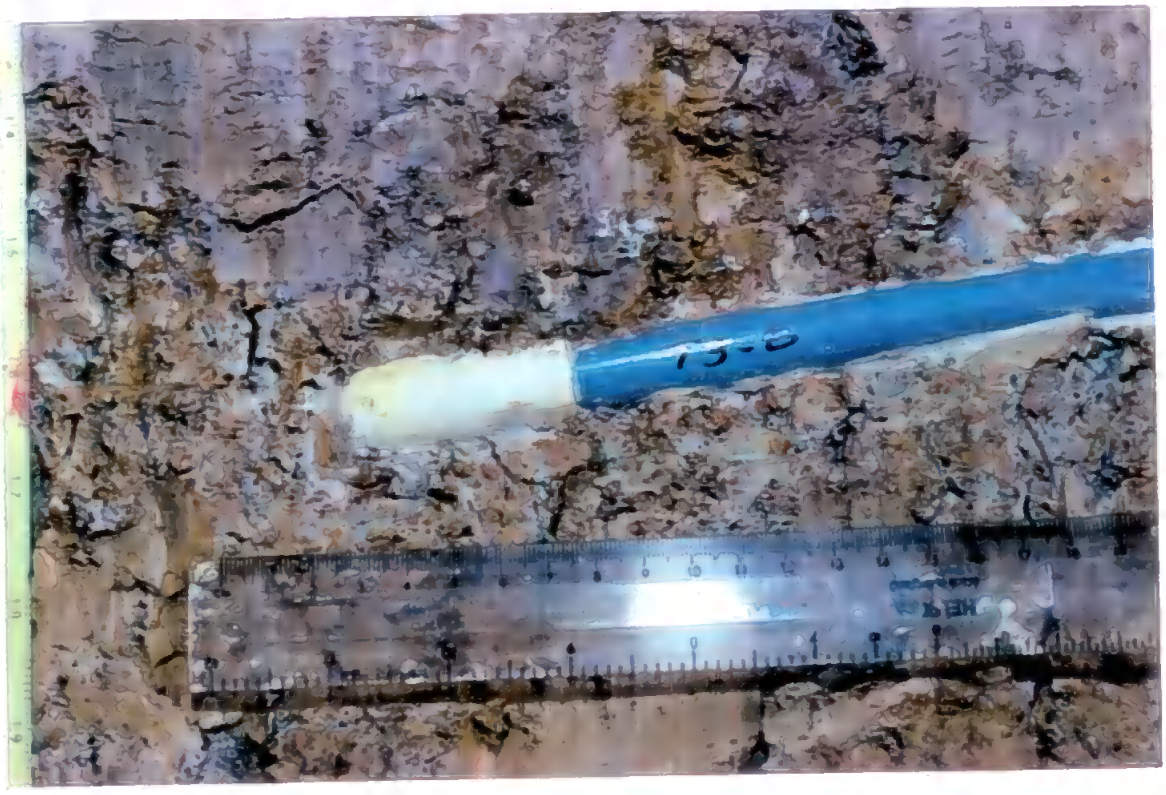

Plate 4.1 - Illustration of the contact between a tensiometer cup and the soil.

Plate 4.2 - Examples of tensiometers in the soil profile.

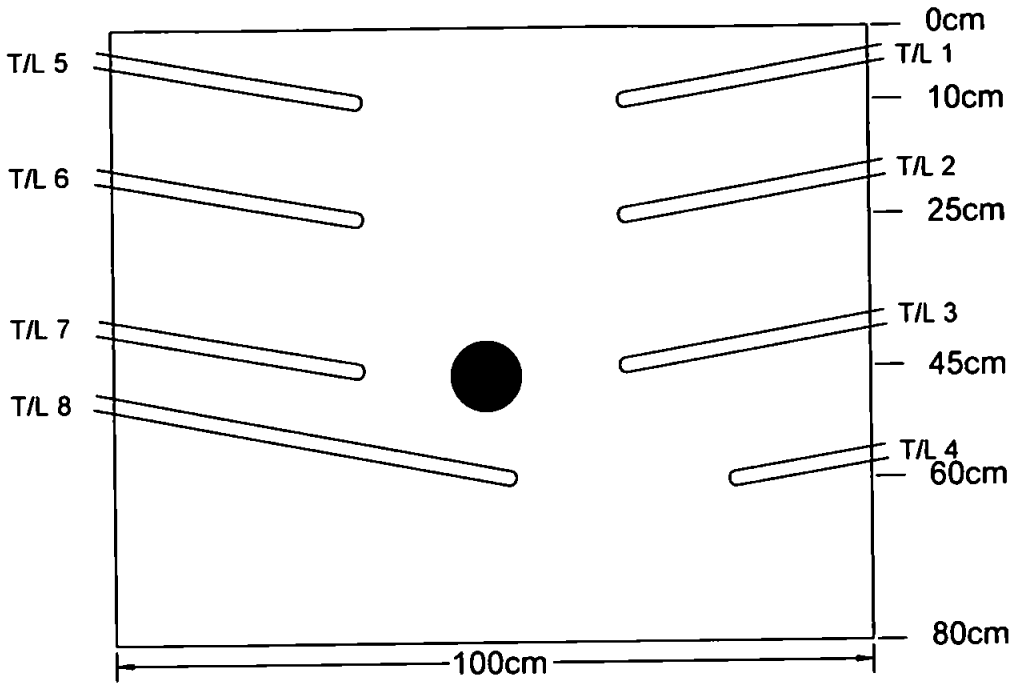

Figure 4.1 - Location of tensiometers in the soil section.

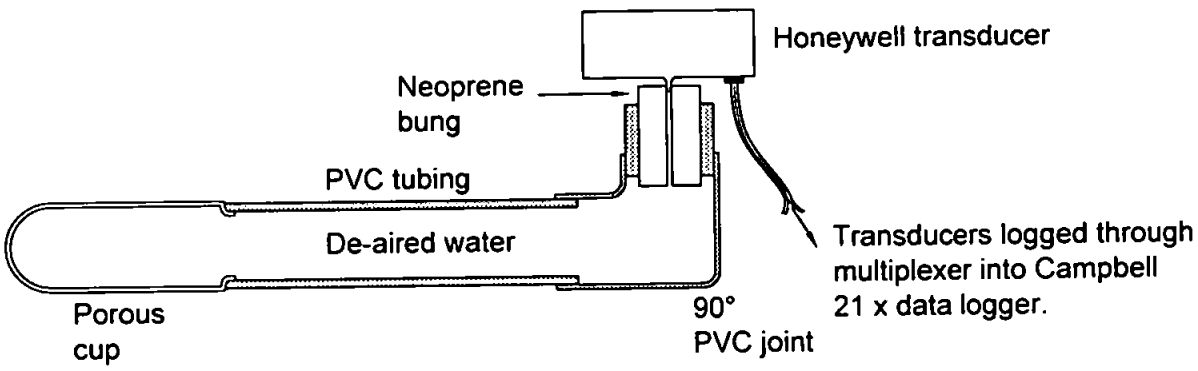

Figure 4.2 - Tensiometer and transducer.

Each of the tensiometers used in this experiment were individually calibrated (the calibration equations are presented in Appendix C). The calibration was carried out over the range 0 - 300 cm head of water using 10 cm intervals from 0 - 100 cm and 50 cm intervals from 100 - 300 cm. The transducers were calibrated through the logging system described below to reduce any error that may be incurred if any part of the system was altered.

The experiment described in this thesis used a combination of electrical pressure transducers and data acquisition system to automatically monitor tensiometer response at a 10 minute interval. Honeywell pressure transducers were attached to each tensiometer and were connected back via a AM 32 multiplexing board to a Campbell 21X data logger. The multiplexing board allowed up to thirty two inputs (transducers) to be linked to one logger. The data logger controlled when the multiplexing board started to switch from one transducer to the next, how quickly it stepped through, the number of recordings made in each pass through and where the data was stored in the logger. The Campbell 21X logger can be programmed to step through the multiplexing board at any time interval exceeding the time needed to complete the stepping sequence. The logger recorded and stored the millivolt response of each transducer in sequence. The program used in this experiment is shown in Appendix B. The millivolt response was stored in a SM 192 Solid State Storage Module connected to the Campbell data logger via a SC 9-pin Peripheral Cable. The storage module was periodically down loaded to a computer using a RS 232 interface. The information was down loaded as an ASCII coma deleted file which was imported directly into a spreadsheet where the data was manipulated.

For the purposes of this research the transducers were stepped through every 10 minutes. Such a short repeat interval time was used so that a fine resolution response could be

observed. Subsequent data analysis and results were more selective in actual time intervals used once established responses had been completely understood.

4.3. TIME DOMAIN REFLECTOMETRY.

Soil water content is an important variable within a soil as it affects other physical soil properties, for example, hydraulic conductivity and pore size available to conduct water and solute. Under field conditions water content continuously changes. In laboratory column experiments the ability to be able to control and monitor soil water conditions is paramount to the successful modelling of the system.

Techniques used to measure soil water content have included thermogravimetric method, gamma ray attenuation method, neutron probe and time domain reflectometry (TDR). Of the former the thermogravimetric method entailed removing a core of soil while both the gamma ray attenuation and neutron probe involved potentially harmful emissions of radiation. In more recent years the TDR approach to soil water measurements has become increasingly popular as it allows *in situ* nondestructive measurements of volumetric water content to an accuracy of $\pm$ 0.01 m^3 m^{-3} (Ledieu *et al.*, 1986). The use of TDR in the determination of dielectric permittivity of liquids was first discussed by Fellner-Feldegg (1969). The method has become well established since then in determining soil water content (Topp *et al.*, 1980; Smith and Patterson, 1980; Topp and Davis, 1985; Heimovaara and Boulten, 1990).

TDR is used to determine the volumetric soil water content by the measurement of the velocity of propagation of a high-frequency electromagnetic signal, in the form of a voltage pulse, through a soil. The TDR is synchronized via a timing control unit which measures the difference in time between pulse emission and reflection. The pulsar produces an

electromagnetic signal which travels along a 50Ω co-axial cable, transmission line, and terminates in a parallel pair of steel waveguides embedded in the soil. Some reflection of the signal occurs at the junction between the transmission line and the waveguides. The remaining signal propagates through the soil guided by the waveguide and is reflected back at the end of the waveguide which represent the end of the open circuit. The reflected signal is picked up by the receiver inside the TDR and the signal trace is displayed on an oscilloscope screen. The x-axis of the oscilloscope represents time. The apparent distance/time between the two points of reflection is a function of the relative permittivity of the soil surrounding the waveguide, as the distance increases so too does the time interval, represented between the two points of reflection, and is a function of dielectric constant.

Figure 4.3 shows an example of a signal trace as it may appear on a screen (Topp and Davis, 1985). Point A represents the point on the trace where the waveguide enters the soil. Point B represents the point at which the signal is reflected at the end of the waveguide. The distance between point A and B is the measurement of the time it has taken the signal to propagate through the soil.

Soil water content has the most dominant dielectric constant, air having a dielectric constant equal to 1, solids 4, and pure water 80 (Baker and Lascano, 1989). Thus a measurement of the dielectric constant of soil is a good measurement of its volumetric water content. In soil there is a simple relationship between propagation velocity and dielectric constant as described by Topp and Davis (1985).

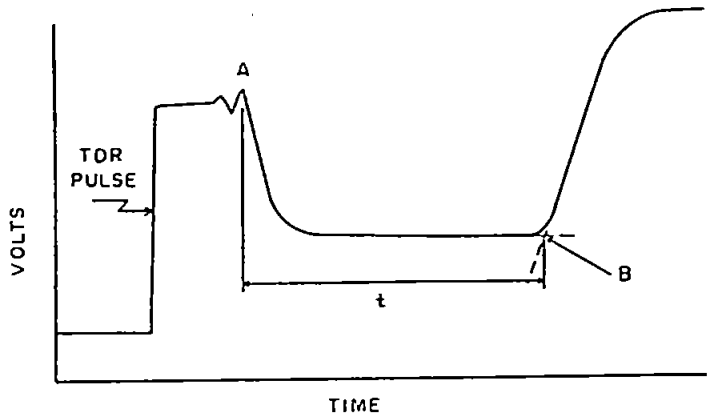

Figure 4.3 - Idealized TDR output trace showing how the propagation time is determined (Topp and Davis, 1985).

Topp and Davis (1985) concluded that dielectric constant (K) is only weakly dependent on soil type, density, soil temperature and pore water conductivity. Topp *et al.* (1980) formulated an empirical equation from which volumetric water content of the soil, θ_v, could be calculated:

$$\theta_v = -5.3\times10^{-2} + 2.9\times10^{-2}K - 5.5\times10^{-4}K^2 + 4.3\times10^{-6}K^3 \quad (4.1)$$

Work by Topp *et al.* (1980) showed this procedure to be insensitive to variations in bulk density, temperature, salinity and mineral composition. This implies that a single empirical calibration curve (volumetric water content verses apparent dielectric constant) can be generally allied to nearly all soil types.

The main advantages of the TDR system are; its nondestructive nature, the speed at which measurements can be made, and its ability to measure water content and soil salinity at the same time.

4.3.1. Sample Volume and Spatial Sensitivity of a TDR System.

Changes in soil water content may vary over a short distance, due to the influence of cracks, biopores and textural layering. The spatial sensitivity of the TDR system depends on the volume of soil sampled and how this volume compares to the REV.

Topp and Davis (1985) described the cross-section of soil sampled by wire guides as an ellipse with vertices at the rods and an approximate sampling area of 3800 mm^2, for waveguides with a 50 mm separation. However, Baker and Lascano (1989) suggest that the sensitivity is largely confined to a cross-sectional area of approximately 1000 mm^2 surrounding the waveguide, with a 50 mm separation, although limited sensitivity extends possibly as much as 3500 to 4000 mm^2. The width of the region of sensitivity normal to the plane containing the waveguide is approximately 30 mm. Knight (1991) suggested that the sampled volume is bias towards the transmission line elements. Sensitivity ends abruptly at the end of the waveguide, therefore, changes in water content just beyond the end of the waveguide have no discernible effect on the signal. Sampling is therefore considered to be uniform along the length of the waveguide but diminishes away from the probe. As the length and spacing between the guidelines increases the resolution of the TDR system decreases. Work by Topp and Davis, (1985) has shown a centre to centre spacing of 50 mm to be a practical compromise estimating this spacing to sample a cross section of 3800 mm^2 and volume sampled to be directly related to the length of the waveguide. In this experiment therefore each pair of rods (40 cm long), according to the above calculation, would represent a sample volume of 1540000 mm^3. Two probe

waveguide samplers were chosen as they sample a larger volume than other systems that implement three probe waveguides (Whalley, 1993).

4.3.2. Speed of Sample Acquisition.

The speed at which values of soil water content needs to be established depends on the prevailing soil water variability. In a field experiment soil water varies continuously both spatially and temporally. Under such conditions quick repetitive observations of soil water content are essential to be able to make detailed assessments of the processes that occur. Under steady state laboratory experiments spatial and especially temporal variations in soil water content will be minimised and therefore the speed of repetitive observation is lessened.

System designs have been improved recently to include fully automated TDR programmes (Baker and Allmaras, 1990; Heimovaara and Boulten, 1990; Wraith *et al.*, 1993). Such systems allow rapid repetition of observations at one particular site and by incorporating a switching mechanism (Baker and Allmaras, 1990) can be used to monitor a multiple of sensors. Automated systems can also be used to capture and store traces for later reference and/or analysis (Dowd *et al.*, pers. com.). The inclusion of waveform analysis programs within the computerised set up permits less subjective interpretations of the waveform to be made (Wraith *et al.*, 1993). Subjective interpretation of waveform made during manual sampling of TDR results can be problematical when more than one person is collecting the readings.

4.3.3. TDR System Design used in this Thesis.

Fourteen pairs of 3 mm diameter, 40 cm long, stainless steel TDR probes were installed in each block with each probe being placed 5 cm apart from its accompanying waveguide.

The co-axial transmission line was attached to each probe by creating a 2 - 3 mm split in the top of the probe in which one side of the transmission line was placed before being crimped and soldered to secure the connection. The other side of the transmission line was attached to the second probe in a similar fashion allowing sufficient flexibility for the probes to be spaced 5 cm apart. Each pair of probes, which constituted the waveguide, was then carefully hammered into the soil takeing care to keep the probes horizontal as well as parallel with its accompanying probe. The positioning of the probes was made easer by using a wooded guide rail. The use of two probe rather than three probe waveguides (Whalley, 1993) or even four probe waveguides (Zegelin *et al.*, 1989) was used as it gave good results in the form of a clear trace. The TDR probes were not impedance balanced (Spaans and Baker, 1993) as a strong signal had been achieved without, both in previous experiments (Addison, 1995) as well as this experiment. The trace allowed the top beginning and end of the waveguides to be easily defined (Figure 4.3). The waveguides were distributed evenly in the horizons relating to the fracture zone created by the mole plough and at similar heights in the soil profile to those of the suction lysimeters and tensiometers, as shown in Figure 4.4. The location of these probes parallel to the mole drain and at different distances away from the mole drain, allowed an average measurement of soil water condition to be made at a known distance away from the mole through time.

The system was semi-automatic in that the TDR probes were linked via a stepper motor, which was stepped by a computer, to a Tektronix 1502C model cable tester. Under the steady state experimental conditions bulk soil water content changed very little and therefore results from the TDR system were only collected once a day. A value for distance (D) was calculated from the wave trace and the representative volumetric water content calculated using Topp's Equation (4.1).

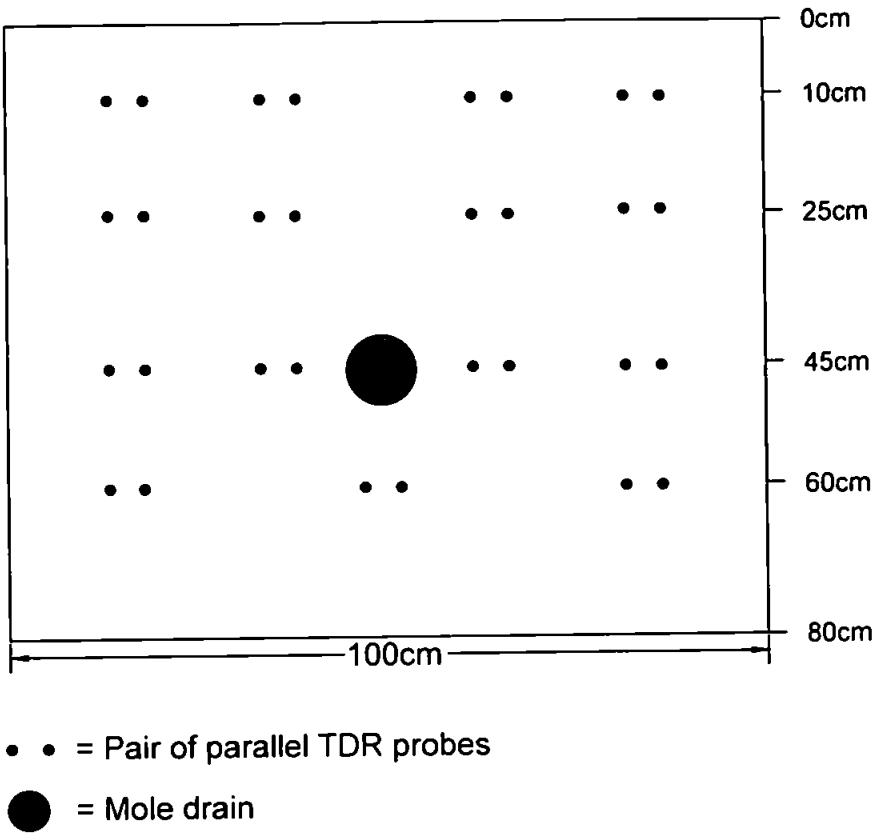

Figure 4.4 - Location of TDR waveguides in the soil section.

4.4. SUCTION CUP LYSIMETERS.

The ability to directly observe detailed movement of solute through the soil has involved the use of traceable substances (Reeves and Beven, 1990). Direct observation of tracers can lead to the clarification of solute pathways from the interpretation of chemical breakthrough curves and mathematical models (Chapter 1 and 7). An ability to sample *in situ* changes in tracer concentration, through time, is essential to the interpretation of spatial and temporal variations of solute movement at the microscale.

The use of a porous ceramic interface has been used in soil physics since 1904, developed initially by Briggs and McCall (1904) to continuously sample soil water solutes, *in situ*. The technique of using porous material, in the form of a porous ceramic cup, to sample soil solute has been referred to as, a porous tube device, tension lysimeter, ceramic points,

tension-free lysimeter, pan and deep pressure vacuum lysimeters, vacuum extractor, soil water sampler, porous ceramic sampler, soil water extractor, and suction and free-drainage soil solution sampler or lysimeter (Litaor, 1988). In this thesis porous ceramic cups will be referred to as suction cup lysimeters.

Suction cup lysimeters are constructed of hydrophillic materials with fine pores, the most common material used is ceramic. A suction is induced in the sampling system, drawing water and solute into the sampler through the porous ceramic wall. Water will flow from the soil through the ceramic wall until the 'capillary' pressure (suction) in the suction cup lysimeter and in the soil are equal. The suction that can be applied to the system is limited by the air entry value of the system, which is dependent on the largest pore. Schubert (1982) expressed this function as (Grossmann and Udluft, 1991):

$$P_c = -2\sigma(T) \cos a \ (rgD_1)^{-1} \times 10^{-9} \qquad (4.2)$$

Where, p_c is capillary pressure (MPa), σ is surface tension (N m^{-1}), T is temperature (°C), a is contact angle, r is radius of the pore (m), D_1 is density of the liquid (kg dm^{-3}) and g is the gravitational constant (m s^{-2})

Care is needed when the instrument is installed to insure a good contact is made between the soil and the sampler, an auger of similar diameter to the probe is therefore used to create an access tunnel. To increase contact and to prevent hydraulic short circuiting a slurry of either sieved fine material removed from the hole or fine quartz silt is injected into the access tunnel before the sampler is installed (Grossmann and Udluft, 1991).

The use of suction lysimeters for soil solute sampling has a number of advantages over other methods as well as disadvantages:

Advantages:

1. The simple design allows for a relatively low cost construction.
2. Installation of the instrument is not complicated and causes only minimal disturbance to the soil profile (especially when installed horizontally).
3. Samples can be drawn continuously at several depths in the profile simultaneously.
4. The method is less destructive than taking individual soil samples and does not require the sample site from which the sample is analysed to be destroyed.
5. The sampler can be left *in situ*.

Disadvantages:

1. The unknown soil volume over which the sample is drawn means that only a qualitative judgement of solute movement can be made, not a quantitative one.
2. Its relatively small surface area compared to the extensive spatial variability of the soil. Macropores may bypass the suction cup lysimeter leading to a unrepresentative sample being taken (Shaffer *et al.*, 1979).
3. The sample taken may be chemically altered by the sampling system. Sorption can be minimised by prewashing the instrument with dilute hydrochloric acid and then rinsing with a nutrient solution similar to the one encountered in the field (Debyle *et al.*, 1988).
4. The removal of large quantities of water by sampling may accelerate downward flow (Lord and Shepherd, 1993).

4.4.1. Sampling Volume.

The suction cup lysimeter can be regarded as a point source of suction which samples a spherical volume (Hemmen, 1990; Grossmann and Udluft, 1991).The recharge area of a suction cup lysimeter is dependent on distance from the ceramic cup, capillary pressure in the soil, the strength of applied suction, diminishing suction in the system, the diameter of the ceramic cup, pore size distribution of the soil, and depth of installation (Wood, 1973; Rhodes, 1986; Grossmann and Udluft, 1991). Grossmann and Udluft, (1991) used the above assumptions to produce an estimate of recharge area of between 0.1 m and 0.5 m. They suggested that the larger the sample pulled the better the spatial resolution but the greater the disturbance caused to water movement within the soil. To reduce the volume of water being channelled from fine pores into larger pores, due to artificial drainage created by the removal of water from the soil to the suction cup lysimeter, Grossmann and Udluft (1991), have suggested that the withdrawn sample volume should be as small as possible and that the sample should be taken over very short time interval, giving a high spatial and temporal resolution to the sampling.

Soil water chemistry is not homogeneous throughout the soil mass (England, 1974). Water collected from large pores at low suctions may have a chemical composition different from water held more tightly round smaller pores. Grossmann and Udluft, (1991) argue that the permeability of the cup should be in excess of the permeability of the saturated soil. The potential gradient generated by the suction cup lysimeter acts on all pores, however, sampling is limited by the suction value of the cup, capillary pressures above this suction will not be sampled. The flow rate from different pore sizes will also vary depending on the diameter of the pores. A quantitative value for the sample pulled by the suction cup lysimeter is not possible because the volume of soil the water sample was extracted from is unknown. This is especially true of a diminishing suction because at initially higher

suctions soil solution will be extracted from fine pores as well as larger pores, but as suction decreases over time the sample becomes more biased towards larger pores where the water is held less tightly. The spatial variability of soil properties is often underestimated. An understanding of which pore water is being sampled for any given matric potential and water content within the soil is needed to provide an accurate interpretation of what is being sampled (Biggar and Nielson, 1976).

4.4.2. Speed of Sampling.

The applied suction in the suction cup lysimeter and the unsaturated permeability of the soil will determine the sampling rate. The more uniform the permeability, the more uniform the flow rate. The time required to collect a water sample varies with suction applied, hydraulic conductivity of the medium and water content of the soil (Rhodes, 1986). Severson and Grigal, (1976) argue that a short extraction time would result in a sample that represents water moving through macropores and held at tensions of 10 kPa or less, where as a sample taken over a longer time period would represent solutes held at higher suctions, approaching that applied to the ceramic cup (45 kPa). Others argue that suction cup lysimeters will preferentially sample mobile solutes held at lower potentials (Hemmen, 1990). Hansen and Harris (1975) found that to reduce sample variability it was necessary to have a short sample interval, uniform sampling lengths, and the same initial vacuum for all samplers.

The use of automated collection and analysis systems, using suction cup lysimeters, has been restricted in the past because of available technology. The adaption of a suction cup system so that solute can be collected whilst suction is maintained within the suction device has been developed by Chow (1977). More recent developments have included not only the external collection of solute from the lysimeter system but also a method to allow

continuous chemical analysis of the solute as it is collected (Marshall, 1994; Holden *et al.*, 1995a). The continuous sampling of solute as it is collected using a flow through spectrophotometer, developed by P. Worsfield at The University of Plymouth, has been successfully adapted to a field plot scale experiment (Holden *et al.*, 1995a & b). Such a continuous monitoring system allows very fine temporal observations of solute transport to be made.

4.4.3. Design of Suction Cup Lysimeter System used in this Experiment.

For this experiment eight porous suction cup lysimeters were installed, 10° off horizontal, in each block at levels in the soil identical to that of the tensiometers (Figure 4.5). Although it was not necessary to install the lysimeters at an angle of 10° by so doing it meant that both the tensiometers and lysimeters had been installed in an identical manor. This design enabled a comparison of water and chemical movement down through the soil profile through time to be made.

The construction of the suction cup lysimeter used in this experiment was similar to the design of the tensiometers (Figure 4.6). Porous ceramic cups, with outside dimensions of 2 cm width by 5 cm length, and a pore size of 20μm (products of the Soil Moisture Corporation, Santa Barbara, California) were attached to ridged PVC tubing, with a smaller diameter sample collection tube inserted down the centre of the rigid tube into the ceramic cup. The smaller tube enters the rigid tube through the neoprene bung which seals the lysimeter system. Some designs incorporate a second small tube into the bung so that lysimeter can be evacuated separately to were the sample is collection. However, a suction within the system can also be achieved successfully with a single tube. The single tube also has the advantage that any residual solute is removed when a suction is applied and therefore less contamination between samples will occur. A suction of 40 cm mercury (53

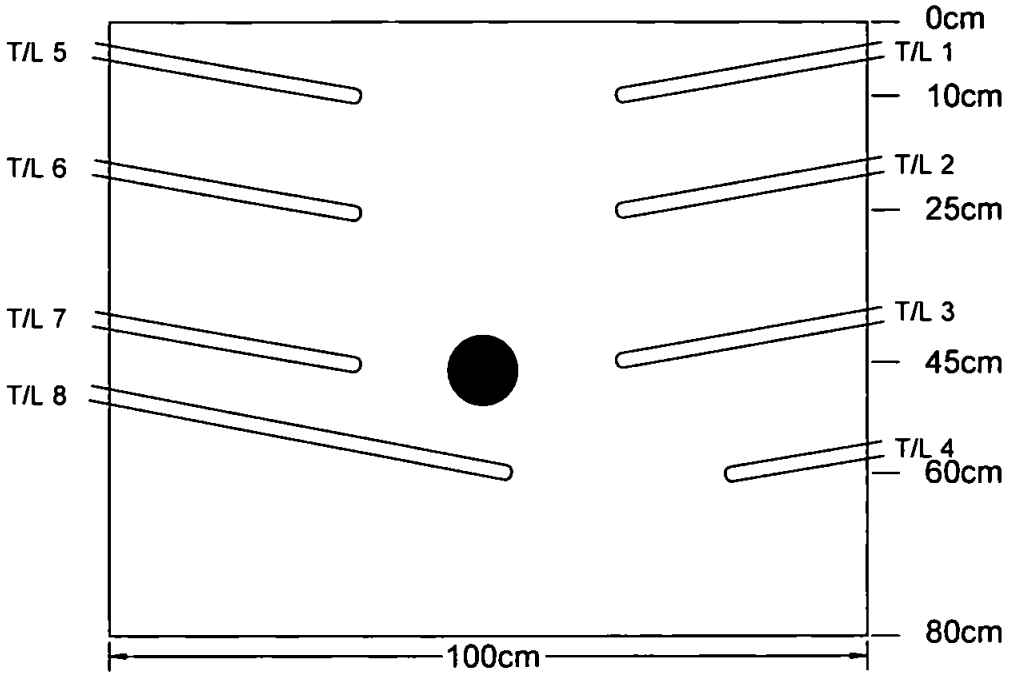

Figure 4.5 - Location of suction cup lysimeters in the soil section.

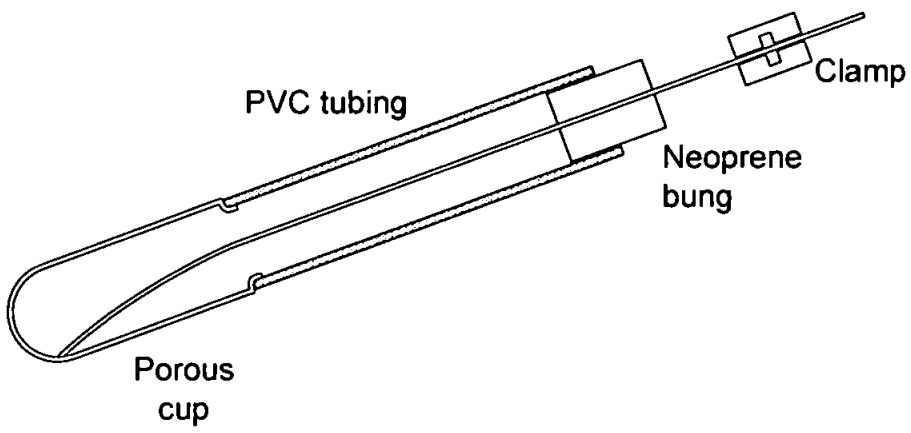

Figure 4.6 - Suction cup lysimeter.

kPa) was applied to all lysimeters and the samples were collected every 4 hours. A 4 hour interval was chosen as it was sufficiently frequent to be sensitive to chemical concentration changes through time, as well as allowing a sufficient volume of sample to be collected from all of the lysimeters (a minimum of 2 ml was needed for analysis) and was also considered to be a practical time interval for manual collection over a prolonged time period.

4.5. TRACER EXPERIMENTS.

Tracers are important when trying to interpret the movement of solutes and water through soil. The use of 'conservative' tracers such as chloride and stable isotopes are of particular importance in tracing water pathways as the isotopic composition of a particular volume of water will not change unless mixed with water of a different isotopic concentration.

Work by Kluitenberg and Horton (1990) has highlighted the importance of detailed description of solute tracer application to a soil containing macropores. They observed that the method of application directly affects the subsequent transport of solutes through the soil.

For this experiment two different types of tracer application were used. The first was a miscible displacement of tracer were the soil water in the block was replaced by water with a known tracer concentration (100 mg l^{-1} or 250 mg l^{-1} chloride). The second application was a pulse of tracer containing 2500 mg l^{-1} Cl and 500 mg l^{-1} NO_3, applied in a litre of water sprayed onto the surface of the block so that no ponding occurred, followed by the start of irrigation with tap water 15 minutes later.

4.5.1. Sampling Locations and Analysis.

Water samples were collected during the experiment from the suction cup lysimeters, mole drain, irrigation system and from below the block (i.e. sample that accumulated on top of the sand table). Samples were chemically analyzed for chloride and total oxidised nitrogen (T.O.N.) using a Technican mark 3 auto analyzer.

The concentration of the samples were determined by a process of colorimetry. Colorimetry is a process where-by the proportion of absorbed light of the appropriate wave length (λ) is measured and is directly proportional to the concentration of the chemical being analyzed. Samples were stored in a frozen state and analysed as soon as possible after the end of each experiment to limit deterioration. Freezing the samples had no determinable effect on the chemical properties of the sample. Previous experiments at North Wyke on nitrate storage has shown that freezing does not effect the chemical composition of the sample (North Wyke, Nitrate experiment, Unpd,. 1993)

Chloride (Cl) concentration measured on the auto analyzer depends on the formation of ferric thiocyanate ions during the reaction between mercuric thiocyanate and chloride. In the presence of the ferric ion, the liberated thiocyanate forms a deep red colour ferric thiocyanate that is in proportion to the original chloride concentration, concentration of chloride is measurable by colorimetry at 480 nm. Chloride can be detected with an accuracy of ± 0.11 mg l^{-1} within the rang of 0 - 20 mg l^{-1} in which chloride variation is linear using the auto analyzer. Where sample concentrations exceeded this limit samples were diluted by a factor of 1 in 10. Some of the higher concentration samples were diluted by a factor of 1 in 20.

Total oxidised nitrogen (T.O.N.) concentration (i.e. nitrate plus nitrite) was measured using

the auto analyzer by the reduction of nitrate to nitrite through a copper-hydrazine reducing reagent. The amount of nitrite is measured by the coupling of N-1-naphthylethylene diamine dihydrochloride (Nedd) and the diazo compound formed during the reaction between nitrite and sulphanilamide. The reaction produces a reddish-purple azo-dye, the intensity of which determines the concentration of nitrite when measured at 520 nm. Total oxidised nitrogen (T.O.N.) can be detected with an accuracy of ±0.008 mg l^{-1} within the range of 0 - 0.5 mg l^{-1} using the auto analyzer. When concentrations exceeded the observable limits a dilution factor of 1 in 10 was used.

The breakthrough curves produced from the samples collected during this experiment are presented and discussed in detail in Section 7.7.

4.6. SUMMARY OF INSTRUMENTATION.

Table 4.3 summarises the instrumentation used in this experiment and gives a brief outline of what part it played in the observation of water and solute movement through the soil.

The preceding chapters have formed the introduction to this thesis including; background information on the topics under consideration, the experimental design of the thesis and of the experiment itself. The following chapters comprise the experimental observations including; soil structure (Chapter 5), soil water movement (Chapter 6) and solute transport through the soil (Chapter 7). Chapter 8 links the three separate components of Chapters 5, 6 and 7, accentuating the importance of multi-technique methods to the detailed interpretation of how and why water and solutes move through the soil.

Table 4.1 - Instrumentation used in this experiment.

Instrument	Scale/sample area	Soil property observed
Tensiometers	Surface area ≈ 42.3 cm^2	Changes in soil suction. Observations made at 10 min. intervals for eight locations in each block.
Time Domain Reflectometry	Cross section of 3800 mm^2	Changes in soil moisture. Observations taken daily from fourteen locations within the soil block.
Suction cup lysimeters	Cup size ≈ 2 cm width by 5 cm length. Applied suction ≈ 40 cm mercury (53 kPa).	Collection of *in situ* solute samples used in combination with tracers to monitor change in known concentration through time. Data interpreted using BTC and models to predict solute pathways travelled.

CHAPTER 5.

SOIL STRUCTURE.

5.1. INTRODUCTION.

The main objective of the research presented in this thesis was to investigate variability of soil water movement and to determine the mechanisms which influence water and solute movement through a soil. The presence of cracks, channels or spaces around and between soil peds is the most important factor controlling water and solute movement (Booltink, 1993) as described in chapter 1. Soil structure is a rather vague term which can be used to describe qualitatively the shape of soil aggregates, for example 'very coarse prismatic' or 'fine sub-angular blocky' (Soil Survey Staff, 1975). The pore space between the peds is generally ignored in a field description. Such a visual interpretation although being important for characterising different soil types provides no detailed (quantitative) information as to pore size distribution, shape of pores or connectivity of pores within the soil profile. Quantitative data of these properties is important when interpreting the fate of solutes moving through a soil profile. However, quantification of soil structure is not easy because of the complex nature of soil structure and the problem of the scale of measurement (Newman and Thomasson, 1979).

Quantitative measurements of soil structure have been undertaken by Jongerius *et al.* (1972) and Murphy *et al.* (1977) to describe pore size distribution. Subsequent workers have characterised and measured soil structure, including pore size distribution as well as pore and ped shape, using digital binary images (Moran *et al.*, 1989; McBrantney and Moran, 1990), image analysis techniques (Bullock and Thomasson, 1979; Walker and Trudgill, 1983; Ringrose-Voase and Bullock, 1984; Ringrose-Voase, 1987) and computerised classification and recognition (Holden, 1993).

In this investigation three techniques were used to provide a quantitative interpretation of soil structure:

1. Profile tracing method.
2. Binary transect method.
3. Resinated core section method.

Each of the three techniques provides a different perspective on structure quantification. The tracings provide a vertical impression of macropore (pore diameter >1 mm or 1000 µm) connectivity throughout the 0.8 m^2 soil section. The binary transects provide a finer detailed description of pore size distribution across a 0.8 m width of the soil profile and at regular intervals of depth in the soil, but with no reference as to how the results of one binary transect line may be associated with another. The resinated soil samples provide an image at a microscopic scale (pore diameter between 1000 - 136 µm) of pore space as represented by a horizontal surface in the soil profile. The resinated core section method allowed pore size distribution and cross-sectional shape of pores to be examined but again provided no indication of connectivity of individual pores into other horizons.

The use of profile tracings and binary transects provides a macro-scale representation of pore size distribution. At the macro-scale pore size diameters >1 mm (1000 µm) were examined over an area which was equivalent to the exposed soil profile (vertical soil section 1 m by 0.8 m). Photographs of polished resin core samples facilitate a more detailed (microscopic) interpretation of size and shape of macropores and mesopores. At the micro-scale, pore size diameters in the size range 1000 to 136 µm were observed over an area restricted by sample core size and resolution of image analyzer. The profile tracing and resinated samples were analyzed using a Quantimet Image Analyzer System described later in this chapter.

A variety of measurements are possible using the Quantimet technique but the measurements most used in soil structure classification include mean size, area, length, perimeter, shape and total count. Movement of fluid through and between pores is controlled by the shape of the pores, pore size distribution and connectivity between pore spaces. Classification based on shape can provide an indication of the efficiency of the pores in storing and moving water. Ringrose-Voase and Bullock (1984) used a Quantimet to classify macropores by shape according to a four class system introduced by Brewer (1964). Each of the four classes were considered to have distinct functional properties (Table 5.1). Similarly, Walker and Trudgill (1983) used four size and three shape classes to classify individual pores based on classifications devised by Bouma *et al.* (1977) (Table 5.2). Brewer (1964) and Bouma *et al.* (1977) both use the same group divisions of packing voids, channels, planar voids and vughs. However, the way in which Ringrose-Voase and Bullock (1984) and Walker and Trudgill (1983) used the classification differed. Ringrose-Voase and Bullock (1984) classified pore shape classes using a learning set to 'teach' the computerised system to recognise different pore shapes, while Walker and Trudgill (1983) classified pore shape from the ratio of pore area to pore perimeter squared which requires no learning set to be established. The classification of pore classes based on Bouma *et al.* (1977) (Table 5.2) was used in this experiment because it was easy to calculate and did not require a data set of shapes to be established first. Work by Bullock and Thomasson (1979) has shown measurements of pore size distribution from Quantimet to be akin to results obtained from suction-plates. Walker and Trudgill (1983) have suggested that it should be possible to use Quantimet data to study the effects of pore geometry on the miscible displacement of a tracer through a soil.

This chapter will describe the three techniques employed in this research to quantify soil structure, starting at the macro-scale of the profile tracings and binary transect before

Table 5.1 - Functional properties of the four main pore classes defined by Brewer (1964) (cited in Ringrose-Voase and Bullock, 1984).

Pore Class	Functional Properties
Packing voids	These pores allow rapid movement of water through the soil although this may decrease on wetting if the void is formed between aggregates.Minimal storage capacity. Also important for root expansion.
Channels	Important for water movement, may reduce in size on wetting but rarely close completely.
Planar voids	Important for water movement in dry soil but tend to close off when the soil wets up.
Vughs	Main recognised function at present is water storage.

Table 5.2 - Bouma *et al.* (1977) classification of pore size (mean pore diameter) and shape (ratio of area (A) to the square of the perimeter (Pe^2)).

Classification by:	Class	Parameters
Pore size	Class 1	> 1000 µm
	Class 2	1000 - 300 µm
	Class 3	300 - 100 µm
	Class 4	< 100 µm
Pore shape	Class 1 - Rounded voids (channels)	$A/Pe^2 > 0.04$
	Class 2 - Voids with intermediate shape (vughs)	$A/Pe^2 < 0.04 > 0.015$
	Class 3 - Elongated voids (planar voids)	$A/Pe^2 < 0.015$

examining the micro-scale approach based on the resinated core samples. As the amount of detailed information is vast, especially in the binary transect method and resinated core section method, summary tables of the mean results for all vertical soil sections and horizons, for block A and B, are presented in the results first. The summary tables are used to simplify the information to make it more readily interpretable. Detailed tables of individual vertical sections showing individual horizon observations are also presented, after the summary tables, so that discrepancies between the two blocks as well as between profiles are highlighted. The success of the three techniques will be discussed at the end of this chapter.

5.2. MACRO-SCALE.

At the macro-scale pores and cracks with a diameter of ≥ 1 mm (1000 μm), were described over an area of 0.8 m^2. Two methods were used at this scale, profile tracings and binary transects.

5.2.1. Profile Tracing Method.

Tracings of cracks and pores, visible to the naked eye (≥ 1 mm), were made for five vertically exposed soil sections of block A (exposed at a distance of 0, 10, 20, 40 and 50 cm from the outer vertical edge into the block), and four vertically exposed sections of block B (10, 20, 40 and 50 cm from outer edge into the block). Each of the selected vertical soil sections, which are also referred to as soil profiles, was carefully plucked clean to produce a flat surface with minimal smearing or disturbance. A4 sheets of over-head projection paper were pinned to the profile (as shown in Plate 5.1) and the cracks and pores drawn in using sharpened chinograph pencils of different colours to distinguish pores/channels and stones. The technique is very basic and inaccuracies occur due to the thickness of pencil compared to the width of crack. However, connectivity and orientation

Plate 5.1 - Illustration of profile tracing method.

of cracks in the profile are picked out by this method. The individual A4 sheets were joined together and reduced in size, to a scale of 1: 2.8 (cm), so that they could be analyzed using the Quantimet, as explained later in this chapter. Figure 5.1 shows two examples of the reduced profile tracings one from each block. The nine profile tracings are presented in Appendix D.

Analysis of Profile Tracings:

The tracings of the profile were analyzed using a Quantimet 570. Each scanned image covered an equivalent frame area of 4325.765 cm^2 and each pixel in the image had a width of 0.136 cm. Values of area, total number of pores, anisotropy and mean tortuosity were calculated for each profile.

(a)

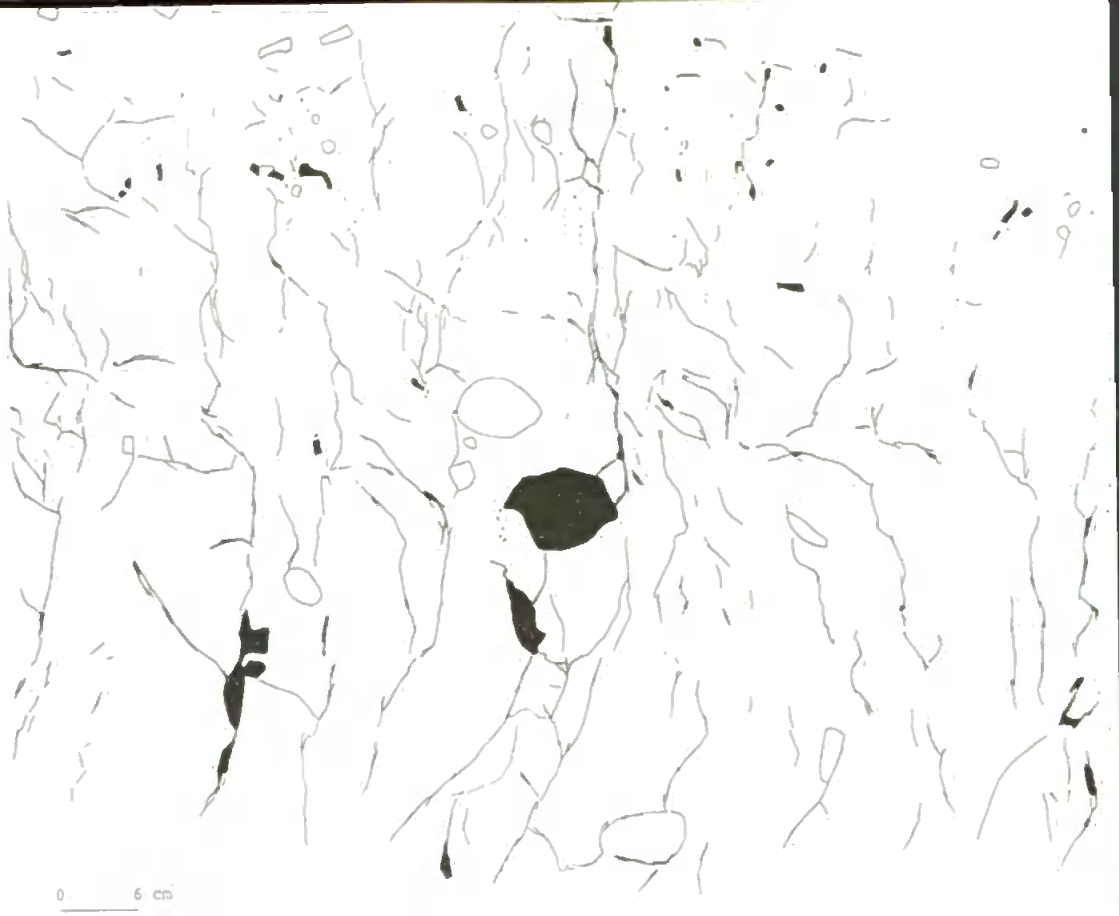

(b)

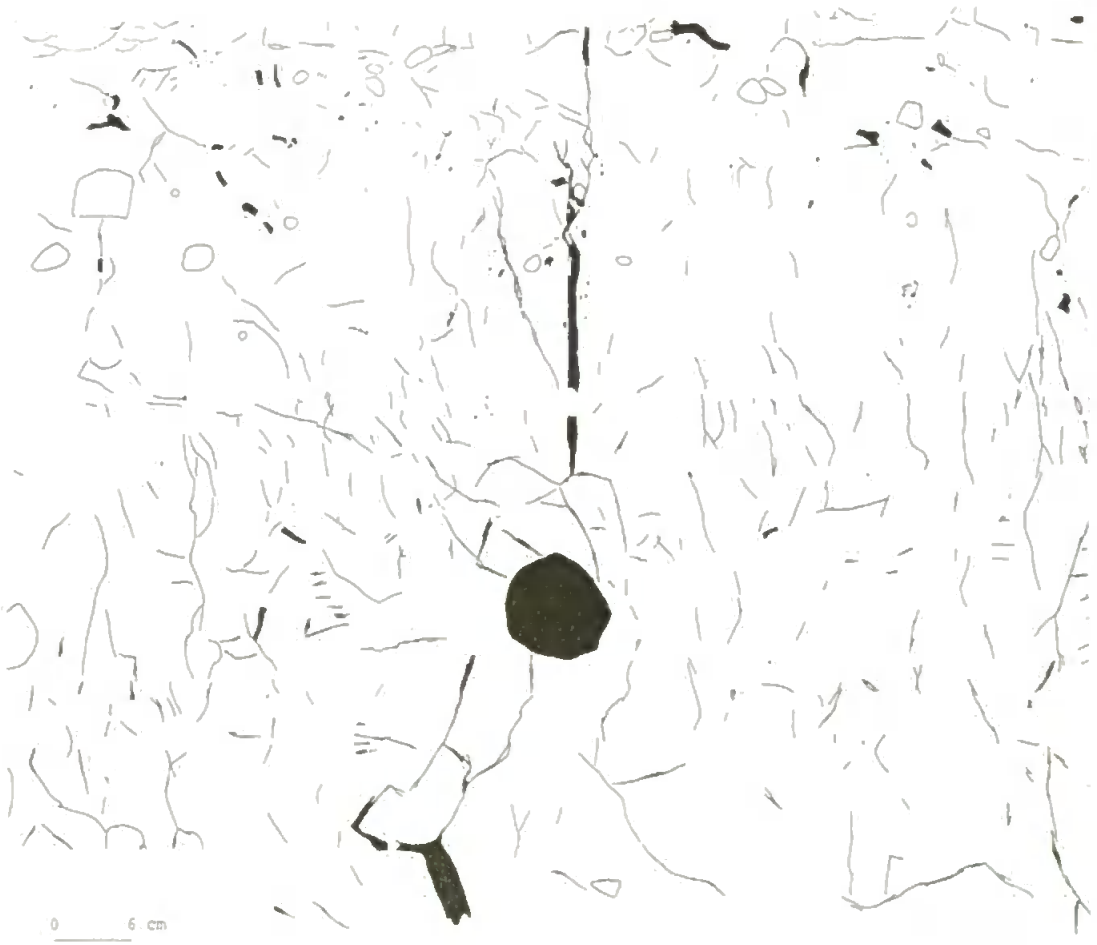

Figure 5.1 - Two examples of profile tracings used in Quantimet analysis for block A (a) and block B (b).

Anisotropy (H/V) is a measurement of vertically (V) intercepted results compared to horizontally (H) intercepted results. As the number of horizontal intercepts increases compared to vertical intercepts it is assumed that there is a more vertically dominant component. Values of anisotropy that are > 1 imply a vertical component while values < 1 imply a more horizontal component.

Tortuosity [L/(P/2)] was calculated assuming the majority of the cracks to be no wider than two pixels. Perimeter (P) was a measurement of actual length of the crack (× 2), while length (L) was a measurement of the shortest distance from start to finish of the crack in a straight line and took no account of deviation of the crack between the two points. Therefore, the closer the value of tortuosity [L/(P/2)] is to 1, the more direct the channel or crack. As tortuosity increases [L/(P/2)] < 1.

Results:

Pore and crack characteristic results based on the profile tracing technique are presented in Tables 5.3 and 5.4 (a and b). A tracing of the vertical section at 0 cm (interface between soil and wax) in block B was not physically possible. A two domain classification was used in which small cracks and pores were defined as those being greater than 1 mm but less than 4 mm and potentially capable of conducting water across their whole cross-sectional area as compared to large cracks, > 4 mm, that were unlikely ever to be totally flooded at the applied irrigation rate (2.76 mm h^{-1}). These results are discussed below.

Table 5.3 - (a) Results of anisotropy (H/V), mean tortuosity [L/(P/2)] and % area of pores, (b) porosity (%), mean porosity (μ) and standard deviation (σ), for profile tracings of block A, at locations of 0, 10, 20 ,40 and 50 cm within the block.

(a)

	ANISOTROPY		MEAN TORTUOSITY		PERCENTAGE AREA OCCUPIED BY PORES (TOTAL COUNT)	
PROFILE LOCATION	small cracks	large cracks	small cracks	large cracks	small cracks	large cracks
0 cm	0.953	0.765	0.80	0.66	5.6 (361)	4.4 (26)
10 cm	1.187	1.325	0.81	0.65	5.3 (331)	2.4 (11)
20 cm	1.15	1.33	0.79	0.66	6.6 (377)	2.8 (11)
40 cm	1.33	1.653	0.80	0.64	5.7 (344)	4.5 (9)
50 cm	1.189	1.458	0.79	0.65	7.9 (430)	5.3 (17)
	μ = 1.16	μ = 1.31	μ = 0.80	μ = 0.65	μ = 6.22	μ = 3.88
	σ = 0.12	σ = 0.30	σ = 0.01	σ = 0.01	σ = 0.95	σ = 1.10

(b)

POROSITY (%).			
position within profile	small cracks	large cracks	combined porosity of small and large cracks.
0 cm	5.6	4.4	10.0
10 cm	5.3	2.4	7.7
20 cm	6.6	2.8	9.4
40 cm	5.7	4.5	10.2
50 cm	7.9	5.3	13.2
	μ = 6.2	μ = 3.9	μ = 10.1
	σ = 0.9	σ = 1.1	σ = 1.78

Table 5.4 - (a) Results of anisotropy (H/V), mean tortuosity [L/(P/2)] and % area of pores, (b) porosity, mean porosity (μ) and standard deviation (σ), for profile tracings of block B, at locations of 10, 20 ,40 and 50 cm within the block.

(a)

	ANISOTROPY		MEAN TORTUOSITY		PERCENTAGE AREA OCCUPIED BY PORES (TOTAL COUNT)	
PROFILE LOCATION	small cracks	large cracks	small cracks	large cracks	small cracks	large cracks
10 cm	1.045	1.538	0.79	0.70	7.2 (517)	1.7 (5)
20 cm	1.019	1.297	0.80	0.69	5.1 (491)	2.6 (12)
40 cm	1.089	1.649	0.80	0.67	5.5 (418)	1.9 (9)
50 cm	0.871	1.812	0.82	0.60	5.1 (430)	2.4 (6)
	μ = 1.01	μ = 1.57	μ = 0.80	μ = 0.67	μ = 5.73	μ = 2.15
	σ = 0.08	σ = 0.19	σ = 0.01	σ = 0.04	σ = 0.87	σ = 0.36

(b)

POROSITY (%).			
position within profile	small cracks	large cracks	combined porosity of small and large cracks
10 cm	7.2	1.7	8.9
20 cm	5.1	2.6	7.7
40 cm	5.5	1.9	7.4
50 cm	5.1	2.4	7.5
	μ = 5.7	μ = 2.2	μ = 7.9
	σ = 0.9	σ = 0.4	σ = 0.6

Interpretation of Profile Tracing Method Results:

The results of the tests for anisotropy conducted for both blocks suggests a predominantly vertical component to the direction of cracks and channels. However, the values of anisotropy for the small cracks were smaller than those for the larger cracks which suggests that the small cracks would have allowed water not only to move down the soil profile but also across it.

The value of 0.765 for the larger cracks in profile 0 cm, block A (Table 5.3a), implies a predominantly horizontal orientation to the larger cracks and channels in this exposed vertical section. The predominantly horizontal orientation of the larger cracks and channels at the sample location 0 cm into the block can be explained by a large proportion of worm channels which were present in this profile. The worm channels were primarily in the top 20 to 30 cm soil layer where soil conditions must have remained tolerable for the worm population to have survived. The worm channels were more obvious in this profile as it contained the interface between the soil and wax and therefore the worms were more restricted in their direction of movement, either having to re-enter the soil or move along the edge of the soil at the interface. As the soil face at 0 cm did not have to be prepared before the tracing was made, the surface characteristics were undisturbed. Pre-treatment of subsequent vertical sections combined with the less restricted movement for the worms resulted in fewer worm channels being intersected along the long axis of the channel.

Mean tortuosity values of on average 0.8 and 0.66 for small cracks and large cracks respectively imply that for both blocks, cracks and channels, were highly directional (where 1 = straight) with only minor deviations. Variability in tortuosity was only marginally greater for large cracks (σ = 0.027) compared to smaller cracks (σ = 0.009) within the profile. In terms of solute and water movement tortuosity values approaching 1.0 would

imply a relatively rapid movement along primarily vertical pathways. Tortuosity values for the larger cracks indicate that they were less directionally uniform. However, the method for calculating tortuosity is based on several assumptions:

1. Cracks are a maximum of two pixels in width.
2. As the width of the crack increase above two pixels the amount of error in the calculation increases slightly. A larger perimeter will result in a smaller tortuosity value and this finding may account for the discrepancy in the result.

Porosity results show the smaller cracks (in the range of 1 < 4 mm) to have had an average percentage porosity greater than that of the larger cracks (> 4 mm). In block A, 61 %, and block B, 72 %, of porosity was accounted for in the smaller cracks. However, the combined mean porosity of the profiles in block A was 10.1 % and in block B was 7.9 % (Tables 5.3b and 5.4b), giving an average profile porosity for both blocks of 9 %.

In summary blocks A and B had predominantly more vertically orientated cracks than horizontal ones, both with a low tortuosity. Although there was a greater number of smaller than larger cracks in all profiles, the area occupied by the small cracks was only marginally larger, 3 %, than that occupied by large cracks. Block A and B had an average pore area (for small pore and cracks only) of 6.2 % and 5.7 % respectively. However, these values do not take into account the potential for water to flow along the edges of the larger cracks which will allow solute to travel as if in a macropore although the whole channel may not be filled. Compared with the block as a whole it would appear that only a small percentage (6 %) of the total area of the block would be available to preferential flow. To put this in context Beven and Germann (1982) note that an increase of macropore space by 0.002% would more than double potential infiltration capacity.

5.2.2. Binary Transect Method.

The presence (1) and absence (0) of pores and cracks, along an 800 mm horizontal line, across the soil profile, were recorded every 1 mm. Since the results are recorded as a series of 1 and 0 the technique will be referred to as the binary transect method. This method was used in order to quantify the distribution of pore space across, as well as at regular depths in the soil vertical section. Binary transects were made for vertically exposed soil sections at 50 cm, 30 cm and 10 cm into the soil blocks. Transects were located every 5 cm up from the mid point of the mole drain (located at a depth of 45 cm in the vertical section) to the surface with one transect -10 cm below the mole. The location of the transects that correspond to a traced profile at 10 and 50 cm into the block were drawn onto the profile and are presented in Figures D.2, D.5, D.6 and D.9 (Appendix D).

Results of Binary Transect Method:

Moran *et al.* (1989) and McBratney and Moran (1990) used digital analysis of soil structure to produce binary digital images. McBratney and Moran (1990) used their binary image to estimate four characteristics of soil structure. The first and most basic of these was an estimation of porosity based on a single row of binary responses to the presence or absence of a pore space. Porosity as a volume proportion (V_{VP}) was estimated along a line using the Delesse principle, which states that the sum of the individual pixels identified as a pore space (N_P) divided by the total number of pixels along the line (N_T) equals the porosity.

$$V_{VP} = N_P / N_T \quad units^3\ units^{-3} \qquad (5.1)$$

The 800 mm horizontal length of the transect was such that the technique was not amenable to digital analysis, but rather the method described by McBratney and Moran (1990) was

adopted as described above. The difference in scale between this experiment and the one carried out by McBratney and Moran makes direct comparisons of results difficult.

The summary of the results using the binary transect method are presented as mean pore count calculated along the total 800 mm transect line (Table 5.5 a) and mean pore count calculated for 160 mm lengths of transect line (Table 5.5 b). The results are presented for both the whole of the transect line (800 mm) and as subsections of the transect line (160 mm × 5) to establish whether any pattern of variability in the results alters with changing scale of observation.

The results of the binary transect for individual vertical sections are presented in Tables 5.6 to 5.11. Results of pore count are presented for both total transect length (800 mm) and for subsections (160 mm) of the transect. Porosity associated with the pore count are indicated in brackets, calculated using Delesse principle as described by McBratney and Moran (1990). The bottom row of each table represents the transect line taken at -10 cm below the mole, the row above is the transect across the mole at 45 cm and each row above that represents a 5 cm increase in distance above the mole.

Tables 5.6 to 5.11 show the absolute response of pore space (1) along the transect line for each 160 mm segment as well as the total occurrences of pore space for each complete transect line. Although the method used to estimate porosity in this experiment was the same as used by McBratney and Moran (1990) the method is limited as it takes no account of pore size along the line. The analysis tallies the number of occurrences of pore space (1's) identified along the transect line but cannot provide any information on the pore size distribution since only an aggregate total is given, irrespective of location of other pore spaces. The measurement of porosity is thus only an estimate. Table 5.12 to 5.18 present

Table 5.5 - (a) Mean (μ), standard deviation (σ), variability ((μ/σ) × 100) and mean porosity (μ/800) calculated from total pore count along the 800 mm transect line (Tables 5.6 to 5.11). (b) Mean (μ), standard deviation (σ), variability ((μ/σ) × 100) and mean porosity (μ/160) calculated from pore count every 160 mm along each transect line (Tables 5.6 to 5.11). Shaded area represents location of transect line that intersects the mole drain in the vertical section.

(a)

Depth in profile	Mean pore count per 800 mm (μ)	Standard deviation (σ)	Variability, % (σ/μ)	Mean porosity, % (μ/800)
5 cm	215	34.7	16.1	27
10 cm	165.3	28.0	16.9	21
15 cm	158	36.6	23.2	20
20 cm	146.2	40.9	28.0	18
25 cm	166.7	29.8	17.9	21
30 cm	181.8	44.8	24.7	23
35 cm	170.3	23.1	13.5	21
40 cm	157.0	13.7	8.7	20
45 cm	183.2	24.8	13.5	23
55 cm	117.5	43.2	36.8	15
		Mean porosity for profile, %		20.9
		Standard deviation of porosity for profile		3.0

(b)

Depth in profile	Mean pore count for every 160 mm (μ)	Standard deviation (σ)	Variability, % (μ/σ)	Mean porosity (μ/160)
5 cm	43.0	14.8	34.3	27
10 cm	33.1	13.2	39.8	21
15 cm	31.6	14.1	44.6	20
20 cm	29.2	10.8	37.1	18
25 cm	33.3	10.7	32.0	21
30 cm	36.4	11.7	32.2	23
35 cm	34.1	9.7	28.5	21
40 cm	31.4	8.2	26.1	20
45 cm	36.6	26.5	72.4	23
55 cm	23.5	11.5	49.0	15
		Mean porosity for profile, %		20.9
		Standard deviation of porosity for profile		3.0

Table 5.6 - Transects taken 10 cm into block A. Shaded area represents location of mole in the vertical section.

Pore count per 160 mm across profile (Estimate of porosity,%)					Total pore count	Depth
23 (14.0)	8 (5.0)	33 (21.0)	32 (20.0)	22 (14.0)	118	10 cm
20 (13.0)	16 (10.0)	33 (21.0)	31 (19.0)	9 (6.0)	109	15 cm
16 (10.0)	19 (12.0)	28 (18.0)	7 (40.0)	19 (12.0)	89	20 cm
38 (24.0)	23 (14.0)	44 (28.0)	26 (16.0)	8 (5.0)	139	25 cm
42 (26.0)	44 (28.0)	33 (21.0)	52 (33.0)	36 (23.0)	207	30 cm
26 (16.0)	35 (22.0)	38 (24.0)	51 (32.0)	23 (14.0)	173	35 cm
36 (23.0)	24 (15.0)	26 (16.0)	57 (36.0)	13 (8.0)	156	40 cm
13 (8.0)	10 (6.0)	101 (63.0)	11 (7.0)	12 (8.0)	147	45 cm
16 (10.0)	19 (12.0)	22 (14.0)	11 (7.0)	6 (4.0)	74	55 cm

Table 5.7 - Transects taken 30 cm into block A. Shaded area represents location of mole in the vertical section.

Pore count per 160 mm across profile (Estimate of porosity,%)					Total pore count	Depth
21 (13.0)	24 (15.0)	61 (38.0)	13 (8.0)	51 (32.0)	170	10 cm
31 (19.0)	18 (11.0)	44 (28.0)	10 (6.0)	52 (33.0)	155	15 cm
19 (12.0)	21 (13.0)	34 (21.0)	24 (15.0)	10 (6.0)	108	20 cm
22 (14.0)	28 (18.0)	52 (33.0)	25 (16.0)	11 (7.0)	138	25 cm
26 (16.0)	31 (19.0)	19 (12.0)	17 (11.0)	9 (6.0)	102	30 cm
24 (15.0)	24 (15.0)	23 (14.0)	37 (23.0)	20 (13.0)	128	35 cm
26 (16.0)	28 (18.0)	30 (19.0)	24 (15.0)	20 (13.0)	128	40 cm
24 (15.0)	23 (14.0)	90 (56.0)	24 (15.0)	10 (6.0)	171	45 cm
28 (18.0)	11 (7.0)	31 (19.0)	23 (14.0)	17 (11.0)	110	55 cm

Table 5.8 - Transects taken 50 cm into block A. Shaded area represents location of mole in the vertical section.

Pore count per 160 mm across profile (Estimate of porosity, %)					Total pore count	Depth
37 (23.0)	25 (16.0)	59 (37.0)	17 (11.0)	19 (12.0)	157	10 cm
30 (19.0)	28 (18.0)	46 (29.0)	17 (11.0)	20 (13.0)	141	15 cm
26 (16.0)	22 (14.0)	44 (28.0)	26 (16.0)	16 (10.0)	134	20 cm
36 (23.0)	27 (17.0)	33 (21.0)	28 (18.0)	32 (20.0)	156	25 cm
25 (16.0)	31 (19.0)	39 (24.0)	42 (26.0)	36 (23.0)	173	30 cm
36 (23.0)	25 (16.0)	28 (18.0)	36 (23.0)	46 (29.0)	171	35 cm
35 (22.0)	21 (13.0)	45 (28.0)	41 (26.0)	27 (17.0)	169	40 cm
27 (17.0)	48 (30.0)	103 (64.0)	36 (23.0)	15 (9.0)	229	45 cm
49 (31.0)	36 (23.0)	36 (23.0)	32 (20.0)	47 (29.0)	200	55 cm

Table 5.9 - Transects taken 10 cm into block B. Shaded area represents location of mole in the vertical section.

Pore count per 160 mm across profile (Estimate of porosity, %)					Total pore count	Depth
47 (29.0)	44 (28.0)	49 (31.0)	49 (31.0)	68 (43.0)	257	5 cm
27 (17.0)	36 (23.0)	46 (29.0)	30 (19.0)	26 (16.0)	165	10 cm
30 (19.0)	27 (17.0)	54 (34.0)	28 (18.0)	19 (12.0)	158	15 cm
30 (19.0)	36 (23.0)	33 (21.0)	33 (21.0)	31 (19.0)	163	20 cm
30 (19.0)	41 (26.0)	41 (26.0)	35 (22.0)	34 (21.0)	181	25 cm
46 (29.0)	43 (27.0)	42 (26.0)	47 (29.0)	33 (21.0)	211	30 cm
31 (19.0)	35 (22.0)	38 (24.0)	35 (22.0)	24 (15.0)	163	35 cm
36 (23.0)	34 (21.0)	30 (19.0)	34 (21.0)	33 (21.0)	167	40 cm
25 (16.0)	22 (14.0)	81 (51.0)	27 (17.0)	35 (22.0)	190	45 cm
32 (20.0)	29 (18.0)	29 (18.0)	29 (18.0)	25 (16.0)	144	55 cm

Table 5.10 - Transects taken 30 cm into block B. Shaded area represents location of mole in the vertical section.

Pore count per 160 mm across profile (Estimate of porosity, %)					Total pore count	Depth
49 (31.0)	31 (19.0)	40 (25.0)	42 (26.0)	10 (6.0)	172	5 cm
56 (35.0)	32 (20.0)	44 (28.0)	32 (20.0)	50 (31.0)	214	10 cm
47 (29.0)	44 (28.0)	67 (42.0)	42 (26.0)	31 (19.0)	231	15 cm
47 (29.0)	37 (23.0)	46 (29.0)	41 (26.0)	40 (25.0)	211	20 cm
58 (36.0)	42 (26.0)	48 (30.0)	38 (24.0)	39 (24.0)	225	25 cm
57 (36.0)	52 (33.0)	63 (39.0)	38 (24.0)	31 (19.0)	241	30 cm
35 (22.0)	48 (30.0)	55 (34.0)	43 (27.0)	24 (15.0)	205	35 cm
31 (19.0)	35 (22.0)	37 (23.0)	29 (18.0)	29 (18.0)	161	40 cm
41 (26.0)	25 (16.0)	67 (42.0)	33 (21.0)	21 (13.0)	187	45 cm
8 (5.0)	30 (19.0)	13 (8.0)	7 (4.0)	25 (16.0)	83	55 cm

Table 5.11 - Transects taken 50 cm into block B. Shaded area represents location of mole in the vertical section.

Pore count per 160 mm across profile (Estimate of porosity, %)					Total pore count	Depth
32 (20.0)	49 (31.0)	69 (43.0)	22 (14.0)	44 (28.0)	216	5 cm
40 (25.0)	24 (15.0)	41 (26.0)	32 (20.0)	31 (19.0)	168	10 cm
27 (17.0)	21 (13.0)	56 (35.0)	25 (16.0)	25 (16.0)	154	15 cm
35 (22.0)	28 (18.0)	52 (33.0)	24 (15.0)	33 (21.0)	172	20 cm
32 (20.0)	31 (19.0)	39 (24.0)	39 (24.0)	20 (13.0)	161	25 cm
29 (18.0)	32 (20.0)	40 (25.0)	22 (14.0)	34 (21.0)	157	30 cm
38 (24.0)	40 (25.0)	51 (32.0)	18 (11.0)	35 (22.0)	182	35 cm
39 (24.0)	33 (21.0)	37 (23.0)	22 (14.0)	30 (19.0)	161	40 cm
24 (15.0)	22 (14.0)	58 (36.0)	17 (11.0)	54 (34.0)	175	45 cm
12 (8.0)	13 (8.0)	41 (26.0)	12 (8.0)	16 (10.0)	94	55 cm

the pore size groupings based on single, double, treble, quadruple etc. occurrences of pores (1's) (representing pore sizes of 1, 2, 3, 4 and ≥5 mm) that occur along each transect line in each of the profiles. The results are summarised in Table 5.12 and 5.19 and are discussed below.

Tables 5.20 and 5.21 show the calculated porosity per 160 mm section across the block and at specified heights above the mole for block A and B. Calculations for these tables were made using pore sizes between 1 and 4 mm, pore spaces ≥5 mm were disregarded as saturation throughout the block was not reached and therefore it would have been unlikely that these pores were involved in solute transport. Porosity values in bold correspond to positions of suction cup lysimeters and tensiometer in the vertical section.

Table 5.12 - Mean number of pores in each size group and for the total number of pores across the binary transect lines (showing the standard deviation, σ, for the readings), as calculated from Tables 5.13 to 5.18. Shaded area represents location of transect through the mole drain.

Mean number of pores for each size class for both block A and B.						
depth in profile	1 mm (σ)	2 mm (σ)	3 mm (σ)	4 mm (σ)	≥ 5 mm (σ)	mean total number of pores
5 cm	91.3 (10.0)	23.3 (1.9)	7.7 (2.1)	1.7 (1.7)	4.3 (0.5)	128.3 (11.0)
10 cm	70.7 (35.3)	10.0 (6.9)	3.8 (2.1)	3.0 (2.6)	4.0 (2.4)	91.5 (40.5)
15 cm	71.3 (42.1)	13.7 (5.2)	2.7 (1.7)	2.3 (1.7)	4.7 (2.3)	94.7 (42.0)
20 cm	73.2 (48.0)	9.7 (6.5)	3.7 (2.1)	2.2 (1.5)	4.3 (2.9)	93.0 (48.5)
25 cm	78.5 (38.4)	11.2 (4.6)	6.0 (2.2)	2.0 (1.2)	4.5 (2.4)	102.8 (39.4)
30 cm	83.5 (40.3)	12.3 (7.9)	4.5 (1.9)	3.2 (1.9)	6.5 (4.2)	110.0 (44.2)
35 cm	69.0 (29.6)	12.3 (3.9)	5.8 (3.0)	2.5 (1.6)	5.5 (2.3)	96.0 (26.9)
40 cm	62.7 (27.0)	14.8 (2.7)	5.2 (2.3)	2.2 (2.3)	5.3 (3.2)	90.2 (24.6)
45 cm	39.3 (20.1)	9.2 (4.5)	4.7 (1.5)	1.8 (1.1)	4.8 (1.9)	60.0 (22.2)
55 cm	45.8 (19.2)	11.5 (4.9)	4.0 (1.7)	1.8 (1.8)	3.2 (2.0)	66.3 (24.0)
Profile mean (μ)	68.53	12.8	4.81	2.27	4.71	93.28

Table 5.13 - Total number of pores in each pore class (1, 2, 3, 4 and ≥5 mm) along each transect line 10 cm into block A. Shaded area represents location of transect through mole drain.

Number of pores occurring in each pore size group.					Total number of actual pores along each transect.	Depth
1 mm	2 mm	3 mm	4 mm	≥ 5 mm		
22	9	6	2	5	44	10 cm
16	5	6	2	7	36	15 cm
13	2	1	1	9	26	20 cm
34	8	7	1	5	55	25 cm
40	12	7	5	15	79	30 cm
32	15	10	2	8	67	35 cm
64	16	7	1	5	93	40 cm
25	4	3	1	2	35	45 cm
22	2	3	2	2	31	55 cm

Table 5.14 - Total number of pores in each pore class (1, 2, 3, 4 and ≥5 mm) along each transect line 30 cm into block A. Shaded area represents location of transect through mole drain.

Number of pores occurring in each pore size group.					Total number of actual pores along each transect.	Depth
1 mm	2 mm	3 mm	4 mm	≥5 mm		
25	1	7	0	8	41	10 cm
18	17	3	4	8	50	15 cm
19	10	7	2	6	44	20 cm
24	9	5	4	8	50	25 cm
25	2	2	1	8	38	30 cm
34	12	10	1	4	66	35 cm
12	16	3	1	9	41	40 cm
15	3	6	2	7	34	45 cm
22	17	5	0	5	49	55 cm

Table 5.15 - Total number of pores in each pore class (1, 2, 3, 4 and ≥5 mm) along each transect line 50 cm into block A. Shaded area represents location of transect through mole drain.

Number of pores occurring in each pore size group.					Total number of actual pores along each transect.	Depth
1 mm	2 mm	3 mm	4 mm	≥5 mm		
64	1	2	1	4	72	10 cm
70	17	1	1	4	93	15 cm
52	6	5	4	4	71	20 cm
76	6	4	3	5	98	25 cm
78	6	4	5	6	99	30 cm
63	8	3	3	7	84	35 cm
49	19	4	0	10	82	40 cm
27	14	7	2	7	57	45 cm
74	13	6	5	6	104	55 cm

Table 5.16 - Total number of pores in each pore class (1, 2, 3, 4 and ≥5 mm) along each transect line 10 cm into block B. Shaded area represents location of transect through mole drain.

Number of pores occurring in each pore size group.					Total number of actual pores along each transect.	Depth
1 mm	2 mm	3 mm	4 mm	≥5 mm		
94	26	10	4	4	138	5 cm
103	16	4	3	1	127	10 cm
94	14	1	0	4	113	15 cm
97	22	2	4	0	125	20 cm
101	20	8	1	1	131	25 cm
116	27	4	2	4	153	30 cm
91	14	4	5	2	116	35 cm
89	11	7	3	3	113	40 cm
61	15	4	4	3	87	45 cm
60	16	6	1	4	87	55 cm

Table 5.17 - Total number of pores in each pore class (1, 2, 3, 4 and ≥5 mm) along each transect line 30 cm into block B. Shaded area represents location of transect through mole drain.

Number of pores occurring in each pore size group.					Total number of actual pores along each transect.	Depth
1 mm	2 mm	3 mm	4 mm	≥5 mm		
78	22	8	1	4	113	5 cm
104	17	3	8	5	137	10 cm
129	20	3	5	4	161	15 cm
131	13	2	2	5	153	20 cm
129	10	9	2	6	156	25 cm
137	16	7	5	4	169	30 cm
114	18	3	2	4	141	35 cm
92	15	2	1	4	114	40 cm
71	10	3	1	5	90	45 cm
43	11	2	3	0	59	55 cm

Table 5.18 - Total number of pores in each pore class (1, 2, 3, 4 and ≥5 mm) along each transect line 50 cm into block B. Shaded area represents location of transect through mole drain.

Number of pores occurring in each pore size group.					Total number of actual pores along each transect.	Depth
1 mm	2 mm	3 mm	4 mm	≥5 mm		
102	22	5	0	5	134	5 cm
106	16	1	4	1	128	10 cm
101	9	2	2	1	115	15 cm
127	5	5	0	2	139	20 cm
107	14	3	1	2	127	25 cm
105	11	3	1	2	122	30 cm
80	7	5	2	8	102	35 cm
70	12	8	7	1	98	40 cm
37	9	5	1	5	57	45 cm
54	10	2	0	2	68	55 cm

Table 5.19 - Mean porosity as a percentage, %, for each size class as well as a total porosity percentage for pore sizes 1 - 4 mm and 1 - ≥5 mm. Shaded area represents location of transect through mole drain.

	Mean porosity for each size class, as a percentage %.					total porosity	
position in profile	1 mm	2 mm	3 mm	4 mm	≥ 5 mm	1 - 4 mm	1 - ≥5 mm
5 cm	11.4	5.8	2.9	0.9	17.8	21.0	38.8
10 cm	8.8	2.5	1.4	1.5	38.3	14.2	52.5
15 cm	8.9	3.4	1.0	1.2	31.9	14.5	46.4
20 cm	9.2	2.4	1.4	1.1	27.0	14.1	41.1
25 cm	9.8	2.8	2.3	1.0	28.4	15.9	44.3
30 cm	10.4	3.1	1.7	1.6	35.8	16.8	52.6
35 cm	8.6	3.1	2.2	1.3	35.9	15.2	51.1
40 cm	7.8	3.7	2.0	1.1	30.3	14.6	44.9
45 cm	4.9	2.3	1.8	0.9	77.1	9.9	87.0
55 cm	5.7	2.9	1.5	0.9	21.3	11.0	32.3
			Sum of the total porosity			147.2	491.0
			Mean of the total porosity			14.72	49.1
			Standard deviation of the total porosity			2.88	14.0

Table 5.20 - Porosity (%) per 160 mm across block A using binary transect method. Porosity calculated for pore sizes between 1 and 4 mm in diameter. Shaded area represents location of transect through mole drain.

Depth	1 - 160	161 - 320	321 - 480	481 - 640	641 - 800
10 cm	3.8	**9.4**	7.5	**7.9**	11.1
15 cm	13.3	13.4	10.4	6.7	8.3
20 cm	8.8	6.9	10.0	7.3	6.1
25 cm	9.2	**13.4**	9.6	**12.3**	10.6
30 cm	11.9	14.2	8.4	9.2	11.9
35 cm	11.5	12.7	13.6	11.0	13.1
40 cm	11.5	11.2	11.3	16.5	7.3
45 cm	7.3	**5.2**	7.5	**10.6**	6.7
55 cm	9.8	12.3	**8.8**	16.1	**12.1**

Table 5.21 - Porosity (%) per 160 mm across block B using binary transect method. Porosity calculated for pore sizes between 1 and 4 mm in diameter. Shaded area represents location of transect through mole drain.

Depth	1 - 160	161 - 320	321 - 480	481 - 640	641 - 800
5 cm	25.6	23.3	21.7	20.7	13.6
10 cm	23.3	**17.9**	26.3	**19.6**	16.3
15 cm	20.4	19.2	20.0	19.8	15.6
20 cm	21.7	21.0	16.4	19.4	20.4
25 cm	23.1	**21.7**	20.0	**21.9**	18.4
30 cm	24.2	25.2	24.2	20.7	19.0
35 cm	18.8	21.0	17.9	18.6	16.3
40 cm	22.1	17.1	15.2	17.7	16.0
45 cm	14.2	**12.5**	7.3	**15.0**	13.6
55 cm	9.6	12.5	**13.1**	8.8	**13.7**

Interpretation of Binary Transect Method Results:

Summary Table 5.5 shows that mean pore count and hence porosity decreased from the surface to a depth of 20 cm and then generally increased towards the mole. A 20 % increase in variability of porosity was observed between the calculations made from the total pore count along the 800 mm transect line (mean variability 19.93 %) compared to the ones calculated every 160 mm (mean variability 39.6 %) (Table 5.5 a and b). These results indicate the high degree of variability of pore count across the profile associated with a heterogeneous soil. An average porosity of 21 % was calculated, for the combined profiles of block A and B, using the Delesse principle.

Tables 5.6 to 5.11 show a general trend of increasing pore count and thus porosity from the mole upwards. This increase in pore count was not simply restricted to the column directly above the mole but was also evident to either side of the mole. This may be a reflection of either the natural change that occurs in the soil between the upper and lower horizons or it may be a reflection of stress cracking induced by the mole plough. No regular pattern occurs between the vertical soil sections.

Table 5.12 shows the mean number of pores in size group 1 mm to be significantly greater than any other size group. For example from the soil surface down to 35 cm there are on average 6 times more pores recorded in the 1 mm group than in the 2 mm group (Table 5.12). Below 35 cm the difference in numbers of recorded pores, in each size group, reduces as the soil structure changes from 'fine sub-angular blocky' to 'coarse prismatic'.

Tables 5.13 to 5.18 show that the majority of transect rows were dominated by pores that were 1 mm wide with a diminishing occurrence of pores as they increase in size from 2 mm to 4 mm. The occurrence of pores shows a general increase from the transect taken

across the mole towards the surface. This trend is most noticeable in the transect profiles of block B (Tables 5.16, 5.17 and 5.18).

The biggest difference between transect profiles taken from block A compared to block B was that the total number of pores for each transect line tended to be higher in block B (mean 119.1 %) than in block A (mean 60.7 %). This result demonstrates the heterogeneous nature of the soil since soil conditions were similar when the transects were taken and the same technique was used on both blocks.

Mean porosity for the profiles based on pore size distribution are shown in Table 5.19. Porosity calculated from pore size gave a predicted mean profile porosity of 15 % for pore sizes 1 - 4 mm, and 49 % when the ≥ 5 mm pore group was also included. Porosity for the mean profile calculated by the Delesse principle, of 21 %, under-estimates the porosity according to calculations based on pore size distribution. Mean porosity in Table 5.19 increases from the mole (45 cm) towards the surface, with only a slight reduction in porosity between 10 and 20 cm (depth).

Tables 5.20 and 5.21, which show porosity at 160 mm across the blocks and at specified heights above the mole, indicate that block B (Table 5.21) had a larger occurrence of pores in the range 1 - 4 mm than block A (Table 5.20). The mean profile porosity calculated using the values in Tables 5.20 and 5.21 show block B to have had a mean porosity of 18.4 % compared to block A which had a mean porosity of only 10.17 %. From this it may be expected that block B would have a quicker response to tracer application than block A, this will be examined in Chapter 8.

5.3. MICRO-SCALE

5.3.1. Resin Samples.

This technique allowed the number of pores to be counted and characteristics of pores (shape, perimeter and area) to be examined for pores as small as 0.1 mm (100 μm). However, the area of soil under consideration was extremely limited (38.5 cm^2).

Sample Collection and Preparation:

Eight undisturbed soil samples were collected from each of the two blocks. Samples were collected using Pitman Corer tins (38.5 cm^2 × 5 cm), from locations related to the positioning of the ceramic cups of the lysimeters and tensiometers in the profile (Figure 5.2 and Plate 5.2) so that a comparison could be made between soil structure and the data obtained from the suction cup lysimeters and tensiometers at equivalent locations. This comparison will be made in Chapter 8.

The samples were taken back to the laboratory to be impregnated with Crystic resin. The soils were first dried by acetone replacement of water as follows. Samples were immersed in acetone and sealed off to reduce evaporation. After a week the acetone was siphoned off and replaced with fresh acetone. This process was repeated four times. At the end of the four weeks the samples were impregnated with crystic resin (SR17449) which with the addition of a catalyst (methyl ethyl ketone peroxide (catalyst 'o')) hardened the soil sample so that sections could be cut from it using a geological saw (chemicals supplied by B and K Resins Ltd., Bromley, Kent, England). An ultra violet sensitive, fluorescent dye (Uvitex OB) was added to the impregnating mixture so that voids in the soil could be easily distinguished under U.V. light and photographed. The dye was dissolved in acetone and added to the mixture which was stirred for 5 minutes. The mixture was then poured around the edge of the sample to half way up the sample and left to stand for and hour so that the

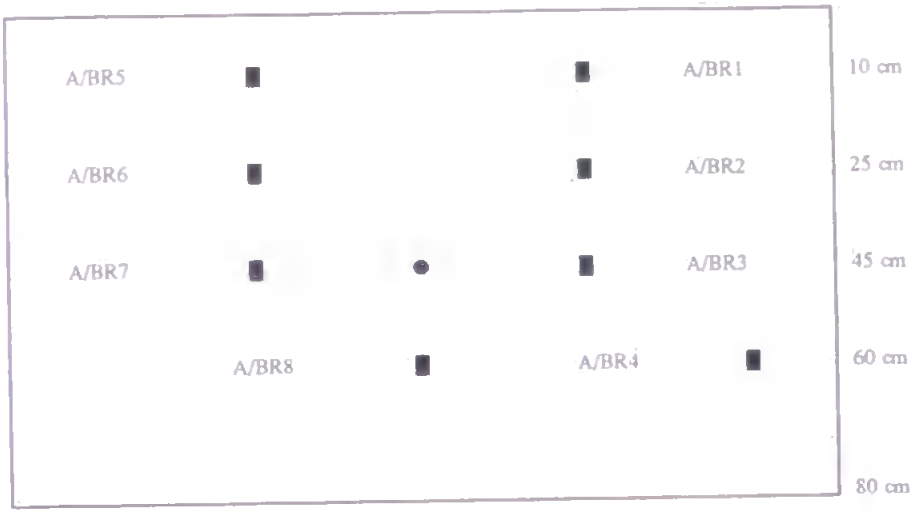

Figure 5.2 - Sample location, in vertical soil profile, of soil cores taken for resinated soil section sampling.

Plate 5.2 - Collection of soil cores for resination sampling.

resin could begin to penetrate by capillary action. The sample was then covered with resin and left to stand until air bubbles had ceased to coming out and then put under vacuum of -700 mbar (0.69 atm) for 12 hours (vacuum diminishing slowly through time). The samples were left to harden in a fume cupboard for 10 -12 weeks during which time loss in volume due to evaporation was replaced by addition of more resin to prevent air re-entering the sample. Once the volume loss was stabilised the samples were left to harden. The samples can be made to harden more rapidly by adding more catalyst, however, allowing polymerisation to occur over a long a period of time as possible reduces the likelihood of cracking occurring within the sample.

Each sample was then cut horizontally into four slices using a geological saw. A problem of cracking occurred when sawing the samples taken from the lower clay rich horizons. Release of internal forces when cut resulted in the sample fissuring, a problem also found when thin sectioning fine sedimentary rock samples. However, this cracking did not affect the results obtained by image analysis as cracking that occurred after resination showed up dark on the photographs whereas cracks in the sample before resination appeared white in the photographs, so that the Quantimet only analysed resin filled cracks. The resin technique used was very successful, impregnating between clay rich particles, as proven by the ability to polish the surface of the sample using water and not oil. If the resin had not impregnated the clay particles the water would have washed the clay out. From each sub-division two faces were selected to be polished and subsequently photographed, using a × 2 magnification, under UV-light following similar procedures as described by Geyger and Beckmann (1967) (cited in Ringrose-Voase, 1987).

A total of 32 photographs were made, representing two photographs for each location in Figure 5.2 and a combined total of eight photographs for each of the four sampling

horizons (10, 25 45 and 60 cm down the profile). Four examples of the photographs are given for depths representing 10 cm and 60 cm for block A (Plate 5.3) and block B (Plate 5.4). All photographs used for analytical purposes are held for reference by Dr. A. Williams (University of Plymouth).

Analysis of Photographs Using The Quantimet:

The photographs were analyzed using a Quantimet 570. Jongerius *et al.* (1972) and Murphy *et al.* (1977) were the first to utilise an image analysis computer, such as Quantimet, in order to measure and characterise soil structure. The Quantimet allows an objective and rapid quantitative measurement of pore size and shape, in 2-dimensions, to be made either from a thin section or from photographs of a flat surface. The image of the soil, formed by a thin section under a microscope or a photograph under an epidiascope, is scanned by a television camera. The signal produced by the scan is sent to a detector module where each pixel of the image is analysed for its 'representative grey-level'. Pores are identified by setting the instrument to detect pixels with a grey-level equivalent to that represented by a pore.

The advantages and disadvantages of image analysis using a Quantimet have been discussed by Bullock and Thomasson (1979) and include the following observations:-

Advantages:

1. Physical measurement of pore features can be directly compared to visual interpretations of samples.
2. The system is not only capable of measuring total pore count but also other parameters including length, perimeter, shape and orientation.
3. Sensitivity of the system is high 500000 points being analyzed in each image.

(a)

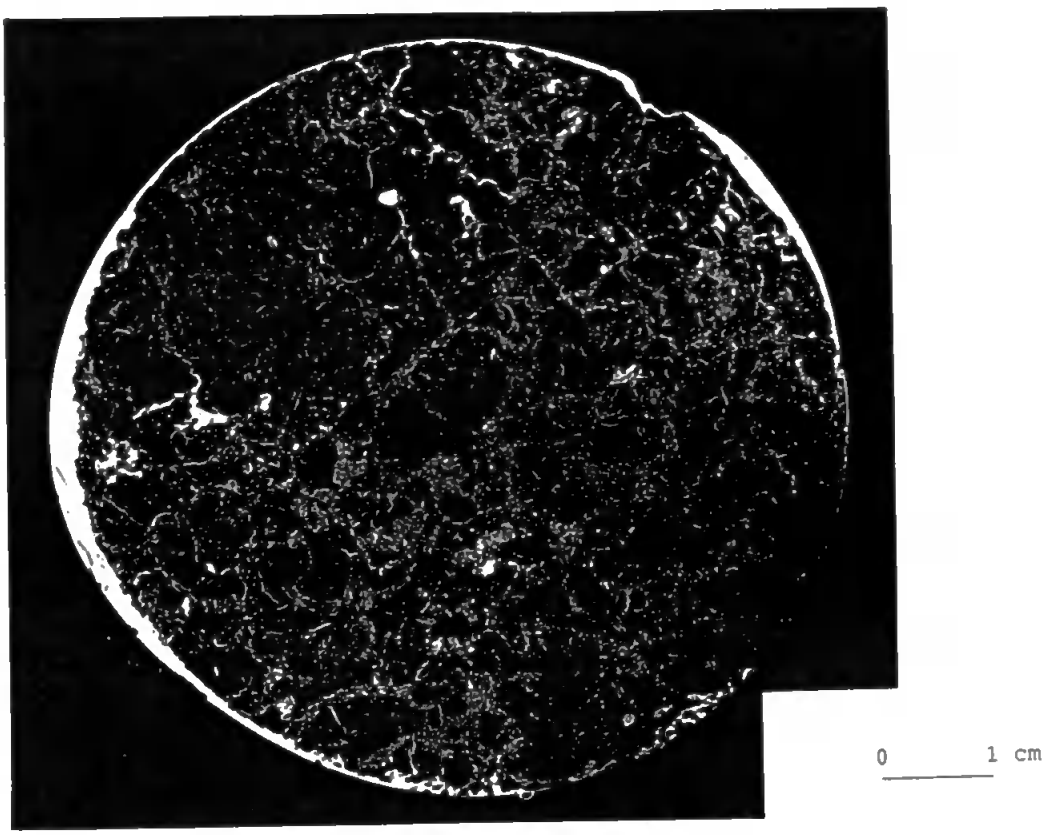

(b)

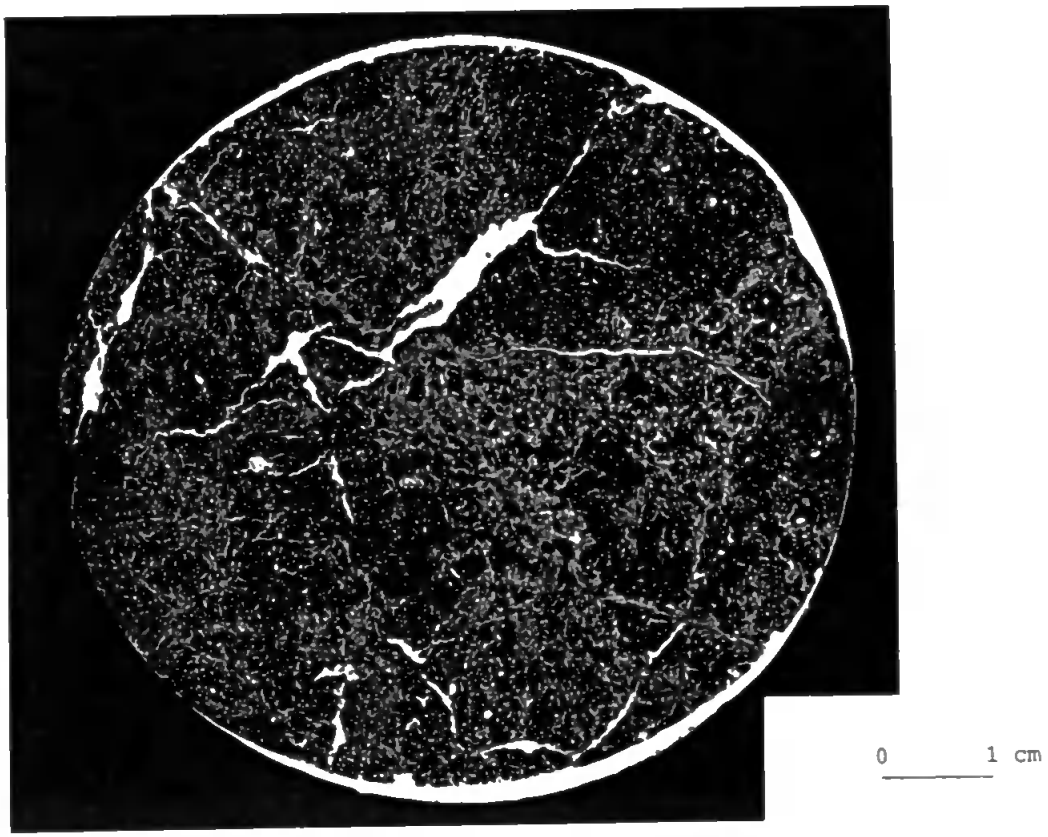

Plate 5.3 - Photographs of resin samples at (a) 10 cm depth, (b) 60 cm depth, in block A.

(a)

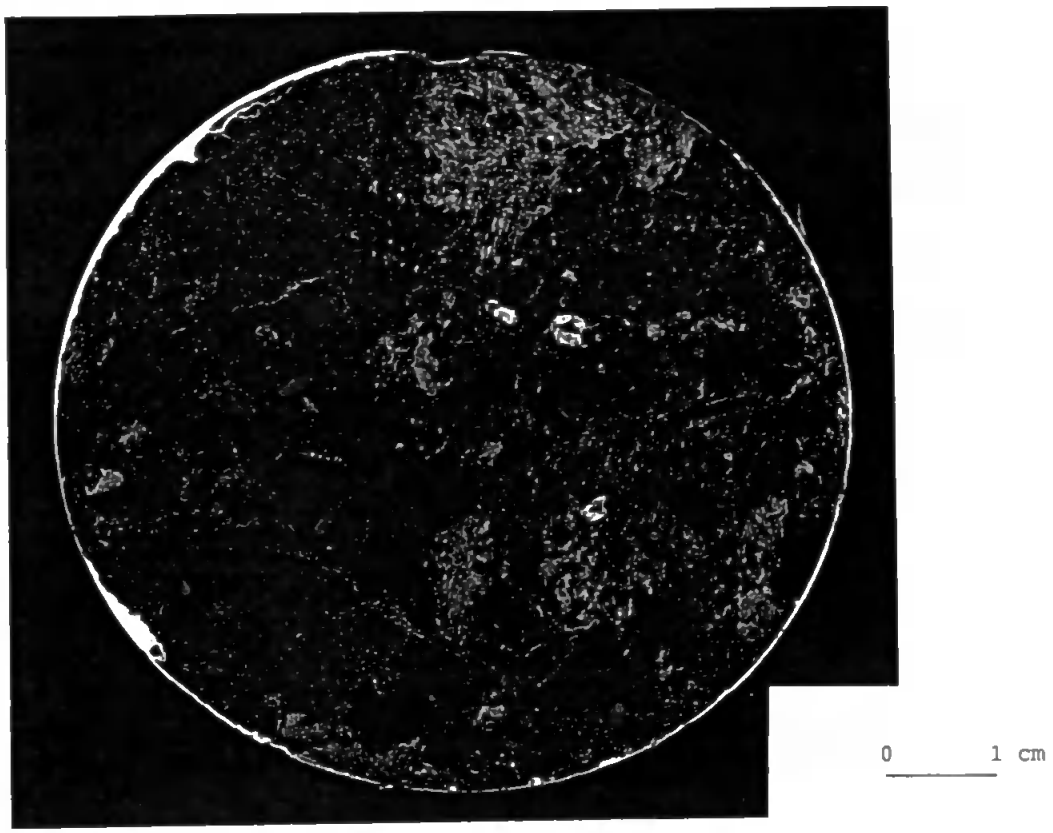

(b)

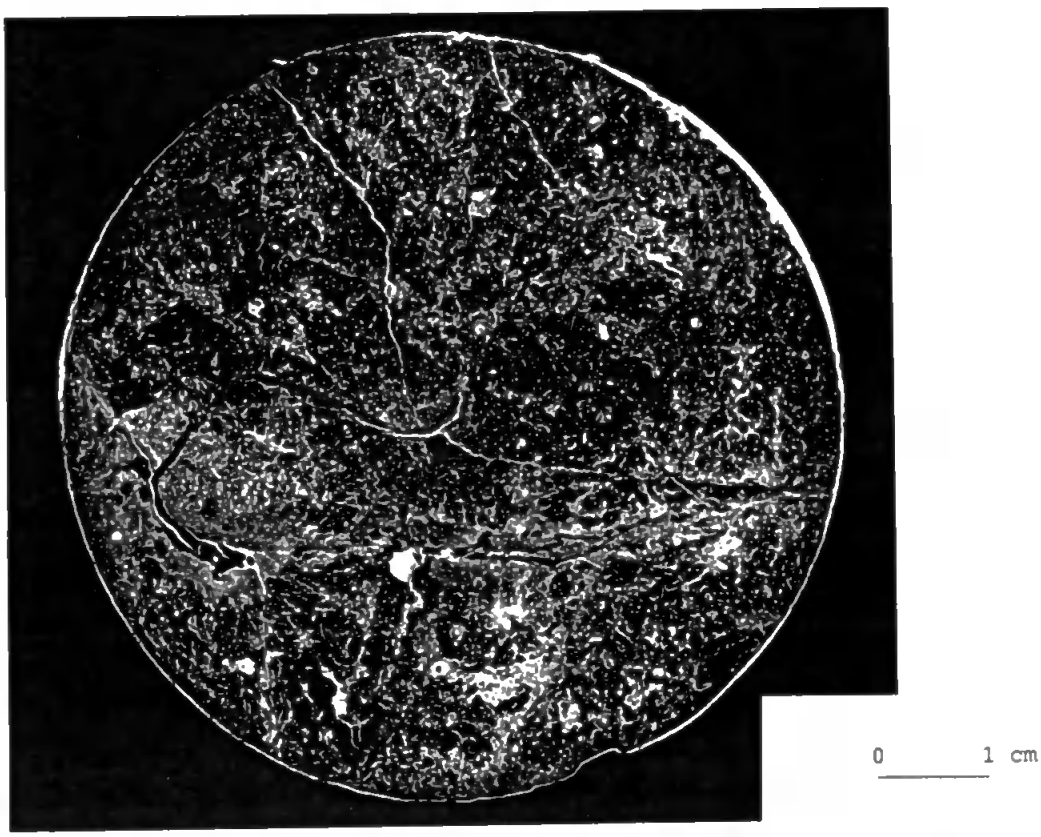

Plate 5.4 - Photographs of resin samples at (a) 10 cm depth, (b) 60 cm depth, in block B.

4. Analysis of the image takes only a few minutes.

Disadvantages:

1. It is only a 2-dimensional interpretation and therefore pores appear as discrete features.
2. Pore space corresponds to time of sampling only.
3. The size of the smallest pore measurable is limited by pixel size.
4. The grey-level response of pores within a sample is selected subjectively by an operator. The size of a pore effects the grey-level response emitted by that pore. A small pore may not appear as brightly as a larger pore and may emit a grey-level lower than defined, for a pore, by the operator. This will result in an inaccuracy in the observed pore count especially of the smaller pores within the sample. Inaccuracies due to grey-level response increase as the range of pore sizes increases within the sample.
5. Size of image may not be appropriate to the variability of pore size within the sample.

An area of 33 mm × 33 mm located around the centre of the sample was looked at, randomly orientated with respect to the horizontal axis of the original block. This frame size gave the most satisfactory image given the wide pore size variability in the samples. Each pixel of the image represented a diameter of 0.068 mm of the sample. The images were analyzed for area, length, perimeter and mean diameter (average of eight diameters) for each pore and a total pore count was made.

Each area was classified according to size and shape as defined by Walker and Trudgill (1983). For each classification the total area, mean area and number of pores were

calculated. The size class was calculated from mean pore diameter and divided into >1000 μm (class 1), 1000 - 300 μm (class 2), 300 - 136 μm (class 3) and < 136 μm (class 4). The smallest classification was 36 μm different from that defined by Walker and Trudgill because of the pixel size used. The shape class was calculated as defined by Walker and Trudgill (1983) according to the ratio of pore area (A) compared to pore perimeter (P) squared (A/P^2). The three classes were divided into >0.04 (class 1, round voids), 0.04 - 0.015 (class 2, voids with intermediate shape) and < 0.015 (class 3, elongated voids).

Results of Resinated Core Sample Method:

For each sampling location indicated in Figure 5.2 two images were analyzed. The results of the analysis are presented as a classification based on size of pore (Tables 5.22 to 5.27) and pore shape (Tables 5.28 to 5.32). The results are discussed below.

Results of Size Classification:

Table 5.22 - Mean values for size classes 1 - 4 (>1000, 1000 - 300, 300 - 136 and <136 μm) calculated from Tables 5.24 - 5.27. Values of mean total area (MTA), mean area (MMA), mean pore count (MPC) and mean porosity (MPr), and standard deviation (σ) for each value. Size classes shown for 10, 25, 45 and 60 cm depth down soil profile from surface.

		Class 1		Class 2		Class 3		Class 4	
		mean	σ	mean	σ	mean	σ	mean	σ
10 cm	MTA	21.0	11.1	19.63	13.13	6.73	4.71	1.02	0.671
	MMA	3.2	1.3	0.18	0.011	0.047	0.001	0.021	0.0003
	MPC	7.0	3.5	108.3	72.48	144.5	101.0	48.38	31.41
	MPr	1.9	1.0	1.8	1.2	0.6	0.4	0.1	0.04
25 cm	MTA	45.26	25.11	38.17	7.30	14.23	2.9	1.89	0.43
	MMA	3.03	1.21	0.16	0.05	0.048	1.17	0.021	0.0003
	MPC	14.38	6.82	213.9	43.02	297.4	63.36	89.13	20.13
	MPr	4.0	2.0	4.0	0.7	1.3	0.3	0.2	0.05
45 cm	MTA	21.97	28.80	17.40	13.80	6.77	3.16	1.30	0.40
	MMA	2.18	2.17	0.18	0.02	0.05	0.002	0.022	0.003
	MPC	7.38	6.58	89.75	64.36	148.9	64.79	59.50	20.40
	MPr	2.0	3.0	2.0	1.0	0.6	0.3	0.1	0.04
60 cm	MTA	28.88	21.78	15.73	7.66	6.86	3.40	1.31	0.49
	MMA	4.61	3.13	0.17	0.01	0.05	0.001	0.021	0.0
	MPC	5.88	2.67	90.88	45.62	147.1	71.36	62.0	23.05
	MPr	3.0	2.0	1.0	0.7	0.6	0.3	0.1	0.05

Table 5.23(a) - Mean total area for all size classes at four depth locations in the soil profile for block A and B combined. Mean porosity given as a percentage.(b) Mean porosity (%) for sampling locations in blocks A and B.

(a)

Depth	Mean total pore area	Standard deviation (σ)	Mean total porosity (%)	Standard deviation (σ)
10 cm	48.36	23.38	4.4	2.1
25 cm	99.55	28.59	9.1	2.6
45 cm	47.44	40.71	4.4	3.7
60 cm	52.75	25.31	4.8	2.3
		Mean porosity for profile	5.7	

(b)

Depth (cm)	Block A		Block B	
10	A5 5.85	A1 5.85	B5 4.5	B1 1.86
25	A6 5.65	A2 11.4	B6 10.5	B2 9.0
45	A7 4.44	A3 10.15	B7 1.85	B3 1.1
60	A8 5.85	A4 7.75	B8 4.0	B4 1.7

Table 5.24 - Area (mm^2), mean area, and number of pores per size class for block A.

SAMPLE	PORE	CLASS 1	CLASS 2	CLASS 3	CLASS 4
AR1	Total area	24.600	46.270	17.049	2.467
	Mean area	2.236	0.180	0.046	0.021
	Total pore count	11	257	367	115
	Porosity (%)	2.3	4.2	1.6	0.2
AR1	Total area	5.232	21.367	9.123	1.586
	Mean area	1.308	0.163	0.047	0.021
	Total pore count	4	131	195	75
	Porosity (%)	0.5	2.0	0.8	0.1
AR2	Total area	52.344	35.617	11.931	1.605
	Mean area	3.272	0.194	0.050	0.021
	Total pore count	16	184	241	76
	Porosity (%)	4.8	3.3	1.1	0.1
AR2	Total area	93.325	37.757	14.521	1.472
	Mean area	4.444	0.180	0.049	0.021
	Total pore count	21	210	299	71
	Porosity (%)	8.6	3.5	1.3	0.1
AR3	Total area	49.229	45.294	12.603	1.667
	Mean area	2.591	0.209	0.048	0.021
	Total pore count	19	217	263	78
	Porosity (%)	4.5	4.2	1.2	0.2
AR3	Total area	85.381	18.592	6.036	1.349
	Mean area	7.762	0.192	0.044	0.031
	Total pore count	11	97	137	44
	Porosity (%)	7.8	1.7	0.6	0.1
AR4	Total area	57.079	16.836	7.812	1.439
	Mean area	5.708	0.170	0.047	0.021
	Total pore count	10	99	167	67
	Porosity (%)	5.2	1.5	0.7	0.1
AR4	Total area	55.724	20.983	8.991	1.823
	Mean area	6.192	0.159	0.047	0.021
	Total pore count	9	132	190	86
	Porosity (%)	5.1	1.9	0.8	0.2

Table 5.25 - Area (mm^2), mean area, and number of pores per size class for block A.

SAMPLE		CLASS 1	CLASS 2	CLASS 3	CLASS 4
AR5	Total area	34.675	23.014	8.304	0.914
	Mean area	3.853	0.178	0.046	0.021
	Total pore count	9	129	180	44
	Porosity (%)	3.2	2.1	0.8	0.1
AR5	Total area	21.210	30.944	7.883	1.132
	Mean area	1.768	0.195	0.048	0.021
	Total pore count	12	159	165	54
	Porosity (%)	1.9	2.8	0.7	0.1
AR6	Total area	5.653	27.251	7.665	1.098
	Mean area	1.131	0.020	0.048	0.021
	Total pore count	5	136	159	52
	Porosity (%)	0.6	2.5	0.7	0.1
AR6	Total area	13.924	48.007	16.750	2.452
	Mean area	1.547	0.172	0.048	0.021
	Total pore count	9	279	350	116
	Porosity (%)	1.3	4.4	1.5	0.2
AR7	Total area	5.052	11.188	5.752	1.023
	Mean area	1.010	0.170	0.043	0.021
	Total pore count	5	66	133	49
	Porosity (%)	0.5	1.0	0.5	0.1
AR7	Total area	27.062	34.131	10.529	1.629
	Mean area	1.691	0.202	0.047	0.021
	Total pore count	16	169	225	79
	Porosity (%)	2.5	3.1	1.0	0.1
AR8	Total area	27.393	24.430	10.894	1.865
	Mean area	6.848	0.167	0.048	0.021
	Total pore count	4	146	228	88
	Porosity (%)	2.5	2.2	1.0	0.2
AR8	Total area	53.959	5.284	2.097	0.720
	Mean area	10.792	0.176	0.047	0.021
	Total pore count	5	30	45	34
	Porosity (%)	5.0	0.5	0.2	0.1

Table 5.26 - Area (mm^2), mean area, and number of pores per size class for block B.

SAMPLE		CLASS 1	CLASS 2	CLASS 3	CLASS 4
BR1	Total area	9.365	3.129	2.826	0.511
	Mean area	3.122	0.174	0.045	0.020
	Total pore count	3	18	63	25
	Porosity (%)	0.9	0.3	0.3	0.5
BR1	Total area	8.347	7.386	2.244	0.213
	Mean area	4.173	0.176	0.046	0.021
	Total pore count	2	42	49	10
	Porosity (%)	0.8	0.7	0.2	0.02
BR2	Total area	48.272	31.063	17.072	1.889
	Mean area	3.713	0.155	0.047	0.021
	Total pore count	13	201	362	89
	Porosity (%)	4.4	2.9	1.6	0.2
BR2	Total area	43.794	35.191	15.922	2.282
	Mean area	4.379	0.171	0.046	0.021
	Total pore count	10	206	344	108
	Porosity (%)	4.0	3.2	1.5	0.2
BR3	Total area	0.961	3.002	2.500	0.900
	Mean area	0.961	0.158	0.046	0.021
	Total pore count	1	19	54	43
	Porosity (%)	0.1	0.3	0.2	0.1
BR3	Total area	2.187	7.201	4.966	0.810
	Mean area	1.094	0.176	0.045	0.021
	Total pore count	2	41	110	39
	Porosity (%)	0.2	0.7	0.5	0.1
BR4	Total area	14.246	10.307	3.390	0.952
	Mean area	2.374	0.198	0.046	0.021
	Total pore count	6	52	74	45
	Porosity (%)	1.3	0.9	0.3	0.1
BR4	Total area	1.472	4.734	2.457	0.568
	Mean area	1.472	0.158	0.043	0.021
	Total pore count	1	30	57	27
	Porosity (%)	0.1	0.4	0.2	0.1

Table 5.27 - Area (mm^2), mean area, and number of pores per size class for block B.

SAMPLE		CLASS 1	CLASS 2	CLASS 3	CLASS 4
BR5	Total area	32.440	13.375	3.996	0.686
	Mean area	3.604	0.186	0.048	0.021
	Total pore count	9	72	84	33
	Porosity (%)	3.0	1.2	0.4	0.1
BR5	Total area	31.934	11.590	2.429	0.644
	Mean area	5.322	0.200	0.046	0.021
	Total pore count	6	58	53	31
	Porosity (%)	2.9	1.1	0.2	0.1
BR6	Total area	49.073	40.470	15.354	2.216
	Mean area	3.775	0.181	0.048	0.021
	Total pore count	13	224	323	104
	Porosity (%)	4.5	3.7	1.4	0.2
BR6	Total area	55.706	49.982	14.611	2.093
	Mean area	1.989	0.184	0.049	0.022
	Total pore count	28	271	301	97
	Porosity (%)	5.1	4.6	1.3	0.2
BR7	Total area	3.698	9.005	3.991	1.027
	Mean area	1.233	0.200	0.043	0.022
	Total pore count	3	45	93	47
	Porosity (%)	0.3	0.8	0.4	0.1
BR7	Total area	2.178	10.813	7.769	2.007
	Mean area	1.089	0.169	0.044	0.021
	Total pore count	2	64	176	97
	Porosity (%)	0.2	1.0	0.7	0.2
BR8	Total area	8.044	17.361	8.735	1.297
	Mean area	1.609	0.187	0.046	0.021
	Total pore count	5	93	190	61
	Porosity (%)	0.7	1.6	0.8	0.1
BR8	Total area	12.916	25.897	10.492	1.837
	Mean area	1.845	0.179	0.046	0.021
	Total pore count	7	145	226	88
	Porosity (%)	1.2	2.4	1.0	0.2

Results of Shape Classification:

Table 5.28 - Mean values for, mean total pore area (MTA), mean area (MMA) and mean total pore count (MPC) calculated from results of block A and B, at four depths in the soil profile (10, 25, 45 and 60 cm, from surface). Shape class 1 (>0.04), class 2 (0.04 - 0.015) and class 3 (<0.015).

		Class 1		Class 2		Class 3	
Depth	Pore	mean	σ	mean	σ	mean	σ
10 cm	MTA	17.073	10.62	18.476	9.31	12.812	9.51
	MMA	0.071	0.007	0.349	0.109	3.865	3.322
	MPC	246.0	163.45	59.0	40.78	3.125	2.571
25 cm	MTA	37.766	8.52	35.251	14.26	26.529	23.59
	MMA	0.084	0.030	0.356	0.111	3.904	2.22
	MPC	512.63	109.38	96.625	13.88	5.5	3.46
45 cm	MTA	13.323	8.88	18.639	17.23	15.480	24.86
	MMA	0.054	0.013	0.204	0.082	3.034	4.86
	MPC	226.5	103.08	77.38	42.66	4.13	2.57
65 cm	MTA	14.540	7.51	18.710	11.80	19.504	18.53
	MMA	0.060	0.006	0.338	0.204	5.089	6.74
	MPC	240.25	113.55	61.5	29.01	4.125	2.67

Table 5.29 - Area (mm^2), mean area and number of pores for each pore shape class, block A.

SAMPLE		CLASS 1	CLASS 2	CLASS 3
AR1	Total area	38.799	37.180	14.407
	Mean area	0.066	0.243	2.401
	Total pore count	591	153	6
AR1	Total area	20.623	16.684	0
	Mean area	0.061	0.242	0
	Total pore count	336	69	0
AR2	Total area	33.870	49.233	18.393
	Mean area	0.161	0.478	4.598
	Total pore count	410	103	4
AR2	Total area	34.505	35.840	76.731
	Mean area	0.071	0.351	6.976
	Total pore count	488	102	11
AR3	Total area	32.100	51.648	25.045
	Mean area	0.077	0.338	3.578
	Total pore count	417	153	7
AR3	Total area	14.530	18.602	78.227
	Mean area	0.063	0.255	15.645
	Total pore count	231	73	5
AR4	Total area	17.660	38.538	26.967
	Mean area	0.064	0.622	5.393
	Total pore count	276	62	5
AR4	Total area	18.957	15.808	52.756
	Mean area	0.059	0.180	6.594
	Total pore count	321	88	8

Table 5.30 - Area (mm^2), mean area and number of pores for each pore shape class, block A.

SAMPLE		CLASS 1	CLASS 2	CLASS 3
AR5	Total area	22.536	23.066	21.305
	Mean area	0.074	0.452	4.261
	Total pore count	306	51	5
AR5	Total area	22.598	24.581	13.990
	Mean area	0.074	0.311	1.999
	Total pore count	304	79	7
AR6	Total area	20.746	20.922	0
	Mean area	0.074	0.299	0
	Total pore count	282	70	0
AR6	Total area	46.781	27.398	6.955
	Mean area	0.072	0.271	3.477
	Total pore count	651	101	2
AR7	Total area	11.169	9.388	2.457
	Mean area	0.056	0.177	1.229
	Total pore count	198	53	2
AR7	Total area	21.916	43.211	8.224
	Mean area	0.064	0.315	1.175
	Total pore count	345	137	7
AR8	Total area	27.763	35.901	0.918
	Mean area	0.070	0.536	0.918
	Total pore count	398	67	1
AR8	Total area	5.885	12.097	44.078
	Mean area	0.063	0.637	22.039
	Total pore count	93	19	2

Table 5.31 - Area (mm^2), mean area and number of pores for each pore shape class, block B.

SAMPLE		CLASS 1	CLASS 2	CLASS 3
BR1	Total area	6.747	3.953	5.132
	Mean area	0.073	0.247	5.132
	Total pore count	92	16	1
BR1	Total area	6.453	11.737	0
	Mean area	0.079	0.559	0
	Total pore count	82	21	0
BR2	Total area	37.246	17.712	43.339
	Mean area	0.065	0.219	5.417
	Total pore count	576	81	8
BR2	Total area	36.001	22.967	38.221
	Mean area	0.063	0.242	6.370
	Total pore count	567	95	6
BR3	Total area	3.347	4.015	0
	Mean area	0.038	0.134	0
	Total pore count	87	30	0
BR3	Total area	7.949	6.221	0.994
	Mean area	0.052	0.164	0.994
	Total pore count	153	38	1
BR4	Total area	6.761	9.497	12.636
	Mean area	0.054	0.202	2.527
	Total pore count	125	47	5
BR4	Total area	4.801	4.431	0
	Mean area	0.054	0.170	0
	Total pore count	89	26	0

Table 5.32 - Area (mm^2), mean area and number of pores for each pore shape class, block B.

SAMPLE		CLASS 1	CLASS 2	CLASS 3
BR5	Total area	12.613	17.044	20.841
	Mean area	0.081	0.416	10.421
	Total pore count	155	41	2
BR5	Total area	6.212	13.564	26.821
	Mean area	0.061	0.323	6.705
	Total pore count	102	42	4
BR6	Total area	42.752	55.573	8.787
	Mean area	0.077	0.540	2.197
	Total pore count	557	103	4
BR6	Total area	50.223	52.363	19.804
	Mean area	0.088	0.444	2.200
	Total pore count	570	118	9
BR7	Total area	5.662	7.045	5.014
	Mean area	0.042	0.144	1.003
	Total pore count	134	49	5
BR7	Total area	9.909	8.981	3.878
	Mean area	0.040	0.104	0.646
	Total pore count	247	86	6
BR8	Total area	16.258	10.496	8.683
	Mean area	0.060	0.150	1.240
	Total pore count	272	70	7
BR8	Total area	18.237	22.915	9.990
	Mean area	0.052	0.203	1.998
	Total pore count	348	113	5

Interpretation of Results of Resin Samples:

Size class:

The summary of the size classification shown in Table 5.22, for the four depths (10, 25, 45 and 60 cm) in the profile shows that the mean total area, for each height in the profile, decreases with diminishing pore size. Mean pore count increased from class 1 to class 2 by 93 %, from class 2 to class 3 by 33 % and then decreased from class 3 to class 4 by 64 %. Pores in the range 300 - 136 μm (class 3) dominated the soil samples compared to larger pore sizes. The decrease in pores from class 3 to class 4 may be due to the sensitivity of the measurement which was limited by pixel size. The number of observations in class 4 may therefore not truly depict the total population of pores < 136 μm.

Mean porosity values (Table 5.22) were very similar for classes 1 and 2 at equivalent depths of 10, 25 and 45 cm in the vertical sections. Between classes 2, 3 and 4 mean porosity decreased as mean pore size reduced. Mean porosity for the combined size classes and vertical sections (block A and B) was the greatest at 25 cm (9.1 %) (Table 5.23a). The predicted mean porosity for the combined profiles using this method was 5.7 % (Table 5.23a).

Table 5.23(b) shows the mean porosity for blocks A and B at sampling locations. From this table it can be seen that porosity calculated in a pore size range of between 1000 - 136 μm was greater in block A compared to block B. Mean porosity for each block calculated using the values in Table 5.23(b) show block A to have had a porosity of 7.11 % compared to 4.31 % for block B.

The variability in total number of pores, size and porosity between sample locations even from within the same sample were perceptible (Tables 5.24 to 5.27). Noticeably differences

in pore count and porosity were also observed between the two blocks (Table 5.23b, Tables 5.24 - 5.27). These observations show just how variable soil conditions can be even within a very short distance and therefore highlight the necessity for detailed structural observations when dealing with solute movement.

One pattern that re-occurred in the vertical soil sections was an increase, in all size classes, of total pores from the 10 cm horizon to the 25 cm horizon. Below the 25 cm horizon some of the size classes showed a decrease in observed pore count in the vertical soil section with depth while other vertical sections showed no obvious trend.

Although differences in observation did occur between the left and right hand side of the vertical soil sections the differences were only slight.

Shape class:

The summary Table 5.28 shows that the vertical sections were dominated by class 1 (round, Table 5.2) pores, with class 3 (elongated, Table 5.2) pores occurring the least in the soil samples. The mean total area occupied by each pore shape class was very similar with class 2 (intermediate) pores occupying only a marginally larger area than the other two classes (9 % more than class 2 and 18 % more than class 3).

Class 1 pores (round) were the most numerous in the soil samples (Tables 5.29 - 5.32). Class 2 pores (intermediate) were observed in soil samples throughout the vertical soil section although they were less frequently observed than class 1 pores. Class 3 (elongated) were the least frequently observed pore group and in some parts of the vertical section were absent (for example Table 5.31, BR1, BR3 and BR4). An increase in total pore count was observed from 10 cm to 25 cm for soil pore classes 1 and 2. Fewer pores were observed

in all three shape classes in block B than in block A.

5.4. COMPARISON OF MACRO AND MICRO SCALE STRUCTURAL ANALYSIS TECHNIQUES.

5.4.1. Criticisms.

Each of the three methods had advantages and disadvantages over the other two methods:

Profile tracing method: this allowed a large soil area to be quantified in a realistic time period of approximately one day. The technique not only allows porosity and pore count to be made but can also be used to show connectivity between surface and lower horizons, and thus can provide an indication of how water may move through the profile. Further developments might include application of a dye in the irrigation which would stain any pores and cracks that the solution flowed through. Stained pores and cracks could then be highlighted on the tracing to show evidence of where the water plus dye had moved. Such a visual record would aid interpretation of connectivity between pores and cracks, and hence water and solute movement through the soil section. This method can also be used to show tortuosity and orientation (anisotropy) of pores and cracks in the soil section, which are important in determining the length of pathway solutes had to travel through as well as the predominant direction of movement.

Disadvantages of the profile tracing method include limitations of size of pore that can be realistically traced (> 1 mm). The method takes little account of pores and cracks that may be orientated into or out of the profile.

Binary transect method: Allowed pore size distribution, above 1 mm, across the vertical soil section to be examined in detail and thus provide important information as to why water

may move quickly through a particular location in the soil compered to other locations. It is limited compared to the profile tracing method because it provides no information concerning connectivity between transect lines and therefore no direct information as to direction of water movement through the soil profile. A combination of binary transect method and profile tracing method may be useful in assessing connectivity as well as pore size distribution. The binary transect method is more time consuming than the profile tracing method but may be improved by using a micro-video camera set on a movable platform which could automatically record the transect. The camera would be more reliable than a manual recorder in making observations at precisely 90° to the soil profile.

The representativeness of this technique is dependent of the number of transect lines made down the vertically exposed soil section, in this experiment 10 transect lines were used which represented 1.25 % of the soil section. Table 5.5 showed variability to be minimal, the results of the 160 mm transects were comparable to the 800 mm transects. From this result, it can be concluded that 160 mm transects in this type of soil are representative. Reduction of the number of transects to perhaps 2 × 160 mm transects per metre width would offer a rapid method of assessing structure (this should only be undertaken after variability has been determined). Furthermore a greater number of transects could be taken down the soil section to build up a picture of the connectivity of pores.

Resinated core section method: This is a more widely accepted technique for quantifying soil structure as it is relatively easy to collect and prepare. This method allowed recognition of shape of pores which influence flow through the soil as well as pore size distribution at the meso-scale (1000, 1000 - 300, 300 - 136 and >136 μm). Compared to the profile tracing and binary transect methods it allows a more detailed analysis of the finer pores below 1 mm which the other techniques were not capable of examining. The technique however,

is limited when a wide range of pore sizes are present as an appropriate resolution for all pore sizes may be hard to achieve. Structural information gathered by this method provides information about potential storage but little about water movement through the soil section and therefore it is limited in its usefulness with regards to research on solute movement. The method may be improved by using a dye in the irrigation water which would highlight active solute pathways. The main disadvantages are that the process of resination may alter the structural properties of the soil sample, particularly if a catalyst is used to speed up the hardening process.

Comparisons made between the three structural techniques was restricted by orientation of the sample and area sampled. The profile tracing and the binary transect methods are both vertical interpretations of the soil structure section while the resinated core section method examined a horizontal area. The biggest difference was the sample area size particularly between the profile tracing method compared to the binary transect method and resinated core section method. The profile tracing method covered an area of 4325.765 cm^2 compared to 8 cm^2 for the binary transect method (per line) and 10.89 cm^2 for each resinated core section.

Certain limitations of the methods may be overcome by combining techniques as in the case of the binary transect method and resinated core section method, so that both a macro- and micro- scale perspective is achieved. The combination of these three techniques allows connectivity, tortuosity, pore size distribution, pore shape and porosity at both the macro- and micro- scale to be quantified.

5.4.2. Integration.

The three structural quantification methods used in this experiment had three structural characteristics in common; pore area, porosity and total pore count (Table 5.33). Estimated values of porosity were largest using the binary transect method and ranged from 49 % to 3% depending on the method chosen (Table 5.34). The largest mean porosity value was obtained using the binary transect method (1 - > 5 mm) in which the area of the mole dominated the results. If the aforementioned result is disregarded porosity for the three techniques ranged from 21 % to 3.0 % with the largest results being obtained by the binary transect method (the Delesse principle). It must, however, be reemphasize that differences in pore size range observed do occur between the different techniques and therefore porosity is not necessarily based on a common pore size. Porosity calculated by the profile tracing method, 6 % for 1 - 4 mm cracks, is similar to that calculated by the resinated core section, 5.8 % for 1000 - 136 µm cracks and pores (Table 5.34). However, mean porosity calculated by the profile tracing method (6 %) compared to the binary transect method (14.72 %), for a pore size range 1 - 4 mm, was very different. This difference may arise due to the difference in sampling area covered by the two aforementioned techniques.

Table 5.34 shows that pore count per area (cm^2) increased as sampling technique becomes more detailed. For example, the profile tracing method is not sensitive to pores/cracks < 1 mm, as it is limited by the width of the pencil and as a result of this, the pore count per unit area using this method was the lowest (0.1 per cm^2). The resinated core section method examined pores in minute detail as small as 136 µm, as a result pore count per unit area (35.2 per cm^2) was much larger than determined by the other two techniques which were not intended to observe mesopores (Table 5.34). However, larger pores and cracks (> 1 mm) are not easily taken into account using the resinated core section method due to sampling

Table 5.33 - Summary of structural characteristic measured by each of the three techniques used in this research.

Structural quantification method.	Sampling scale	Structural characteristic measured
Profile tracing method (PTM)	macro	Pore area, porosity, total pore count, anisotropy, tortuosity.
Binary transect method (BTM)	macro	Pore area, porosity, total pore count, pore size distribution.
Resinated core section method (RCSM)	micro	Pore area, porosity, total pore count, pore size distribution, pore shape.

Table 5.34 - Summary of mean porosity and mean pore count per unit area (cm^2) using the three structural techniques.

Method	Pore size	Mean porosity	Mean number of pores per unit area (cm^2)
Profile tracing method	1 - 4 mm	6.0 %	0.096
	> 4 mm	3.0 %	0.003
	total	9.0 %	0.099
Binary transect method	Delesse principle	21 %	20.8
	1 - 4 mm	14.72 %	11.1
	1 - >5 mm	49.1 %	11.7
Resinated core section method		5.8 %	35.2

Table 5.35 - Summary of the changes in porosity and pore count per unit area (cm^2) for four sampling horizons (10, 25, 45 and 60 cm) using binary transect method and resinated core section method.

	Binary transect method			Resinated core section method
Porosity at:	Delesse principle	1 - 4 mm	1 - > 5 mm	
10 cm	21 %	14.2 %	52.5 %	4.4 %
25 cm	21 %	15.9 %	44.3 %	9.5 %
45 cm	23 %	9.9 %	87.0 %	4.7 %
60 cm	15 %	11.0 %	32.3 %	4.7 %
Mean pore count per area at:	Delesse principle	1 - 4 mm	1 - > 5 mm	
10 cm	20.7	10.9	11.4	28.3
25 cm	20.8	12.3	12.9	56.5
45 cm	22.9	6.9	7.5	28.1
60 cm	14.7	7.9	8.3	28.1

Limitations.

All three techniques were limited either to the large or small scale. Combining the different techniques may help to eliminate problems such as under estimation of small pores, or over-estimation of large pores, due to limitation of scale. Table 5.35 summarises porosity and pore count at sampling horizon depths of 10, 25 45 and 60 cm in the vertical soil section. By combining the porosity calculated by the binary transect method (1 - >5 mm) with porosity calculated by the resinated core section method (1000 - 136 µm) (Table 5.35) the porosity value at 10 cm was 56.9 %, at 25 cm was 53.8 % and at 60 cm was 37.0 %. These values compare favourably to porosity calculated from bulk density samples in

Section 2.3.3. of 58 % (10 cm), 55 % (25 cm) and 46 % (60 cm).

Table 5.35 also shows that mean pore count was greater at 25 cm in the vertical soil section using both the binary transect and resinated core section method and decreased with depth in the soil in the size range > 4 mm. Percentage porosity was also greatest at the 25 cm horizon for pore sizes > 4 mm.

From the experimental results of soil structure the soil blocks can be classified as having predominantly round or intermediate pore shapes, with direct vertically orientated channels through a vertical soil section. The soil had a porosity of 57 %, 54 % and 37 % at depths of 10, 25 and 60 cm. Approximately 5 % of porosity was due to pores of < 1 mm diameter. In conclusion, this soil structure has the potential to allow rapid movement of water and solute through the soil profile.

5.4.3. Implications.

All three techniques showed that pore numbers increased as size class reduced; however, total area of the smaller macropores or mesopores (< 1 mm diameter) tended to be less than that of the larger macropores (> 1 mm diameter) (for example, Table 5.22). Although there would appear to be more chance of solute moving into smaller sized macropores because they were more abundant in the soil, the actual volume that could be carried by each individual smaller pore is limited compared to a larger pore. However, if there are sufficient numbers of fine pores the combined potential flow rate may provide an equivalent rate of flow to a single larger pore. This idea will be examined more thoroughly in Chapter 8. At low irrigation rates, not exceeding the infiltration capacity of smaller mesopores, it can be surmised that small pores will become saturated before larger pores. Therefore, at low irrigation rates water movement through the soil may be confined

exclusively to mesopores. The implication of this would be an increased residence time for any solute moving through the soil and a greater potential for interaction between resident soil water and new irrigation. At higher irrigation rates exceeding infiltration capacity of the smaller pores or when the smaller pores become saturated larger pores may become more actively involved in transporting solute and water. The larger area occupied by bigger pores means that an increased percentage of water is able to move more rapidly through the profile compared to a reduced percentage through smaller pores. The faster the solute and water can move through the soil the less chance it has to interact with the majority of the soil matrix. The concentration of solute moving through rapid pathways is not altered as much as when it moves more slowly through the soil and as a result a larger peak concentration is observed at depth.

From results in Tables 5.20, 5.21 and 5.23(b) it can be said that although block A and B were taken from within 1 m of each other there were noticeably differences between them structurally. The results would imply that block B had a larger porosity in the pore size range 1 - 4 mm than block A (18.43% and 10.17% respectively), but had a smaller porosity in the size range 1000 - 136 μm (4.3% and 7.11% respectively). It may be expected from these results that tracers applied to block B may appear at sample locations more quickly than in block A because there are a greater number of larger macropore pathways present in block B. The proportion of fast pathways compared to slower narrow pathways has an important implications on the shape of the breakthrough curve. A rapid peak followed by a smaller but significant movement of slower moving solute in the smaller pores resulting in a long slow tail-off to the breakthrough curve. The effect, on concentration of solute, of different pathways (macropore and mesopore) is examined in Chapter 7 using breakthrough curve analysis and the relationship between tracer movement and structure is examined in Chapter 8.

CHAPTER 6.

WATER MOVEMENT.

6.1. INTRODUCTION.

Part of the first aim of this investigation was to examine in detail the movement of water and solutes along specific pathways. Soil water status can be used to set limits to the calculation of soil water movement through the soil block. The soil block experiments were designed to investigate solute movement under steady state conditions. In this chapter, the patterns of water movement are investigated to determine whether steady state conditions were achieved. However, consideration of flow or discharge alone does not adequately characterise the water pathways or solute movement. To characterise water and solute movement tracers were applied to investigate in more detail which pathways were considered to be involved and the interaction between mobile and immobile zones, both of which will be discussed separately in Chapter 7. The information on soil water status, structure and solute movement in the blocks will be integrated in Chapter 8.

The techniques used for monitoring soil water characteristics are now well established and include the use of tensiometer with transducers and time domain reflectometry (TDR), which were used in this experiment to monitor water content as described in Chapter 3. Transducers measure soil water status directly, as a measurement of energy or potential at a point within the soil. By using two or more tensiometers at different locations within the soil the hydraulic gradient between different points can be predicted. TDR is a complementary technique and involves the measurement of dielectric permittivity from which the volumetric water content, θ, can be calculated and hence soil water status may be derived. The principles of these two techniques and the differences in soil properties being characterised were outlined in Chapter 4. The relevant points of that chapter are

summarised below. Differences in the nature of the results obtained from the tensiometers and those collected from the TDR include both the type of soil water characteristics being monitored and the area over which they sampled. Tensiometers measure matric potential surrounding a porous cup which provides an indication of changing soil potential at a point. The TDR measures soil water content between the two probes, set 5 cm apart and 40 cm in length and thus provides information about soil water conditions within that horizontal plane. The sampling volume of the TDR (1000 mm^2 cross sectional area along the probes (Baker and Lascano, 1989)) is larger than that of the tensiometer which monitors the area around the cup (reactive surface area 42.3 cm^2 (Hendrickx *et al.*, 1994)). Averaging results over a large volume of soil, as the TDR does, may give a better interpretation as to soil water conditions over a large volume, through time, but it may conceal detailed patterns of water movement through macropores.

The direction of water movement is influenced partly by matric potential which in turn is a function of soil water conditions. Direction of water movement can be obtained directly from soil matric potential results obtained from tensiometers, whereas such information can only be gained indirectly from the TDR. Water will move from areas of high pressure, low capillary tension to low pressure, higher capillary tension, which is generally from areas of high to low water content.

This chapter will examine the changes in response recorded by the tensiometers and TDR probes through time. Similarities and differences between measurements will be highlighted. A very brief review of each technique is presented before the results obtained from the tensiometer and TDR are discussed in order.

6.2. TENSIOMETERS.

Although results were collected every 10 minutes results are presented as hourly responses to simplify the information. The hourly response represents a time five minutes after an irrigation event occurred.

The response to changing matric potential was monitored from the tensiometers by electrical pressure transducers (Honeywell 150PC series flow-thru pressure sensor) and logged as a milli-volt (mV) response, via a multiples board, to a Campbell 21X data logger, as described in Chapter 4. The electrical responses from the pressure transducers for the five experiments were converted from mV to head of suction (cm H_2O) using calibration curves for each transducers. The calibration equations are presented in Appendix C. The location of the tensiometers within the soil block are indicated in Figure 4.1.

6.2.1. Soil Water Potential Results.

Figures 6.1 to 6.6 (a and b) show the soil water potential as determined by the hourly response of the tensiometers for the right (a) and left (b) side of blocks A (Figure 6.1 to 6.3) and B (Figure 6.4 to 6.6). The first experiment (run 1) which consisted of a weak concentration (100 mg l^{-1} Cl) miscible displacement (as described in Section 3.10.), followed by a flush then a stronger concentration (250 mg l^{-1} Cl) miscible displacement, was divided into two parts. Figures 6.1 (Run 1(I)) represents the period over which the weak concentration miscible displacement followed by the flush occurred. Figure 6.2 (Run 1 (II)) represents the period of the stronger concentration miscible displacement. The Y-axis represents an increasing (+) suction, in cm head of water.

To determine whether steady state conditions were achieved in the blocks, in line with the intentions of the experiment, a linear regression of change in suction through time was used

(a)

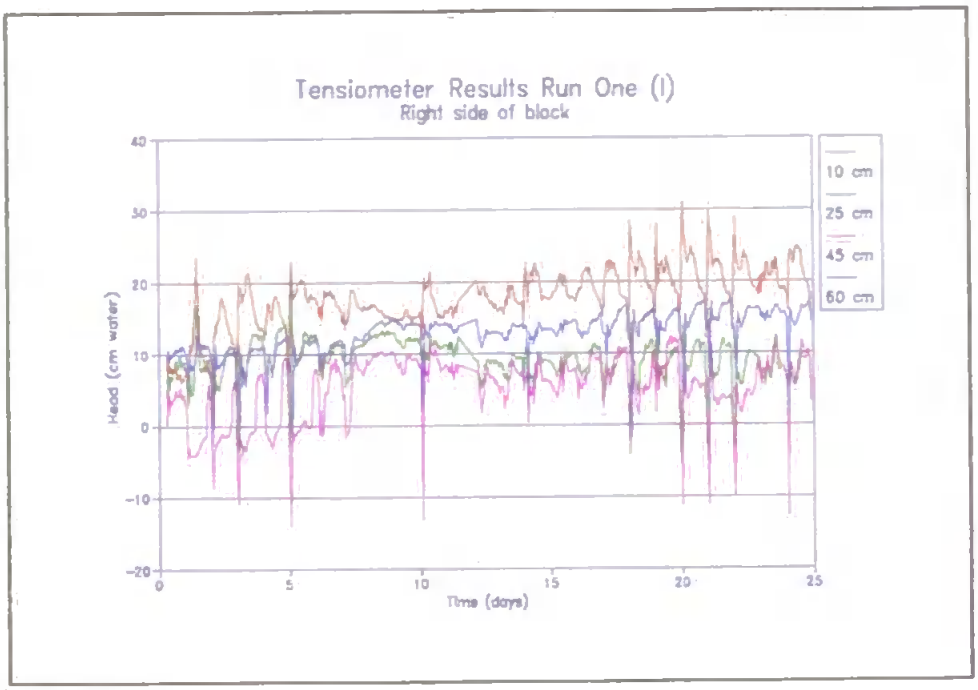

(b)

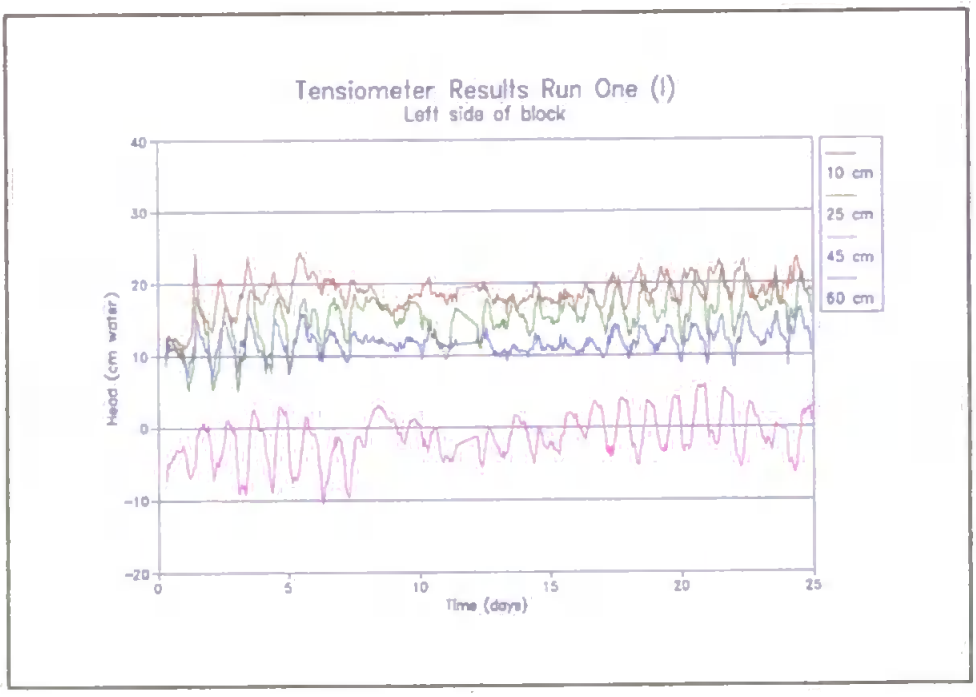

Figure 6.1 - Change in soil water potential through time at depths of 10, 25, 45 and 60 cm for run 1 (I), block A. (a) right side (b) left side of the soil block.

(a)

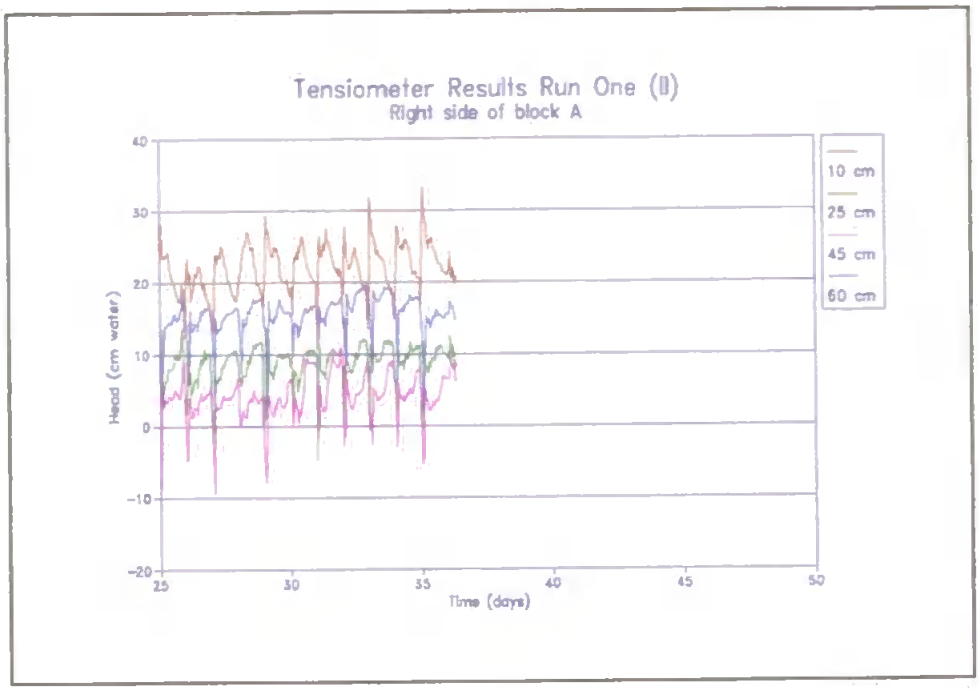

(b)

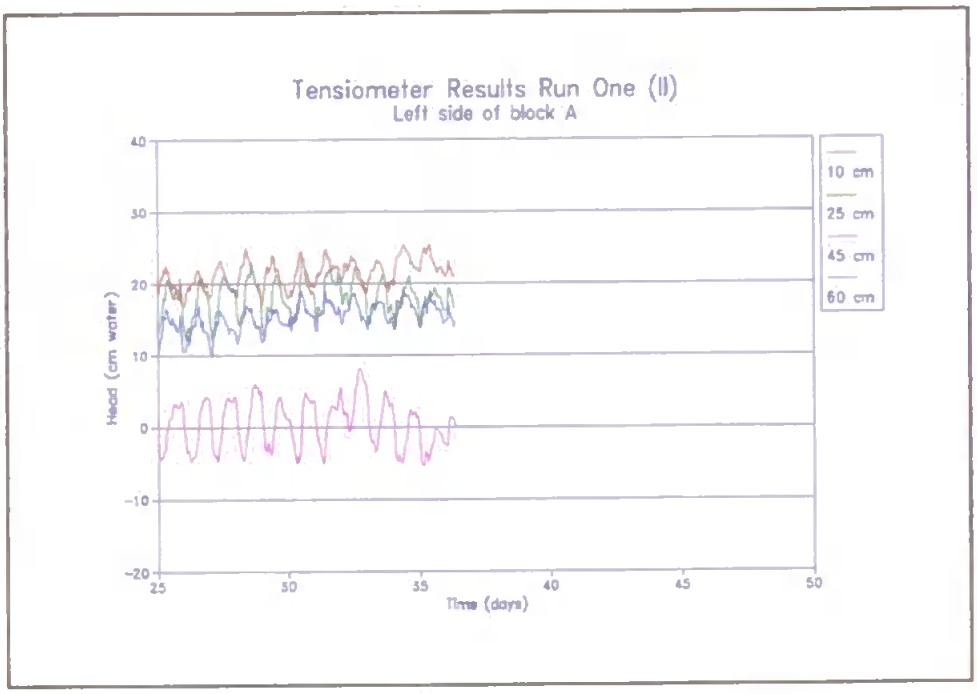

Figure 6.2 - Change in soil water potential through time at depths of 10, 25, 45 and 60 cm for run 1(II), block A. (a) right side and (b) left side of the soil block.

(a)

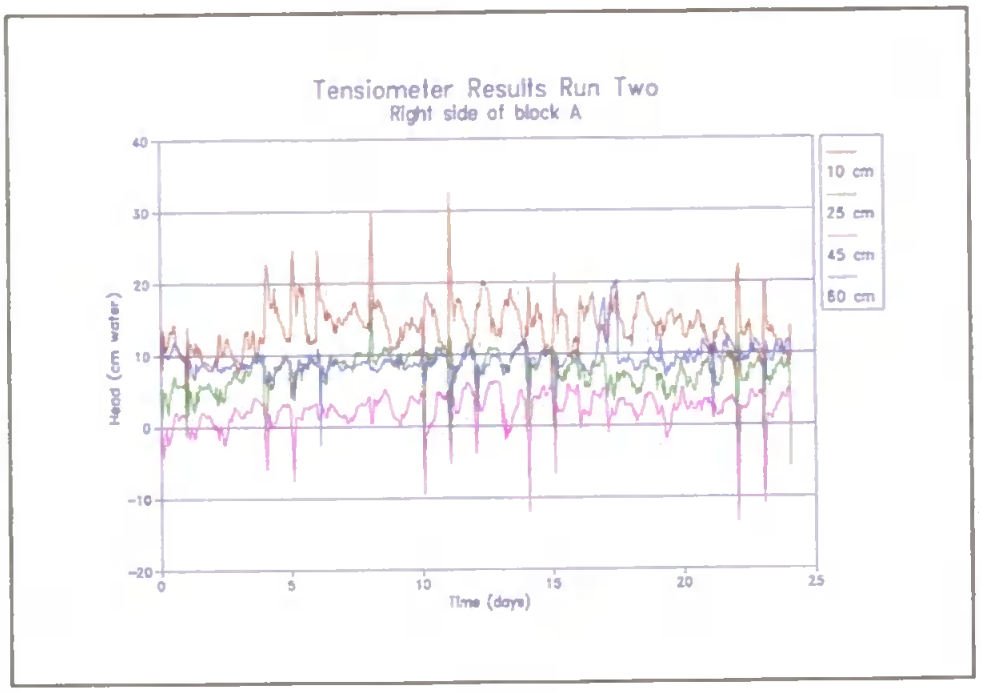

(b)

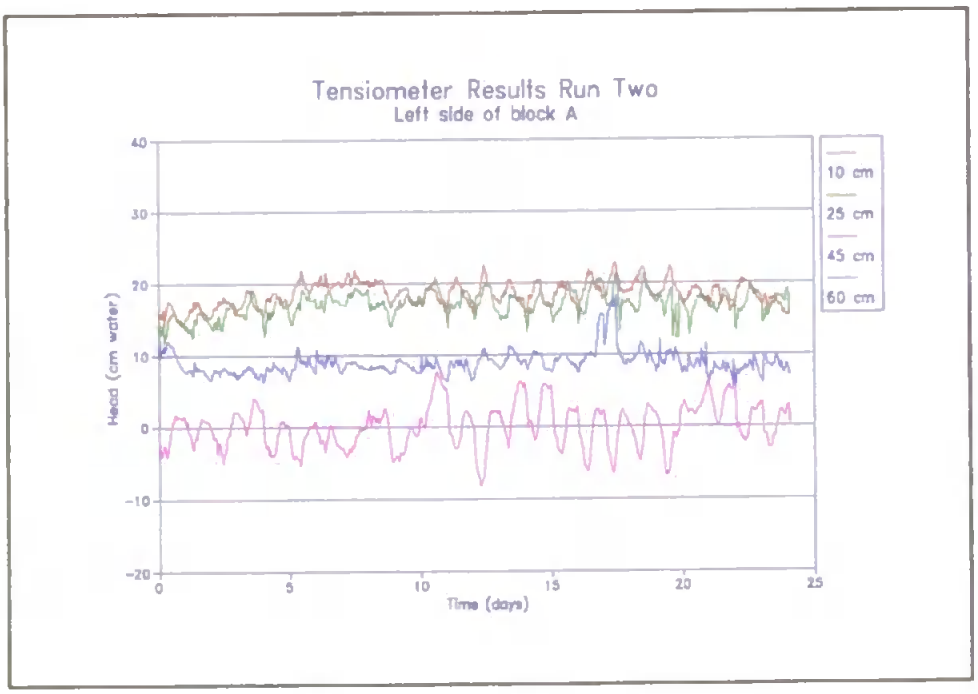

Figure 6.3 - Change in soil water potential through time at depths of 10, 25, 45 and 60 cm for run 2, block A. (a) right side and (b) left side of the soil block.

(a)

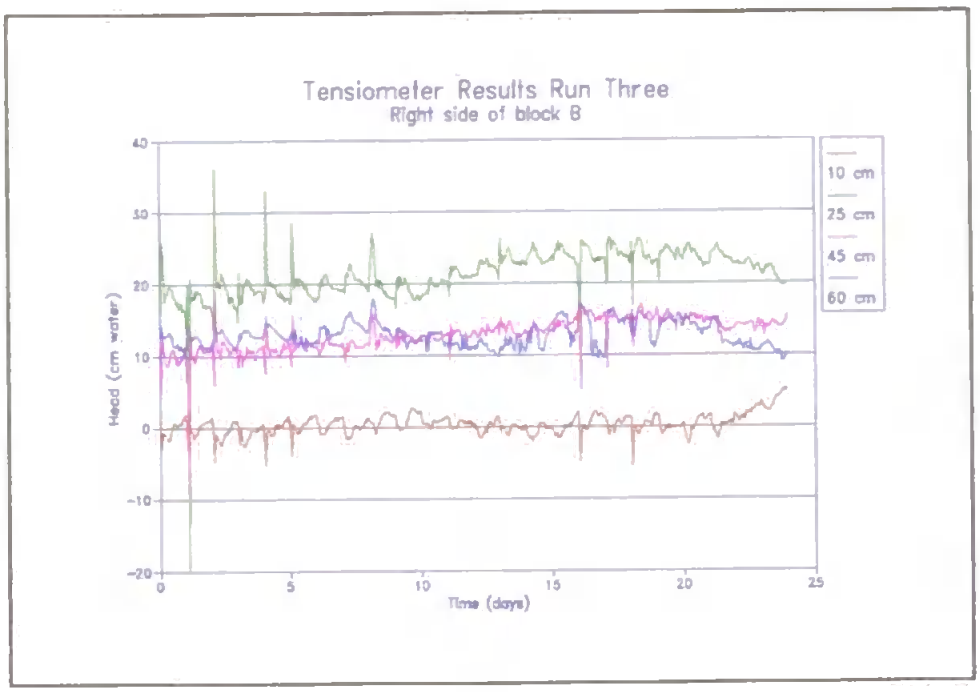

(b)

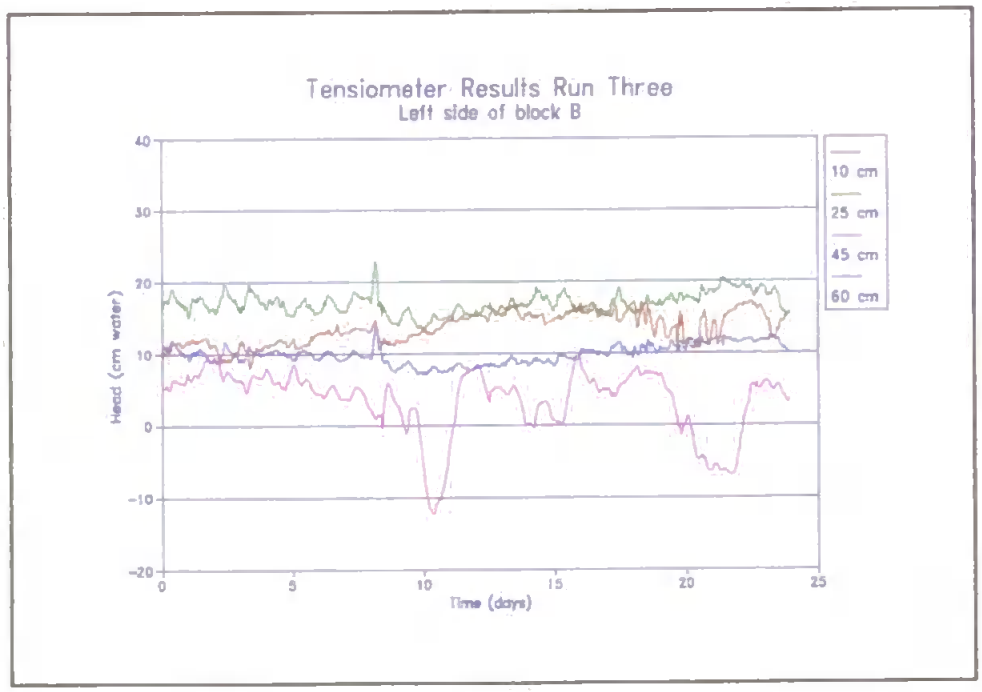

Figure 6.4 - Change in soil water potential through time at depths of 10, 25, 45 and 60 cm for run 3, block B. (a) right side and (b) left side of the soil block.

(a)

(b)

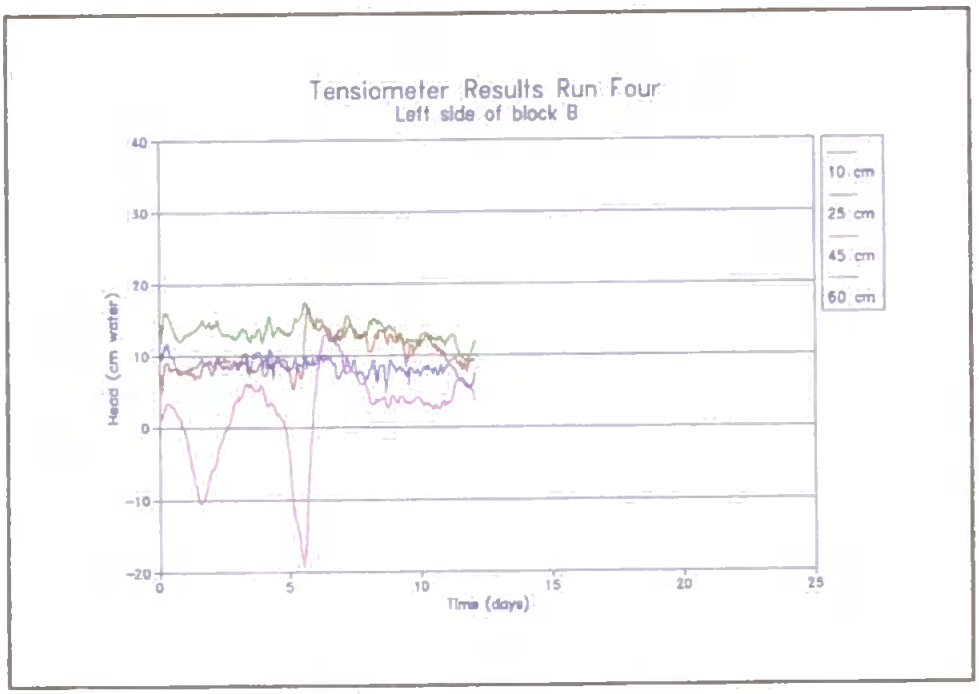

Figure 6.5 - Change in soil water potential through time at depths of 10, 25, 45 and 60 cm for run 4, block B. (a) right side and (b) left side of the soil block.

(a)

(b)

Figure 6.6 - Change in soil water potential through time at depths of 10, 25, 45 and 60 cm for run 5, block B: (a) right side and (b) left side of the soil block.

to examine the response of the tensiometers, to see if the soil water potential was changing progressively through time. The regression equation for each of the experiments is presented in Appendix E. The gradient (m) of the line is presented in Table 6.1, as calculated from the regression of change in suction through time for tensiometer results for each experiment shown in Figure 6.1 to 6.6 (a and b). A positive gradient implies the suction was increasing through time which would be associated with a drying out of the soil and a subsequent decrease in pressure in the tensiometer. A negative gradient implies that the soil was wetting up through time. The larger the gradient the more extreme the condition of either wetting or drying over time. A gradient of zero would suggest steady unchanging soil water conditions over the time period.

Table 6.1 - Calculated gradient (m) of line from the regression analysis of head of suction (cm H_2O) through time, for tensiometer results of the five experimental runs (Figures 6.1 to 6.6 (a and b)). The tensiometers on the left (L) hand side of each block represent T5 to T8 (10 - 60 cm), on the right (R) hand side of the block represent T1 to T4 (10 - 60 cm).

Depth	Run 1 (I)		Run 1 (II)		Run 2		Run 3		Run 4		Run 5	
	L	R	L	R	L	R	L	R	L	R	L	R
10 cm	0.12	0.39	0.28	0.24	0.05	0.03	0.20	0.07	0.32	0.27	0.05	-0.09
25 cm	0.24	-0.08	0.06	0.21	0.07	0.00	0.04	0.27	-0.18	0.43	-0.06	-0.02
45 cm	0.16	0.24	-0.04	0.27	0.09	0.08	-0.22	0.24	0.66	0.19	-0.74	-0.25
60 cm	0.05	0.25	0.31	0.23	0.03	0.07	0.06	0.00	-0.18	0.07	0.07	0.02

From the computed regression lines the suction at the start and finish of each experiment was calculated, to establish how stable soil water conditions had remained through time. These results are presented in Tables 6.2 - 6.7 below.

Table 6.2 - Suction at the start and finish of Run 1 (I).

	Suction (cm water)					
	Left			Right		
Depth	at start (day 0)	finish (day 25)	Difference	at start (day 0)	finish (day 25)	Difference
10 cm	16.99	19.99	+ 3.00	12.93	22.68	+ 9.75
25 cm	12.29	18.29	+ 6.00	10.10	8.10	- 2.00
45 cm	-3.31	0.69	+ 4.00	2.10	8.10	+ 6.00
60 cm	11.18	12.43	+ 1.25	9.54	15.79	+ 6.25

Table 6.3 - Suction at the start and finish of Run 1 (II).

	Suction (cm water)					
	Left			Right		
Depth	at start (day 25)	finish (day 36)	Difference	at start (day 25)	finish (day 36)	Difference
10 cm	19.76	22.84	+ 3.08	20.59	23.23	+ 2.64
25 cm	17.65	18.31	+ 0.66	7.66	9.97	+ 2.31
45 cm	0.56	0.12	- 0.44	2.66	5.63	+ 2.97
60 cm	13.51	16.92	+ 3.41	14.20	16.73	+ 2.53

Table 6.4 - Suction at the start and finish of Run 2.

	Suction (cm water)					
	Left			Right		
Depth	at start (day 0)	finish (day 25)	Difference	at start (day 0)	finish (day 25)	Difference
10 cm	17.77	19.02	+ 1.25	13.46	14.21	+ 0.75
25 cm	16.13	17.88	+ 1.75	7.62	7.67	+ 0.05
45 cm	-1.12	1.13	+ 2.25	1.25	3.25	+ 2.00
60 cm	8.44	9.19	+ 0.75	8.37	10.12	+ 1.75

Table 6.5 - Suction at the start and finish of Run 3.

	Suction (cm water)					
	Left			Right		
Depth	at start (day 0)	finish (day 25)	Difference	at start (day 0)	finish (day 25)	Difference
10 cm	11.07	14.24	+ 3.17	-0.49	1.26	+ 1.75
25 cm	16.37	17.37	+ 1.00	18.06	24.81	+ 6.75
45 cm	6.08	0.58	- 5.50	9.99	15.99	+ 6.00
60 cm	9.08	10.58	+ 1.50	12.74	12.82	+ 0.08

Table 6.6 - Suction at the start and finish of Run 4.

	Suction (cm water)					
	Left			Right		
Depth	at start (day 0)	finish (day 12)	Difference	at start (day 0)	finish (day 12)	Difference
10 cm	8.32	12.16	+ 3.84	0.75	3.99	+ 3.24
25 cm	14.32	12.16	- 2.16	11.64	16.80	+ 5.16
45 cm	-1.83	6.09	+ 7.92	11.15	13.43	+ 2.28
60 cm	9.50	11.66	+ 2.16	12.15	12.99	+ 0.84

Table 6.7 - Suction at the start and finish of Run 5.

	Suction (cm water)					
	Left			Right		
Depth	at start (day 0)	finish (day 12)	Difference	at start (day 0)	finish (day 12)	Difference
10 cm	8.22	8.82	+ 0.60	2.74	1.66	- 1.08
25 cm	14.93	14.21	- 0.72	12.87	12.63	- 0.24
45 cm	5.07	-3.81	- 8.88	13.60	10.60	- 3.00
60 cm	7.55	8.39	+ 0.84	14.35	14.59	+ 0.24

Table 6.8 - 6.12 record the mean, maximum, minimum, range and standard deviation of suctions that were recorded in each experiment (run 1 to run 5 respectively). The results are shown for four depths in the profile (10, 25, 45 and 60 cm) and for both the left (L) and right (R) side of the blocks.

Table 6.8 - Mean, maximum, minimum, range and standard deviation of suctions for run 1 block A.

Depth in profile	Mean suction		Max. suction		Min. suction		Range of suction		Standard deviation (σ)	
	L	R	L	R	L	R	L	R	L	R
10 cm	19.64	19.72	25.38	33.19	10.04	5.52	15.34	27.68	2.57	4.28
25 cm	16.45	8.83	23.19	19.47	5.10	-5.51	18.09	24.98	3.18	2.93
45 cm	-0.43	4.47	8.14	13.54	-10.56	-13.93	18.70	27.47	3.31	4.12
60 cm	13.38	13.88	19.74	19.76	6.92	-2.56	12.83	22.32	2.33	3.17

Table 6.9 - Mean, maximum, minimum, range and standard deviation of suctions for run 2 block A.

Depth in profile	Mean suction		Max. suction		Min. suction		Range of suction		Standard deviation (σ)	
	L	R	L	R	L	R	L	R	L	R
10 cm	18.40	13.83	22.80	32.48	14.22	2.52	8.58	29.95	1.62	3.27
25 cm	17.00	7.64	21.41	17.68	11.80	-9.18	9.61	26.85	1.69	2.63
45 cm	-0.01	2.19	7.61	6.21	-8.30	-13.44	15.91	19.65	2.96	2.89
60 cm	8.83	9.23	18.06	20.20	4.98	-2.56	13.08	22.76	1.65	1.94

Table 6.10 - Mean, maximum, minimum, range and standard deviation of suctions for run 3 block B.

Depth in the profile	Mean suction		Max. suction		Min. suction		Range of suctions		Standard deviation (σ)	
	L	R	L	R	L	R	L	R	L	R
10 cm	13.44	0.31	17.14	5.20	7.95	-5.43	9.19	10.63	2.06	1.36
25 cm	16.89	21.29	22.78	35.97	13.27	-27.91	9.51	63.88	1.40	3.39
45 cm	3.45	12.84	9.72	18.98	-12.30	-9.87	22.02	28.84	4.55	2.22
60 cm	9.83	12.79	13.72	17.94	7.09	9.04	6.63	8.90	1.27	1.67

Table 6.11 - Mean, maximum, minimum, range and standard deviation of suctions for run 4 block B.

Depth in profile	Mean suction		Max. suction		Min. suction		Range of suctions		Standard deviation (σ)	
	L	R	L	R	L	R	L	R	L	R
10 cm	10.24	2.37	16.67	5.62	4.58	-1.87	12.09	7.49	2.38	1.52
25 cm	13.23	14.22	17.46	19.76	9.16	4.44	8.30	15.32	1.40	2.68
45 cm	2.12	12.28	13.69	15.49	-19.24	6.30	32.93	9.19	6.11	0.97
60 cm	8.40	12.56	11.87	14.83	4.84	9.81	7.03	5.02	1.14	1.04

Table 6.12 - Mean, maximum, minimum, range and standard deviation of suctions for run 5 block B.

Depth in profile	Mean suction		Max. suction		Min. suction		Range of suctions		Standard deviation (σ)	
	L	R	L	R	L	R	L	R	L	R
10 cm	8.54	2.18	47.03	29.22	-3.30	-0.30	50.34	29.52	3.73	1.90
25 cm	14.56	12.73	41.30	49.65	11.35	6.44	29.95	43.21	2.43	4.04
45 cm	0.61	12.08	13.52	46.85	-21.02	10.07	34.53	36.78	6.35	3.33
60 cm	7.99	14.46	37.67	36.48	3.78	11.10	33.89	25.38	2.97	2.47

6.2.2. Interpretation of Soil Water Potential.

Figures 6.1 to 6.6 (a and b) show characteristic signs of diurnal fluctuation in pressure as described by Haise and Kelley (1950). Diurnal fluctuations due to a temperature gradient between the porous cup and soil causes water to diffuse from the warmer surface to the cooler surface. As air temperature fluctuates more readily than soil temperature, tensiometer response can be influenced by the changes in air temperature and result in distinctive diurnal rises and falls in pressure response above and below suction due to soil water conditions. Unlike the results obtained by Haise and Kelley where daily variations in tension of 350 to 400 cm water were recorded, the maximum range in tension in these experiments was 64 cm water and the minimum 6.63 cm water. Fluctuations were less extreme in this experiment due to improved thermal properties of the tensiometer system

including temperature compensated tensiometers. and possibly soil type. Minimum values (high pressure, low suction) were recorded in the morning, between 7 and 10 am and maximum readings (low pressure, high suction) were recorded between 7 and 10 pm, which concur with the results obtained by Haise and Kelley. The results on the right side of the block showed signs of greater fluctuation, this is most likely the result of being closer to a more exposed location. Fluctuations become less pronounced by run 3 to 5, this may be due to a change over in tensiometers from block A to B or it may more likely be a reflection of changing external air temperatures. Run 1 and 2 were conducted over the summer of 1993. During this period the difference in air temperature between day and night was on average 8°C. Run 3 to 5 were conducted in Autumn and Winter 1993. The difference between day and night time temperatures was less 6°C (North Wyke Meterological Data, unpd., 1993).

From Table 6.1 the gradient of the regression line for Figures 6.1 to 6.6 (a and b) shows block A to have been predominantly drying through time (positive gradient). Although by run 2 the gradient throughout was negligible. Results for block B also would suggest that the block was initially drying (run 3). However, by run 4 and especially run 5 the gradient was minimal or even negative, implying a wetting up of the block.

The largest differences in suction occurred more often at 25 and/or 45 cm depth in the soil (Table 6.2 to 6.7). The difference in suction always remains positive at 60 cm, which was below the level of the mole drain, as well as at a depth of 10 cm for all but the final run (run 5, Figure 6.7). These results would imply that suction increased from the start to the finish at these points and therefore drying occurred through time. Although the actual difference is only small, maximum recorded difference in any part of the soil block was 9.75 cm water (Table 6.2). A wetting up of the soil through time was observed at location

depths of 45 cm (L) (Table 6.3), 45 cm (L) (Table 6.5), 25 cm (L) (Table 6.6) and 25 cm, 45 cm (L), 10 cm 25 cm, 45 cm (R) (Table 6.7). The predominantly negative difference in suction (Table 6.7) indicating wetting of the soil through time was most likely the result of initially (gravimetrically) drained soil conditions at the start of run 5. The position of other 'wetting' locations observed in other experimental runs may be influenced by soil structure this will be examined in Chapter 8.

Even though the water table was raised to the base of the mole drain in runs 2 and 3 tensiometer results indicated that the soil below the mole was not saturated (Tables 6.9 and 6.10). The positive suction below the mole drain at 60 cm depth would suggest that either the internal water table was not raised, although externally it did appear to be, or that the spatial location of the sampler in someway affected the observation. It was observed, during destructive sampling that tensiometers at 60 cm (in both blocks) were not intercepted by macropores. The recorded unsaturated conditions at 60 cm may be explained by the location of the samplers within a matrix dominated zone. Matrix soil water conditions take longer to equilibrate than the macropore system so although macropores may have been fully saturated below the mole the matrix may not have had time to reach saturation.

For runs 1 to 3 a greater range of suctions was observed on the right hand side of the block than on the left (Tables 6.8 to 6.10). Greater fluctuations in pressure on the right hand side may be attributed to its closer proximity to external climate, as explained earlier in this chapter. The range in suctions recorded in run 5 was high due to the drying out period between run 4 and 5 which resulted in high initial suctions being recorded but after initial irrigation these fluctuations reduced. The lowest mean suction was always recorded at 45 cm depth on the left side of each block for all five experiments (Tables 6.8 to 6.12). This may be a reflection of soil structure and will be considered in Chapter 8.

In summary, although the observed water tensions in the soil (recorded by the tensiometers) did fluctuate they were within acceptable experimental limits determined by technology available at present. It was therefore accepted that the system was as close to steady state as possible.

6.2.3. Hydraulic Conductivity.

From Darcy's Law the flux (q) of water is given by:

$$q = -K \frac{\delta H}{\delta L} \qquad (6.1)$$

Where, K is the hydraulic conductivity and $\delta H/\delta L$ is the gradient of the hydraulic head.

Under steady water flow conditions in an open system the unsaturated hydraulic conductivity, $K(\psi_m)$, can be calculated as a function of matric head, ψ_m, by applying Darcy's Law for values of q (Miyazaki, 1993)

$$K(\psi_m) = \frac{q}{\delta H/\delta L} \qquad (6.2)$$

Hydraulic gradient and thence K was calculated using the mean transducer suction as well as suction calculated from the regression line for the start and finish of each experiment. These values, for hydraulic gradient and K, are presented in Tables 6.13 to 6.18. Water flux, q, was known for each experiment from the constant irrigation. The mean water flux

for each experiment was respectively 3, 3, 23, 25 and 3 mm h^{-1}. Water flux is important because it affects soil water conditions, within the soil, and hence hydraulic conductivity (from Equation 6.1). The influence of soil water conditions on hydraulic conductivity will be considered at the end of this chapter.

The values of unsaturated K is compared with those calculated in Chapter 2 using the Falling Head Permeameter from which the saturated hydraulic conductivity was shown to be 34.56 cm h^{-1} in the first 10 cm of soil and 0.0157 cm h^{-1} below 45 cm.

Results of Unsaturated Hydraulic Conductivity:

Table 6.13 - Gradient (dH/dL) and unsaturated hydraulic conductivity (K) between 10 - 25, 25 - 45 and 45 - 60 cm in block A, run 1 (I). Saturated hydraulic conductivity for 10 - 25 and 45 - 60 presented in brackets.

Gradient and hydraulic conductivity between	Run 1 (I) - Gradient and hydraulic conductivity Left					Right				
	dH/dL	mean K (cm h^{-1})	range	K at start	K at finish	dH/dL	mean K (cm h^{-1})	range	K at start	K at finish
10 - 25 cm (k=34.56 cm h^{-1})	0.79	0.38	- 0.10	0.44	0.34	0.42	0.72	+10.33	0.37	10.7
25 - 45 cm	1.17	1.78	- 0.10	0.22	0.12	0.80	0.38	- 0.20	0.50	0.30
45 - 60 cm (k=0.0157 cm h^{-1})	1.88	0.16	- 0.19	1.97	1.78	1.51	0.20	+ 0.0	0.20	0.20

Table 6.14 - Gradient (dH/dL) and unsaturated hydraulic conductivity (K) between 10 - 25, 25 - 45 and 45 - 60 cm in block A, run 1 (II). Saturated hydraulic conductivity for 10 - 25 and 45 - 60 presented in brackets.

Gradient and hydraulic conductivity between	Run 1 (II) - Gradient and hydraulic conductivity Left					Right				
	dH/dL	mean K (cm h^{-1})	range	K at start	K at finish	dH/dL	mean K (cm h^{-1})	range	K at start	K at finish
10 - 25 cm (K=34.56 cm h^{-1})	0.78	0.38	+ 0.08	0.35	0.43	0.11	2.65	+ 0.42	2.17	2.59
25 - 45 cm	0.12	2.48	+ 1.26	2.06	3.32	0.77	0.39	- 0.02	0.40	0.38
45 - 60 cm (K=0.0157 cm h^{-1})	1.99	0.15	- 0.02	0.16	0.14	1.75	0.17	0.0	0.17	0.17

Table 6.15 - Gradient (dH/dL) and unsaturated hydraulic conductivity (K) between 10 - 25, 25 - 45 and 45 - 60 cm in block A, run 2. Saturated hydraulic conductivity for 10 - 25 and 45 - 60 presented in brackets.

Gradient and hydraulic conductivity between	Run 2 - Gradient and hydraulic conductivity Left					Right				
	dH/dL	mean K (cm h^{-1})	range	K at start	K at finish	dH/dL	mean K (cm h^{-1})	range	K at start	K at finish
10 - 25 cm (k=34.56 cm h^{-1})	0.91	0.33	- 0.01	0.34	0.33	0.59	0.51	+ 0.04	0.49	0.53
25 - 45 cm	0.15	2.01	- 0.33	2.18	1.85	0.73	0.41	- 0.05	0.44	0.39
45 - 60 cm (k=0.0157 cm h^{-1})	1.59	1.19	+ 0.0	0.18	0.18	1.47	0.20	+ 0.01	0.20	0.21

Table 6.16 - Gradient (dH/dL) and unsaturated hydraulic conductivity (K) between 10 - 25, 25 - 45 and 45 - 60 cm in block B, run 3. Saturated hydraulic conductivity for 10 - 25 and 45 - 60 presented in brackets.

Gradient and hydraulic conductivity between	Run 3 - Gradient and hydraulic conductivity Left					Right				
	dH/dL	mean K (cm h^{-1})	range	K at start	K at finish	dH/dL	mean K (cm h^{-1})	range	K at start	K at finish
10 - 25 cm (k=34.56 cm h^{-1})	1.23	0.19	+ 0.02	0.17	0.19	2.40	0.10	- 0.01	0.10	0.09
25 - 45 cm	0.33	0.70	+ 0.96	0.47	1.43	0.58	0.40	+ 0.02	0.39	0.41
45 - 60 cm (k=0.0157 cm h^{-1})	1.43	0.16	- 0.05	0.19	0.14	1.00	0.23	+ 0.10	0.19	0.29

Table 6.17 - Gradient (dH/dL) and unsaturated hydraulic conductivity (K) between 10 - 25, 25 - 45 and 45 - 60 cm in block B, run 4. Saturated hydraulic conductivity for 10 - 25 and 45 - 60 presented in brackets.

Gradient and hydraulic conductivity between	Run 4 - Gradient and hydraulic conductivity Left					Right				
	dH/dL	mean K (cm h^{-1})	range	K at start	K at finish	dH/dL	mean K (cm h^{-1})	range	K at start	K at finish
10 - 25 cm (k=34.56 cm h^{-1})	1.20	0.21	+ 0.02	0.18	0.20	1.79	0.14	- 0.09	0.31	0.22
25 - 45 cm	0.45	0.56	- 0.94	1.30	0.36	0.90	0.28	+ 0.04	0.26	0.30
45 - 60 cm (k=0.0157 cm h^{-1})	1.42	0.18	+ 0.04	0.14	0.18	1.02	0.25	+ 0.03	0.23	0.26

Table 6.18 - Gradient (dH/dL) and unsaturated hydraulic conductivity (K) between 10 - 25, 25 - 45 and 45 - 60 cm in block B, run 5. Saturated hydraulic conductivity for 10 - 25 and 45 - 60 presented in brackets.

Gradient and hydraulic conductivity between	Run 5 - Gradient and hydraulic conductivity Left					Right				
	dH/dL	mean K (cm h^{-1})	range	K at start	K at finish	dH/dL	mean K (cm h^{-1})	range	K at start	K at finish
10 - 25 cm (k=34.56 cm h^{-1})	1.40	2.14	+ 0.01	0.21	0.22	1.70	0.18	- 0.01	0.18	0.17
25 - 45 cm	0.30	0.99	+ 2.44	0.59	3.03	0.97	0.31	+ 0.04	0.29	0.33
45 - 60 cm (k=0.0157 cm h^{-1})	1.49	0.20	- 0.09	0.26	0.17	2.77	0.11	- 0.05	0.29	0.24

Interpretation of Unsaturated Hydraulic Conductivity:

Hydraulic gradient within the soil blocks did not remain constant throughout the experiments. In run 1 (I) the hydraulic gradient was larger on the left side of the block than on the right but also increased with depth in the profile on both sides (Table 6.13). In run 1 (II) the hydraulic gradient was higher on the left side at 10-25 cm and 45-60 cm than on the right. At 25-45 cm hydraulic gradient decreased on the left side and was lower on the left side than on the right of the block (Table 6.14). In run 2 a similar response pattern as run 1 (II), in hydraulic gradient, was observed (Table 6.15). In run 3 in the top 10-45 cm

hydraulic gradient was larger on the right side of the block than on the left. Hydraulic gradient decreased from 10 to 45 cm and then increased to 60 cm, on both sides of the block (Table 6.16). In runs 4 and 5 hydraulic gradient responded in a similar way to the response recorded in run 3. The lowest hydraulic gradients were recorded; for block A, more frequently between 25-45 cm (L) and between 10-25 cm (R) (Tables 6.13 to 6.15); for block B, between 25-45 cm on the left side of the block (Tables 6.16 to 6.18). From Equation 6.2 it can be seen that as hydraulic gradient increases hydraulic conductivity (K) decreases. Regions of larger hydraulic gradient are therefore associated with regions of slower moving solute and water in the soil. In Chapter 8 a link between speed of movement, driving force and change in concentration through time will be made to see whether the observed pattern of water movement can be associated with observed solute movement.

The largest K values throughout the five experiments were recorded between 25-45 cm on the left side of both blocks (Table 6.13 to 6.18). The location of other large values of K occurred between 10-25 cm (R) run 1 (II) and run 5. For the majority of the experiments the lowest values of K were recorded between 45-60 cm. Other low values of K were also recorded between 10-25 cm, for example, run 2(L), run 3(R) and run 4. Higher values of K above the mole drain (at 45 cm) would imply that flow of solute and water was potentially rapid while below the mole drain level the rate of flow reduced. Although hydraulic conductivity is higher towards the mole drain level the mole did not flow readily, as water would have had to overcome the pressure gradient between the soil and air interface. Water will only move from the soil into the mole drain when the soil surrounding the mole is saturated allowing water to move into the air. Water was therefore more likely to continue through cracks and channels that it already occupied which meant that the mole drain was bypassed. As a consequence of this only a small flow rate was recorded from the

mole, on average 0.02 mm h^{-1} (block A) and 0.002 mm h^{-1} (block B) compared to the mean irrigation rate of 2.76 mm h^{-1}. Mole drain flow represented 0.7 % and 0.07 % (block A and B respectively) of irrigation input. Solute, in these two experimental blocks of soil was therefore carried past the mole drain to depth. In a field situation similar to the experiment this may potentially lead to an accumulation of chemicals within the ground water aquifer.

Unsaturated K in the top 10 to 25 cm of soil was in most cases a factor of 100 smaller in value than K sat. This would imply that the irrigation rate was such that the soil structure was capable of conducting the water and therefore saturation did not occur in this part of the block. Mean K predicted from tensiometer data exceeded calculated K sat. by a factor of 10 between 45 to 60 cm. As K sat. represents the maximum potential velocity the unsaturated K values can only be explained by differences due to variation in scale of observation. At 45 to 60 cm the structure has been described as very coarse prismatic, in Chapter 2, therefore samples taken for K sat. values may only reflect the matric part of the soil and take no account of macropores.

6.3. SOIL WATER CONTENT (TDR).

TDR readings were taken at 24 hour intervals to monitor changes in soil water content through time. Tables 6.20 to 6.24 show the mean volumetric water content, θ_v, as calculated using Topp's Equation (Topp *et al.*, 1980), that is:

$$\theta_v = -5.3\times10^{-2} + 2.9\times10^{-2}K - 5.5\times10^{-4}K^2 + 4.3\times10^{-6}K^3 \quad (6.2)$$

Areas, in Tables 6.20 to 6.24, with no readings in either represent locations where there was no TDR probe or the TDR probe failed due to loss of contact. The maximum,

minimum, range and standard deviation for each experimental run for volumetric water content are presented in Tables 6.25 to 6.29. The location of the TDR probes in the profile are shown in Figure 6.7.

Table 6.19 - Location of TDR in profile

9	10		11	12
6	7		8	13
3	4	●	5	14
2		1		15

Results of Soil Water Content:

Table 6.20 - Mean volumetric water content (cm^3 H_2O cm^{-3}) for block A, run 1, as calculated using TDR readings in the soil profile. The Table shows the relative positioning of the TDR probes in the soil profile with regard to the mole, ●.

0.42	0.40		0.41	0.40
0.37	0.35		0.36	0.32
0.30	0.33	●	0.33	0.30
0.30		0.32		0.33

Table 6.21 - Mean volumetric water content (cm^3 H_2O cm^{-3}) for block A, run 2, as calculated using TDR readings in the soil profile. The Table shows the relative positioning of the TDR probes in the soil profile with regard to the mole, ●.

	0.41		0.41	0.45
0.57	0.37		0.37	0.37
0.29	0.33	●	0.33	0.37
0.36		0.39		0.41

Table 6.22 - Mean volumetric water content (cm^3 H_2O cm^{-3}) for block B, run 3, as calculated using TDR readings in the soil profile. The Table shows the relative positioning of the TDR probes in the soil profile with regard to the mole, ●.

0.39	0.42		0.41	0.40
0.37	0.37		0.37	0.35
0.34	0.38	●	0.38	0.35
0.37		0.39		0.37

Table 6.23 - Mean volumetric water content (cm^3 H_2O cm^{-3}) for block B, run 4, as calculated using TDR readings in the soil profile. The Table shows the relative positioning of the TDR probes in the soil profile with regard to the mole, ●.

	0.41		0.42	
0.37	0.37		0.37	0.35
0.29	0.39	●	0.37	0.35
0.35		0.37		0.37

Table 6.24 - Mean volumetric water content (cm^3 H_2O cm^{-3}) for block B, run 5, as calculated using TDR readings in the soil profile. The Table shows the relative positioning of the TDR probes in the soil profile with regard to the mole, ●.

0.40	0.40		0.42	
0.37	0.37		0.37	0.36
0.29	0.37	●	0.37	0.36
0.35		0.37		0.37

Table 6.25 - Mean, maximum, minimum, standard deviation and range for θ_v calculated from TDR results obtained during run 1, block A.

TDR	mean	maximum	minimum	standard deviation	range
1	0.32	0.33	0.31	0.01	0.01
2	0.30	0.33	0.29	0.01	0.04
3	0.30	0.33	0.28	0.02	0.05
4	0.33	0.34	0.33	0.00	0.01
5	0.33	0.34	0.33	0.00	0.01
6	0.37	0.39	0.36	0.01	0.03
7	0.35	0.36	0.33	0.02	0.03
8	0.36	0.36	0.35	0.00	0.01
9	0.42	0.43	0.41	0.01	0.02
10	0.40	0.41	0.37	0.02	0.04
11	0.41	0.42	0.38	0.01	0.04
12	0.40	0.41	0.39	0.01	0.02
13	0.32	0.33	0.31	0.01	0.01
14	0.30	0.31	0.29	0.01	0.02
15	0.33	0.35	0.31	0.01	0.03

Table 6.26 - Mean, maximum, minimum, standard deviation and range for θ_v calculated from TDR results obtained during run 2, block A.

TDR	mean	maximum	minimum	standard deviation	range
1	0.39	0.41	0.31	0.03	0.10
2	0.36	0.40	0.29	0.02	0.11
3	0.29	0.30	0 .28	0.01	0.02
4	0.33	0.33	0.33	0	0
5	0.33	0.33	0.33	0	0
6	0.37	0.37	0.36	0.00	0.01
7	0.37	0.37	0.36	0.00	0.01
8	0.37	0.37	0.36	0.00	0.01
9	0	0	0	0	0
10	0.41	0.41	0.41	0.00	0
11	0.41	0.43	0.41	0.00	0.02
12	0.45	0.49	0.41	0.02	0.08
13	0.37	0.39	0.33	0.02	0.06
14	0.37	0.38	0.33	0.02	0.05
15	0.41	0.45	0.37	0.02	0.08

Table 6.27 - Mean, maximum, minimum, standard deviation and range for θ_v calculated from TDR results obtained during run 3, block B.

TDR	mean	maximum	minimum	standard deviation	range
1	0.39	0.39	0.38	0.00	0.01
2	0.37	0.37	0.35	0.00	0.02
3	0.34	0.35	0.33	0.01	0.02
4	0.38	0.39	0.37	0.01	0.02
5	0.38	0.39	0.37	0.01	0.02
6	0.37	0.38	0.37	0.00	0.01
7	0.37	0.37	0.37	0	0
8	0.37	0.37	0.37	0	0
9	0.39	0.41	0.37	0.02	0.04
10	0.42	0.43	0.41	0.01	0.02
11	0.41	0.45	0.13	0.06	0.31
12	0.40	0.43	0.13	0.06	0.30
13	0.35	0.37	0.34	0.01	0.03
14	0.35	0.35	0.34	0.00	0.01
15	0.37	0.37	0.36	0.00	0.01

Table 6.28 - Mean, maximum, minimum, standard deviation and range for θ_v calculated from TDR results obtained during run 4, block B.

TDR	mean	maximum	minimum	standard deviation	range
1	0.37	0.37	0.36	0.00	0.01
2	0.35	0.350	0.35	0	0
3	0.29	0.29	0.28	0.01	0.01
4	0.39	0.39	0.37	0.01	0.02
5	0.37	0.37	0.37	0.00	0.00
6	0.37	0.37	0.37	0.00	0.00
7	0.37	0.37	0.36	0.00	0.01
8	0.37	0.37	0.36	0.01	0.01
9	0	0	0	0	0
10	0.41	0.41	0.41	0.00	0.00
11	0.42	0.43	0.41	0.01	0.02
12	0	0	0	0	0
13	0.35	0.36	0.35	0.00	0.01
14	0.35	0.38	0.35	0.01	0.03
15	0.37	0.37	0.36	0.00	0.01

Table 6.29 - Mean, maximum, minimum, standard deviation and range for θ_v calculated from TDR results obtained during run 5, block B.

TDR	mean	maximum	minimum	standard deviation	range
1	0.37	0.40	0.37	0.01	0.03
2	0.35	0.37	0.34	0.01	0.03
3	0.29	0.35	0.28	0.03	0.07
4	0.37	0.39	0.37	0.01	0.02
5	0.37	0.38	0.37	0.00	0.01
6	0.37	0.39	0.37	0.01	0.02
7	0.37	0.37	0.37	0.00	0.00
8	0.37	0.37	0.35	0.01	0.02
9	0.40	0.40	0.40	0.00	0.00
10	0.40	0.41	0.38	0.01	0.03
11	0.42	0.43	0.41	0.01	0.02
12	0	0	0	0	0
13	0.36	0.37	0.35	0.01	0.02
14	0.36	0.37	0.35	0.01	0.02
15	0.37	0.37	0.35	0.01	0.02

Interpretation of Soil Water Content:

Soil water content, θ_v, (cm^3 H_2O cm^{-3}) declined from an average of 0.41, at 10 cm, to 0.36, at 60 cm, in the profiles (Tables 6.20 to 6.24). A reduction in soil water content is consistent with an increasing bulk density due to changes in soil texture with depth (Section 2.3.1.).

In Tables 6.25 to 6.29 soil water content remained reasonably stable through time with a maximum standard deviation in any part of the profile being 0.03. The maximum range of soil water content from the TDR was 0.31 although the range was more commonly < 0.1.

In summary, results from the TDR showed that soil water content throughout the soil blocks varied very little between experiments and between blocks. It can therefore be concluded from these results that a steady state had been achieved within the blocks.

6.4. INTERPRETATION OF TENSIOMETER AND TDR DATA.

Even though q fluctuated slightly between experiments (0.3 to 0.21 cm h^{-1}) TDR results showed soil water conditions to remain constant through time, although it may normally be expected that soil water content would decline as q declined. Hydraulic conductivity, K, which is a function of soil water content would also be expected to reduce as soil water content reduced. However, from tensiometer results, although calculations of K, did vary slightly the values were considered to be acceptably stable through time. A new hydraulic equilibrium may therefore have been reached within the soil blocks with respect to pore sizes actively involved in transmitting water.

6.4.1. Summary of Tensiometer and TDR Techniques.

Tensiometer results showed small but real fluctuations in pressure that have been accepted

by Haise and Kelley (1950) as not being significant to the overall pattern. The process of installing these instruments is straightforward and involves minimal disturbance to the site. The major advantage of the transducer system was its ability to monitor change in pressure continuously at a fine temporal scale. The small soil volume over which it sampled allowed the tensiometer to be of use in interpreting fine detailed structural influences on solute movement and was therefore ideal for an experiment such as this one.

TDR results showed a stable state to have existed throughout the soil blocks. Rods were installed easily into the soil causing very little disturbance during installation, making them a less intrusive method than the tensiometer system. The main limitation of the TDR results was the large volume over which they sampled meant that fine detailed structural influences on solute movement were lost. Also, the system at the time was not reliably automated and therefore sampling intervals were not as consistent as the tensiometer data.

Both tensiometer and TDR data would suggest that a steady water state was achieved within the soil blocks as was the intentions of the experiment. Therefore it can be suggested that the spray-rig used in these experiments worked well in applying an even application of water.

The following chapter (Chapter 7) will investigate the movement of solutes as they pass through the soil using chemical tracers. Chapter 8 will amalgamate the findings of Chapters 6 and 7 to explain what factors were influencing solute movement through the soil blocks.

CHAPTER 7.

SOLUTE MOVEMENT.

7.1 INTRODUCTION.

The soil water status within the two soil blocks was examined in Chapter 6 where spatial and temporal variations in soil water content were used to explore variability in water movement through the soil. Although the direction and rate of flow of water can be inferred from soil water status the transport of solutes through the soil is more complex than is explained by the movement of water alone. To examine the transport of solutes through the soil, in response to the second aim of this experiment (Section 1.4), the variation of solute movement through space and time must consider both the movement of water through the soil as well as the hydrodynamic dispersion of the chemical. It is, however, recognised that soil water potential influences the transport of solutes through the soil with regard to the degree of dispersion that takes place (Kluitenberg and Horton, 1990). Hydrodynamic dispersion is a combination of mechanical dispersion and molecular diffusion, as defined in Section 1.11.2. The importance of dispersion compared to diffusion in the movement of solute in a soil has been discussed by Biggar and Nielsen (1962) who have suggested that dispersion is the more dominant process. Hu and Brusseau (1994) have, however, stated that diffusion can contribute significantly to solute movement at low flow velocities (less than 0.1 cm h^{-1}), while dispersion dominates solute movement at velocities exceeding 1 cm h^{-1} .

Tracer studies are commonly used to predict solute movement through soils. Using this approach the implications of solute application method (Kluitenberg and Horton, 1990), the effect of structure on solute movement (Walker and Trudgill, 1983), the effect of aggregate size distribution on solute transport (Hayot and Lafolie, 1993) and preferential flowpaths

through soil (Singh and Kanwar, 1991) have been examined. All of these experiments were conducted on soil columns under controlled conditions, using non-sorptive chemicals, such as chloride. Under such conditions the soil column has been regarded as a model that can be used to simulate field conditions (Schweich and Sardin, 1981) although invariably questions are raised about both soil variability (representative elementary volume) and laboratory techniques as discussed in Chapter 1.

The way in which a solute moves through a soil is governed by a number of soil variables (Harvey,1993); Soil structure is fundamental because of its influence on available pathways, soil water content determines which pathways are potentially available to transmit solutes, suction within the soil determines the hydraulic gradients along which solute can flow while the hydraulic conductivity of the soil restricts the speed of solute movement and also the rate of dispersion. These variables are interdependent, although by comparing them with the results obtained in the individual experiments, the more dominant variable(s) will be identified. The effect of these variables on solute movement will be briefly examined in this chapter, although a more thorough integration between variables and solute movement will be made in Chapter 8.

A particular problem has been identified concerning solute transport in soils containing preferential flowpaths through which water and solute may travel bypassing much of the soil matrix (Beven and Germann, 1982). The presence of preferential flowpaths can permit surface applied chemicals to move rapidly through the soil with little interaction occurring between storage (matrix) water and rapidly moving water. One potential of this bimodal transport of chemicals is that it can lead to problems of economic loss and increase environmental pollution hazard (Kluitenberg and Horton, 1990), although the reverse can also be true (Scholefield *et al.* 1993).

The existence of preferential flow within soils has clearly been demonstrated by Andreini and Steenhuis (1990). Preferential or bypass flow occurs along non-capillary pores defined by Radulovich *et al.* (1992) as pores drained under tensions ranging from just measurable up to tensions related to field capacity. The size of pores potentially involved in bypass flow therefore include both macropores and mesopores as defined by Luxmoore (1981) (Section 1.10.). Until recently preferential flow was assumed to occur when the soil was close to or fully saturated with ponded surface water. However, Radulovich *et al.* (1992) found bypass flow to occur in well aggregated soils at irrigation rates lower than saturated flow rate. The ability of a soil to conduct water and solute preferentially through the soil, below saturation, has been explained by Radulovich *et al.* (1992). In a soil with bimodal transport the difference in hydraulic conductivity of the soil matrix compared to macropores is great. Since, as explained by Poiseuille's law flow (Q) is proportional to the pore radius to the power four (r^4). The soil matrix, although possessing more pores (total number of pores) per unit area than pores that circumvent the soil matrix, consists of pore spaces of low infiltrability. When rate of water input exceeds the hydraulic conductivity of the micropores water accumulates on the aggregate surface and moves off in the direction of easiest flow. The water becomes channelled into larger macropores or converges into fingers causing localization of flow, the majority of the soil matrix is therefore bypassed.

This chapter will explain how the tracer experiments used in this research were conducted and will explore the implications of the results to both water and solute movement, through the soil blocks. Solute data will be described firstly as changes in concentration through time, and secondly selective results will be presented as breakthrough curves (relative concentration verses relative pore volume) to try and investigate the presence of preferential flowpaths. The final part of this chapter will verify a one dimensional flow model.

7.2 TRACER EXPERIMENT.

In this experiment tracers were applied to the soil surface and samples of the solute were collected *in situ* using suction cup lysimeters at various locations in the soil blocks, as discussed in Chapters 3 and 4. Solute samples were also collected from the mole drain and at the base of the block. The solute sample taken from the base of the block represented the average concentration of the solute leaving the soil and possibly some of the more immobile water held within the sand table.

Samples were collected every 4 hours throughout the five experiments. A 4 hour sampling interval was used as it allowed sufficient time for a useful volume of solute to be collected from all of the lysimeters since a minimum of 2 mls was needed for analysis. This sampling interval was also believed to be sensitive to rapid changes occurring in the solute concentration, as well as being a practical time span for manual collection of samples over a prolonged period of time. During the final two experiments an 8 hour time span was used at night. For a more sensitive sampling protocol an automated system would be needed and such a system will be discussed in Chapter 9.

One important consideration in this experiment was the way in which the tracers were applied to the soil surface since according to Kluitenberg and Horton (1990) the method will influence the movement of the solute through the soil. The five experiments can be split into two categories depending on whether the tracers were applied continuously or as a pulse (Table 7.1). The first category involved the application of a conservative tracer (chloride) as a miscible displacement (experiments 1, 2 (block A) and 3 (block B)). Miscible displacement experiments are widely used and accepted means of investigating the transport and fate of solute in soil (Walker and Trudgill, 1983; Kluitenberg and Horton, 1990; Singh and Kanwar, 1991; Brusseau, 1993). The second category involved the

Table 7.1 - Summary of tracer experiments, run 1 to run 5, tracer application method and duration.

Sampling Run - Location of water table.	Method	Number of days applied and sampled for.
1 (block A) - low water table, block draining	miscible displacement flush miscible displacement	12 days irrigation with 100 mg l^{-1} Cl. 12 days irrigation at background, 10 mg l^{-1} Cl. 12 days irrigation with 250 mg l^{-1} Cl.
2 (block A) - water table at base of mole	miscible displacement flush	12 days irrigation with 250 mg l^{-1} Cl. 12 days irrigation at background.
3 (block B) - water table at base of mole	miscible displacement flush.	12 days irrigation with 250 mg l^{-1} Cl. 12 days irrigation at background.
4 (block B) - low water table, block draining	slug of KCl and KNO_3.	Day 1 applied tracer and flushed through with background water for 12 days.
5 (block B) - low water table, block draining	slug of KCl and KNO_3.	Day 1 applied tracer and flushed through with background water for 12 days.

application of a pulse of both a conservative (chloride) and biological (nitrate) tracer (experiments 4 and 5 (block B)). Pulse experiments are used to simulate the effects of applying chemicals to the surface of the soil followed by a rainstorm event (Shuford *et al.*, 1977; Sassner *et al.*, 1994), by using such a procedure both preferential flowpaths and dilution can be observed spatially and temporally. The tracer method used and the number of days that the tracers were applied for each experiment are summarised in Table 7.1.

7.3. TEMPORAL CHANGE IN SOLUTE CONCENTRATION THROUGH TIME.

The following discussion describes how solute concentration at the different sampling locations varied through time and throughout the two soil blocks. The relative timings of the different experiments are given in Appendix A. The explanation includes both types of tracer application method as described above. Each experiment will be briefly outlined with the aims of the individual experiment cited. A description of the results will be presented

followed by an explanation of which processes were potentially involved and a summary of the observations at the end of each section. Each block was divided into equal halves to allow a degree of replication during the experiments and they will be referred to as the left and right hand side of the block. Sampling location will be discussed in the order of A1/B1 - A4/B4 (right), followed by A5/B5 - A8/B8 (left) maintaining a general order of surface to depth.

7.4. MISCIBLE DISPLACEMENT EXPERIMENTS.

7.4.1. Sampling Run 1.

The first run consisted of two miscible displacement experiments, one of 100 mg l^{-1} Cl and the second of 250 mg l^{-1} Cl. At a mean irrigation rate of 3 mm h^{-1}. The aim of the first experiment was partly to establish the behaviour of a tracer at a relatively reduced concentration as well as to compared the two different concentrations of tracers, with the intention of monitoring the significance of increased diffusion with increasing concentration gradient. Furthermore, the larger tracer concentration facilitated a repeat of the experiment while ensuring that the input was sufficiently greater than the background concentration so that a clear trace could be distinguished. The second aim of this initial experiment was to begin to distinguish specific pathways through which solute moved within the soil and to examine temporal and spatial changes in pathways. The third and final aim of this experiment was to observe which pathways transmitted solute in a soil that was draining, in an attempt to simulate spring time conditions within a mole drained soil and for this reason water was not permitted to accumulate at the base of the block. Run 1 was also used to establish how long each tracer experiment would be conducted for, from results of time taken to reach peak concentration.

Between the two miscible displacements the block was flushed with tap water which had

an average background concentration of 10 mg l^{-1} Cl. Each miscible displacement and flush lasted for a period of 12 days.

Suction cup lysimeters:

Chloride concentration (right), 100 mg l^{-1} Cl: The times and concentrations for the initial breakthrough and peak/background response of tracer for run 1 are summarised in Table 7.2. Figure 7.1 shows the change in chloride concentration observed on the right hand side of block A. Initial solute breakthrough occurred in samples collected from locations A1(10 cm), A2(25 cm) and A3(45 cm) within one day of irrigation (Table 7.2). Sampler A4 (60 cm) did not collect a solute sample until eight days after the start of irrigation. By 8.6 days solute collected from sampler A4 (60 cm) had reached the peak irrigation concentration. Solute concentration in samples collected from samplers A1(10 cm) and A2(25 cm) increased rapidly reaching a concentration of 100 mg l^{-1} Cl just in excess of one day after the start of irrigation (Table 7.2). The rise in solute concentration at A3 (45 cm) was more delayed compared to change in concentration at A1(10 cm) and A2(25 cm), taking 8.6 days to reach 100 mg l^{-1} Cl.

Flushing with tap water (right), 10 mg l^{-1} Cl: Samples collected at samplers A1(10 cm) and A2(25 cm) were again observed to responded quickly to the change in concentration (Table 7.2). Initial (dilution) breakthrough occurred within half a day of the change over to tap water and reached a background concentration of 10 mg l^{-1} Cl in 1.2(A1) and 1.7(A2) days respectively. Change in solute concentration at samplers A3(45 cm) and A4(60 cm) both recorded a delay in initial response to the change over in irrigation concentration compared to the first miscible displacement experiment (Table 7.2), taking 1 and 2.8 days respectively to show an initial response, and 5 and 7.5 days to reach background concentrations.

Table 7.2 - Response times of the change in concentration curves (Figures 7.1, 7.2, 7.3 and 7.4) for sampling run 1. Values in brackets represent maximum/minimum concentration obtained if below irrigation concentration.

Sampler	Irrigation with 100 mg l^{-1} Cl (part I).		Flush with tap water 10 mg l^{-1} Cl.		Irrigation with 250 mg l^{-1} Cl (part II).	
(depth in soil, cm)	Time of initial break-through (hrs)	Time to peak (hrs)	Time of initial break-through (hrs)	Time to back-ground (hrs)	Time of initial break-through (hrs)	Time to peak (hrs)
A1 (10)	4	27	12	28	12	124
A2 (25)	5	27	12	40	12	120
A3 (45)	11	207	24	120	24	148
A4 (60)	-	207	68	180	32	272 (226 mg l^{-1})
A5 (10)	8	231	60	340 (27.5 mg l^{-1})	32	272 (166 mg l^{-1})
A6 (25)	47	215	96	352 (21.8 mg l^{-1})	44	272 (201 mg l^{-1})
A7 (45)	11	231	60	332 (23 mg l^{-1})	24	272 (157 mg l^{-1})
A8 (60)	8	227	4	252	4	220 (239 mg l^{-1})
Mole (50)	1	83	0.5	152	4	100
Base of Block (85)	1	231 (88.5 mg l^{-1})	4	305	4	272 (205 mg l^{-1})

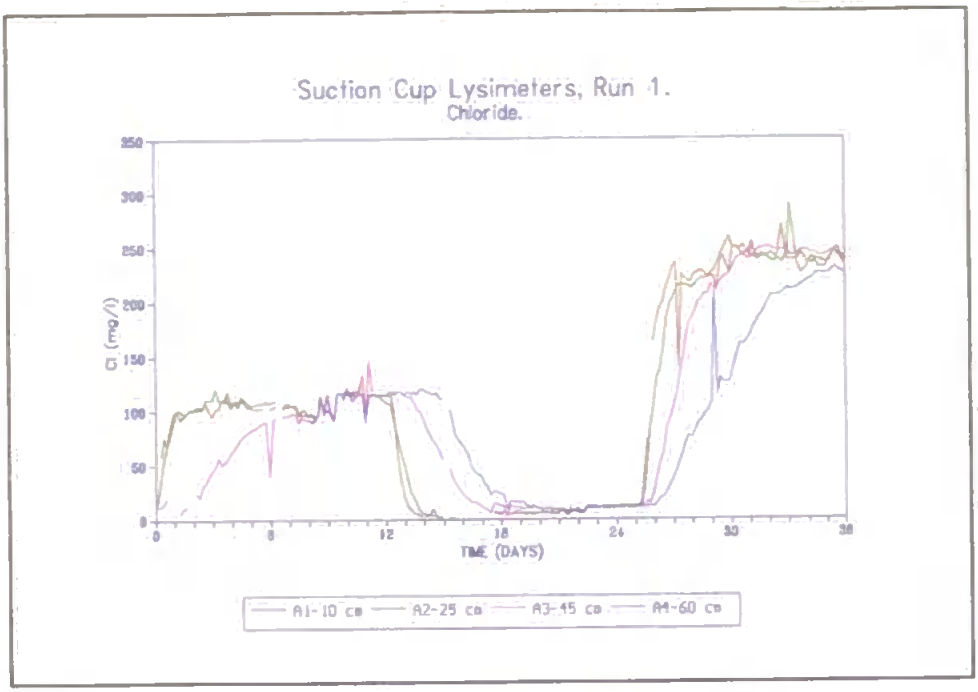

Figure 7.1 - Change in chloride concentration through time at suction cup lysimeters A1 to A4 (right), run 1 (block A).

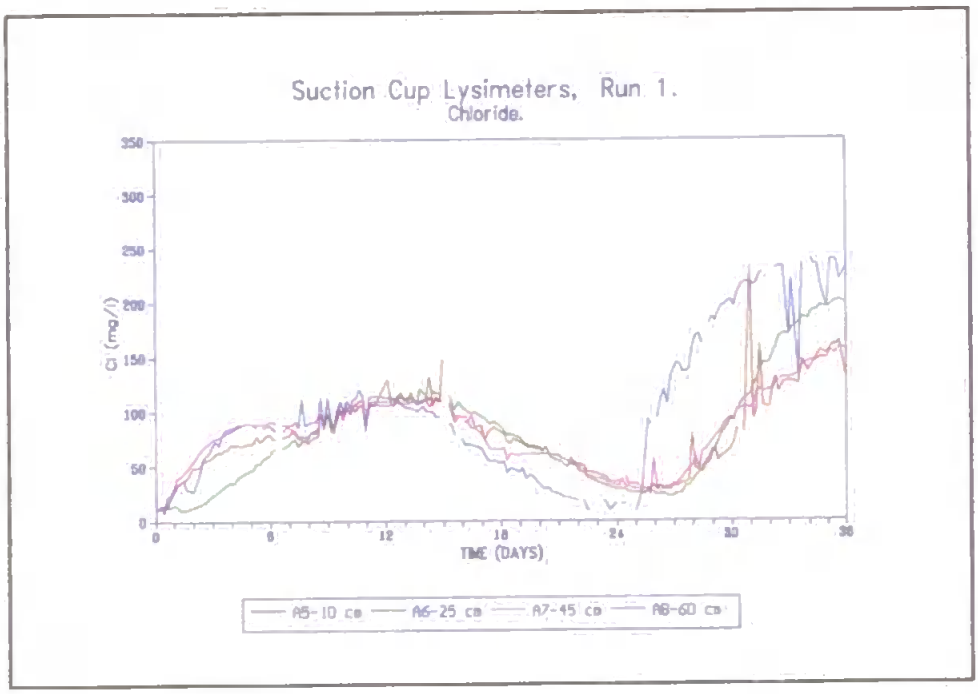

Figure 7.2 - Change in chloride concentration through time at suction cup lysimeters A5 to A8 (left), run 1 (block A).

Increased chloride concentration (right), 250 mg l^{-1} Cl: A similar response was observed to the earlier results when the irrigation concentration was raised. The concentration of samples collected at A1(10 cm) increased slightly quicker than at A2(25 cm) although both locations reached peak concentrations at similar times. Change in solute concentration at location A3(45 cm) was again slightly slower than at A2(25 cm), and A4(60 cm) was notably slower than the other sampling locations. Peak concentrations were reached within 5(A1), 5(A2), 6(A3) and 11(A4) days from the change over in irrigation concentration. Only samples collected at A4(60 cm) did not reach the irrigated concentration of 250 mg l^{-1} Cl (Table 7.2).

Chloride concentration (left), 100 mg l^{-1} Cl: At the start samples collected from A5(10 cm), A7(45 cm) and A8(60 cm) displayed a rapid change in concentration (Figure 7.2) with an initial breakthrough within the first half a day (Table 7.2). Solute collected at A6(25 cm) was more delayed in its initial rise in concentration taking almost 2 days to respond. Despite the slow initial rise in concentration of solute collected at A6 the sample location was the first at which irrigation concentration reached 250 mg l^{-1} Cl, taking 9 days, while A5(10 cm), A7(45 cm) and A8(60 cm) took about 9.6 days (Table 7.2).

Flush with tap water (left), 10 mg l^{-1} Cl: A change in the order of response of the samplers was noted. Solute collected from sampler A8(60 cm) displayed the quickest change in concentration compared to the other samples during the flush with the initial decrease in concentration occurring after only 4 hours and background concentration being reached in 10.5 days. The location of sampler A8(60 cm) immediately under the mole could account for this. Solute concentration collected at A5(10 cm) and A7(45 cm) responded in a similar manner to each other taking 2.5 days to show an initial (dilution) breakthrough, while solute collected from A6(25 cm) took 4 days. Solute collected from samplers A5(10

cm), A6(25 cm) and A7(45 cm) reached their lowest concentration approximately 14 days after the initiation of the flush. The lowest recorded concentration for these samplers were 27.5(A5), 21.8(A6) and 23(A7) mg l^{-1} Cl.

Increased chloride concentration (left), 250 mg l^{-1} Cl: Following the change over to the more concentrated tracer the increase in concentration of solute collected from samplers A5(10 cm), A6(25 cm) and A7(45 cm) was again noticeably delayed compared to location A8(60 cm) taking 1.3(A5), 1.8(A6), 1(A7) and 0.17(A8) days to show an initial breakthrough. None of the solute samples collected from these samplers reached the background concentration of 250 mg l^{-1} Cl within 12 days. The maximum concentrations reached were 166(A5), 201(A6), 157(A7), and 239(A8) mg l^{-1} Cl. Samples collected from A5(10 cm) at the top of the profile and therefore closest to the site of irrigation were noticeably repressed.

Mole and base of block:

Chloride concentration, 100 mg l^{-1} Cl: Data for the mole and base of block (Figures 7.3 and 7.4) showed that the initial breakthrough occurred within one hour after the start of irrigation and that a similar rate of rise in concentration occurred. The sample collected from the mole drain reached a background concentration of 100 mg l^{-1} Cl within 3.5 days. Results from the base of block showed that the solute concentration peaked at 88.5 mg l^{-1} Cl, 9.6 days after the start. The smaller peak concentration at the base of the block is most likely a result of dilution with water in the top of the sand table.

Flushing with tap water, 10 mg l^{-1} Cl: Dilution of concentration after the beginning of the flush was more delayed in the sample taken from the base of block compared to the mole (Table 7.2). Background concentration was similarly reached first by the sample

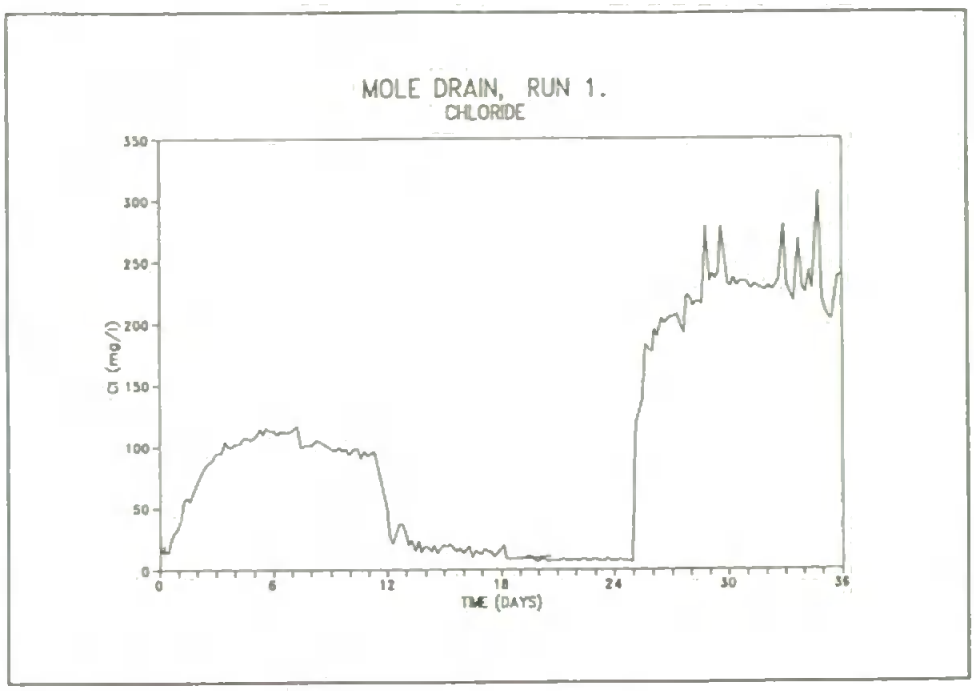

Figure 7.3 - Change in chloride concentration through time from samples collected from the mole drain, run 1 (block A).

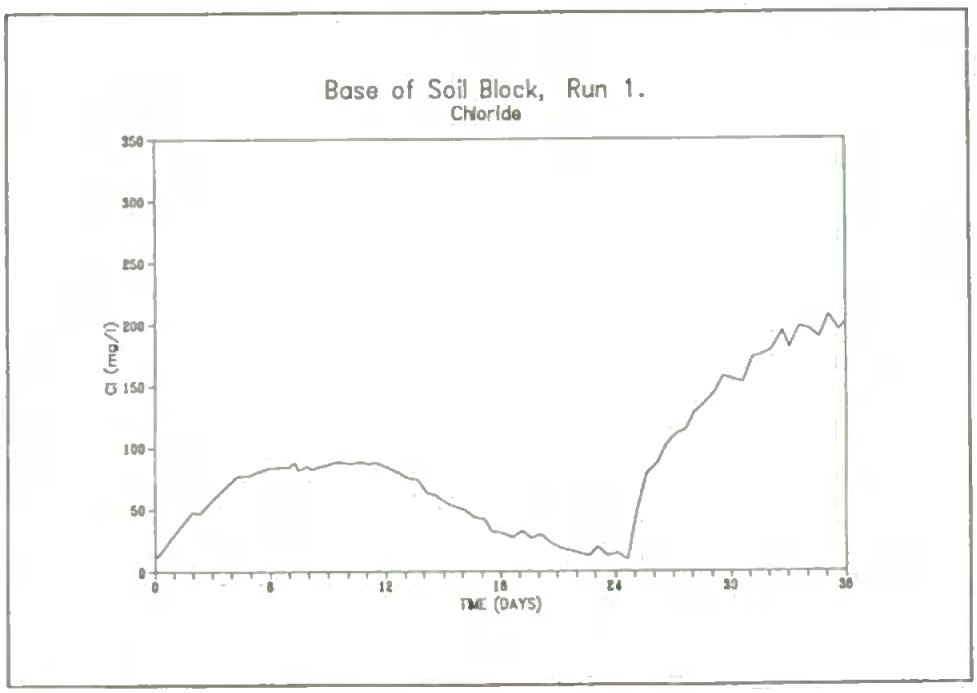

Figure 7.4 - Change in chloride concentration through time from samples collected from the base of the block, run 1 (block A).

collected from the mole drain (Table 7.2).

Increased chloride concentration, 250 mg l^{-1} Cl: Similar results as those observed during the irrigation with 100 mg l^{-1} Cl were noted when applying the 250 mg l^{-1} Cl tracer. Samples taken from the mole showed an increase in concentration within 4 hours and reached peak concentration within 4 days. Samples taken from the base of block showed an initial breakthrough within 4 hours and took 12 days to reach a peak concentration of 205 mg l^{-1} Cl.

Explanation:

The pattern of chloride response observed at these samplers suggests that both hydrological pathways and depth from surface play an important role in influencing the shape of the solute curves (Figures 7.1, 7.2, 7.3 and 7.4). The initial rapid response indicated by the curves could be the result of transport along preferential flowpaths where minimal mixing and limited dilution of solute occurred. The quick response observed at the mole and at sampler A8(60 cm) may be accounted for by preferential or macropore flow of surface water to the mole drain. A crack was observed that directly linked sampler A8 to the base of the mole which would explain the similar response detected at these two locations.

The concentration of the sample collected from sampler A5(10 cm) changed much more slowly than the sample at A1(10 cm) even though both samplers were located at similar depths in the soil. The delayed response in solute concentration observed at A5 (10 cm, left) may be linked to a band of clay rich soil observed between 5 and 10 cm depth in the soil section. A band of low permeability soil found above sampler A5(10 cm) would explain the dampened response to irrigation concentration. During destructive sampling of the soil block A1(10 cm) was observed to have been located in an area where the clay band

was cracked and therefore more permeable.

Changes in response times of the samples collected from the lysimeters may also be explained by changes in macropore pathways occurring during the experiment as a result of soil fauna activity. The difference in the response between samples collected from A5 to A8 (left) and A1 to A4 (right), may also be explained by the difference in predominance of preferential flowpaths intercepted by the different samplers. Faster pathways seem to be more active on the right hand side of the block. Changes in solute concentration occurred more quickly at A6(25 cm) and A8(60 cm) than at A5(10 cm) and A7(45 cm) probably because of the locality of the samplers to preferential flowpaths. The different responses between the left and right side of the block may be an indication of uneven fracturing of the soil by the mole plough due to soil moisture variations in the profile.

The sample collected from the base of block reached peak concentration more slowly and also attained a smaller concentration than the mole drain sample. The reduced concentration at the base of the block may be accounted for by the increased distance to the base of the block compared to the mole, which would allow more time for reaction and mixing to take place. The existence of artificially induced macropores orientated towards the mole drain may also have resulted in an increased proportion of the solute reaching the mole drain via preferential flowpaths compared to pre-existing pathways that connected the surface of the soil to the base. The sample collected at the base represented a wider sampling area compared to the mole and may have therefore been influenced more by the larger volume of slower moving water.

Changes in response times of samples collected from A5(10 cm) to A8(60 cm) through the 36 days may be associated with spatial variations in soil water content throughout the

block. The block was irrigated, at a rate of 3 mm h^{-1}, for one month prior to the start of the experiment and only slight temporal variations in soil water content were observed, as detailed in Chapter 6. Tables 6.2 and 6.3 show that suction from the start of run 1 (part I) to the end of run 1 (part II) increased slightly (mean increase +5.2 cm H_2O in suction). An increase in suction would suggest that drying occurred in the block over this time. The extended time (from initial breakthrough values, Table 7.2) taken for tracer to move to depth in part II compared to part I may have been due to observed drying of the block. Drying would have reduced the size of available pathways able to transmit solute, resulting in a slower flow rate and greater potential for diffusion to occur. Maximum drying occurred at sampler A1(10 cm) which recorded an increase in suction of 10.3 cm H_2O from the start of part I to the end of part II, this can be linked to an observed increase in time to initial breakthrough.

The hydraulic gradient between A6(25 cm) and A7(45 cm) (left), and A1(10 cm) and A2(25 cm) (right) showed a decrease between part I and II, whilst the hydraulic conductivity (K) increased (doubled) at these locations (Table 6.13 and 6.14). This would imply that a faster flow rate at depth in the soil was possible and would explain why some of the deeper samplers showed changes in concentration earlier than samplers closer to the soil surface.

Summary of run 1:

Run 1 was divided into two parts, part I 100 mg l^{-1} chloride concentration and part II increased chloride concentration (250 mg l^{-1} Cl), between which block A was flushed with tap water (10 mg l^{-1} Cl). A highly variable picture emerged of solute movement through time and space. A summary of the order in which solute concentration at different sample locations reached initial breakthrough (the first observed change in concentration) and time

Table 7.3 - Order of response of initial breakthrough and peak concentration/dilution for run 1 part I, flush and part II.

Sampler	Part I (100 mg l^{-1} Cl)		Flush		Part II (250 mg l^{-1} Cl	
(Depth in soil, cm)	Initial break-through	Peak	Initial (dilution) break-through	Lowest conc.	Initial break-through	Peak
A1 (10)	2	1	3	1	2	3
A2 (25)	3	1	3	2	2	2
A3 (45)	5	3	4	3	3	4
A4 (60)	-	3	6	5	4	6
A5 (10)	4	6	5	9	4	9
A6 (25)	6	4	7	10	5	8
A7 (45)	5	6	5	8	3	10
A8 (60)	4	5	4	6	1	5
Mole (50)	1	2	1	4	1	1
Base of block (85)	1	6	2	7	1	7

to peak concentration is given in Table 7.3. A brief review of the different response rates of the suction cup lysimeters to change in solute concentration is presented in Table 7.4.

In general, the response to initial breakthrough in the soil profile, occurred most rapidly in part I, more slowly in part II and the slowest during the flush with tap water. The time at which the initial breakthrough occurred and peak irrigated concentration was reached at samplers A1(10 cm) to A4(60 cm) (right) increased with depth for both part I and II. A similar response order to the tracer application was also observed during the flush. The concentration of solute samples collected at A5(10 cm) to A8(60 cm) (left), did not respond in an order associated with depth in the soil. Samples collected from A6(25 cm) took the longest time for the tracer to appear in solution after initial application while the solute

Table 7.4 - Summary of result of suction cup lysimeter responses for run 1.

Experiment	Location - left of block (A5(10 cm), A6(25 cm), A7(45 cm) and A8(60 cm))	Location - right of block (A1(10 cm), A2(25 cm), A3(45 cm) and A4(60 cm))
Run 1	Initial breakthrough occurred fastest at A8. A6 taking the longest to show initial breakthrough. Peak irrigation concentration was reached first at A6 (part I). During flush A8 reached background concentrations first, A6 reached the next lowest concentration followed by A7 and A5. (part II) A5 and A8 did not reach applied irrigation concentration. A8 reached the largest concentration followed by A6, A5 and A7.	A1 to A4, increase in time of initial breakthrough and peak irrigation concentration with depth for both tracer and flush.

concentration at A8(60 cm) changed the quickest although it was one of the deepest samplers in the profile, at 60 cm depth. With the exception of location A8(60 cm), in general, the right side of the block responded faster than the left.

A rapid initial breakthrough was observed in the solute samples taken from the mole and base of block (Table 7.2).The sample collected from the mole reached peak concentration in less than half the time than at the base of block. Similarly, solute collected from the mole reached a peak concentration equivalent to irrigation concentration in all three cases (100 mg l^{-1} Cl irrigation, flush and 250 mg l^{-1} Cl irrigation), although the sample collected at the base of block did not reach peak irrigated tracer concentration for either tracer application.

In general initial breakthrough and time to peak were reached more quickly and indeed, in some cases took less than half the time, during part I irrigation compared to part II

irrigation. Samples collected from A3(45 cm, right) and A7(45 cm, left) both show initial breakthrough to occur at the same time as each other for tracer applications, although samples collected from A7(45 cm) peaked later than samples from A3(45 cm). The pattern of solute movement, down the soil profile, was more variable during the initial breakthrough A5 to A8 (left) than A1 to A4 (right). Initial response through time although taking longer to appear in part II, the sequence of response in the soil profile were similar for all locations except A5 (Table 7.2). The delay in initial breakthrough and time to peak in part II as compared to part I may be linked with the increased concentration gradient between applied tracer and matrix water leading to a larger rate of diffusion. Increased diffusion resulted in increased retention of solute in the soil matrix. This would explain why peak irrigation concentration was not reached in 6 out of 10 sample locations (part II).

7.4.2. Sampling Run 2.

The second experiment conducted on block A alone consisted of a twelve day miscible displacement using 250 mg l^{-1} Cl solution followed by a twelve day flush with tap water (10 mg l^{-1} Cl) at an irrigation rate of 3 mm h^{-1}. Block A was flushed with tap water for three weeks between the first and second experiment to bring the initial concentrations of chloride in soil water back down to approximately 10 mg l^{-1} Cl, as well as to maintain soil water conditions within the block. The aim of the second experiment was to observe any changes in pathways as a result of raising the water table to the base of the mole. The water table was raised to simulate autumn/winter conditions to see if this affected solute concentration exiting the mole. As the water was allowed to accumulate and mix with other drainage water in the sand table no sample was collected from the base of the block. The second aim of this experiment was to observe any spatial or temporal variations in solute breakthrough and concentration within the block, as well as between this second experiment and run 1 (part II).

Suction Cup Lysimeters:

Chloride concentration (right), 250 mg l^{-1} Cl: A summary of the time to initial breakthrough and to peak or background concentrations reached for run 2 is presented in Table 7.5. Figure 7.5 shows the solute concentration curves for samplers at A1(10 cm),A2(25 cm),A3(45 cm)and A4(60 cm) (right), of block A. The speed at which solute concentrations collected in the samples reached the concentration of the irrigated water reflected the depth of the sampling position. Initial breakthrough occurred at 8(A1), 8(A2), 12(A3) and 28(A4) hours after the start. Similarly peak concentrations were reached 2.5(A1), 3.5(A2), 4.8(A3) and 8.2(A4) days after the start of irrigation.

Flushing with tap water (right), 10 mg l^{-1} Cl: The initial response of solute samples to the (dilution) breakthrough were similar to those observed during the application of 250 mg l^{-1} Cl occurring at 8, 8, 8 and 24 hours (A1 to A4 respectively). However, the time to reach background concentration was slightly extended compared to the time to peak, taking 2.8, 5.8, 7 and in excess of 12 days (A1 to A4 respectively). This extension may be due to the proportion of diluting solute compared to the concentration of the soil solute.

Chloride concentration (left), 250 mg l^{-1} Cl: Samples collected at A5(10 cm) to A7(45 cm) showed an initial decrease in concentration before initial breakthrough of the irrigated tracer was seen (Figure 7.6). This initial decrease in concentration was probably due to residual chloride left after the end on run 1 and gave an indication that these sampling points were only receiving very slow moving matric water. Initial breakthrough occurred in these samples 8(A5), 44(A6) and 76(A7) hours after the start of irrigation and reached their peak concentration values 12.3(A5), 10.3(A6) and 13(A7) days after the start. The peak concentrations of samples collected at A5(10 cm) and A7(45 cm) were 10 and 14 mg l^{-1} Cl, lower than the peak concentration, of 250 mg l^{-1} Cl (Table 7.5), another indication

Table 7.5 - Response times recorded by the change in concentration curves (Figures 7.5, 7.6 and 7.7) for run 2. Values in brackets represent peak maximum/minimum concentration observed if below irrigation concentration.

Sampler	Initial background	Irrigation with 250 mg l^{-1} Cl.		Flush with tap water (10 mg l^{-1})	
(depth in soil, cm)	conc. (mg l^{-1})	Time of initial break-through (hrs)	Time to peak (hrs)	Time of initial break-through (hrs)	Time to peak (hrs)
A1(10)		8	60	8	68
A2(25)		8	84	8	140
A3(45)	14.5	12	116	8	168
A4(60)	19.4	28	196	24	288 (24.5 mg l^{-1})
A5(10)		8	296 (240 mg l^{-1})	4	288 (95.3 mg l^{-1})
A6(25)	51	44	248	44	288 (26.1 mg l^{-1})
A7(45)		76	312 (236 mg l^{-1})	36	288 (49.4 mg l^{-1})
A8(60)		4	128	4	264
Mole(50)		0.02	220	0.04	39

that these samplers were mainly observing matrix water. Samples collected from A8(60 cm), directly below the mole, showed an initial increase in concentration within 4 hours and reached peak concentration within 5.3 days, which represented the quickest response of locations A5 to A8.

Flushing with tap water (left), 10 mg l^{-1} Cl: At sample locations A5(10 cm), A6(25 cm) and A7(45 cm) change in chloride concentration again occurred slowly taking 4, 44 and 36 hours respectively to show an initial breakthrough and in excess of twelve days to reach background, while samples collected from A8(60 cm) responded the quickest showing

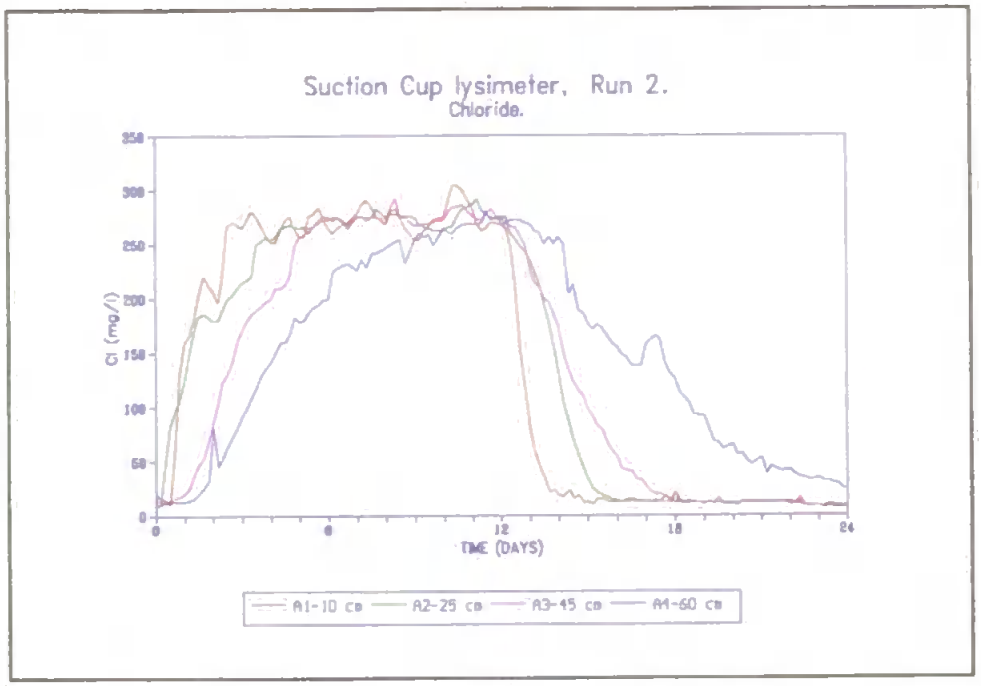

Figure 7.5 - Change in chloride concentration through time at suction cup lysimeters A1 to A4 (right), run 2 (block A)..

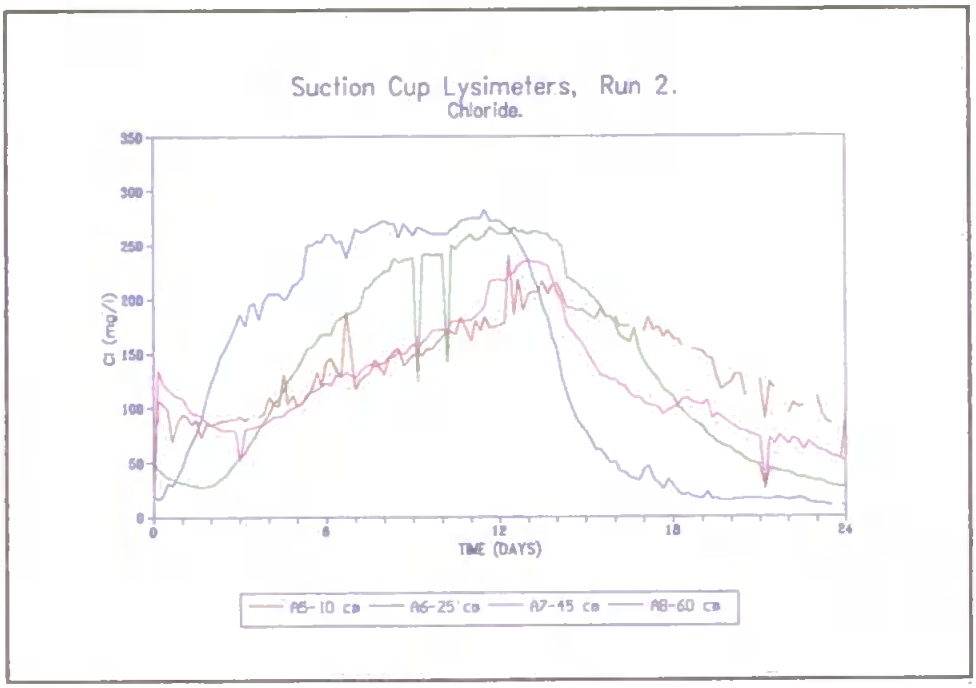

Figure 7.6 - Change in chloride concentration through time at suction cup lysimeters A5 to A8 (left), run 2 (block A).

initial breakthrough in 4 hours and reaching the background concentration within 11 days (Figure 7.6). During the dilution it took longer for all samplers to reach background concentration than during the tracer application (Table 7.5). Solute collected from A5(10 cm) responded the slowest to changes in irrigated concentration.

Mole Drain:

Chloride concentration,250 mg l^{-1} Cl: The mole drain responded to the irrigation within 0.02 of an hour of the start of irrigation and reached the peak concentration 9.2 days after the start (Figure 7.7 and Table 7.5).

Flush with tap water, 10 mg l^{-1} Cl: Unlike the suction cup lysimeters the concentration level at the mole reduced more quickly during the flush taking just 17 minutes to initially respond and under 2 days to reach the background concentration (Figure 7.7).

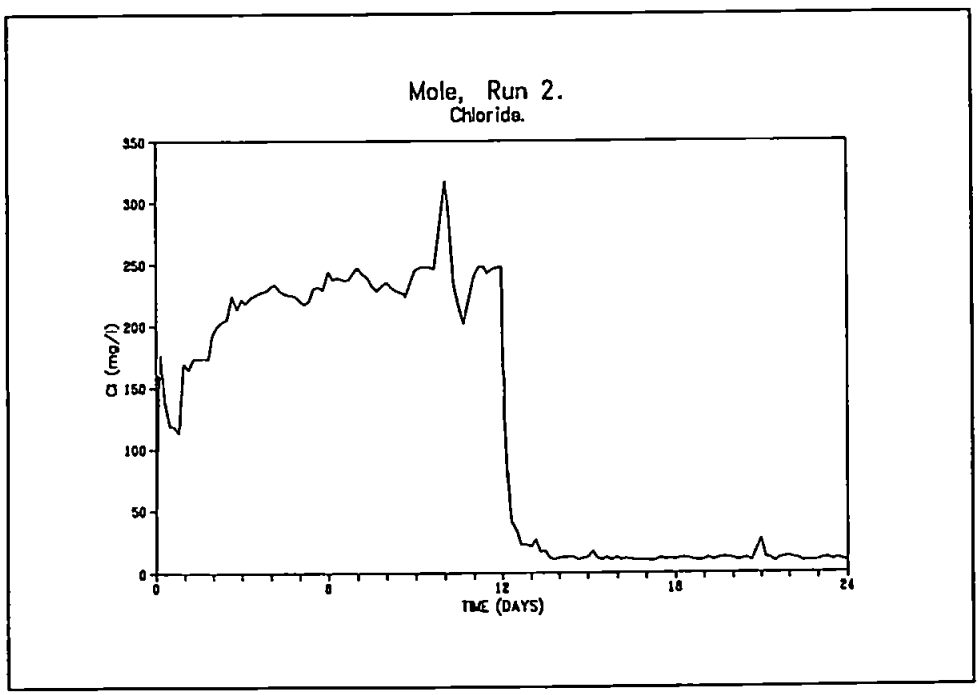

Figure 7.7 - Change in chloride concentration through time from samples collected from the mole drain, run 2 (block A).

Explanation:

Structure again seemed to play an important role in determining the speed of solute movement to depth in the soil. The faster response observed at depth, of change in sample concentration, at A6(25 cm), A8(60 cm) and from the mole drain may have been the result of short path length from point of irrigation to sample location. At the mole the larger proportion of mechanically produced preferential flowpaths may have allowed solute to move through the soil with minimal contact time.

From Chapter 6 (Table 6.8 and 6.9) a general decrease in suction and thus increase in soil water content was observed between run 1 (part II) and run 2 due to the increased height of the water table which reduced the soil water gradient. The resultant increase in hydraulic conductivity allowed a more rapid movement of solute to depth, and therefore less time for diffusion to occur and less solute loss to the soil matrix. A stronger concentration of solute would therefore have been left in solution and may explain the larger peak concentrations reached in run 2 compared to run 1 (part II). Hydrodynamic dispersion would also have increased as flow rate and number of pathways increased which may have delayed peak concentrations emerging.

A faster initial breakthrough in run 2 compared to run 1 (part II) and stronger peak concentrations during tracer irrigation may also be linked to residual chloride in the soil. Accumulation of solute in the matrix, by diffusion, in run 1 (part II) may not have been leached out by flushing in between the two experiments. At sample locations A3(45 cm), A4(60 cm) and A6(25 cm) the concentration of chloride in initial soil water samples taken prior to the experiment were greater than those in the tap water used to flush the soil (Table 7.5). A larger residual concentration of chloride in the soil matrix would have reduced the gradient between irrigated tracer concentration and *in situ* soil water

concentration. A reduced concentration gradient would reduce the rater of diffusion to the soil matrix and therefore leave a greater concentration in the mobile solution.

The fact that the samplers responded in a similar sequence, although at different rates, during run 1 (part II) and run 2 would suggest that similar pathways were active, although dispersion was different which may be linked to hydraulic conductivity and/or hydraulic/chemical concentration gradients. This will be discussed in Chapter 8.

Although a raised water table was observed on the out side of the block, the transducer readings as described in Chapter 6 monitored unsaturated conditions below the mole drain internally. Only at sample locations A3 and A7 (45 cm) did tensiometer results indicate soil water conditions to be close too or actually saturated. The saturated conditions observed at 45 cm may have been as a result of the tensiometer cup intersecting a large pore or crack that was saturated, or may have been due to a change in structure, from fine sub-angular blocky to very coarse prismatic. The change in structure observed between 30 and 50 cm may have lead to the development of an internal catchment which would explain the saturated conditions observed at 45 cm. Tensiometer samplers below the mole, A8 and A4 (60 cm), recorded suction to still be present and therefore soil water conditions to be unsaturated. Unsaturated conditions may have been observed below the mole because of the location of the samplers within peds where only slow equilibrium may have occurred between water in faster flowing pathways and finer pathways. Larger pores and channels may have been filled to the base of the mole but the tensiometers would have only reflect this if larger pore or crack were intersected.

Summary:

Run 2 consisted of an irrigation of tracer for 12 days followed by a flush using tap water for 12 days (Table 7.1). The water table had been allowed to accumulate to the base of the mole drain, in an attempt to simulate winter field conditions. The time of initial breakthrough and time taken to reach irrigation concentration for all sample locations is summarised in Table 7.5. A summary of the order of response to initial breakthrough and peak concentration at all sample locations is given in Table 7.6, while a summary of the different order of response at the suction cup lysimeter samplers is given in Table 7.7.

For this second experiment the right side of the block again reacted more quickly to changes in irrigation concentration than the left. There was also evidence, from the initially large residual chloride concentrations at some sample locations at the start of run 2, of the problem of matrix water retaining an increased concentration even after intensive flushing

Table 7.6 - Order of response of initial breakthrough and peak concentration/dilution for run 2.

Sampler	250 mg l^{-1} Cl		Flush	
(depth in soil, cm)	Initial break-through	Peak	Initial (dilution) breakthrough	Lowest conc.
A1(10)	3	1	3	2
A2(25)	3	2	3	3
A3(45)	4	3	3	4
A4(60)	5	5	4	6
A5(10)	3	8	2	9
A6(25)	6	7	6	7
A7(45)	7	8	5	8
A8(60)	2	4	2	5
Mole(50)	1	6	1	1

Table 7.7 - Summary of result of suction cup lysimeter responses for run 2.

Experiment	Location - left of block (A5(10 cm), A6(25 cm), A7(45 cm) and A8(60 cm))	Location - right of block (A1(10 cm), A2(25 cm), A3(45 cm) and A4(60 cm))
Run 2	A8 showed initial breakthrough and reached irrigation concentration first. Initial breakthrough (tracer) A5 to A7 occurred in order of depth in soil. A6 was the only other sampling location, apart from A8, to reach irrigation concentration. Initial breakthrough (flush) took longest at A6. A6 reached a lower concentration at the end of the flush than A5 which had a larger residual concentration than A7.	A1 to A4, increased in time to initial breakthrough and peak irrigation concentration with depth in the soil for both tracer and flush.

with diluting solution (Table 7.5).

The fastest initial breakthrough for both tracer and flush was recorded at the mole. However, during the tracer irrigation the sample from the mole took twice as long as samples collected from A8(60 cm) to reach irrigation concentration, whilst during the flush samples collected from the mole reached irrigation concentration six times faster than samples at A8 (60 cm).

With the exception of A8(60 cm) samples collected from A1 to A4 (right) responded more quickly than samples collected form A5 to A8 (left). Results from sample locations A1 to A4 showed that solute movement took progressively longer with depth, while solute movement, A5 to A8, was more variable.

The variability of solute response times within the soil block was observed, between run

1 (part II) and run 2, to have been similar. A comparison between run 1 (part II) and run 2 during tracer irrigation shows that for sample locations A1(10 cm) to A4(60 cm) both initial breakthrough and time to irrigation concentration occurred more rapidly during run 2. For sample, at location A5(10 cm) to A8(60 cm) initial breakthrough occurred at the same rate at locations A6(25 cm) and A8(60 cm), faster in run 2 at A5(10 cm), and slower in run 2 at A7(45 cm). Time to attain irrigation concentration was faster in run 2 at location A6(25 cm) and A8(60 cm) and slower in run 2 at locations A5(10 cm) and A7(45 cm). Although irrigation concentration was reached more slowly than in run 1 (part II), concentrations reached in run 2 were closer to the irrigation concentration. Results for the mole drain sample were rather complicated because the initial breakthrough occurred faster in run 2 but time to irrigation concentration took twice as long than in run 1 (part II). Further more, peak irrigation concentration was reached in run 2 unlike run 1 (part II).

7.4.3. Sampling Run 3.

The aim of run 3, conducted on block B alone, was to make a comparison of solute variability between two seemingly identical soil blocks to see how variable solute movement was when soils were initially located only a small distance apart. Sampling locations within the block were made as similar as possible to those in block A using the position of the mole drain as a reference point. Prior to sampling block B was irrigated with tap water for a month. Run 3 consisted of a 12 day miscible displacement using 250 mg l^{-1} Cl solution, followed by a 12 day flush using tap water (10 mg l^{-1} Cl) (Table 7.1) at an irrigation rate of 2.3 mm h^{-1}. As with run 2 (block A) the water at the base of the block was allowed to accumulate to just below the mole to simulating winter type conditions as before. No solute sample was taken from the base of the block because of this.

Table 7.8 summarises the times and concentrations for the initial breakthrough and time to peak/background for the suction cup lysimeters and the mole drain of run 3.

Suction Cup Lysimeters:

Chloride concentration (right), 250 mg l^{-1} Cl: Solute collected from B1(10 cm) responded the first to the change in concentration applied at the surface (Figure 7.8), taking 4 hours to show an initial breakthrough and 3.3 days to reach the peak irrigation concentration of 250 mg l^{-1} Cl. Initial time to breakthrough occurred in 8(B2), 16(B3) and 16(B4) hours respectively and time to peak concentration 12.2(B2), 11.7(B3) and 22(B4) days (Figure 7.8 and Table 7.8). Although samples collected from B3(45 cm) peaked faster than samples collected from B2(25 cm) peak concentration observed at B3(45 cm)was below the irrigation concentration (Table 7.8). The peak concentrations at B3(45 cm) and B4(60 cm) were respectively 236 and 173 mg l^{-1} Cl (Table 7.8).

Flush with tap water (right), 10 mg l^{-1} Cl: The responses were slightly slower than the initial rise during irrigation with 250 mg l^{-1} Cl, with samples collected form samplers B1(10 cm) to B3(45 cm) showing an initial breakthrough within 8, 24 and 16 hours respectively. Sampler B1(10 cm) was the only location at which solute concentration reached background concentration within the 12 days, taking 10.5 days to do so (Figure 7.8). At the other sampling locations solute concentration reached 25.8(B2), 108(B3) and 162(B4) mg l^{-1} Cl respectively.

Chloride concentration, 250 mg l^{-1} Cl and flush (left): Solute concentration sampled at B5(10 cm) showed a very gradual rise and fall in concentration over the 24 day period (Figure 7.9), taking 15.7 days to reach a peak concentration of 194 mg l^{-1} Cl and returning to a concentration of 146 mg l^{-1} Cl by the last day. Initial breakthrough occurred at B6(25

Table 7.8 - The response times recorded by the change in concentration curves (Figures 7.8 to 7.10) for run 3 showing times from start of irrigation or flush, and concentration values if irrigated concentration not reached (250 mg l^{-1} Cl for initial 12 days and 10 mg l^{-1} Cl for the final 12 days).

Sampler	Irrigation with 250 mg l^{-1} Cl.		Flush with tap water, 10 mg l^{-1} Cl.	
(depth in soil, cm)	Time of initial break-through (hrs)	Time to peak conc (hrs)	Time of initial break-through (hrs)	Time to background (hrs)
B1(10)	4	80	8	252
B2(25)	8	292	24	288 (25.8 mg l^{-1})
B3(45)	16	280 (236 mg l^{-1})	16	288 (61.1 mg l^{-1})
B4(60)	16	528 (173 mg l^{-1})	-	288 (162 mg l^{-1})
B5(10)	56	376 (194 mg l^{-1})	96	288 (146 mg l^{-1})
B6(25)	12	280 (228 mg l^{-1})	24	288 (61.1 mg l^{-1})
B7(45)	32	312 (182 mg l^{-1})	40	288 (78.2 mg l^{-1})
B8(60)	32	288 (121 mg l^{-1})	4	288 (69.1 mg l^{-1})
Mole(50)	1	272 (225.1 mg l^{-1})	16	288 (38 mg l^{-1})

cm) 44 hours before it occurred at B5(10 cm) even though the sample was collected from a deeper location within the soil. Solute collected from sampler B6(25 cm) peaked to 228 mg l^{-1} Cl in 12 days and responded in a similar manner to the flush until 6 days into the flush when the rate of dilution was dramatically reduced (Figure 7.9). In the first 6 days solute concentration at B6(25 cm) decreased from 228 to 70 mg l^{-1} Cl. In the final 6 days concentration at B6(25 cm) only decreased from 70 to 60 mg l^{-1} Cl. Solute collected at sampler B7(45 cm) peaked at 182 mg l^{-1} Cl and decreased slowly during flushing to a concentration of 78.2 mg l^{-1} Cl (Figure 7.9). Samples collected from sampler B8(60 cm)

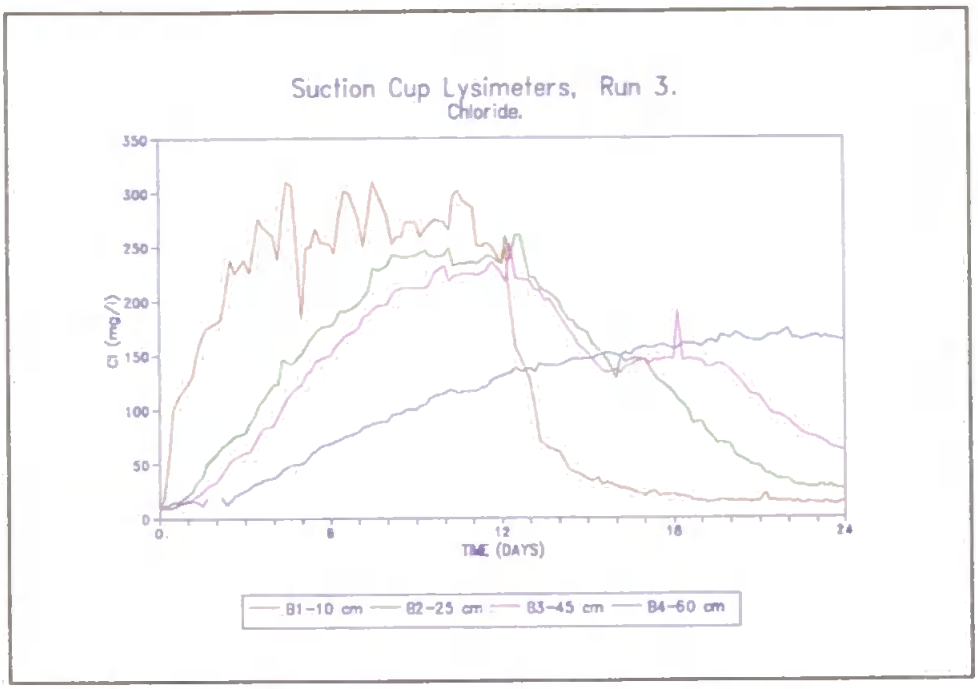

Figure 7.8 - Change in chloride concentration through time at suction cup lysimeters B1 to B4 (right), run 3 (block B).

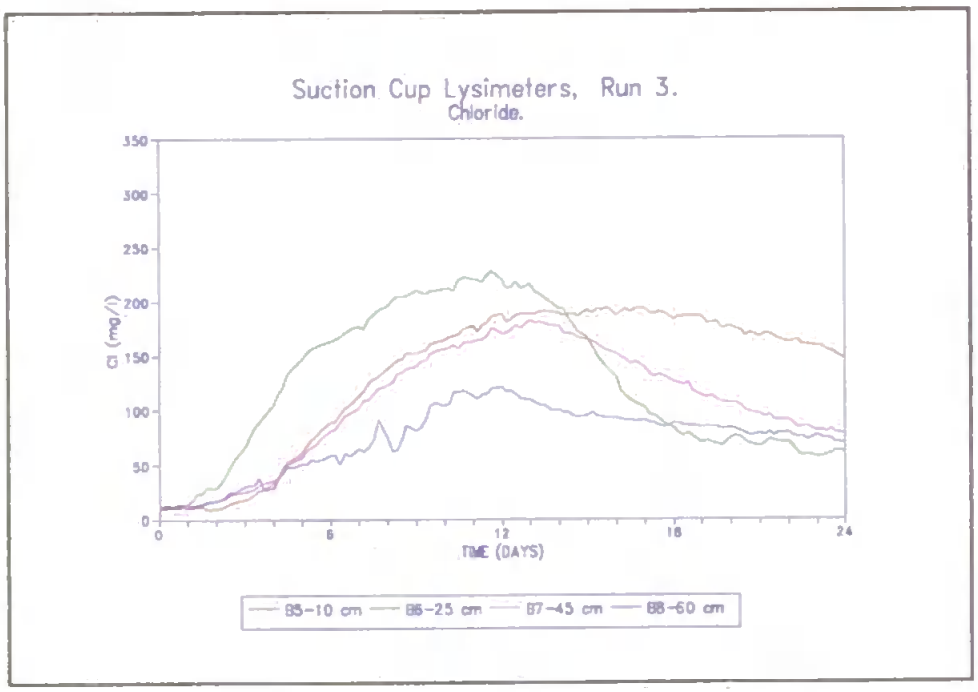

Figure 7.9 - Change in chloride concentration through time at suction cup lysimeters B5 to B8 (left), run 3 (block B).

located directly under the mole drain did not respond in a similar manner to samples collected from the mole drain. After 12 days solute concentration at B8(60 cm) had only reached 121 mg l^{-1} Cl. Similarly after 12 days of flushing solution at B8(60 cm) had only reduced in concentration by less than 50%, to a concentration of 69.1 mg l^{-1} Cl.

Mole Drain:

Chloride concentration, 250 mg l^{-1} Cl: The initial breakthrough occurred within 1 hour of the start. However, peak concentration was reached only 11.3 days later and the peak concentration was 25 mg l^{-1} Cl below the irrigation concentration (Figure 7.10).

Flush with tap water, 10 mg l^{-1} Cl: The dilution of solute concentration took longer than rise in concentration, taking 16 hours to show any response and only reaching a concentration of 38 mg l^{-1} Cl by the final day (Figure 7.10).

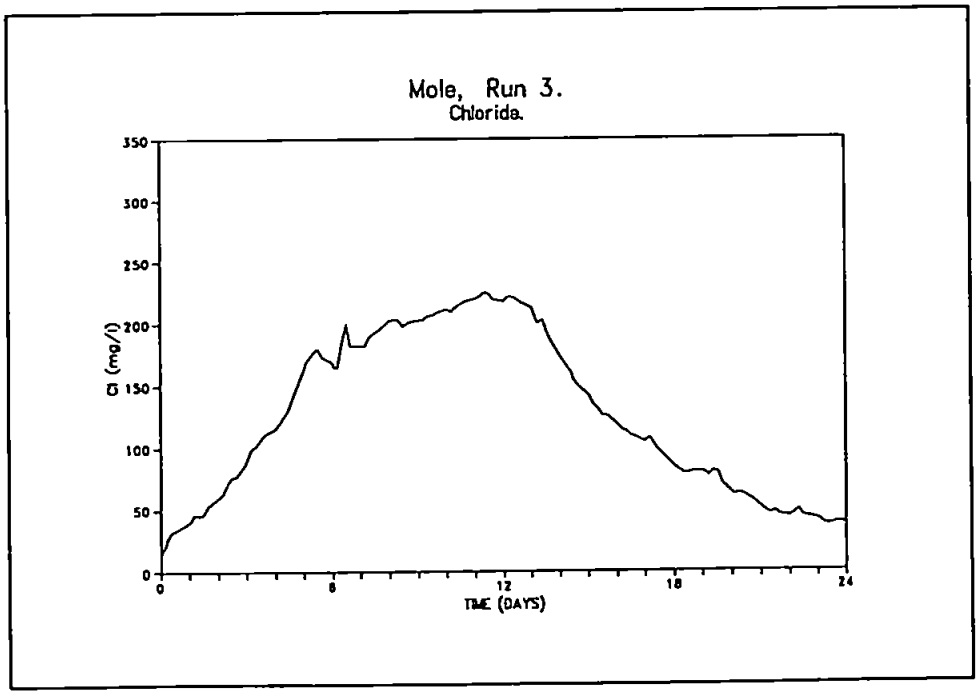

Figure 7.10 - Change in chloride concentration through time from samples collected from the mole drain, run 3 (block B).

Explanation:

Right: The delay in change of concentration of samples collected at B2(25 cm), B3(45 cm) and B4(60 cm) reflected their increased depth in the soil. The changes in solute concentration observed at samplers B1(10 cm) to B3(45 cm) reacted in a manner associated with the intersection of both preferential and matrix flow. The second peak in concentration observed at B3(45 cm) (Figure 7.8) during the flush may have been the result of changing pathways during the experiment caused by faunal activity. Solute collected from sampler B4(60 cm) reacted in a manner associated with slow matrix flow, responding slowly to change as a result of solute mixing.

Left: Solute concentration at sampler B8(60 cm) changed more slowly and attained a weaker peak concentration during run 3 than A8 during run 2. In block A, a crack was observed to link the base of the mole drain to the sampler at A8. No macropores were found to connected the base of the mole directly to B8. The sample collected at B8 must have come either from solute moving slowly through micropores or as a result of the raised water table.

The decline in speed of dilution observed in the sample collected at B6(25 cm) may be explained by a change in predominant pathways. The slow response to change in concentration of solute collected at B5(10 cm) and the fact that the smallest volume of water was collected at this point would suggest that this suction cup was located in a low porosity area and, as in block A, a clay rich band was observed in the locality of B5(10 cm) in the soil section during destructive sampling.

Comparison of experiments: Pattern of response (order) was slightly different in run 3 compared to run 2, possibly as the result of variability in pathways due to the

heterogeneous nature of the soil. The relatively small concentration peaks observed during tracer application in run 1 (part II) and run 3 may have been due to diffusion. A stronger chloride concentration tracer input combined with a weak chloride concentration matrix water resulted in an increased potential gradient between irrigation solution and matrix. Such a large concentration gradient would be likely to increase diffusion into the soil matrix. Larger peak concentrations in run 2 relative to those in run 1 may have been the result of incomplete leaching of chloride from the matrix during flushing leading to a reduced potential gradient between applied tracer and matrix solution thus reducing diffusion between mobile and immobile zones. A reduction in diffusion would lead to a larger concentration of chloride being left in the mobile solution.

A faster response was observed during tracer application than during the flush, in runs 1, 2 and 3, which may be associated with solute ions being repelled by similarly charged particles on the soil surface resulting in a faster movement of solute than water.

Mean suction was larger at locations B2 to B4 (right) than at A2 to A4 (run 2, right) (Tables 6.9 and 6.10). In general mean suction at B6 to B8 (left) was similar to that at A6 to A8 (left) (Tables 6.9 and 6.10). However, samplers, in run 3 located at 10 cm (B1 and B5) record smaller mean suctions than run 2 at similar locations. Only suction sampler B1(10 cm) showed signs of being saturated. Suction samplers below the mole drain (B4 and B8, 60 cm) both recorded a positive suction even though the water table within the soil was believed to have been raised to the hight of the mole drain. This result indicated that perhaps pockets of saturated soil existed. As explained earlier, sampler location may be an important factor in determining the suction recorded. The slow time to peak solute concentration at B4(60 cm) and the even slower dilution rate observed there may have been a result of the raised water table. The effect of raising the water table seemed to cause

dilution of concentration in run 3 at locations B4 and B8 (60 cm). The small peak concentration may be due to the raised water table increasing dilution of these sample locations. This was not as evident in run 2 except at A4(60 cm, right).

In runs 1, 2 and 3 samples collected from the mole drain responded quickly and reached irrigation concentration. Such similarities between the two blocks must be linked to induced pathways, created by the mole plough. Other sample locations within the blocks showed a larger degree of variability, a reflection of dissimilar pathways in a natural soil structure.

Summary:

Run 3 consisted of a 12 day irrigation of tracer followed by 12 days of leaching using tap water (Table 7.1). The high water table was expected to increase the soil water content, especially at the base of the block, with the aim of inducing more drainage from the mole drain. The time of initial breakthrough and time to attain irrigation concentration are summarised in Table 7.8. A summary of the order in which the samples taken from both suction cup lysimeters and mole drain reached initial breakthrough and peak concentration is given in Table 7.9 while a brief summary of how the suction cup lysimeters responded according to depth in the soil is given in Table 7.10.

In general initial breakthrough occurred more rapidly during the tracer irrigation than during flushing. Results observed at B5 to B8 (left) showed that a large residual concentration was maintained at these locations after flushing than at the majority of the right hand readings (B1 to B4), the only exception being the results observed at B4(60 cm) (Table 7.8). Peak concentrations were also observed to be larger on the right side than on the left. The results for block B are not all that dissimilar to those of block A and would suggest that block B behaved in a similar manner to block A.

Table 7.9 - Order of response of initial breakthrough and peak concentration/dilution for run 3.

Sampler	250 mg l^{-1} Cl		Flush	
(depth in soil, cm)	Initial breakthrough	Peak	Initial (dilution) breakthrough	Lowest conc.
B1(10)	2	1	2	1
B2(25)	3	5	4	2
B3(45)	5	3	3	4
B4(60)	5	8		8
B5(10)	7	7	6	7
B6(25)	4	3	4	4
B7(45)	6	6	5	6
B8(60)	6	4	1	5
Mole(50)	1	2	3	3

Table 7.10 - Summary of result of suction cup lysimeter responses for run 3.

Experiment	Location - left of block (B5(10 cm), B6(25 cm), B7(45 cm) and B8(60 cm))	Location - right of block (B1(10 cm), B2(25 cm), B3(45 cm) and B4(60 cm))
Run 3	B5 took the longest to react to both tracer and flush, retained largest concentration of chloride. Peak irrigation concentration not reached at any sampler location (B5 to B8). B6 reached larger peak concentration than B7 followed by B8. During flushing initial breakthrough B8 responded the fastest. At end of flush residual chloride larger in B7 than B8 followed by B6 and B5.	B1 to B4 showed an increase in time to depth for initial breakthrough. Time to peak B2 took longer than B3, otherwise an increase tome to peak irrigation was observed with depth. After flushing there was an increase in residual tracer concentration left with depth.

Initial breakthrough occurred more rapidly at sample locations B1(10 cm), B4(60 cm), B6(25 cm) and B7(45 cm) in run 3 compared to run 2. However, initial breakthrough occurred more slowly at sample locations B3(45 cm), B5(10 cm), B8(60 cm) and at the mole(B) in run 3 compared to run 2. Only results recorded at location B2 had an identical initial breakthrough speed in both run 3 and run 2. Change in chloride concentration observed at the mole took longer to reach initial breakthrough and irrigation concentration during the flush than during the tracer application. This patten of response at the mole drain was also observed in run 1 and run 2 .

Time to peak irrigation concentration (tracer) occurred more slowly in run 3 compared to run 2. As with run 1 (part II) the majority of the sample locations in run 3 (7/9) did not reach irrigation concentration during the tracer application. In general the peak concentrations reached in run 1 (part II) and run 3 were less concentrated than samples collected in run 2. Similarly, after leaching the block 8 out of 9 sampling locations did not reach background concentrations in run 3. A larger residual chloride concentration was left in the soil solute at the end of run 3 similar to large concentrations observed at the beginning and end of run 2 after flushing.

7.5. PULSE EXPERIMENTS.

7.5.1. Sampling Run 4.

The aim of run 4 was to observe the differences in appearance times and changes in concentration for two pulse tracers (chloride and nitrate) at depth in the soil: Soil water status within the soil block was set up to simulate spring time soil conditions with a larger soil water content and low water table, below the level of the mole drain. As no significant effect had been observed in solute movement by raising the water table in runs 2 and 3 it was decided that the base of the block should be drained, so that a solute sample could be

collected from this location. The advantage of sampling solutes emerging from the base of the block was that it gave an indication as to the potential leaching of chemicals at depth in the soil, which could lead to a build up in chemical or pollutant concentration at depth and increase the potential for release into river systems when the water table rises. A pulse of tracer, 2500 mg l^{-1} Cl and 500 mg l^{-1} NO_3 was applied to the surface of block B and flushed through with tap water, at an irrigation rate of 2.5 mm h^{-1}, for 12 days. The stronger concentration of chloride was used to simulate a chloride fertilizer (KCl) and to dominate any residual chloride left in the soil from run 3. The amount of nitrate applied was equivalent to 50 kg N Ha^{-1}, and is a typical amount of fertilizer applied to grassland in early spring.

The results of the chloride and nitrate pulse will be presented separately, followed by a brief explanation of how such solute variations may arise. A summary of the general patterns of solute spatial and temporal variability will be made after the results which will include similarities and differences observed between the chloride and nitrate pulses.

Suction Cup Lysimeters:

Chloride pulse: The response times and concentration of initial breakthrough and peak or background concentration are summarised in Table 7.11. Figures 7.11 and 7.12 show the change in chloride concentration through time at the sampling locations B1 to B4, and B5 to B8 respectively. With the exception of solute collected at B1(10 cm) (Figure 7.11) no other sample collected from any suction cup lysimeters recorded a distinct peak in chloride concentration (Figures 7.11 and 7.12). Solute concentration at sampler B1(10 cm) reached a peak of 109 mg l^{-1} Cl within the first 4 hours of application and took 2 days to return to background concentration levels. The speed and concentration of the pulse observed at B1(10 cm) may have occurred sooner and to a greater concentration than the 4 hour

interval suggests.

Mole drain:

Chloride pulse: The change in solute concentration observed at the mole, Figure 7.13, was not very distinct, the main problem being a large residual chloride level from run 3. Two

Table 7.11 - Chloride concentration curve for run 4 (Figures 7.11 to 7.14), showing times from start of irrigation and concentrations (mg l^{-1} Cl). (-) equal unidentifiable results.

Sampler (depth in soil, cm)	Initial background conc. (mg l^{-1} Cl)	Initial breakthrough (hrs)	Time to peak (hrs)	Time to background (hrs)
B1(10)	109	4	4 (109 mg l^{-1} Cl)	48 (12.1 mg l^{-1} Cl)
B2(25)	36.9	-	-	288 (18 mg l^{-1} Cl)
B3(45)	44.2	-	-	288 (28 mg l^{-1} Cl)
B4(60)	121	-	140 (84.1 mg l^{-1} Cl) 188 (71.6 mg l^{-1} Cl) 224 (62.3 mg l^{-1} Cl)	288 (51.9 mg l^{-1} Cl)
B5(10)	53.7	-	100 (46.9 mg l^{-1} Cl)	288 (30.7 mg l^{-1} Cl)
B6(25)	41.5	-	76 (32 mg l^{-1} Cl)	288 (12.5 mg l^{-1} Cl)
B7(45)	40.8	-	92 (40 mg l^{-1} Cl)	288 (26.1 mg l^{-1} Cl)
B8(60)	66.3	-	108 (64.2 mg l^{-1} Cl)	284 (45.9 mg l^{-1} Cl)
Mole(50)	83.5	-	23 (67.7 mg l^{-1} Cl)	288 (12.9 mg l^{-1} Cl)
Base of Block(85)	48.4	8	8 (52.7 mg l^{-1} Cl)	288 (25.7 mg l^{-1} Cl)

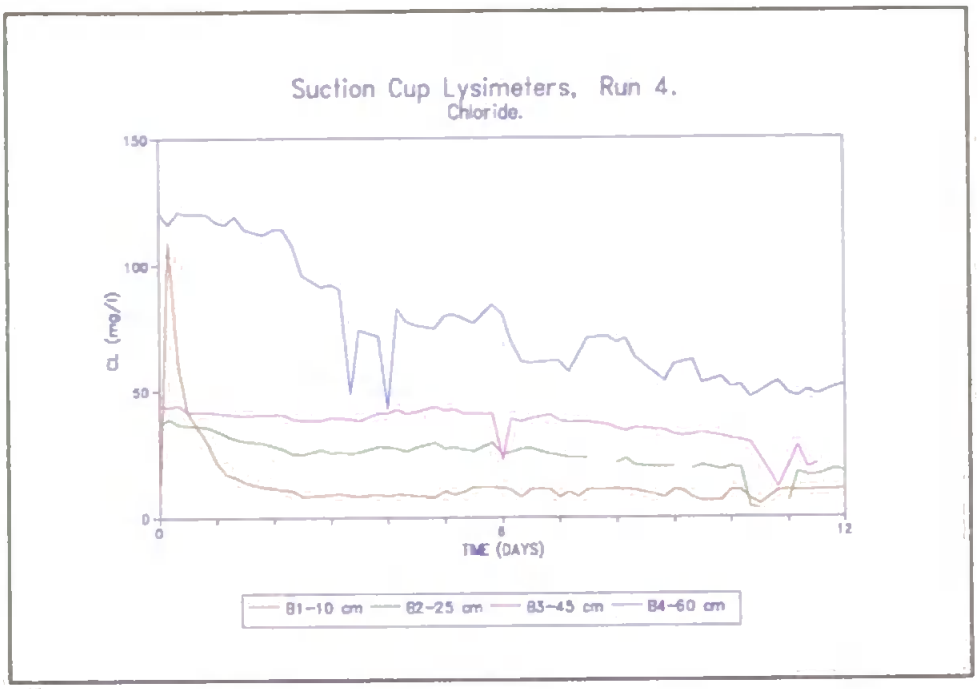

Figure 7.11 - Change in chloride concentration through time at suction cup lysimeters B1 to B4 (right), run 4 (block B).

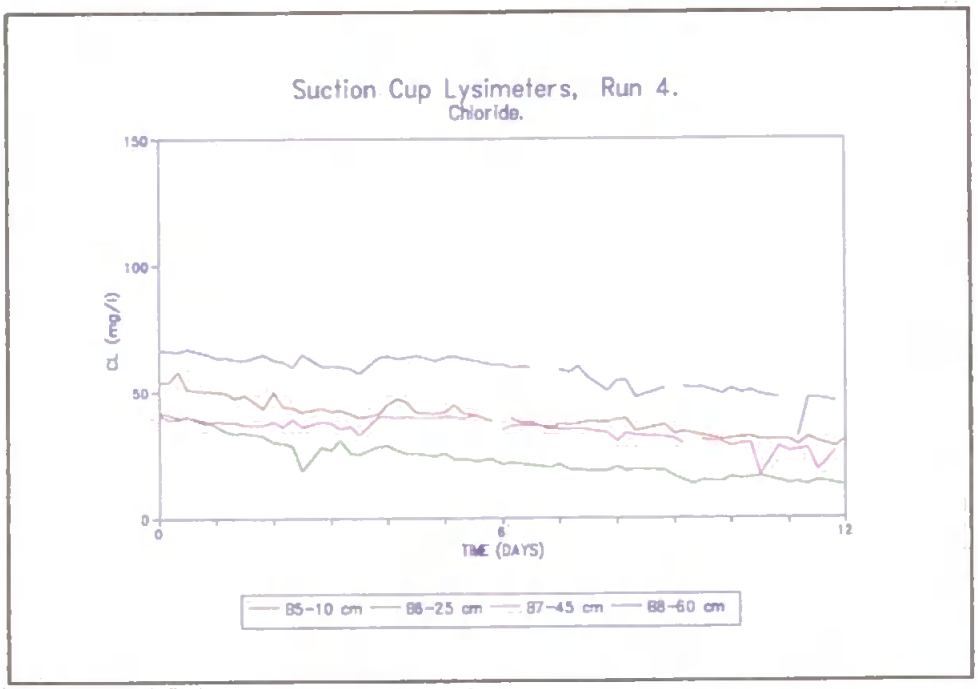

Figure 7.12 - Change in chloride concentration through time at suction cup lysimeters B5 to B8 (left), run 4 (block B).

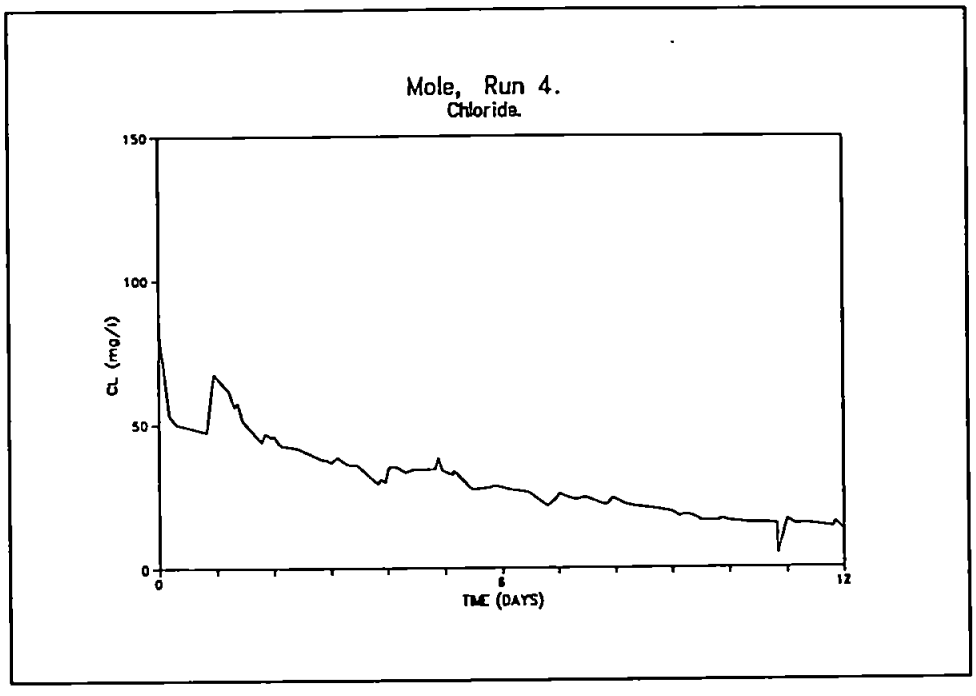

Figure 7.13 - Change in chloride concentration through time from samples collected from the mole drain, run 4 (block B).

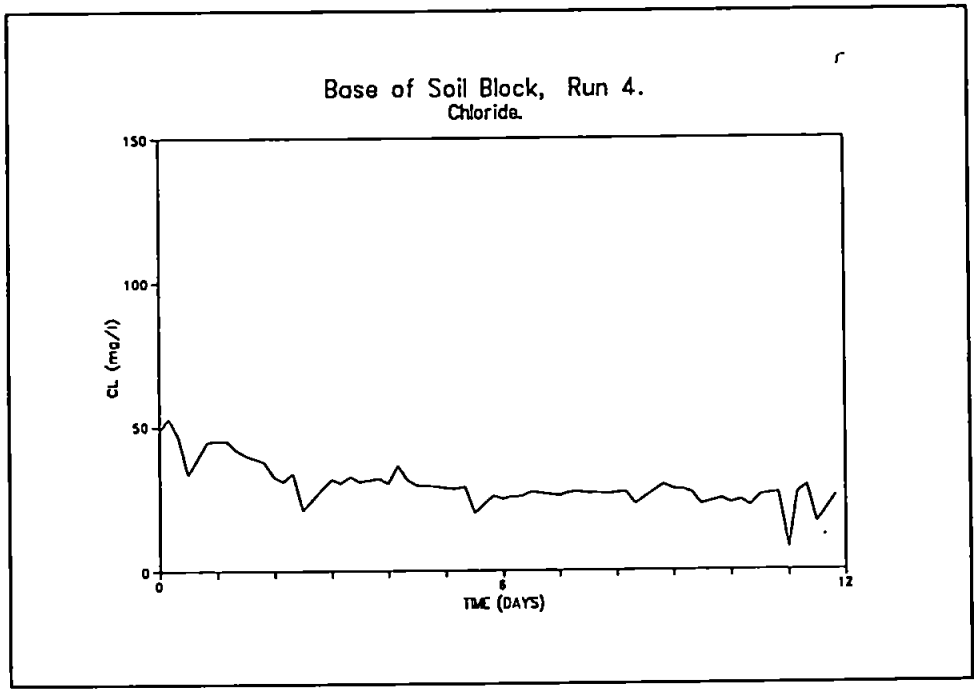

Figure 7.14 - Change in chloride concentration through time from samples collected from the base of the block, run 4 (block B).

pulses were evident, the first peak was observed in the first sample, peaking at 83.5 mg l^{-1} Cl and returning to 47.4 mg l^{-1} Cl within 4 hours. The second peak of chloride occurred 0.96 days after the start of the experiment, peaking to 67.7 mg l^{-1} Cl and took 12 days to reach a concentration of 25.7 mg l^{-1} Cl. A double peak occurring in a pulse experiment has also been noted by Marshall (1994) and Holden *et al.* (1995b) who have suggested that it indicates the interaction of two different sets of pathways.

Base of block:

Chloride: A pulse chloride was observed 8 hours after the start of run 4 (Figure 7.14) although this pulse was not very distinctive, peaking at 52.7 mg l^{-1} Cl, an increase in concentration of 4.3 mg l^{-1} Cl compared to the initial background concentration and may only have represent 'old' solute moving through the block.

Suction Cup Lysimeters:

Nitrate Pulse (right): The response times and concentration of initial breakthrough and irrigation concentration are summarised in Table 7.12 for nitrate. Solute concentration sampled at B1(10 cm) changed rapidly (Figure 7.15), as with the chloride pulse, and peaked 4 hours after the application of the pulse at a concentration of 77.5 mg l^{-1} TON. A second peak of 20.8 mg l^{-1} TON was observed at B1(10 cm) 20 hours after the application (Figure 7.15). Sampler B1(10 cm) eventually reached a background concentration 3.8 days after the start of the experiment. Solute collected from sampler B2(25 cm) showed only a small increase in concentration (6.55 mg l^{-1} TON) 4 hours after application (Figure 7.15), however, solute concentration at B2(25 cm) and B3(45 cm) also showed a very slow rise to a peak 5.2 days after the start of the experiment reaching concentrations of 8.35 and 6.14 mg l^{-1} TON respectively (Figure 7.15). Solute collected from sampler B4(60 cm) showed no indication that nitrate reached this location within the 12 days (Figure 7.15).

Table 7.12 - Change in nitrate concentration curves for run 4 (Figures 7.15 to 7.18), showing times from irrigation and concentration reached (mg l^{-1} TON).

Sampler (depth in soil, cm)	Initial background conc. (mg l^{-1} TON)	Time to initial breakthrough (hrs)	Time to peak (hrs)	Time to background (hrs)
B1(10)	0.469	4	4 (77.5 mg l^{-1} TON) 20 (20.8 mg l^{-1} TON)	92
B2(25)	3.97	4	4 (6.55 mg l^{-1} TON) 124 (8.35 mg l^{-1} TON)	228 (3.56 mg l^{-1} TON)
B3(45)	1.13	4	124 (6.14 mg l^{-1} TON)	288 (3.8 mg l^{-1} TON)
B4(60)	0.405	-	-	288 (1.06 mg l^{-1} TON)
B5(10)	0.237	24	104 (1.23 mg l^{-1} TON) 168 (1.36 mg l^{-1} TON)	144 (0.241 mg l^{-1} TON) 212 (0.287 mg l^{-1} TON)
B6(25)	0.676	12	76 (10.1 mg l^{-1} TON)	288 (0.909 mg l^{-1} TON)
B7(45)	0.263	4	120 (10.4 mg l^{-1} TON)	288 (3.54 mg l^{-1} TON)
B8(60)	0.3	8	140 (2.9 mg l^{-1} TON)	288 (2.21 mg l^{-1} TON)
Mole(50)	1.4	7.71	44.5 (12 mg l^{-1} TON)	244 (1.49 mg l^{-1} TON)
Base of Block(85)	7.6	4	8 (15.75 mg l^{-1} TON)	108 (1.43 mg l^{-1} TON)

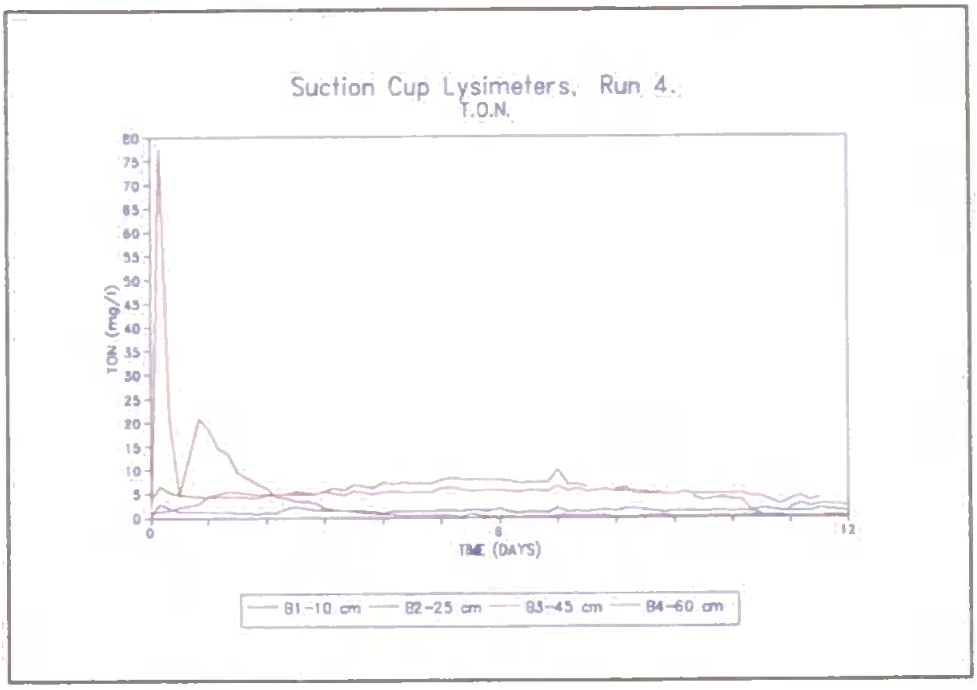

Figure 7.15 - Change in nitrate concentration through time at suction cup lysimeters B1 to B4 (right), run 4 (block B).

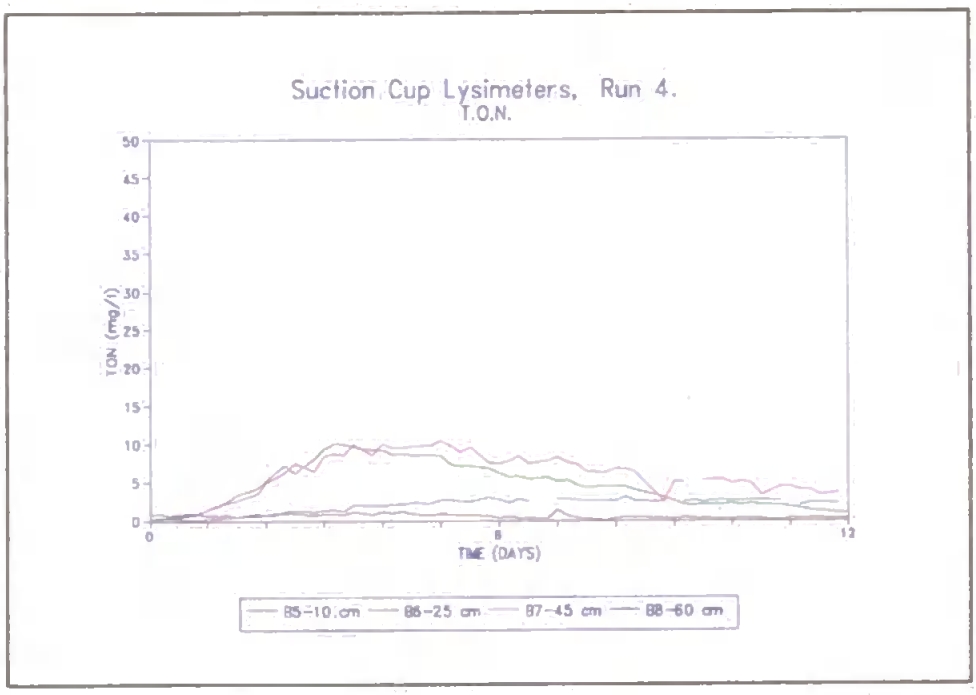

Figure 7.16 - Change in nitrate concentration through time at suction cup lysimeters B5 to B8 (left), run 4 (block B).

Nitrate pulse (left): Solute concentration at B5(10 cm) showed only a very minor change in concentration to the pulse of nitrate although two distinct peaks can be identified (Figure 7.16). The first peak came after a gentle rise in concentration, 4.3 days after the start of the experiment and peaked at 1.23 mg l^{-1} TON. The second peak (B5) occurred as a spike rising from background concentration level to 1.36 mg l^{-1} TON within 8 hours and back down to background concentration within 12 hours. This second peak occurred 7 days after the start of the experiment. Solute collected at sampler B6(25 cm) peaked at 10.1 mg l^{-1} TON in 3.2 days and reduced in concentration, with several sub-peaks (Figure 7.16), over the following 9 days to a background concentration of 0.909 mg l^{-1} TON. Solute concentration at sampler B7(45 cm) rose at a similar rate to solute concentration at B6(25 cm) (Figure 7.16) but reached a larger concentration, peaking 5 days after the start of the experiment (Table 7.12). The concentration of the samples at B7(45 cm) were greater than at B6(25 cm) as the concentration pulse reduced, sample concentration at B7(45 cm) eventually reached a concentration of 3.54 mg l^{-1} TON at the end of the experiment, 2.6 mg l^{-1} TON larger in concentration than the solute concentration at B6. Solute collected from sampler B8(60 cm) (located directly under the mole drain) only showed a gentle rise to a peak concentration of 2.9 mg l^{-1} TON, 5.8 days from the start (Figure 7.16). The reduction in solute concentration at B8(60 cm) was also very gradual and by the end of the experiment the concentration had only reduced to 2.21 mg l^{-1} TON.

Mole Drain:

Nitrate pulse: Figure 7.17 clearly shows that a pulse of nitrate occurred 1.9 days after the start of the experiment and reached a peak nitrate concentration of 12 mg l^{-1} TON (Table 7.12). The rate at which the concentration reduced from its peak concentration was slower than the time to peak taking 10.2 days to reach a background observation.

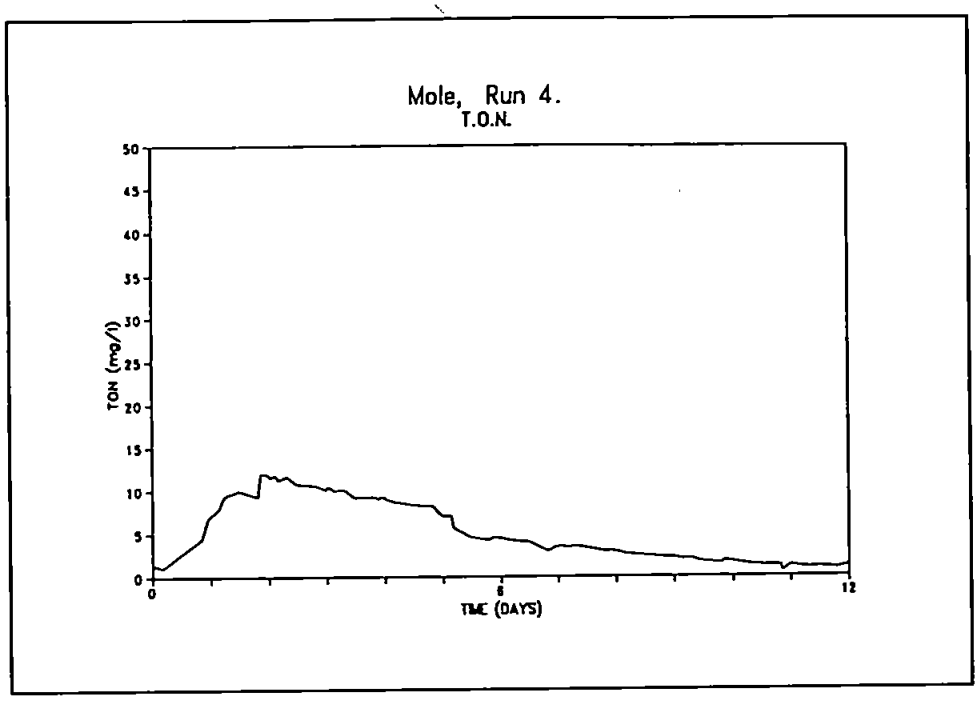

Figure 7.17 - Change in nitrate concentration through time from samples collected from the mole drain, run 4 (block B).

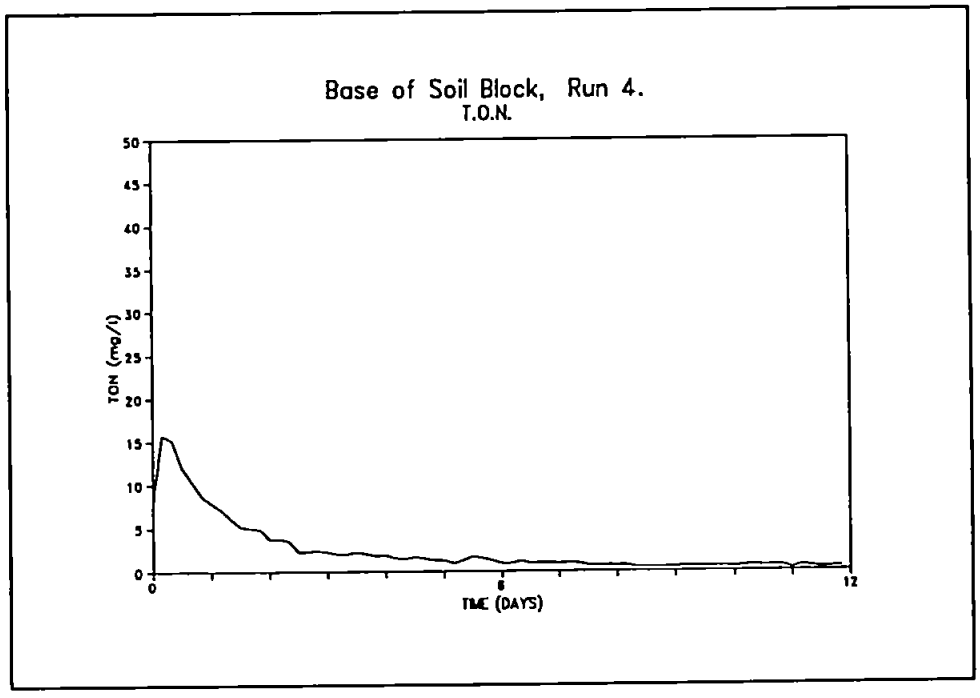

Figure 7.18 - Change in nitrate concentration through time from samples collected from the base of the block, run 4 (block B).

Base of Block:

Nitrate pulse: The pulse of nitrate came through 8 hours after the application of tracer at the surface (Table 7.12), although an initial breakthrough was seen within 4 hours. The peak nitrate concentration reached was 15.75 mg l^{-1} TON. The rate at which the concentration reduced from the peak concentration reached took longer than the initial rise to peak, taking 4.5 days from peak to background level (Figure 7.18).

Explanation:

Chloride: Although the block was flushed for 2 weeks after the end of run 3 the residual chloride concentration within the block was still in-excess of the background concentration (Table 7.11), demonstrating the potential for matrix storage of solutes in the soil. A distinct chloride pulse was not recorded at the majority of sampling locations most likely because even though a stronger concentration of chloride was used than nitrate a dilution of solute to half its original concentration within one hour was plausible making it difficult to distinguish the chloride pulse from the residual chloride concentration in the soil. Other less likely reasons why a distinct chloride peak was not seen may be due to the fact that the applied pulse of tracer did not find its way into a pathway that connected to the lysimeters, highlighting the problems of sampling in a heterogeneous material using at a point samplers, also the pathways through which the solute pulse travelled may have been predominantly slow with a large potential for mixing to occur between flowpaths and stagnant zones within the soil. The fact that nitrate was detected would, however, makes the first theory the more probable explanation.

Nitrate: Although the nitrate tracer had a smaller concentration than that of the chloride pulse residual nitrate in solution prior to the pulse application was small and therefore the nitrate signature was more distinctive in the observed solute samples (Figures 7.15 to 7.18).

Solute collected from sampler B1(10 cm) increased in concentration rapidly in a fashion that could be associated with bypass flow, while solute samples at B2(25 cm) and B3(45 cm) showed a slower rise in concentration characteristic of slower moving water. All results showed very weak peak concentrations from that applied, an indication of mixing, dilution and absorption.

The results observed at B7(45 cm) would suggest that both preferential flow as well as matrix flow influenced the observations at this location. The observed peak concentration in the samples collected from B6(25 cm) and B7(45 cm) showed signs of the presence of rapid pathways to these locations. The slower reduction in concentration of solute collected from B7(45 cm) compared to B6(25 cm) may be due to leaching of nitrate from higher in the soil profile. Sampler B6(25 cm) had less leached area above it and had a weaker peak solute concentration. The very slow rise in solute concentration observed at sampling locations B2(25 cm), B3(45 cm), B5(10 cm) and B8(60 cm) were characteristic of mixing having occurred within slower pathways. The weak peak concentration may be due to diffusion or absorption of nitrate into the soil peds, or lose of nitrate by denitrification or mineralization although this lose was assumed to be minimal due to prevailing soil conditions.

Concentration of samples collected from the mole drain showed a steep rise to peak followed by a slower dilution of concentration. The shape of the curve, from mole drain samples, could be associated with the movement of solute through initially rapid pathways, were a reduced level of mixing lead to a larger concentration at depth, followed by a gentle reduction in concentration associated with slower solute movement, increased mixing and adsorption into matrix.

The results observed at the base of block would suggest that a link may have existed to the surface via preferential flow pathways resulting in a quick peak with a slow reduction in concentration due to increase mixing and absorption with depth and slower pathways. This highlights the potential for rapid movement of chemicals and pollutants to depth, below the mole drain, in a draining soil.

Summary:

The speed of response to initial breakthrough and peak concentration are summarised in Tables 7.11 and 7.12. A summary of the order of response to time of peak concentration and order of magnitude of pulse (from stronger to weaker concentration) for all sample locations is presented in Table 7.13 for both tracers and a brief summary of the response order with depth in soil for the suction cup lysimeters is given in Table 7.14.

Chloride:

In general the chloride pulse was hard to distinguish from residue chloride concentration in the soil. By the end of run 4 concentrations of chloride in the soil, had in some cases, reduced to less than 50% of the original background concentration at the start of run 4 (Table 7.11). The mole sample peaked more slowly but to a larger concentration than the sample collected from the base of the block (Figures 7.13 and 7.14). Time to peak and the concentration of the peak reached was not apparently related for chloride samples (Table 7.13).

Nitrate:

The sample collected from the base of the block compared to the mole sample peaked more quickly (in 1/5th. of the time) and also reached a larger concentration than the mole (Figure 7.17 and 7.18). Table 7.13 clearly indicates that there was some form of relationship

Table 7.13 - Order of response of time to peak and order of magnitude of peak (from stronger to weaker conc.) for chloride and nitrate tracer pulse run 4.

Sampler	Chloride pulse		Nitrate pulse	
(depth in soil, cm)	Time to peak concentration	Order of peak concentration magnitude	Time to peak concentration	Order of peak concentration magnitude
B1(10)	1	1	1	1
B2(25)	-	-	1	6
B3(45)	-	-	7	7
B4(60	8	2	-	-
B5(10)	6	6	5	9
B6(25)	4	8	4	5
B7(45)	5	7	6	4
B8(60)	7	4	8	8
Mole(50)	3	3	3	3
Base of Block(85)	2	5	2	2

Table 7.14 - Summary of result of suction cup lysimeter responses for run 4.

Experiment	Location - left of block (B5(10 cm), B6(25 cm), B7(45 cm) and B8(60 cm))	Location - left of block (B1(10 cm), B2(25 cm), B3(45 cm) and B4(60 cm))
	Chloride: Fastest peak B7, largest peak concentration at B8. B5 responded as slowly as B8. In general there was an increase in peak concentration with depth. masked by large residual chloride levels. Nitrate: Largest peak concentrations reached at B6 and B7, lowest at B5.	Chloride: B1 to B4 showed a decrease in peak concentration and increase in time to peak with depth. Masked by large residual chloride levels Nitrate: B1 to B4 showed a decrease in peak concentration and increase in time to peak with depth.

between time to peak and magnitude of peak concentration for nitrate. The concentration pulses that came through the quickest tended also to have the larger peak concentrations.

Chloride and Nitrate:

Time to peak at B7, B8 and at the mole appeared in a slower time in the nitrate pulse than in the chloride pulse. Other locations recorded a similar time to peak for both tracers (Table 7.13). In general the chloride pulse increased in concentration with depth in the soil. The concentration of nitrate peak with depth compared to the chloride peak was more variable, although sample locations B1 to B3 showed a decreasing concentration with depth. Table 7.13 highlights the variability of observed responses with depth in the soil.

7.5.2. Sampling Run 5.

The final tracer experiment consisted of a pulse of chloride (2500 mg l^{-1}) and nitrate (500 mg l^{-1}) applied to the top of block B, in a similar fashion as in run 4, followed by 12 days of flushing with tap water at an irrigation rate of 3 mm h^{-1} (Table 7.1). Run 5 occurred 9 days after the end of run 4. No irrigation was applied to block B between the 4th and 5th run to allow the block to drain naturally under gravity. The aim of this experiment was to observe any differences in reaction times and variabilities of solute movement through a soil when initial soil water conditions within the soil block were slightly drier (run 4) compared to a soil that was initially closer to saturation (run 5) at the start of the experiment. Work by Kluitenberg and Horton (1990) has highlighted the importance of initial soil water conditions in influencing the shape of the resultant breakthrough curve of a pulse of chloride. Their work showed that a soil with a larger drainage porosity will peak quicker and at a greater concentration if initially drained than if initially saturated, whereas a soil with a smaller drainage porosity will peak quicker if initially drained compared to initially saturated but will have a smaller concentration peak than the initially saturated soil.

The results of the chloride and nitrate pulse will be presented separately. A brief explanation of how such solute variations may arise will be made after the results. The explanation will be followed by a summary of the general pattern of solute spatial and temporal variability which will include similarities and differences observed between the chloride and nitrate pulses.

Suction Cup Lysimeters:

Chloride pulse (right): A summary of the response times and peak concentrations is given in Table 7.15. At sampling location B1(10 cm) an initially large peak concentration of 100.2 mg l^{-1} Cl, 4 hours after the application of the tracer, was observed followed by a rapid return to a background within 3 days (Figure 7.19) (a similar result to run 4). The next largest concentration was observed at B4(60 cm) (Table 7.15). However, background concentration at B4 was initially 51.9 mg l^{-1} Cl which was due to residual chloride left in the soil at the end of run 4. A rapid reduction in solute concentration was observed at location B4(60 cm) after the peak concentration. A second rise in solute concentration to 35 mg l^{-1} Cl was also observed at B4(60 cm) 3.5 days after the tracer was applied (Figure 7.19). The second peak at B4 may have been the tracer emerging or a secondary pathway opening up. Samples collected from B4(60 cm) maintained a large concentration level, above background concentration, throughout the 12 day period reaching a minimum concentration of 27.1 mg l^{-1} Cl by the 12th day. Samples collected from B2(25 cm) and B3(45 cm) showed no positive signs of the pulse passing through these locations, although concentration remained above background levels for most of the 12 days. A possible peak in solute concentration at sampler B2(25 cm) was detected 2.5 days after the tracer was applied.

Chloride pulse (left): No distinct peak in concentration was observed from any of the

suction cup lysimeters on this side of the block (Figure 7.20, Table 7.15). At sampler B5(10 cm) a slight rise in solute concentration to 23.8 mg l^{-1} Cl was detected 3.3 days after the start of the experiment (Figure 7.20). Solute collected from B5(10 cm) maintained a raised concentration over the remaining time period reaching a low of 16.3 mg l^{-1} Cl by day 12. At B6(25 cm) a peak solute concentration of 16.8 mg l^{-1} Cl was observed 3 days after the start of the experiment, while at B7(45 cm) a peak concentration of 23 mg l^{-1} Cl was observed 7.2 days after the tracer was applied (Table 7.15). The peaks observed in the solute sampled from B6(25 cm) and B7(45 cm) were not very distinctive (Figure 7.20). Solute concentration at sampler B7(45 cm) maintained a larger concentration than B6(25 cm) over the 12 days which may be due to a change in soil texture at depth retaining a larger solute concentration. At Sampler B8(60 cm) (below the mole drain) a slight rise in solute concentration was observed 12 hours after the start of irrigation followed by a very gentle decrease in concentration over the following 12 days (Figure 7.20).

Mole Drain:

Chloride pulse: Initially at the start of run 5 the mole drain did not flow because the block had been allowed to drain between runs 4 and 5. The first drainage water observed at the mole drain occurred 24 hours after the start. This first drainage sample was observed to have the largest concentration (113 mg l^{-1} Cl). The concentration decreased to approximately 20 mg l^{-1} Cl within a day and 7 days after the peak had reached a concentration of 10 mg l^{-1} Cl (Figure 7.21).

Base Of Block:

Chloride pulse: The first reading 8 hours after the start of the irrigation resulted in the largest peak concentration (33.6 mg l^{-1} Cl) at this location, which was very dilute compared to the applied tracer concentration. After the peak solute concentration reduced

Table 7.15 - Change in chloride concentration curves for run 5 (Figures 7.19 to 7.22), showing times from start of irrigation and concentrations reached (mg l^{-1} Cl).

Sampler (depth in soil, cm)	Background conc. at start (mg l^{-1} Cl)	Time to initial breakthrough (hrs)	Time to peak (hrs)	Time to background (hrs)
B1(10)	12.1	4	4 (100.2 mg l^{-1} Cl) 164 (12.2 mg l^{-1} Cl)	288 (10.6 mg l^{-1} Cl)
B2(25)	18.0	-	60 (14.5 mg l^{-1} Cl)	288 (10.7 mg l^{-1} Cl)
B3(45)	28	4	-	288 (13.3 mg l^{-1} Cl)
B4(60)	51.9	4	84 (35 mg l^{-1} Cl)	288 (27.1 mg l^{-1} Cl)
B5(10)	30.7	4	80 (23.8 mg l^{-1} Cl)	288 (16.3 mg l^{-1} Cl)
B6(25)	12.5	4	72 (16.8 mg l^{-1} Cl)	288 (9.5 mg l^{-1} Cl)
B7(45)	26.1	-	172 (23 mg l^{-1} Cl)	288 (17.7 mg l^{-1} Cl)
B8(60)	45.9	-	12 (44 mg l^{-1} Cl)	288 (30.7 mg l^{-1} Cl)
Mole(50)	12.9	24	24 (113 mg l^{-1} Cl)	167.5 (11.2 mg l^{-1} Cl)
Base of Block(85)	25.7	8	8 (33.6 mg l^{-1} Cl)	196 (11.4 mg l^{-1} Cl)

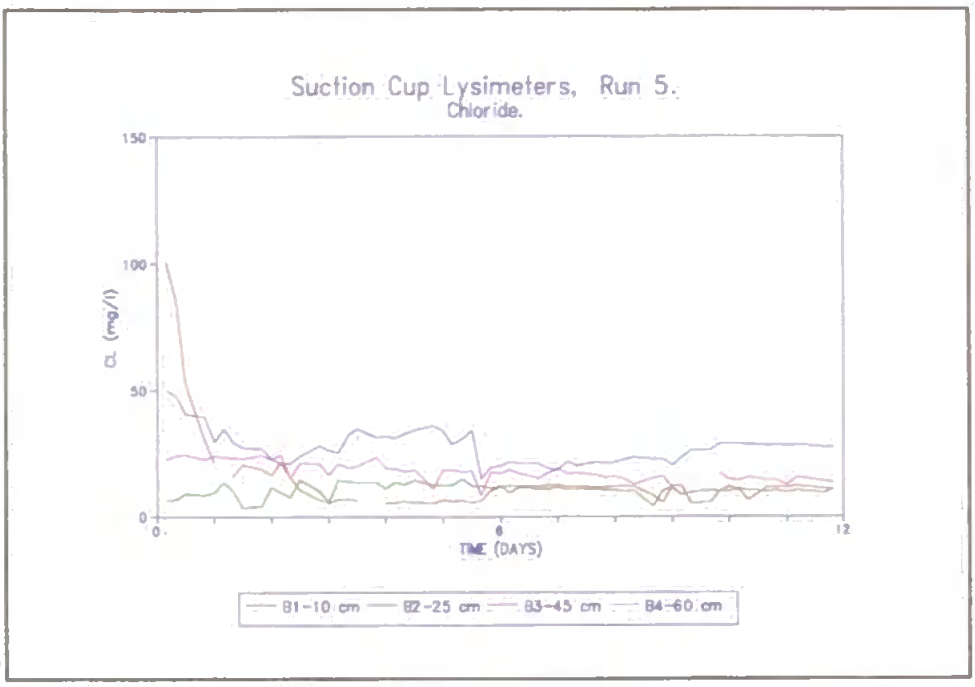

Figure 7.19 - Change in chloride concentration through time at suction cup lysimeters B1 to B4 (right), run 5 (block B).

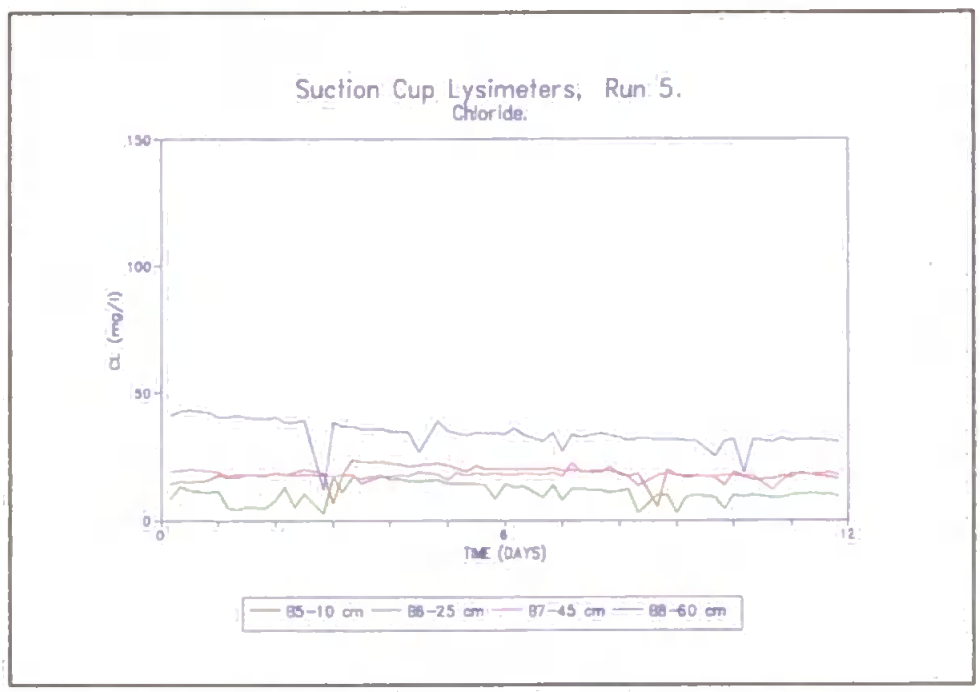

Figure 7.20 - Change in chloride concentration through time at suction cup lysimeters B5 to B8 (left), run 5 (block B).

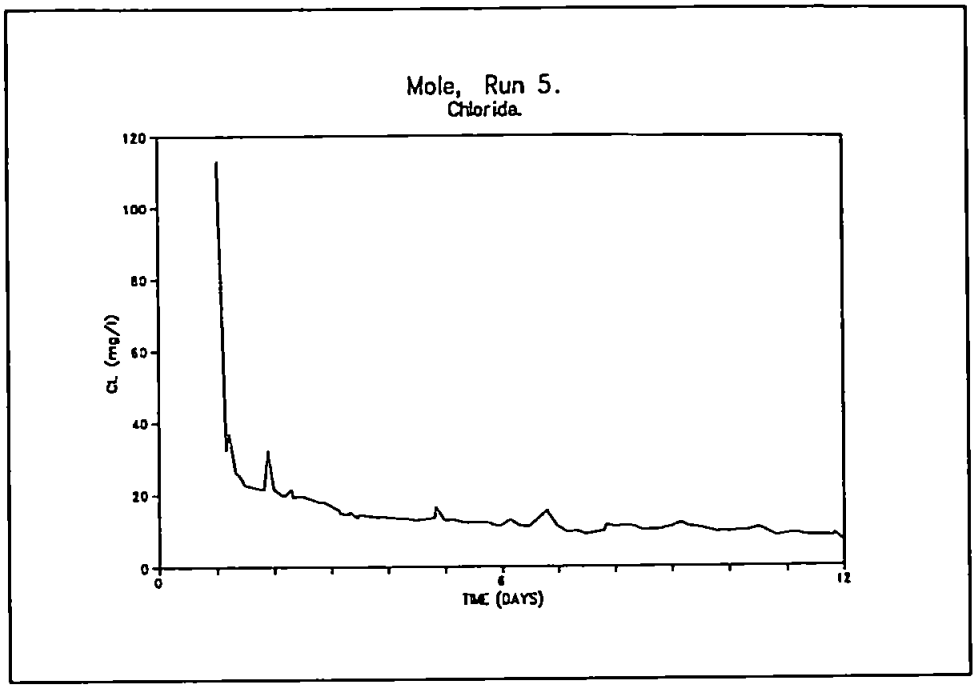

Figure 7.21 - Change in chloride concentration through time from samples collected from the mole drain, run 5 (block B).

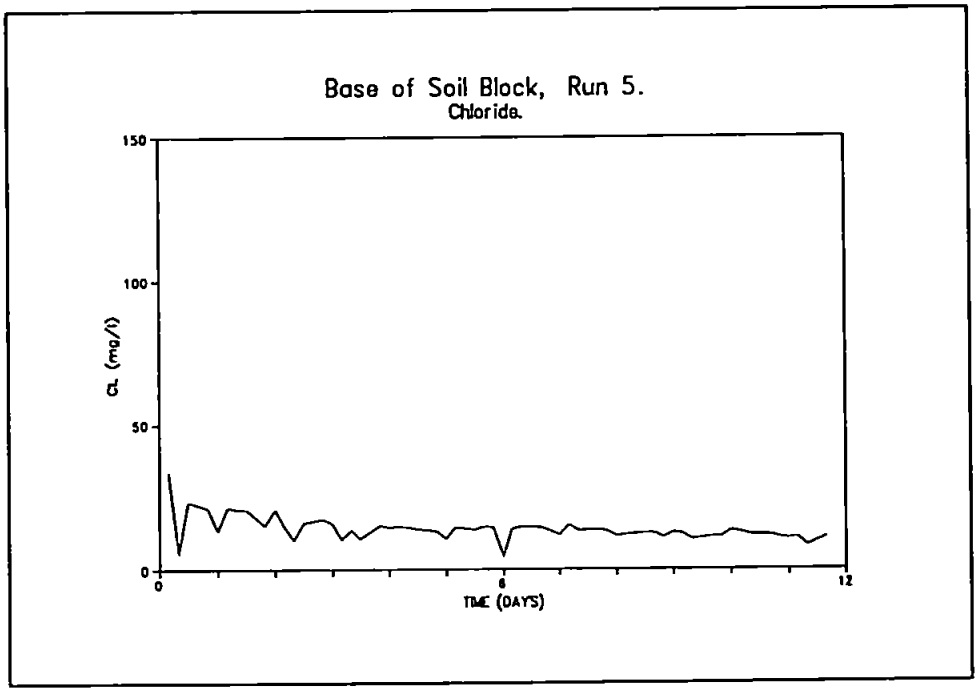

Figure 7.22 - Change in chloride concentration through time from samples collected from the base of the block, run 5 (block B).

slowly reaching 11.4 mg l^{-1} Cl 8.2 days after the start of the run (Figure 7.22).

Suction Cup Lysimeters:

Nitrate pulse (right): A summary of time to peak and peak concentration reached is given in Table 7.16. At sampler B1(10 cm) an initial peak solute concentration of 14.05 mg l^{-1} TON was observed 4 hours after the tracer was applied and a second peak of 46 mg l^{-1} TON 20 hours after the start (Figure 7.23). The concentration observed at B1(10 cm) reduced rapidly after the second peak taking 2.7 days from peak to reach background concentration. The nitrate pulse was detected at B2(25 cm), B3(45 cm) and B4(60 cm) (Figure 7.23, Table 7.16). However, compared to solute concentration at B1(10 cm) the rise to peak at these locations was slower taking 52, 36 and 32 hours respectively. Also the time it took observed concentrations at B2(25 cm), B3(45 cm) and B4(60 cm) to reduce was longer than at B1(10 cm) taking in excess of 12 days to reach concentrations of 3.29(B2), 3.29(B3) and 2.56(B4) mg l^{-1} TON. The peak concentration reached was weaker with increased depth in the soil (Table 7.16).

Nitrate pulse (left): Solute collected from sample locations B5(10 cm) and B6(25 cm) both peak 3.2 days after the start of the experiment, the solute concentration at B6(25 cm) reached a slightly greater concentration (17.94 mg l^{-1} TON) compared with B5(10 cm) (17.44 mg l^{-1} TON) (Figure 7.24). Solute samples from B5(10 cm) and B6(25 cm) showed a slow reduction in concentration over the remaining 8.8 days. At sample location B7(45 cm) and B8(60 cm) no noticeable peak was observed although both locations showed slight signs of a very gentle rise in concentration over the 12 days (Figure 7.24).

Table 7.16 - Change in nitrate concentration curve for run 5 (Figures 7.23 to 7.26), showing times from the start of irrigation and concentration (mg l^{-1} TON).

Sampler (depth in soil, cm)	Initial back-ground conc. (mg l^{-1} TON)	Time to initial breakthrough (hrs)	Time to peak (hrs)	Time to back-ground (hrs)
B1(10)	0.4	4	4 (14.05 mg l^{-1} TON) 20 (46 mg l^{-1} TON)	84 (1.57 mg l^{-1} TON)
B2(25)	3.56	4	52 (13.88 mg l^{-1} TON)	288 (3.29 mg l^{-1} TON)
B3(45)	3.8	x	36 (10.3 mg l^{-1} TON)	288 (3.39 mg l^{-1} TON)
B4(60)	1.06	4	32 (6.26 mg l^{-1} TON) 248 (2.83 mg l^{-1} TON)	288 (2.56 mg l^{-1} TON)
B5(10)	0.241	20	76 (17.44 mg l^{-1} TON)	288 (0.0867 mg l^{-1} TON)
B6(25)	0.909	4	76 (17.94 mg l^{-1} TON)	288 (2.69 mg l^{-1} TON)
B7(45)	3.54	4	220 (8.42 mg l^{-1} TON)	288 (6.75 mg l^{-1} TON)
B8(60)	2.21	4	80 (6.47 mg l^{-1} TON)	288 (5.35 mg l^{-1} TON)
Mole(50)	1.49	24	24 (11.1 mg l^{-1} TON) 59 (14.22 mg l^{-1} TON)	228 (1.97 mg l^{-1} TON)
Base of Block(85)	1.43	8	8 (34.5 mg l^{-1} TON)	168 (1.75 mg l^{-1} TON)

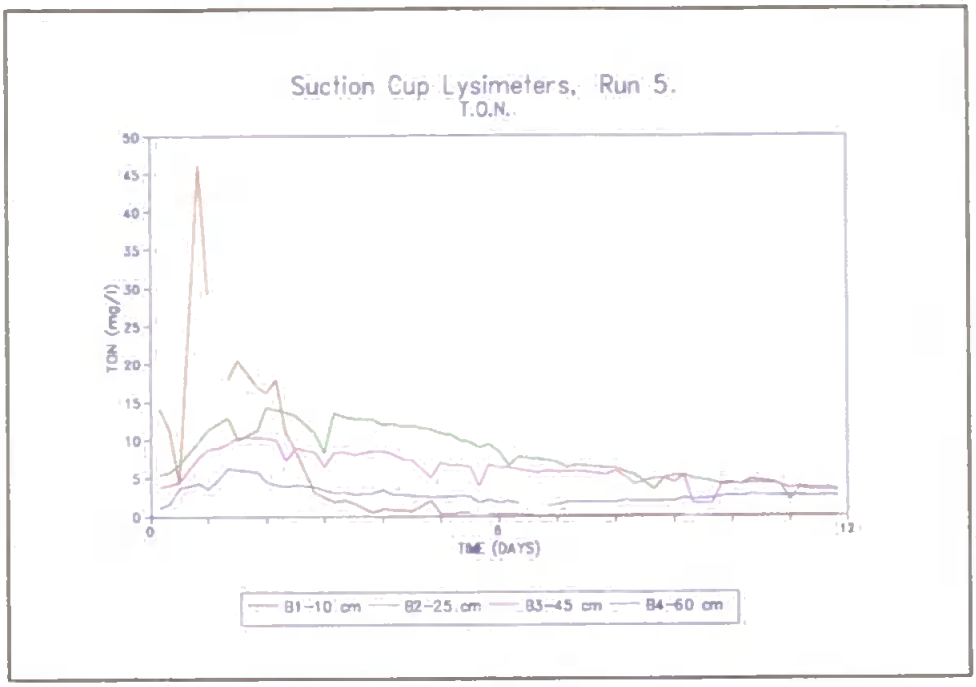

Figure 7.23 - Change in nitrate concentration through time at suction cup lysimeters B1 to B4 (right), run 5 (block B).

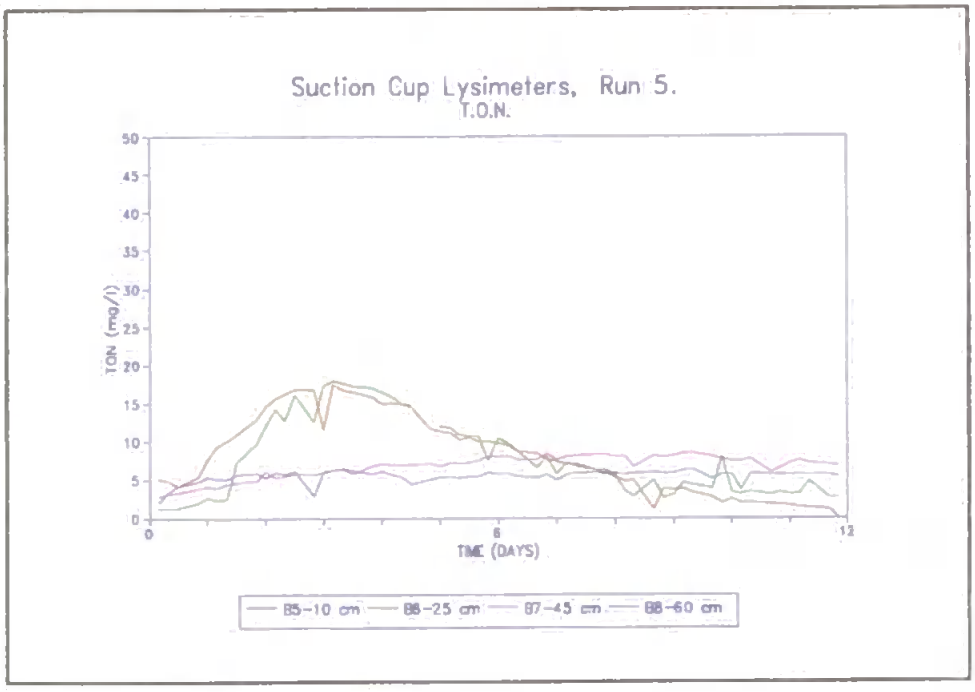

Figure 7.24 - Change in nitrate concentration through time at suction cup lysimeters B5 to B8 (left), run 5 (block B).

Mole Drain:

Nitrate pulse: The first reading from the mole showed an initial peak of 11.1 mg l^{-1} TON which decreased and was followed by a second peak of 14.22 mg l^{-1} TON 2.5 days after the application of the tracer (Figure 7.25). The tail-off from peak concentration was gentle and background concentration was reached 7 days after the pulse was applied.

Base Of Block:

Nitrate pulse: As with the chloride result the first sample, 8 hours after the start, was observed to have the largest concentration of the run, reaching 34.5 mg l^{-1} TON. It took a further 7 days for the concentration to decrease to background levels (Figure 7.26).

Explanation:

The general increase in chloride concentration with depth (from 25 to 60 cm) observed at the suction cup lysimeters, for both run 4 and run 5, may be attributable to leaching of chloride from the higher soil horizons followed by an accumulation of chloride in less porous, deeper soil layers or it may reflect the influence of faster pathways transporting solute to depth with minimal interaction occurring between the faster and slower pathways. At 10 cm a large concentration peak was observed because of its close proximity to solute input which would have allowed less time for mixing and dilution to occur. At the mole a distinct pulse was followed by a rapid decline in concentration which may also have been associated with rapid movement to depth with minimal mixing occurring. The more gradual decrease in concentration after the peak was an indication of slower more tortuous pathways (Figure 7.21). The smaller peak concentration and slower decline in concentration that occurred at the base of block than at the mole (Figures 7.21 and 7.22) would suggests that an increase in mixing occurred with depth, due to slower and more tortuous pathways, than was observed to the mole.

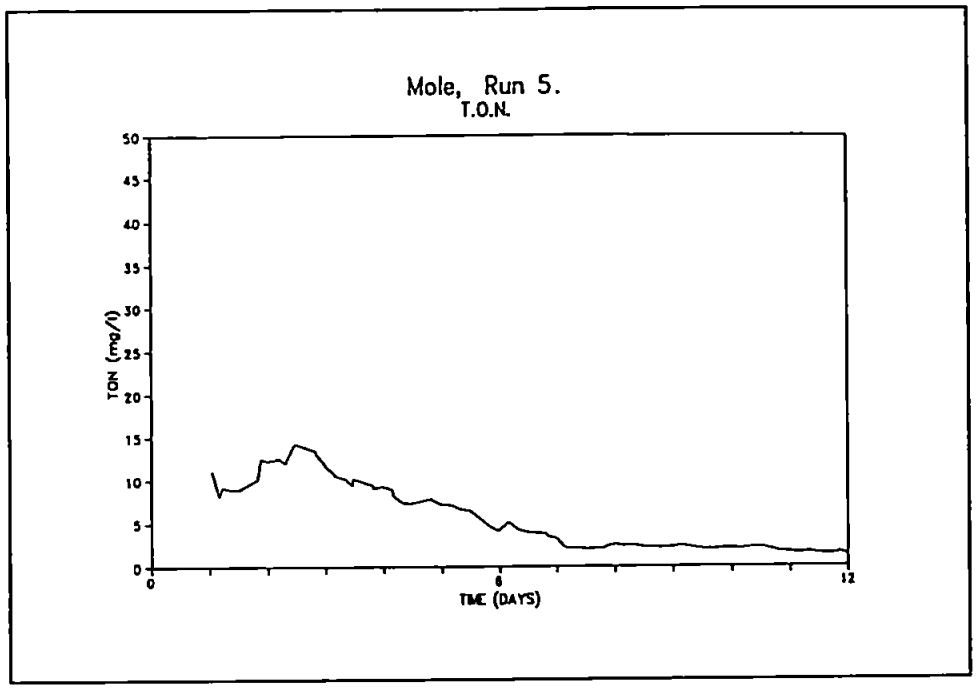

Figure 7.25 - change in nitrate concentration through time from samples collected from the mole drain, run 5 (block B).

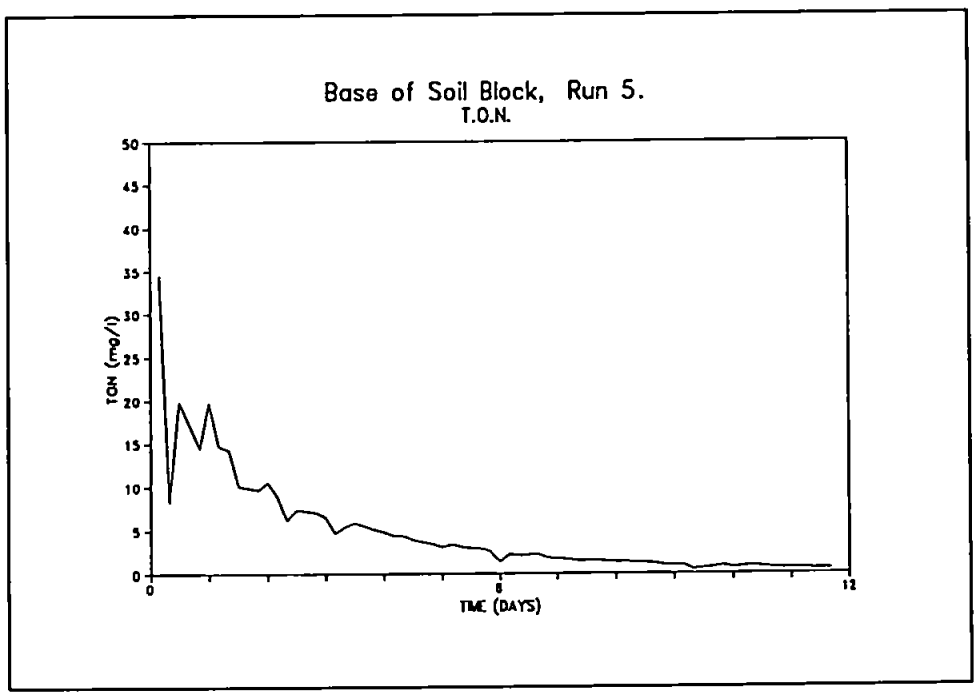

Figure 7.26 - Change in nitrate concentration through time from samples collected from the base of the block, run 5 (block B).

The larger peak chloride concentration at the mole in run 5 compared to run 4, with smaller peak concentrations recorded at other locations conform with observations made by Kluitenberg and Horton (1990). These are that initially drained soils with a large drainage porosity would give rise to greater peak concentrations than originally moist soil. The induced pathways created when the mole was pulled increased drainage porosity to the mole while other locations within the soil did not necessarily possess such a large drainage porosity and hence displayed smaller peak concentrations.

Nitrate concentration in both runs 4 and 5 showed a general decrease in peak concentration with depth at the suction cup lysimeters (Tables 7.15 and 7.16). The lower concentrations of nitrate at depth may have been due to denitrification in the anaerobic, near saturated conditions of the deeper soil. As with chloride, time to peak concentration also increased with depth. The faster response and larger concentrations obtained in run 5 compared to run 4 would suggest that nitrate was absorbed into the soil during run 4. In run 5 less nitrate was taken into the soil, due to the reduced gradient between applied tracer and matrix concentration. As less solute was lost to the matrix, concentrations remaining in solution were stronger than in run 4. The larger peak concentration of nitrate at the base of the block compared to at the mole drain may be an indication of rapid preferential pathways to the base of the block or may be an indication of poor connectivity to the mole. Such rapid movement to depth highlights the potential for rapid loss of chemicals to depths below the mole drain which could lead to the accumulation of chemicals in the water table.

Summary:

Run 5 simulated spring type conditions within the soil, with the application of a chemical to the surface of an initially (gravity) drained soil. The height of the water table was maintained below the level of the mole drain. The aim of the experiment was to observe

the effect of initial soil water conditions on the speed and distribution of solute within the soil. A comparison will be made between observed spatial and temporal variations in solute movement between run 4 and run 5.

A summary of the order of response to time of peak concentration and order of magnitude of pulse (from stronger to weaker concentrations) for all sample locations is presented in Table 7.17 for both tracers. A brief summary of the response order with depth in soil for the suction cup lysimeters is given in Table 7.18.

Table 7.17 - Order of response of time to peak and order of magnitude of peak (from stronger to weaker conc.) for chloride and nitrate tracer pulse run 5.

Sampler	Chloride pulse		Nitrate pulse	
(depth in soil, cm)	Time to peak concentration	Order of peak concentration magnitude	Time to peak concentration	Order of peak concentration magnitude
B1(10)	1	2	2	1
B2(25)	5	9	6	5
B3(45)	-	-	5	7
B4(60)	8	4	4	10
B5(10)	7	6	7	4
B6(25)	6	8	7	3
B7(45)	9	7	9	8
B8(60)	3	3	8	9
Mole(50)	4	1	3	6
Base of block(85)	2	5	1	2

Table 7.18 - Summary of result of suction cup lysimeter responses for run 8.

Experiment	Location - left of block (B5(10 cm), B6(25 cm), B7(45 cm) and B8(60 cm))	Location - left of block (B1(10 cm), B2(25 cm), B3(45 cm) and B4(60 cm))
Run 5	Chloride: In general there was an increase in peak concentration with depth. B8 peaked the quickest, B7 the slowest. Nitrate: Decrease in peak concentration with depth. B7 slowest to peak.	Chloride: B1 peaked first with the largest concentration. B2 to B4 showed an increase in time and concentration of peak with depth. Nitrate: B1 peaked first, B2 peaked last. In general decrease in concentration with depth.

Chloride Pulse:

At locations B5(10 cm) to B8(60 cm) (left) the time to solute peak concentration was more variable than B1(10 cm) to B4(60 cm) (right). A similar response was observed in run 4. B1(10 cm) was the only suction cup lysimeter sample to display a clear peak in concentration, samples from other suction cup lysimeter samplers displayed less obvious rises and falls in concentration (Figure 7.19). The base of block sample peaked before the mole sample (Table 7.17) but the concentration of the pulse at the base of block was not as distinctive as that observed at the mole.

Nitrate pulse:

The fastest and most distinct peak was observed at sample location B1(10 cm). A distinctive peak in concentration was also observed at both the mole drain and base of block. The fastest response was observed at the base of block, as well as the larger peak concentration compared to the mole drain sample.

Nitrate and Chloride Pulse:

With the exception of B8(60 cm) (left), all samples obtained at other sampling locations reached a peak concentration at similar times for both tracers (Tables 7.15 and 7.16). It was easier to distinguish more of the nitrate peaks than the chloride peaks. Distinctive trace signatures were obtained from samples at the mole and base of block compared to most of the suction cup samplers. At the mole, compared with the chloride result, the peak nitrate concentration was delayed and the reduction in concentration from peak concentration was slower, although background concentration was also reached 7 days after the pulse was applied (Figures 7.21 and 7.24).

Results of Run 4 Compared to Run 5:

Chloride: In general timings to peak concentration were similar or slightly slower in run 5. With the exception of the sample collected from the mole drain peak concentrations were smaller in run 5 than in run 4. In both runs 4 and 5 peak chloride emerged at the base of block quicker than at the mole but had a smaller concentration.

Nitrate: In general timings to peak concentration were similar or slightly faster during run 5, also the peak concentration reached was larger in run 5 than in run 4. In both runs 4 and 5 peak concentration emerged at the base of block quicker than at the mole sample and peak concentration reached was larger at the base of the block than at the mole.

7.6. SUMMARY OF CHANGE IN CONCENTRATION THROUGH TIME.

The importance of the different factors controlling solute movement, such as structure, hydraulic conductivity, hydraulic gradient and soil water content will be examined in greater detail in Chapter 8. The general observations and initial impressions from the five experiments are summarised below. A summary of the observations of change in

Table 7.19 - Summary of results of suction cup lysimeter responses to tracer application.

Experiment	Location - left of block (A5/B5(10 cm), A6/B6(25 cm), A7/B7(45 cm) and A8/B-8(60 cm))	Location - right of block (A1/B1(10 cm), A2/B2(25 cm), A3/B3(45 cm) and A4/B-4(60 cm))
Run 1 Block A	Initial breakthrough occurred fastest at A8. A6 takeing the longest to show initial breakthrough. Peak irrigation concentration reached first at A6 (part I). During flush A8 reached background concentration first, A6 reached the next lowest concentration followed by A7 and A5. (part II) A5 to A8 did not reach applied irrigation concentration. A8 reached the largest concentration followed by A6, A5 and A7.	A1 to A4, increased in time to initial breakthrough and peak irrigation concentration with depth for both tracer and flush.
Run 2 Block A	A8 showed initial breakthrough and reached irrigation concentration first. Initial breakthrough (tracer) A5 to A7 occurred in order of depth. A6 was the only other sampling location, apart from A8, to reach irrigation concentration. Initial breakthrough (flush) took longest at A6. A6 reached a lower concentration at the end of the flush than A5 which had a larger residual concentration than A7.	A1 to A4, increased in time to initial breakthrough and peak irrigation concentration with depth for both tracer and flush.
Run 3 Block B	B5 took the longest to react to both tracer and flush, retained largest concentration of chloride. Peak irrigation concentration not reached at any sampler location (B5 to B8). B6 reached larger peak concentration than B7 followed by B8. During flushing initial breakthrough B8 responded the fastest. At end of flush residual chloride larger in B7 than B8 followed by B6 and B5.	B1 to B4 showed an increase in time to depth for initial breakthrough. Time to peak B2 took longer than B3, otherwise an increase time to peak irrigation was observed with depth. After flushing there was an increase in residual tracer concentration left with depth.
Run 4 Block B	Chloride: Fastest peak B7, largest peak concentration at B8. In general there was an increase in peak concentration with depth. Nitrate: Largest peak concentrations reached at B6 and B7, lowest at B5.	Chloride: B1 to B4 showed a decrease in peak concentration and increase in time to peak with depth. Nitrate: B1 to B4 showed a decrease in peak concentration and increase in time to peak with depth.
Run 5 Block B	Chloride: In general there was an increase in peak concentration with depth. B8 peaked the quickest, B7 the slowest. Nitrate: Decrease in peak concentration with depth. B7 slowest to peak.	Chloride: B1 peaked first with largest concentration. B2 to B4 showed an increase in time and concentration of peak with depth. Nitrate: B1 peaked first, B2 peaked last. In general decrease in concentration with depth.

concentration through time made at the suction cup lysimeters for the five experiments were presented in Table 7.19. In the miscible displacement experiment (runs 1, 2 and 3) peak concentration in excess of 250 mg l^{-1} Cl were occasionally observed. Increases in concentration were considered to have been caused by either, settlement of suspended solute or incomplete mixing of the chloride solution in the pressurised reservoir before irrigation, leading to fluctuations in the concentration of the solution applied above and below 250 mg l^{-1} Cl. The initial interpretation from the solute concentration graphs (Figures 7.1 to 7.26) was that the change in solute concentration through time could be explained by a continuum of rapid to slow pathways in this soil. Background concentrations were seemingly reached after only a short period of time suggesting the presence of fast pathways through the soil, while gradual tailing-off in concentration as peak concentration was reached indicated mixing and retention in smaller pores connected to the larger ones.

Solute sampling in both blocks A and B demonstrated clearly the variability in flow patterns that can occur throughout the soil in only a small distance. Some similarities were evident, such as the slow response of A5(10 cm) and B5(10 cm), and the similar response with depth to solute movement at sample locations A1/B1(10 cm) to A4/B4(60 cm) on the right side of the blocks. As depth increased at these locations time to peak concentration took longer to reach for chloride tracer. On the left side of the blocks [samplers A5/B5(10 cm) to A8/B8(60 cm)] time to peak did not always correspond to depth in the soil. This may have been linked to structural differences or soil water variability, which will be examined in Chapter 8.

The effect of raising the water table to just below the height of the mole in run 2 and 3 increased the initial response time of solute leaving the mole drain, although, peak concentration for the miscible displacement experiments was reached at about the same

time whether the base of the soil block was drained or not. Chapter 6 indicated that soil water conditions below the mole drain during run 2 and run 3 may not have been saturated.

Although initial breakthrough occurred at about the same time in both blocks there were obvious differences, for example, samplers A5(10 cm) and B5(10 cm) showed initial breakthrough to occur at 8 hrs and 56 hrs respectively, and sites at A8(60 cm) and B8(60 cm) responded within 76 hrs and 32 hrs respectively. These initial responses, which were primarily determined by bypass or preferential flow, most likely reflect the proximity of the sampler to a major pathway.

The greatest difference in response rate between the two blocks was seen in the recorded time to peak concentration (Tables 7.5 and 7.8). Block A reaches a peak concentration more quickly than block B. Even if chemical absorption is considered by comparing time to peak for run 1 (part I) (Table 7.2) block A still apparently reached peak concentration in a quicker time than block B. Structural and/or hydraulic differences must therefore have been responsible for the observed differences in peak response between the two blocks which will be considered in Chapter 8.

In both pulse experiments (runs 4 and 5) the peak concentration reached was well below the concentration of the applied tracer. In the chloride pulse 2500 mg l^{-1} of Cl was applied to the surface, the maximum peak response observed was 109(run 4, Table 7.11) and 113(run 5, Table 7.15) mg l^{-1} Cl, while for the nitrate pulse 500 mg l^{-1} NO_3 was added to the surface and the maximum peak response observed was 77.5(run 4, Table 7.12) and 46(run 5, Table 7.16) mg l^{-1} TON. Dilution of solute concentration may have been due to the mixing of the solute with weak concentration irrigation water before it entered the soil. Potentially irrigation water could reduce solute concentration of the pulse to half strength

within one hour. Apart from dilution caused by irrigation concentration, solute concentration will also have been reduced as the solute moved through the soil and mixing occurred between fast and slow pathways of different solute concentration. The large difference between applied concentration and maximum peak concentration observed would suggest that a lot of mixing occurred within the soil. This result would indicate that solute pathways were predominantly long and tortuous. However, the fact that peak concentration occurred early on, in some cases within 4 hours, would also suggest these pathways were capable of conducting solute swiftly through the soil. The potential for smaller mesopore pathways to conduct solute swiftly through the soil will be examined in Chapter 8.

The dual peaks observed in the pulse experiments (runs 4 and 5) can be explained by the presence of two different rates of solute transport occurring within the soil (Holden *et al.*, 1995b). Dual peaks were observed to both increase in concentration from first peak to second peak [for example, at sampler B2 and B5 (Table 7.12), B1 and mole (Table 7.16)] as well as to decrease in concentration [for example, at sampler B4 (Table 7.11), B1 (Table 7.12), B1 (Table 7.15) and B4 (Table 7.16)]. All dual peaks that increased in concentration from first to second peak were associated with the nitrate tracer. The reason for the increase in peak concentration from first to second peak requires further investigation. Dual peaks that decreases in concentration from the first peak to the second peak were observed for both chloride and nitrate pulses. The decrease in concentration from first peak to second peak can be associated with an initially observed rapid movement of solute through larger more direct pathways were mixing is minimal, followed by a second peak which reflects movement of solute through slower pathways were mixing between pathways has increased.

Changes in response time may have been due to changes in water content in the soil, although from Chapter 6 it was shown that a stable water state would seem to have existed

in the soil. Other possibilities include new pathways opening up due to fauna activity within the block, available chemical sites being occupied during the preceding experiment leaving fewer sites available for exchange in later experiments, thus allowing more rapid chemical movement and reduced concentration gradients between mobile and immobile zones resulting in reduced dilution of mobile solute. The latter explanations would explain the increased concentration pulses observed in run 5 compared to run 4.

Although block B was allowed to drain between runs 4 and 5 only minor differences were noticeable in the responses between them. Sample locations B2(25 cm), B3(45 cm), B5(10 cm) and B8(60 cm) recorded faster time to peak in run 5 compared to run 4, taking approximately half the time. Residual concentration were larger at B1(10 cm), B4(60 cm), B6(25 cm), B7(45 cm), B8(60 cm) and at the base of block at the end of run 5 compared to run 4. Peak concentration was also larger in run 5 compared to run 4 which may be due to uptake of nitrate in run 4, as explained above, or it may be as Kluitenberg and Horton (1990) defined, a soil with a large drainage porosity (Section 7.5.2.).

7.7. BREAKTHROUGH CURVES.

Sections 7.4 to 7.6 (above) made descriptive observations about the spatial and temporal variability of solute concentrations within the soil. To provide a more quantitative analysis of the data, with regard to the integration of pathways, selective data have been presented in the form of breakthrough curves.

Breakthrough curves have been used by a number of researchers to predict the rate of solute movement through soil based on the shape of the solute curve and have used this information to suggest active pathways and to monitor diffusion and dispersion rates within the soil (Danckwerts, 1953; Bouma and Wösten, 1979; Walker and Trudgill, 1983;

Kluitenberg and Horton, 1990; Singh and Kanwar,1991). A breakthrough curve is a plot of relative concentration (C/Co) versus relative pore volume (PV). Where, C is recorded solute concentration at a specific time, Co equals concentration of applied solute (dimensionless) and PV is the porosity of the column of soil divided by flux of water through time. The shape or skewness of the graph as well as other parameters including initial breakthrough and immobile water fraction are all influenced by the presence or absence of preferential flowpaths (Walker and Trudgill, 1983; Singh and Kanwar, 1991).

If true piston flow occurred through a medium C/Co would equal 1 at 1 PV. Piston flow, however, never occurs in reality because of soil structure. Structure causes the flow of solute through a soil to be turbulent and therefore promotes dispersion and mixing. In a medium that possesses a uniform structure, for example packed glassed beads (Jensen, 1987) perfect dispersion and mixing occurs so that C/Co = 0.5 at 1 PV. Under such uniform displacement the breakthrough curve possesses zero skewness (Walker and Trudgill, 1983). In a soil with a mixed pore size distribution flow, mixing of solutes primarily occurs in the larger pores, while finer pores and dead end pores act as sinks or sources (De Smedt and Wierenga, 1979). A heterogeneous soil causes dispersivity to be much greater than aggregate diameter (Jensen, 1987) and C/Co reaches 0.5 before 1 PV. Walker and Trudgill (1983) showed breakthrough curves which were positively skewed to be associated with rapid water and solute movement along macropores. Displacement of the curve to the left of C/Co = 0.5 at 1 PV, known as the 'holdback' (Danckwerts, 1953), is an indication of the quantity of water not participating in miscible displacement. 'Holdback' is a consequence of poorly connected or dead-end pores, and results in a delay of appearance of tracer in the effluent followed by a rapid rise in concentration. The skewness of the breakthrough curve has been highly correlated with holdback at a 95 per cent confidence level (Walker and Trudgill, 1983). A highly asymmetric shape and early

initial breakthrough with extensive tailing-off at concentrations approaching C/Co =1 was also observed by Kluitenberg and Horton (1990) and Hayot and Lanfolie (1993).

Classical hydrodynamic theory suggests that a uniformly displaced solute will pass through the point C/Co = 0.5, PV = 1, and the graph will posses zero skewness. When macropore or preferential flow is present a concentration of C/Co = 0.5 is reached before PV = 1, and the graph will possess positive skewness. If, however, solute is delayed in the soil or if the sampler is located in an area dominated by matrix flow C/Co = 0.5 may not be reached even after one pore volume has been applied.

The proportion of macropore flow can be estimated from the proportion of mobile pore-water fraction compared to immobile pore-water fraction (Singh and Kanwar,1991). Singh and Kanwar (1991) examined the presence of macropore flow by calculating the fraction of immobile pore-water from the breakthrough curve. The mobile pore-water fraction represents the proportion of rapid macropore flow through the soil. As flow rate increases the effective porosity reduces. The total amount of immobile pore-water fraction increases with increasing macropore flow, as more of the soil is bypassed in preference to faster flowing pathways. An estimate of mobile pore-water fraction can be made from the number of pore-volumes required to reach C/Co = 0.5 (Singh and Kanwar, 1991). The immobile pore-water fraction of the soil is a calculation of one pore volume minus the mobile pore-water fraction.

7.7.1. Results of Breakthrough Curves.

Discussion about breakthrough curves is limited to data collected during run 2 (block A) and run 3 (block B), which represent two experiments that were conducted in a similar fashion. Under such conditions comparisons can be made about spatial and temporal

variations within and between two similar soil volumes (block A and block B). The aim was to observe any similarities or differences that may be linked to spatial heterogeneity of soil structure, by observing two seemingly identical blocks taken from within 1 meter of each other in the field. Selected breakthrough curve parameters and soil properties are presented, for runs 2 and 3, in Tables 7.20 and 7.21 respectively.

It was noticeable that immobile pore-water fractions were small, especially those for run 3 (Table 7.20 and 7.21). This would imply the dominance of slower pathways allowing greater dispersion (mixing). The exception was the fraction calculated for flow to the mole drain, most noticeably in block A, where macropore pathways would appear to have been more dominant from the large fraction of immobile water calculated (Table 7.20 and 7.21).

With the exception of sample locations A5(10 cm), A6(25 cm) and the second peak observed at A7(45 cm), all sample locations, in block A, reached C/Co = 0.5 before PV = 1 (Table 7.20). This would suggest macropore pathways were influencing these breakthrough curves. However, not all these curves possessed a positive skewness as observed by Walker and Trudgill (1983), Kluitenberg and Horton (1990) and Singh and Kanwar (1991) which is an additional indication of rapid initial transport (Figures 7.27 to 7.35). The negative skewness with initially swift movement of solute may have been due to the dominance of both mesopores and matrix pores at these locations, which would have delayed the emergence of the peak concentration.

Time to peak concentration at A5(10 cm) (left) was noticeably delayed although initial breakthrough occurred more rapidly than at some of the other sample locations (Table 7.20). This is a strong indication that samples collected at A5(10 cm) were dominated by slower moving solute due to the impermeability of a clay rich layer of soil at this location.

Table 7.20 - Selected properties of breakthrough curves for run 2.

	A1	A2	A3	A4	A5	A6	A7	A8	MOLE
Bulk density	1.05	1.133	1.438	1.364	1.153	1.255	1.321	1.543	1.543
Porosity (%)	60.5	57.3	45.8	48.6	56.5	52.7	50.2	41.8	41.8
1 Pore Volume (cm^3)	6.05	14.64	23.79	35.47	5.65	13.55	23.58	34.13	25.72
Immobile pore water (%)	0.01	0.508	0.243	0.255	-4.714	-0.593	0.949 -0.034	0.543	0.999 0.769
Flux Input (cm/h)	0.3	0.3	0.3	0.3	0.3	0.3	0.3	0.3	0.3
C/Co = 0.5 (PV)	0.99	0.492	0.757	0.745		1.593	0.051 1.034	0.457	0.001 0.231
Initial Break-through (PV)	0.396	0.164	0.151	0.237	0.423	0.973	0.967	0.035	0.0002
Skewness	0.875	-0.888	0.340	-0.303	-0.010	0.141	0.791	0.226	0.210

Table 7.21 - Selected properties of breakthrough curves for run 3.

	B1	B2	B3	B4	B5	B6	B7	B8	MOLE
Bulk Density	1.403	1.204	1.301	1.280	1.154	1.203	1.363	1.396	1.396
Porosity (%)	47.1	54.6	51.0	51.7	56.5	54.6	48.6	47.4	47.4
1 pore volume (cm^3)	4.71	12.91	23.10	36.48	5.65	13.84	23.56	35.17	25.095
Immobile Pore Water (%)	-0.366	-0.711	-0.195	-0.765	-6.154	-0.728	-0.914	-0.884	0.016
Flux Input (cm/h)	0.23	0.23	0.23	0.23	0.23	0.23	0.23	0.23	0.23
C/Co = 0.5 (PV)	1.366	1.711	1.195	1.765	7.154	1.728	1.914	1.884	0.984
Initial Breakthrough (PV)	0.195	0.143	0.159	0.101	2.276	0.199	0.313	0.209	0.011
Skewness	0.373	-0.278	-0.233	-1.172	-1.419	0.435	-0.192	-0.613	0.456

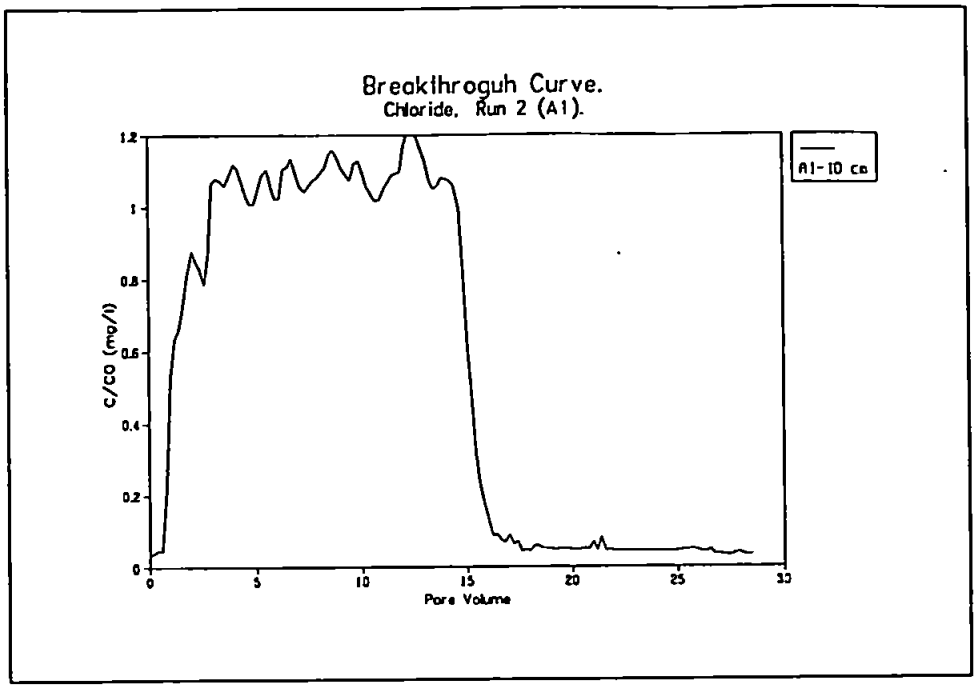

Figure 7.27 - Breakthrough curve for location A1, run 2 block A.

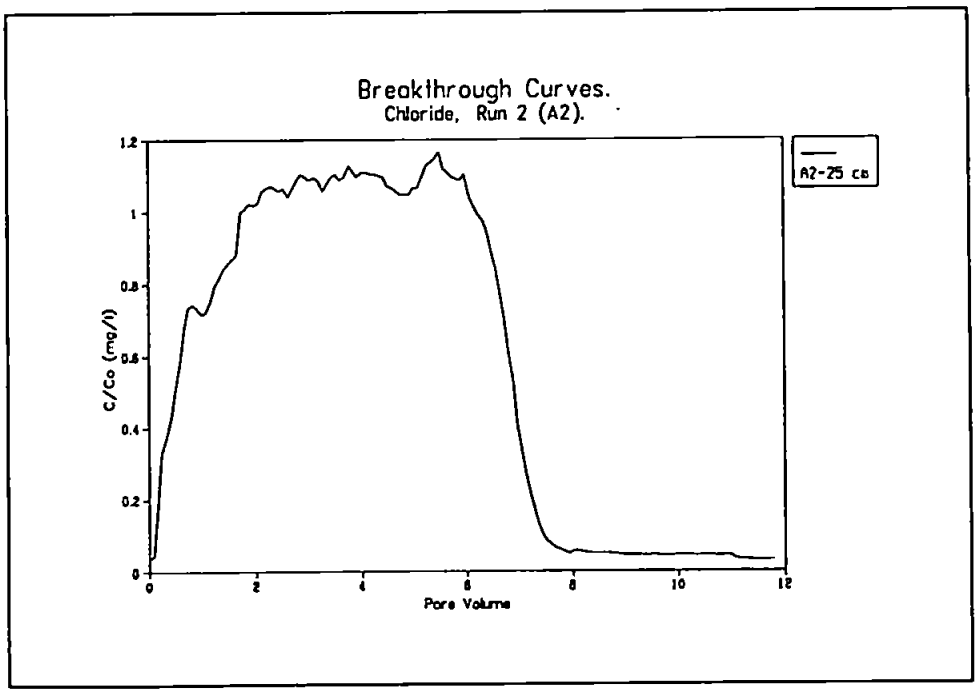

Figure 7.28 - Breakthrough curve for location A2, run 2 block A.

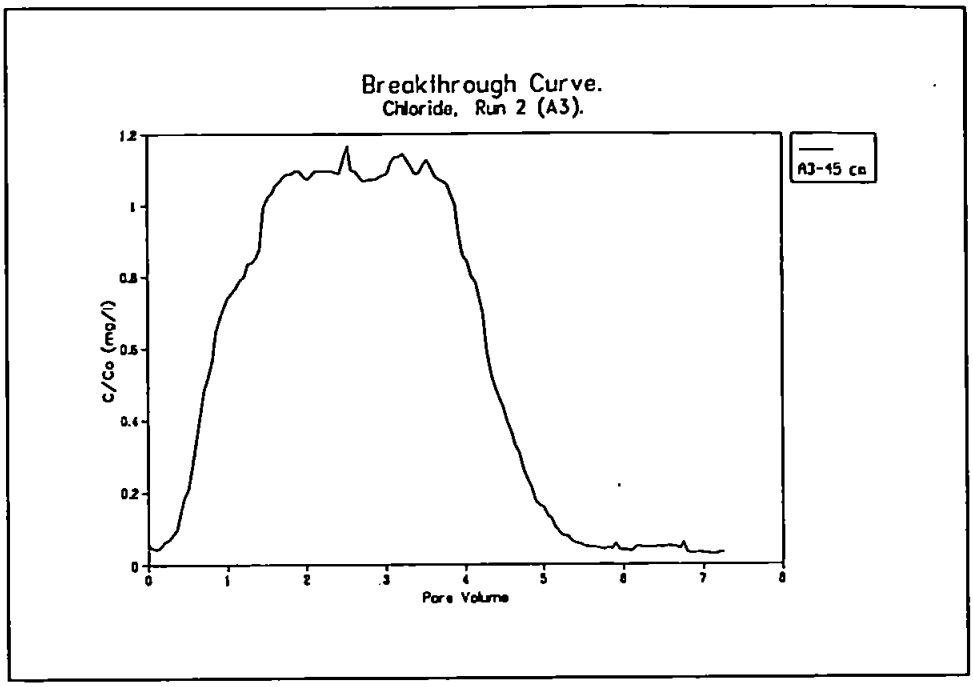

Figure 7.29 - Breakthrough curve for location A3, run 2 block A.

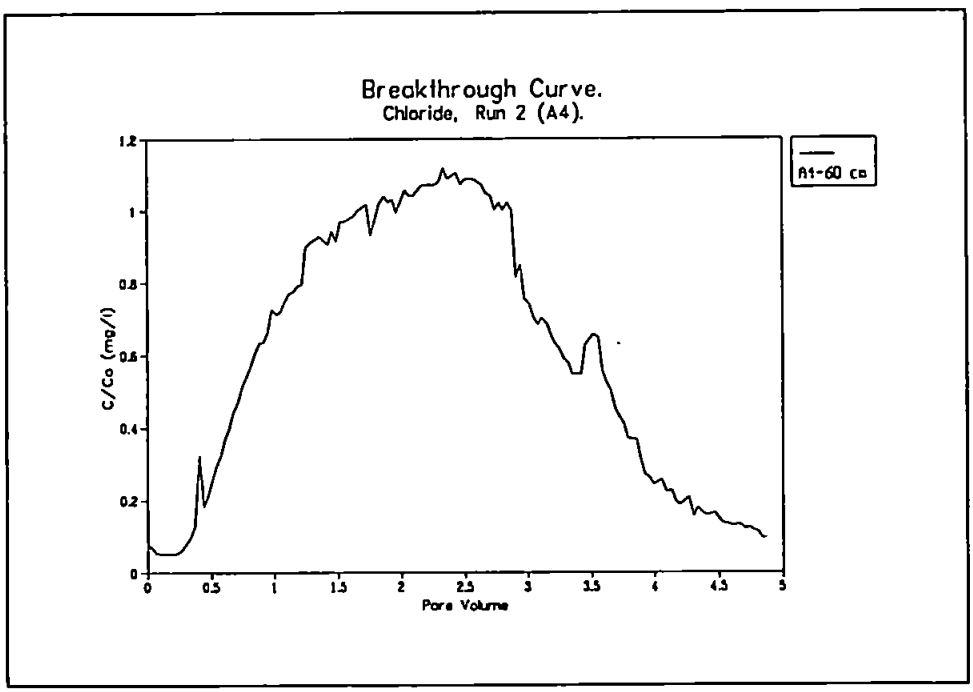

Figure 7.30 - Breakthrough curve for location A4, run 2 block A.

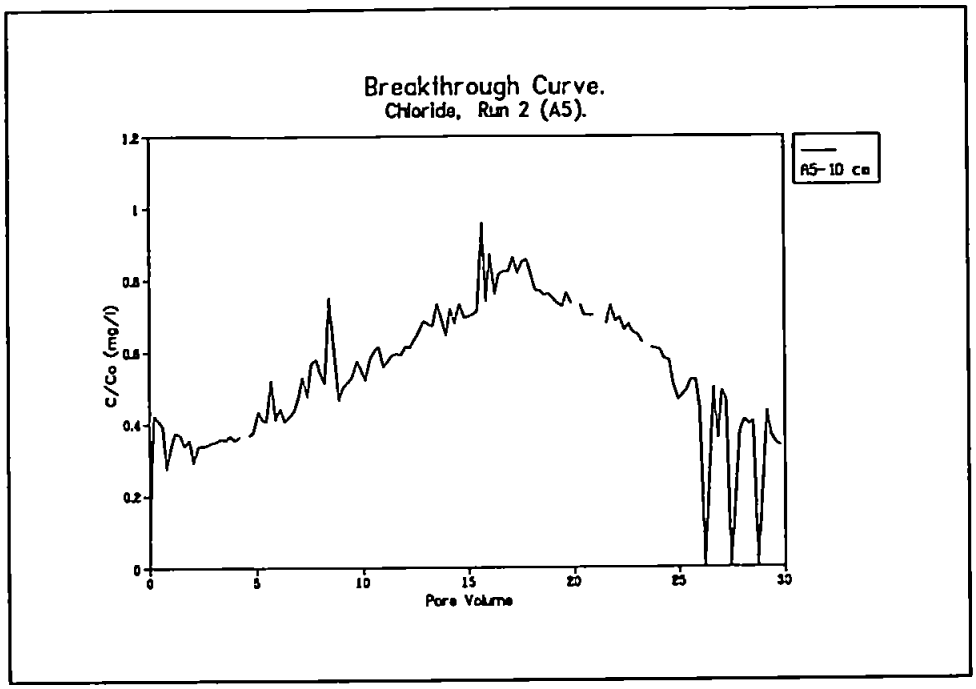

Figure 7.31 - Breakthrough curve for location A5, run 2 block A.

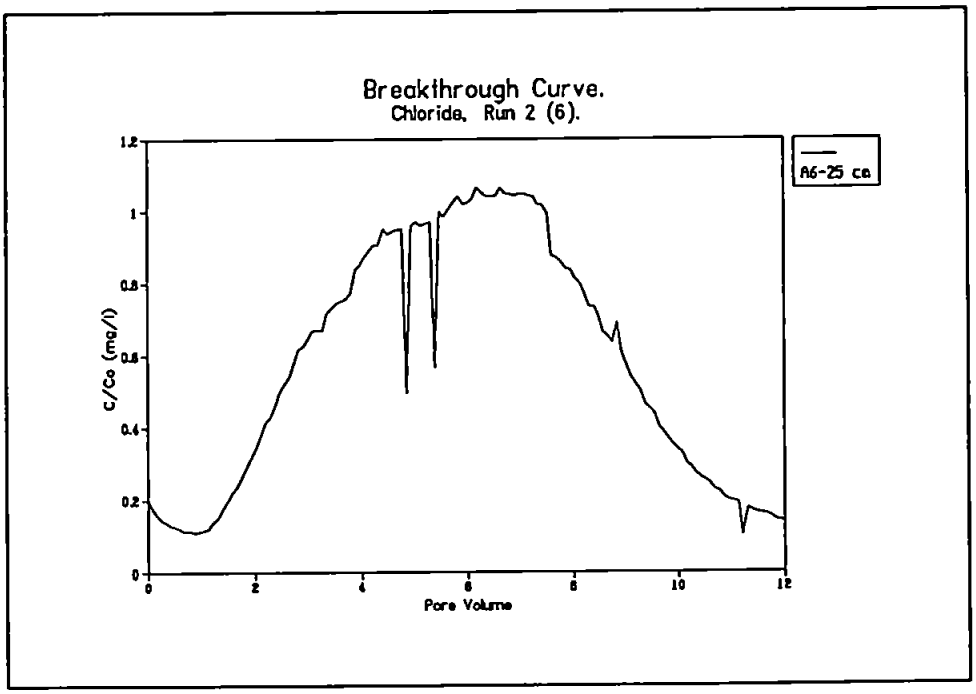

Figure 7.32 - Breakthrough curve for location A6, run 2 block A.

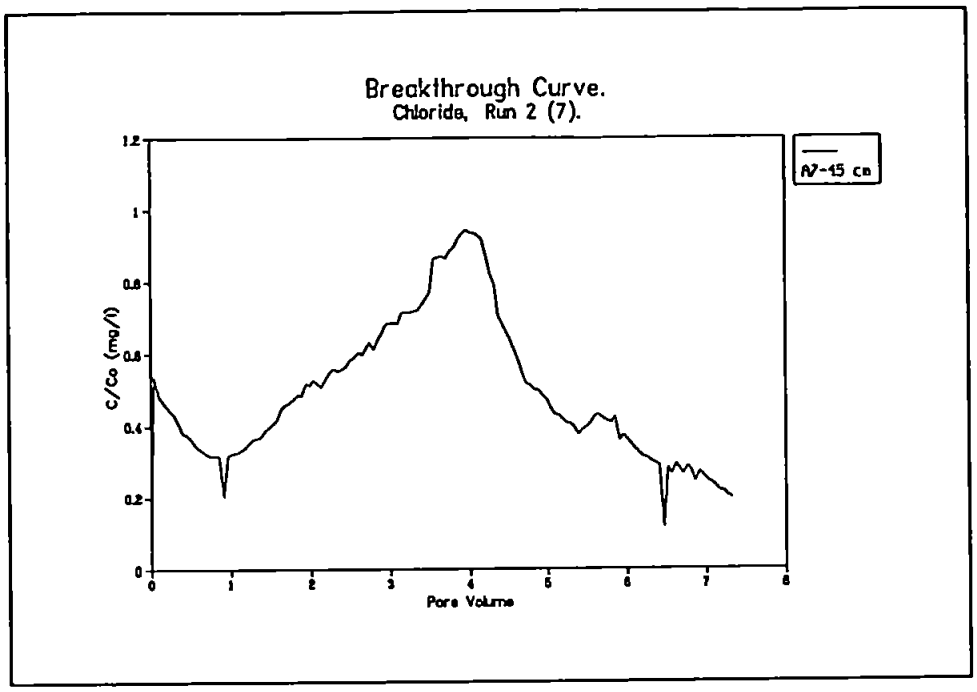

Figure 7.33 - Breakthrough curve for locaton A7, run 2 block A.

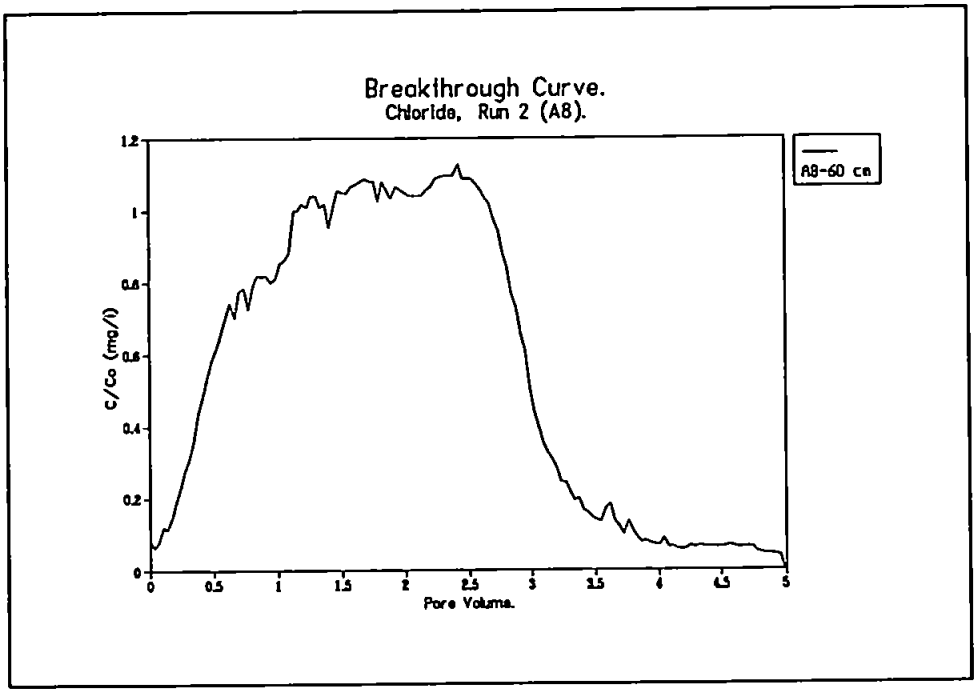

Figure 7.34 - Breakthrough curve for location A8, run 2 block A.

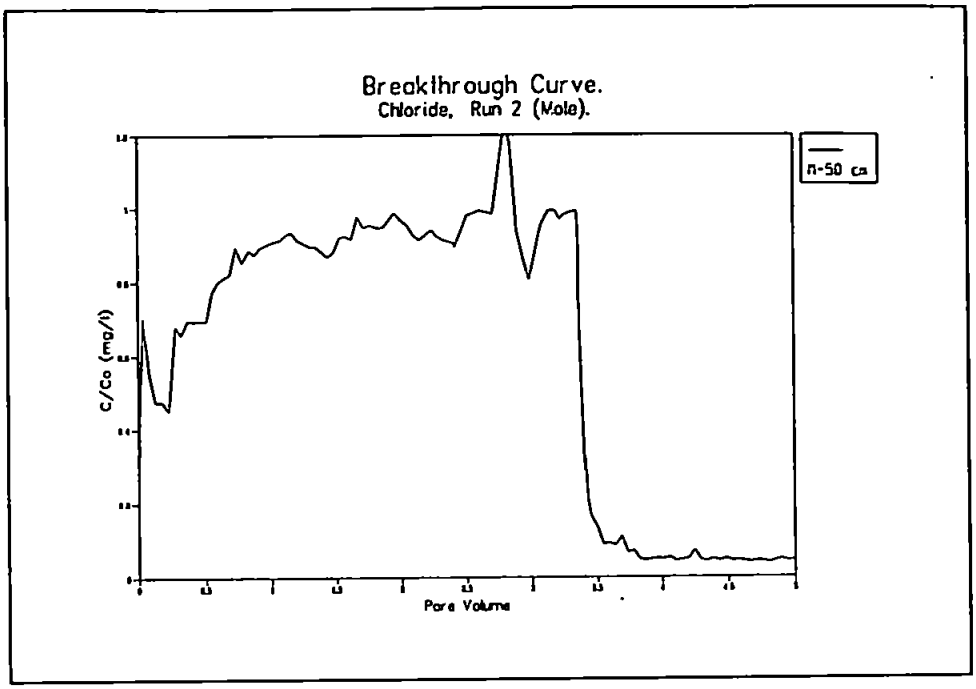

Figure 7.35 - Breakthrough curve for mole drain sample, run 2 block A.

Although the clay rich horizon was evident across the block, A1(10 cm) (right) was less affected by it and must therefore have been located nearby a faster moving pathway through this layer.

Table 7.21 and Figures 7.36 to 7.44 illustrate that the rise in concentration through time in run 3 occurred very slowly. With the exception of that for the mole, no other sample breakthrough curve reached C/Co = 0.5 within 1 PV. Except for sample locations B1(10 cm), B6(25 cm) and the mole(50 cm) all other breakthrough curves were negatively skewed. From the arguments put forward above these features would suggest that mesopore and/or matrix flow dominated soil block B.

The response at B5(10 cm), as at A5, was slow due to the clay rich layer at the top of the

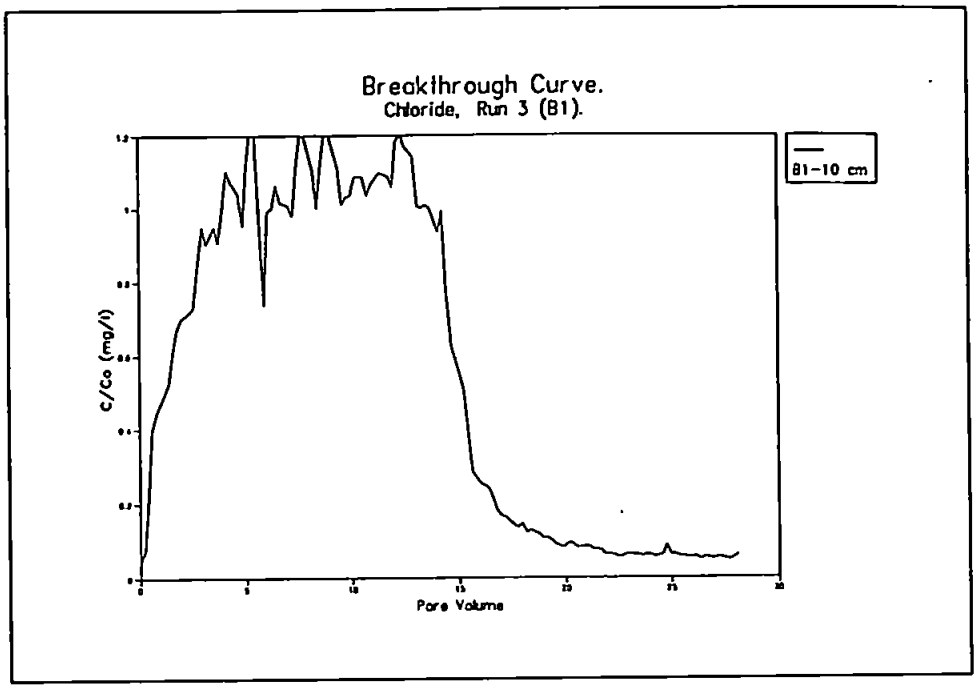

Figure 7.36 - Breakthrough curve for location B1, run3 block B.

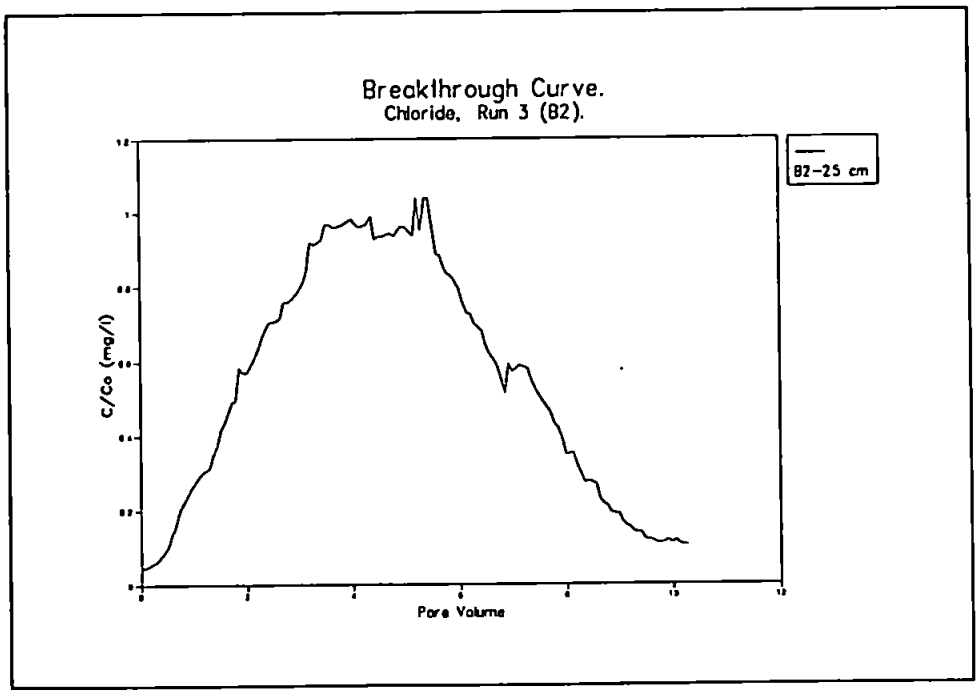

Figure 7.37 - Breakthrough curve for location B2, run 3 block B.

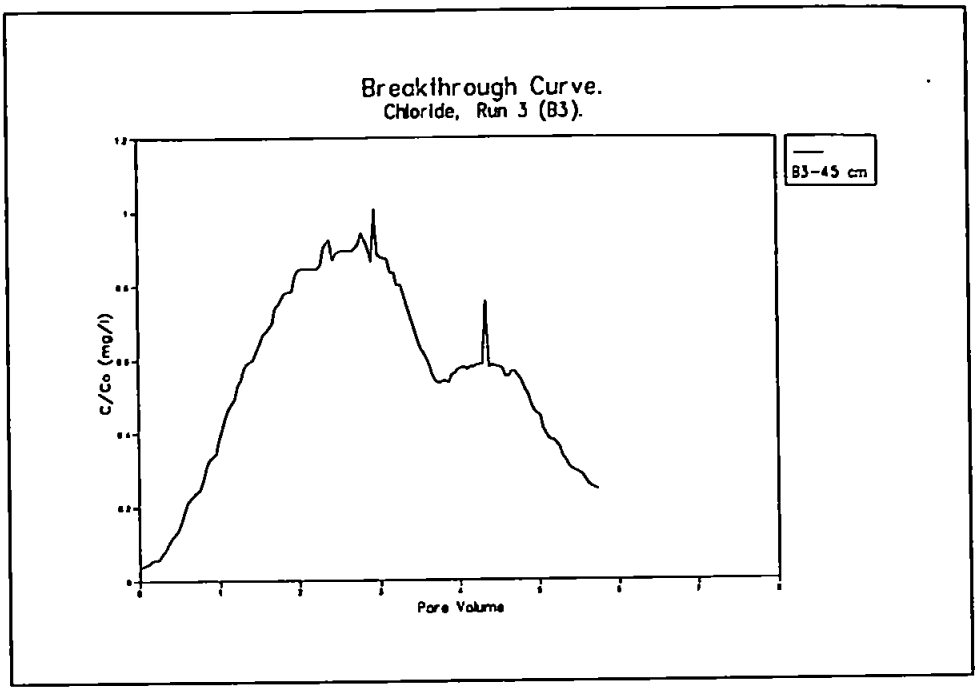

Figure 7.38 - Breakthrough curve for location B3, run 3 block B.

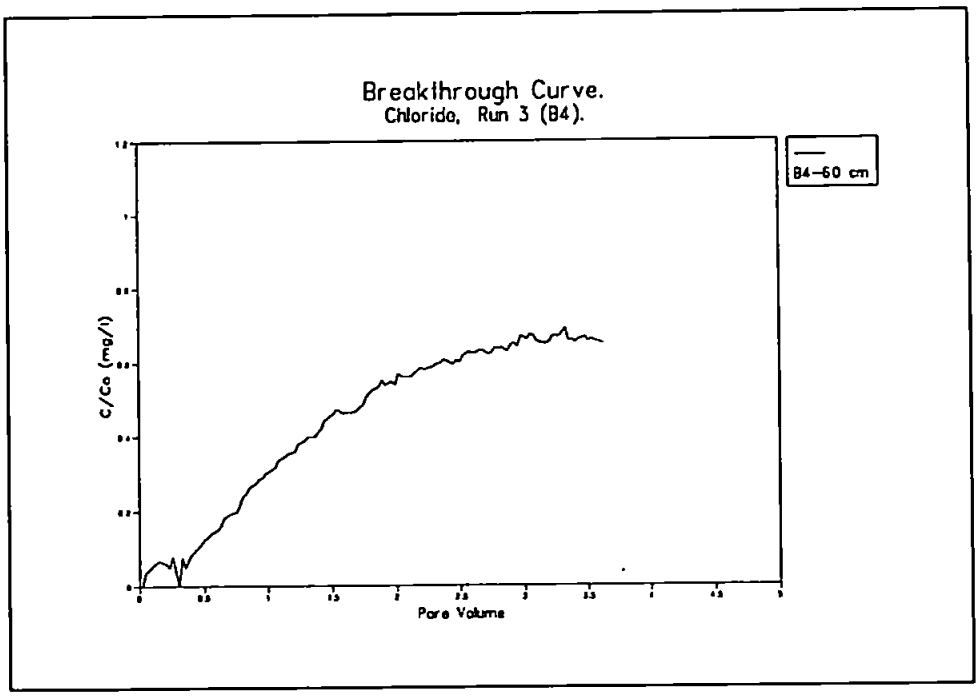

Figure 7.39 - Breakthrough curve for location B4, run 3 block B.

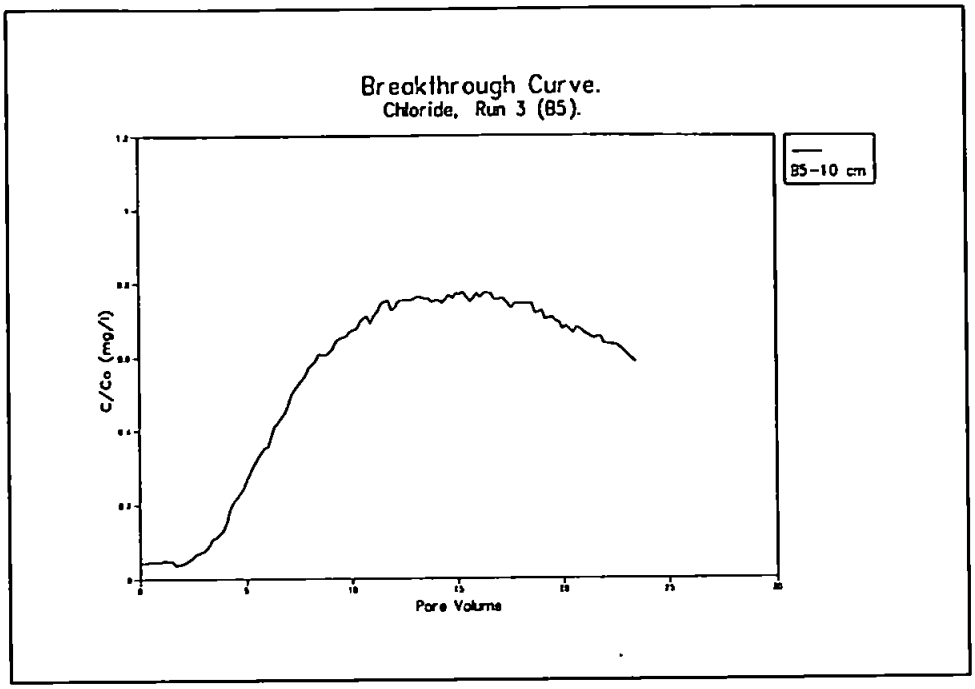

Figure 7.40 - Breakthrough curve for location B5, run 3 block B.

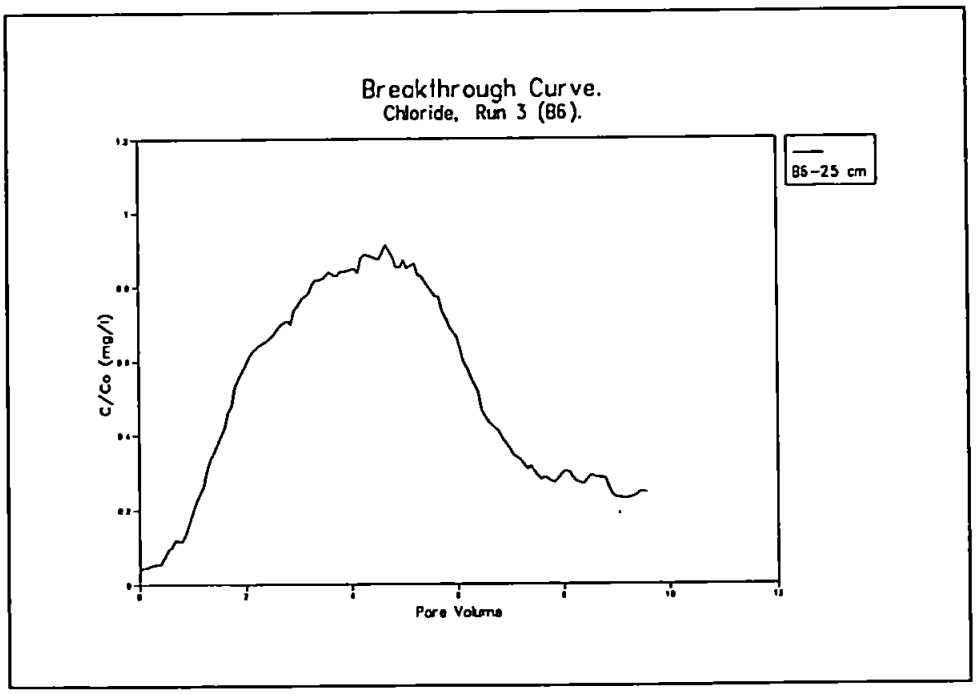

Figure 7.41 - Breakthrough curve for location B6, run 3 block B.

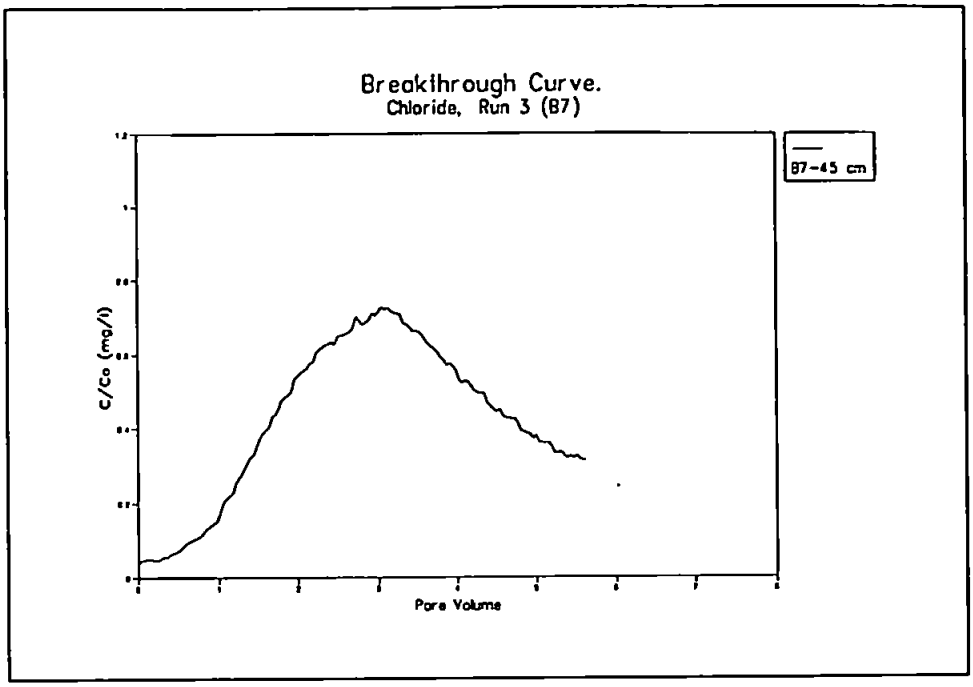

Figure 7.42 - Breakthrough curve for location B7, run 3 block B.

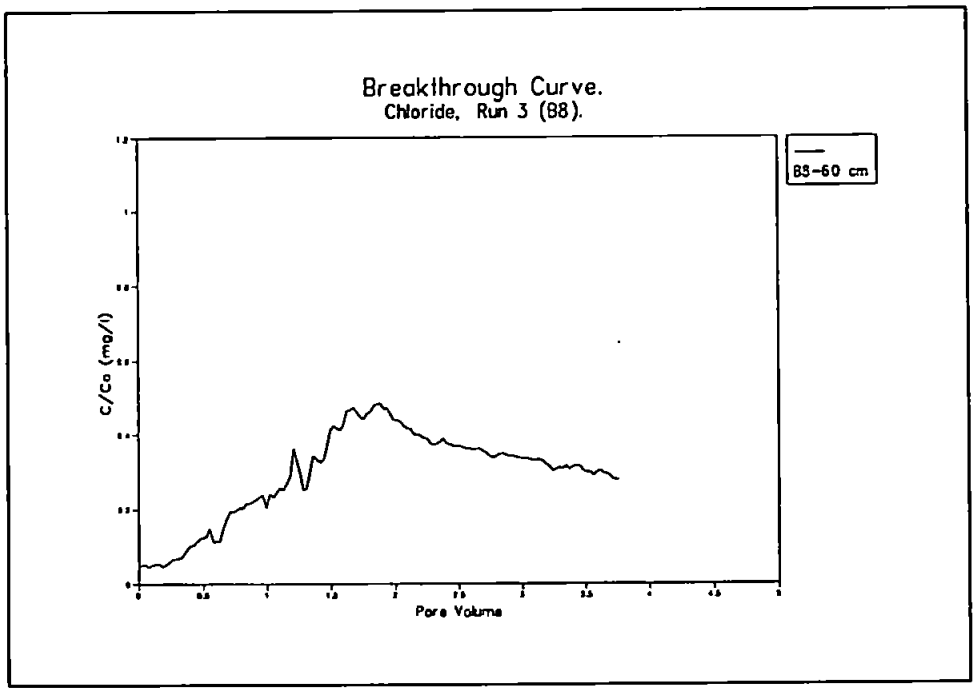

Figure 7.43 - Breakthrough curve for location B7, run 3 block B.

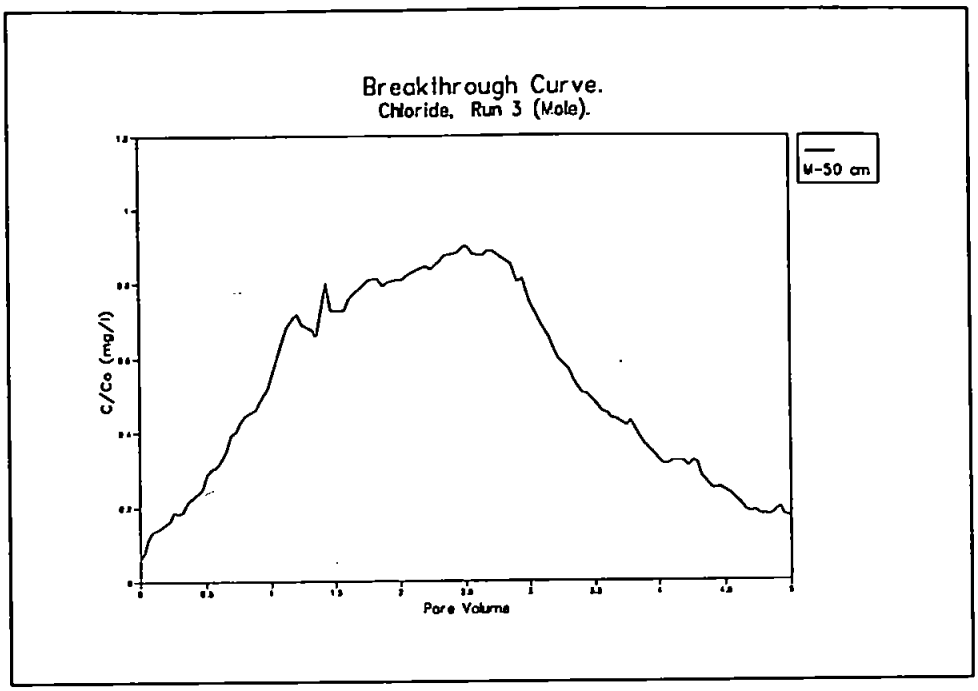

Figure 7.44 - Breakthrough curve for mole drain sample, run 3 block B.

block. A similarity therefore exists between the two blocks at this location within the soil.

Summary:

Breakthrough curve analyses indicated that this type of soil was dominated by matrix flow and/or mesopore flow. Block A, although only taken from 1 m away from where block B was extracted, had more dominant preferential flowpaths. This assertion will be examined in Chapter 8. Variability was observed both within a block as well as between the two soil blocks, for example samples observed at A2, A3, A8 and mole(A) (Figures 7.27, 7.28, 7.33 and 7.34) displayed a faster rising limb to the breakthrough curve than their counterparts B2, B3, B8 and mole(B) (Figures 7.36, 7.37, 7.42 and 7.43). The blocks had certain similarities, for example at sample location A5 and B5(10 cm, left) (Figure 7.30 and 7.39) both breakthrough curves were noticeably delayed compared to sample locations A1 and

B1(10 cm,right) (Figure 7.27 and 7.35) which were at a similar level within the block but represented different sides of the block. Parts of the block were apparently dominated by slower pathways these included locations A1 and B1 (10 cm right), A5 and B5 (10 cm left) and A6 and B6 (25 cm left). At other locations, in particular the mole drain for both blocks, solute samples indicated the presence of faster pathways.

7.7.2. Discussion of Breakthrough Curves.

The results from the breakthrough curves would suggest that the solute samples collected from suction cup lysimeters represented solute that had moved through relatively slower pathways, whereas results from run 2 (mole) indicate the potential for rapid bypass flow. These observations highlight a problem of the approach used in this experiment. Generally breakthrough curves are calculated from the tracer concentration leaving the base of a column of soil through time (Walker an Trudgill, 1983; Kluitenberg and Horton, 1990; Singh and Kanwar, 1991). The technique used by the aforementioned researcher has a number of advantages, the bulk density and porosity of the entire block can be calculated and therefore the total pore volume can be deduced. In this research breakthrough curves were presented for different locations within a block of soil (at 10, 25, 45, and 60 cm) from solute samples collected in porous suction cup lysimeters, 2 cm in diameter and 5 cm in length. Unlike other breakthrough experiments, therefore, the solute concentration did not represent the total concentration of solution exiting a known cross-sectional area. Also an average bulk density had to be used as it was impractical to calculate bulk density from the entire volume of soil. Some doubt must be placed on how representative pore volume calculations, based on a number of smaller bulk density samples, were to the block as a whole. In Chapter 5 it was shown that macropores were less dominant in the soil than smaller pores and therefore, bulk density sampling scale may not have reflected the influence of the macropores within the block. The implication of a misrepresentation of

macropore pathways would lead to a false interpretation of the results. An increase in observed macropores within the sample would reduce the calculated bulk density, increase porosity values and result in a greater throughput being required before 1 PV is reached (Singh and Kanwar,1991). This would result in the breakthrough curve being 'apparently' shifted to the left of where it is in Figure 7.27 to 7.44, and may result in C/Co = 0.5 before PV = 1. As a result of this a comparison between breakthrough curves produced in this experiment and those observed by other researchers would have to be conducted with a degree of caution. A delay in the breakthrough may still be an indication of preferential flow as lysimeters may have been located in an area of the block dominated by matrix flow. Although preferential flow was occurring, solute concentration showed the effect of small advection-dispersion rates, associated with preferential flow bypassing the matrix. By locating samplers in different active zones within the soil, an indication of concentration associated with bypass and that associated with storage can be made, but only if tracer experiments are combined with structural observations. Such a comparisons will be made in Chapter 8.

7.8. MODELLING.

Breakthrough curves and models have been used by a number of researchers to predict dispersion in intact soil columns (Kluitenberg and Horton, 1989; Saleh *et al.*, 1990; Singh and Kanwar, 1991). Experimental work relies on collecting effluent leaving the base of a column. However, in a field environment solute samples are more likely to be collected from *in situ* soil samplers, such as suction cup lysimeters. These samples represent 'at a point' observations unlike those contributing to the more traditional breakthrough curves. The experiments in this investigation were used to test how well models such as the advection-dispersion model could predict 'at a point' breakthrough curves.

Darcian theory assumes all water and solute to flow through a soil at equal velocity across a cross-sectional area. However, Darcian flow can not explain irregular flow that occurs in heterogeneous soils. Models based on Darcy's Law or Richards' equation do not describe water and solute movement through a dual-porous material of limited volume very well, although the basic principles of Darcy's Law cannot be totally rejected as they have been well proven (Beven and Germann, 1981).

Solute transport through homogeneous soil has traditionally been described, for one dimensional steady-state fluid flow, by advection-dispersion equations presented by Lapidus and Amundson (1952). The advection-dispersion equation can be written as:

$$R\frac{\delta C}{\delta t} = D\frac{\delta^2 C}{\delta x^2} - v\frac{\delta C}{\delta x} \qquad (7.1)$$

Where, C is solute concentration (ML^{-3}), x is distance from where solute is introduced (L), t is time (T), D is hydrodynamic dispersion coefficient ($L^2\ T^{-1}$), v is average pore-water velocity ($L\ T^{-1}$), and R is retardation factor (dimensionless) (Singh and Kanwar, 1991).

Most transport models based on advection-dispersion equations assume that an average flowpath exists, and do not consider preferential flow (Andreini and Steenhuis, 1990). Advection-dispersion equation models have been used to fit solute dispersion through repacked soil columns (Beven and Young, 1988). However, solute transport under field conditions and through undisturbed soil columns are less well predicted by the advection-dispersion equation theory, (Parker and Van Genuchten, 1984; Beven and Young, 1988; Saleh *et al.*,1990). Advection-dispersion models have been adapted to try and predict early

breakthrough and tailing by dividing flow into mobile and immobile fractions in which advection-dispersion is assumed to occur in the mobile water only (Rao *et al.*, 1980). However, this adaption to the advection-dispersion model can still only provide an approximation of what is really happening in a heterogeneous soil.

An alternative to the advection-dispersion model with an approach that required limited a prior assumptions of physical processes was presented by Beer and Young (1983). Beven and Young (1988) modified Beer and Young's (1983) approach, which was used to predict solute mixing in rivers, to predict solute movement in soil, and referred to their model as the Aggregated Mixing Zone (AMZ) model. Beven and Young (1988) assumed that similar inefficient mixing occurred between fast flowing pathways and slower flowing matrix solution, referred to as dead zones, as observed in river flow. The mathematical equation of the AMZ model is presented in Beven and Young (1988).

The AMZ model has a number of limitations in that it is a linear methodology similar to the transfer function approach of Jury *et al.* (1986). However, the AMZ model is more flexible with regards to model structure and requires only minimal a priori assumptions about the nature of the flow processes (Beven and Young, 1988). A FORTRAN IV computer program (CXTFIT) was used to curve fit an observed concentration distribution as a function of time using maximum neighbourhood methods to minimize the sum of squares. Data for the CXTFIT program was pre-processed using a program called CDEPREP which produces a CXTFIT data file from ASCII time/concentration data output. This model has been shown by Beven and Young (1988) to produce a good fit to observed breakthrough curves including data that could not be predicted by more conventional advection-dispersion models. For these later reasons this model was chosen to be used to interpret breakthrough curves for this experiment.

In this thesis a comparison is made between predicted parameters, made by the AMZ model and those of a more traditional advection/dispersion model CLEARY (Cleary and Ungs, 1979). The AMZ model represents a deterministic method that optimises parameters while the CLEARY model is both a mechanistic as well as deterministic model.

CLEARY obtained a one-dimensional analytical solution to the advection/dispersion (mass transport) model, using a semi-infinite domain with a type 1 boundary condition. The model is based on the differential equation:

$$\frac{\delta C}{\delta t} + Vx \cdot \frac{\delta C}{\delta x} = Dx \cdot \frac{\delta^2 C}{\delta x^2} - KC \qquad (7.2)$$

Where, C is concentration (C/Co), t is time (days), V is velocity (cm/d), x is distance (cm), D is dispersivity, and K is hydraulic conductivity. The following boundary conditions were imposed on the model

$$@\ x = 0 \qquad C = C_0 e^{-\gamma t} \qquad (7.3)$$

$$@\ x \dashrightarrow +\infty \qquad \frac{\delta C}{\Delta x} \dashrightarrow$$

C and t initially set at 0 at the start of the model.

7.8.1. Results of AMZ and CLEARY Modelling.

Aggregated Mixing Zone Model:

Five breakthrough curves from run 2 and five breakthrough curves from run 3 were curve fitted using the AMZ model. The selected breakthrough curves represented sampling locations at 10 cm and 60 cm depth, either side of the block and from the mole drain. Figures 7.45 to 7.54 show these breakthrough curves plotted with the fitted model (solid line). These figures illustrate that the model had difficulty in matching the responses of A4, A5, B4 and B5 (Figures 7.45, 7.46, 7.50 and 7.51 respectively).

Velocities (cm h^{-1}), estimated from bulk density calculations of porosity were used initially. These values together with the models predicted values of velocity, dispersion and proportion of mobile pore space (β) are shown in Table 7.22 (block A) and 7.23 (block B). Maximum and minimum set ranges of dispersion and mobile water were 1 to 2000, and 0.1 to 1.0 respectively. Predicted velocities, with the exception of the mole from run 2, were well in excess of initial estimated velocity within the soil.

Table 7.22 - Predicted values from AMZ model for run 2, block A.

	A1	A4	A5	A8	Mole
Initial Velocity	0.759	0.640	0.690	0.604	0.622
Predicted Velocity	6.517	71.648	1.196	134.207	0.1
Dispersion	11.683	761.492	4.030	1787.641	2000
β	0.634	1.0	1.0	1.0	0.1

Table 7.23 - Predicted values from AMZ model for run 3, block B.

	B1	B4	B5	B8	Mole
Initial Velocity	0.435	0.470	0.529	0.477	0.474
Predicted Velocity	11.713	3.574	0.734	31.910	32.923
Dispersion	82.845	37.682	1.0	2000	828.360
β	1.0	0.1	0.650	1.0	0.890

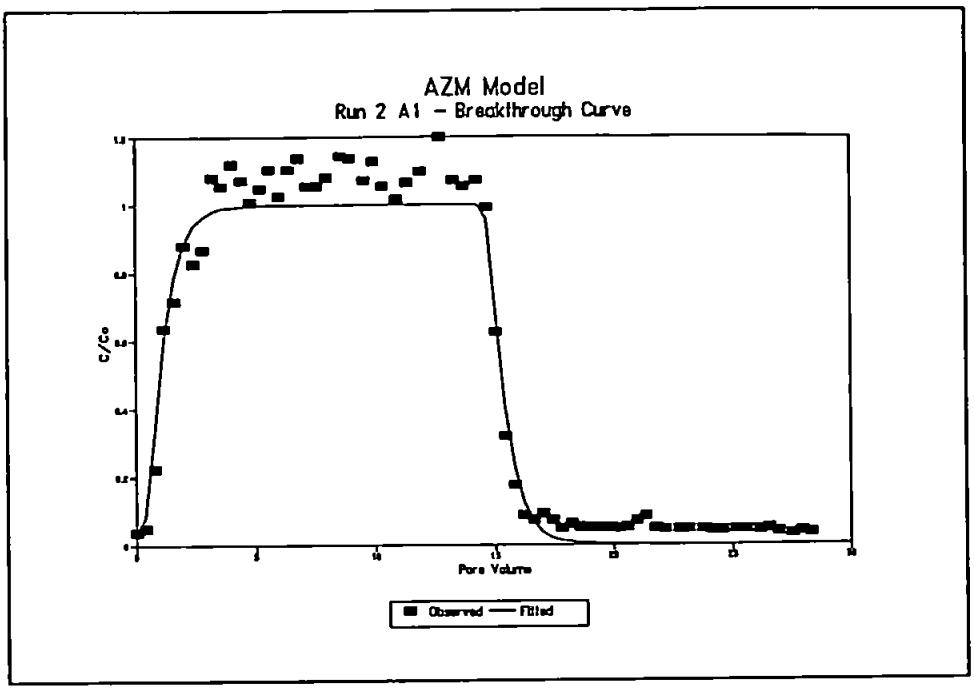

Figure 7.45 - Breakthrough curve A1 (run 2) with AMZ model fitted.

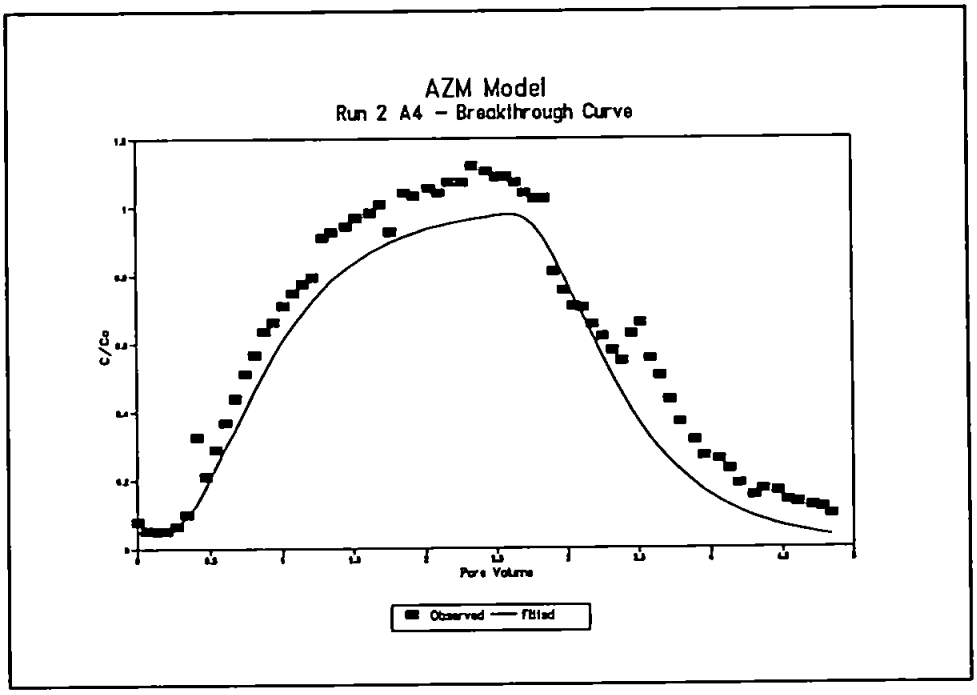

Figure 7.46 - Breakthrough curve A4 (run 2) with AMZ model fitted.

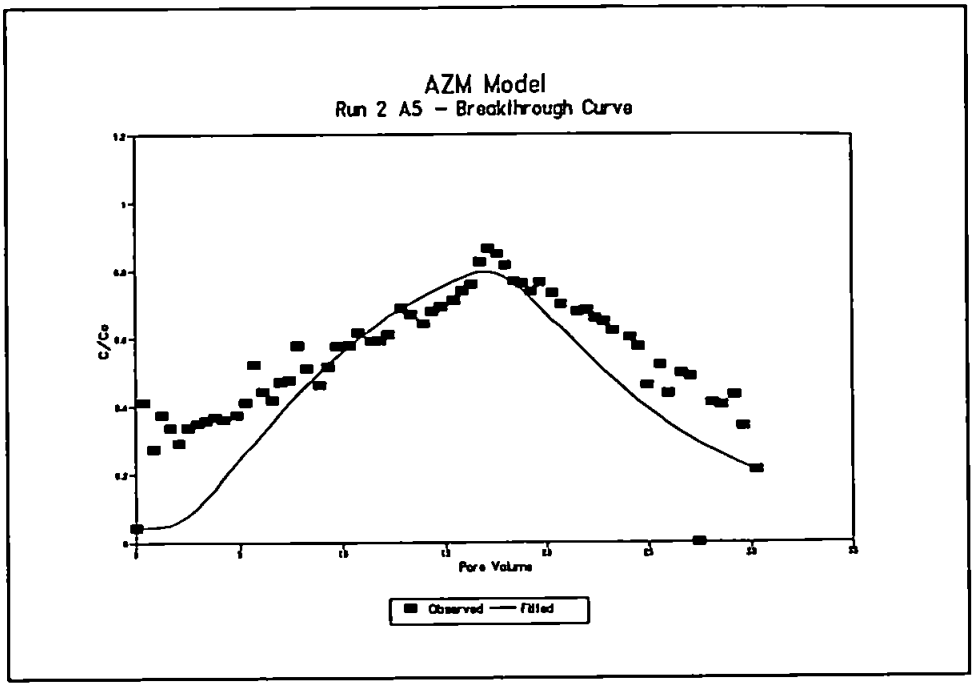

Figure 7.47 - Breakthrough curve A5 (run 2) with AMZ model fitted.

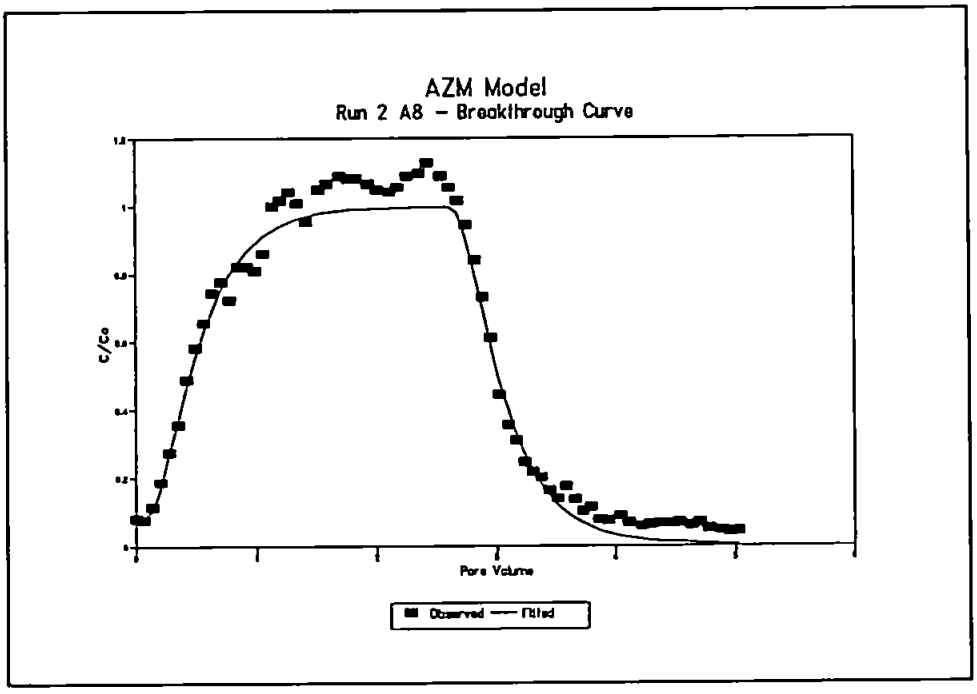

Figure 7.48 - Breakthrough curve A8 (run 2) with AMZ model fitted.

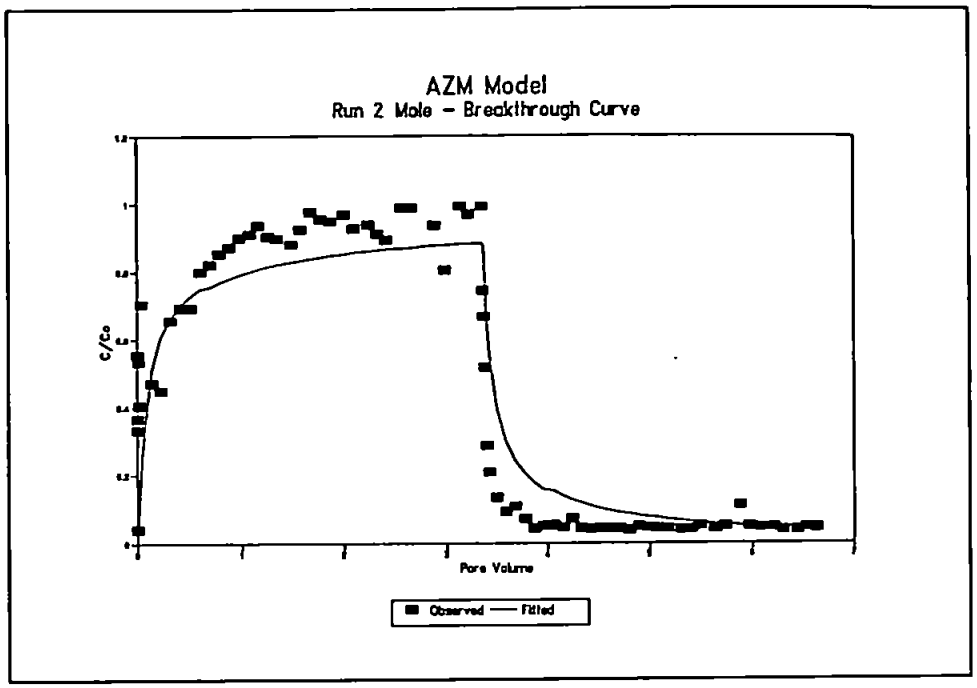

Figure 7.49 - Breakthrough curve for mole drain sample (run 2) with AMZ model fitted.

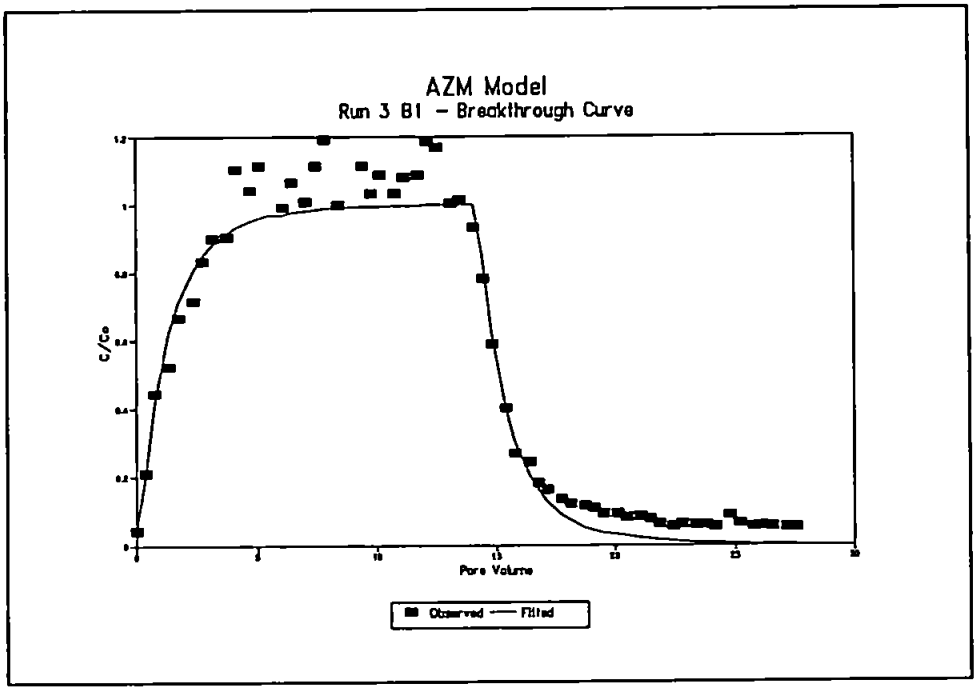

Figure 7.50 - Breakthrough curve B1 (run 3) with AMZ model fitted.

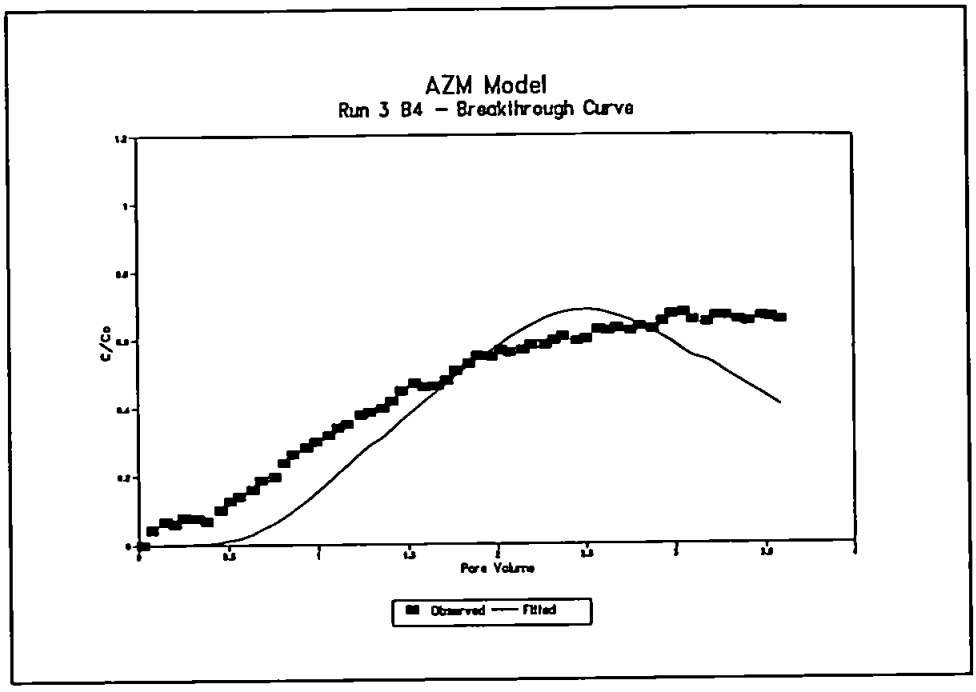

Figure 7.51 - Breakthrough curve B4 (run 3) with AMZ model fitted.

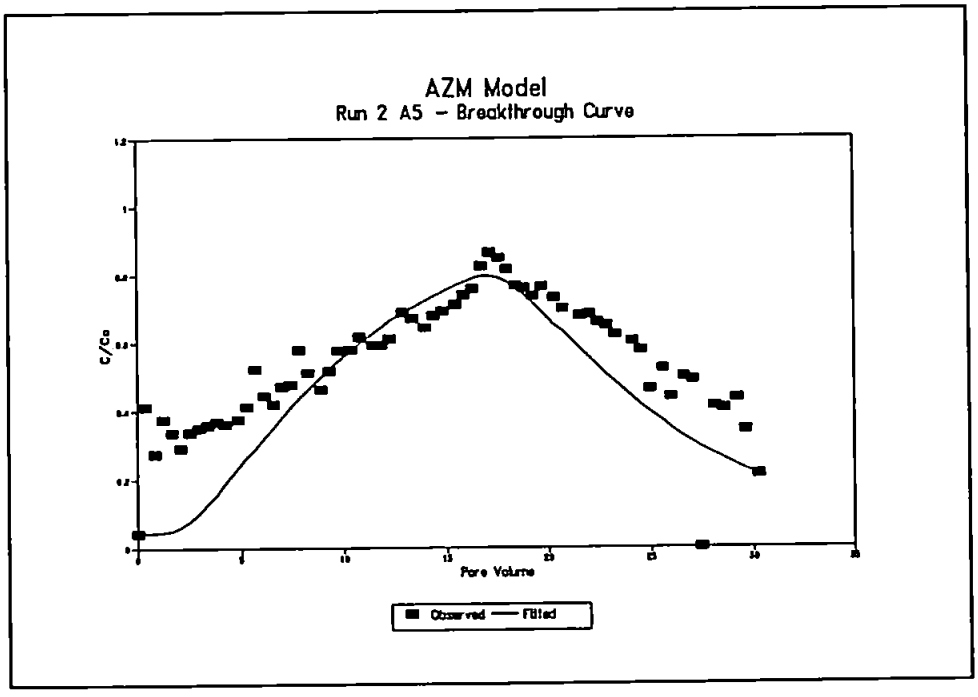

Figure 7.52 - Breakthrough curve B5 (run 3) with AMZ model fitted.

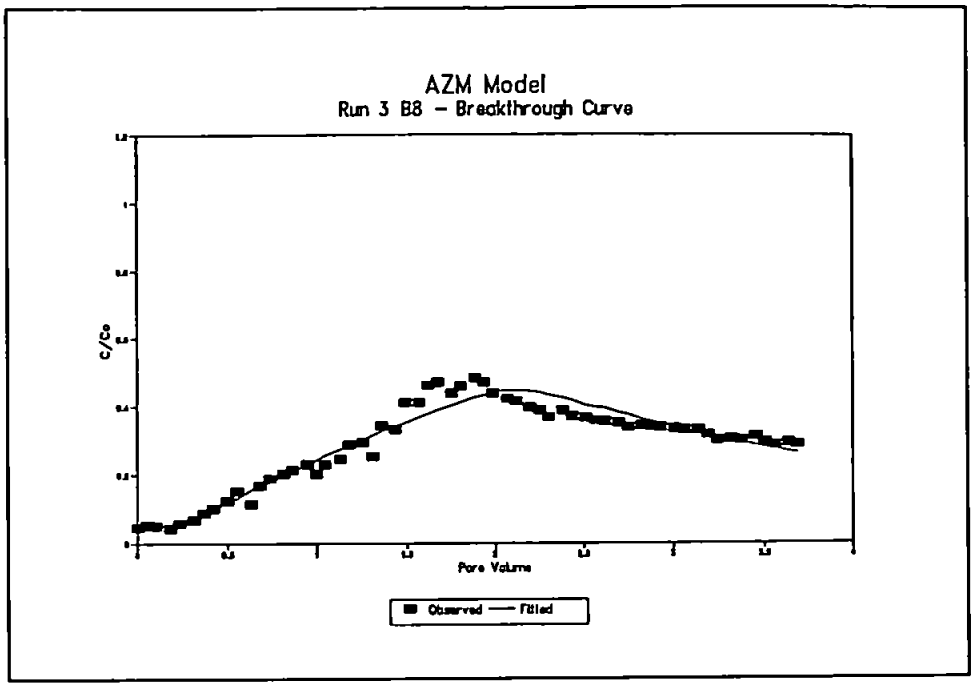

Figure 7.53 - Breakthrough curve B8 (run 3) with AMZ model fitted.

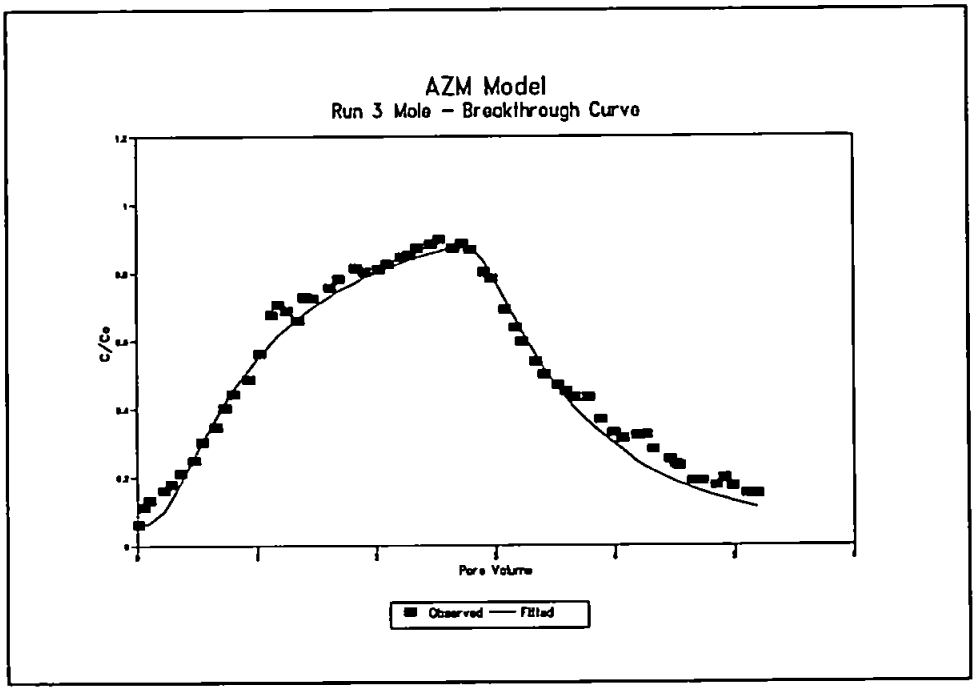

Figure 7.54 - Breakthrough curve for mold drain sample (run 3) with AMZ model fitted.

Advection-Dispersion Model (CLEARY):

CLEARY was used to fit the observed data to predict values of velocity and dispersivity using the same location data as in the AMZ model for samples collected at 10 cm and 60 cm depth, and at the mole, as well as additional locations at 25 and 45 cm depth. Figures 7.55 to 7.72 show the observed and fitted data (solid line) for the eighteen sample locations. Observed velocity and model predicted values of velocity, dispersivity and sink are presented in Table 7.24 (run 2, block A) and Table 7.25 (run 3, block B)

Table 7.24 - Predicted velocity (cm d^{-1}), dispersivity (cm^2 d^{-1}) and sink for run 2, block A, using Cleary advection-dispersion model.

Sample location	A1	A2	A3	A4	A5	A6	A7	A8	Mole
Observed velocity	18.23	17.39	15.29	14.94	16.55	15.72	15.13	14.34	15.22
Predicted velocity	10	18	12	10	0.1	3	1.3	15	50
Predicted dispersivity	10	150	120	150	8	15	50	470	500
Predicted sink	0.2	0.2	0.2	0.2	0.05	0.2	0.2	0.2	0.2

Table 7.25 - Predicted velocity (cm d^{-1}), dispersivity (cm^2 d^{-1}) and sink for run 3, block B, using Cleary advection-dispersion model.

Sample location	B1	B2	B3	B4	B5	B6	B7	B8	Mole
Observed velocity	10.43	11.40	11.33	11.36	16.55	12.38	11.60	11.29	11.48
Predicted velocity	10	1	0.5	3.5	0.1	1	1	3	5
Predicted dispersivity	30	45	100	100	2	30	60	100	300
Predicted sink	0.2	0.2	0.2	0.0	0.2	0.15	0.1	0.0	0.05

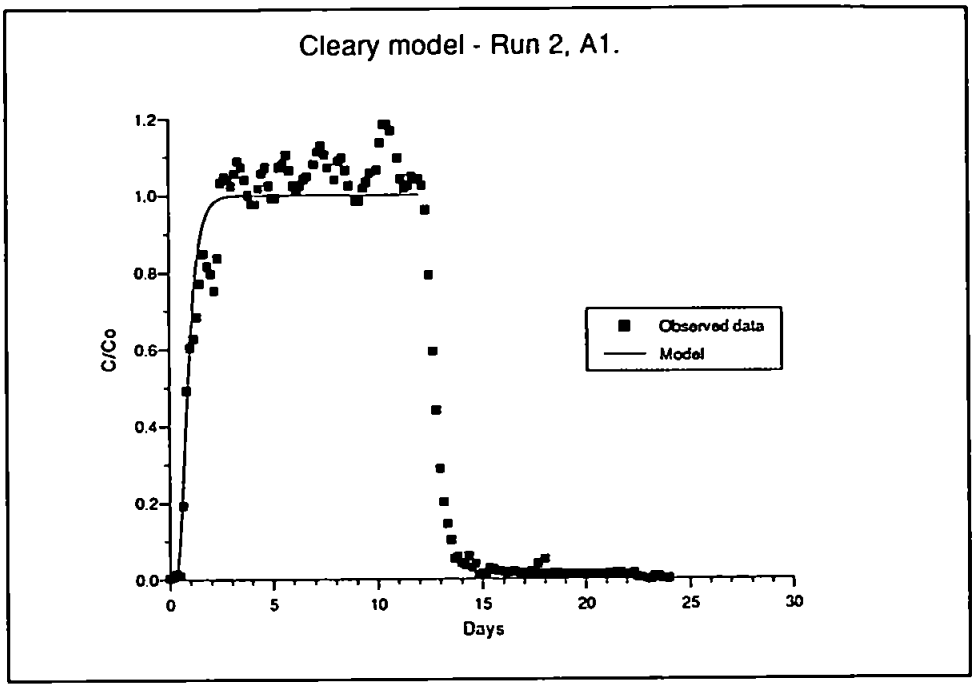

Figure 7.55 - Breakthrough curve A1 (run 2) with CLEARY model fitted.

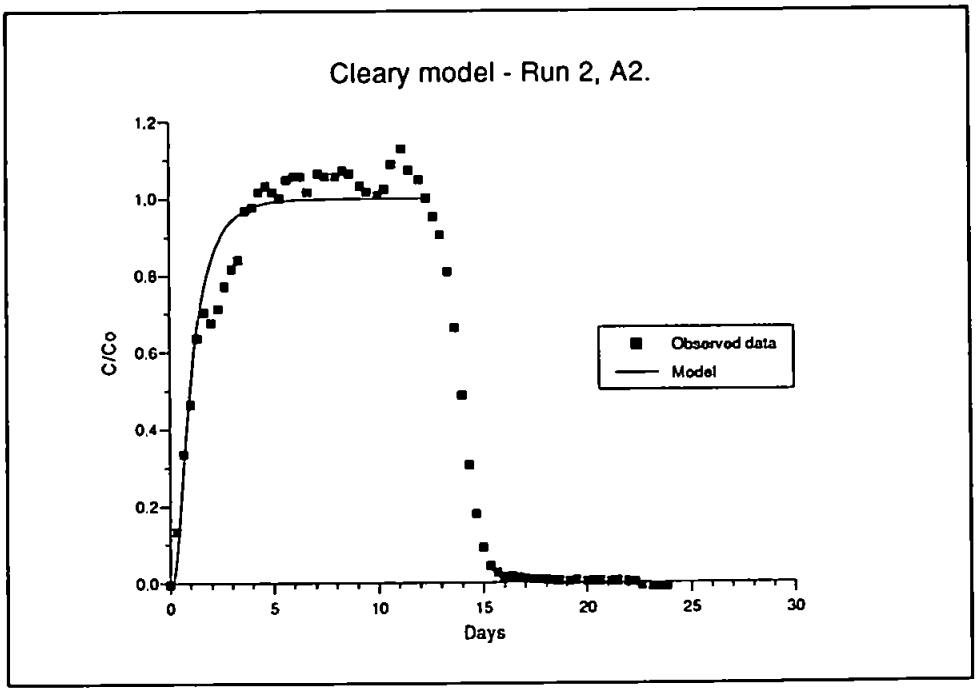

Figure 7.56 - Breakthrough curve A2 (run 2) with CLEARY model fitted.

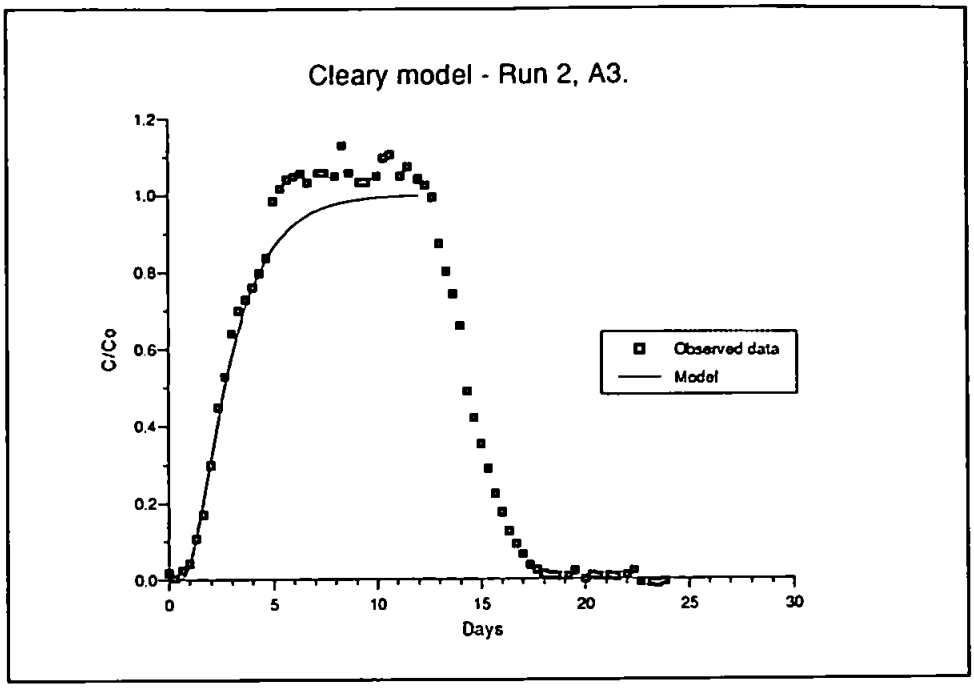

Figure 7.57 - Breakthrough curve A3 (run 2) with CLEARY model fitted.

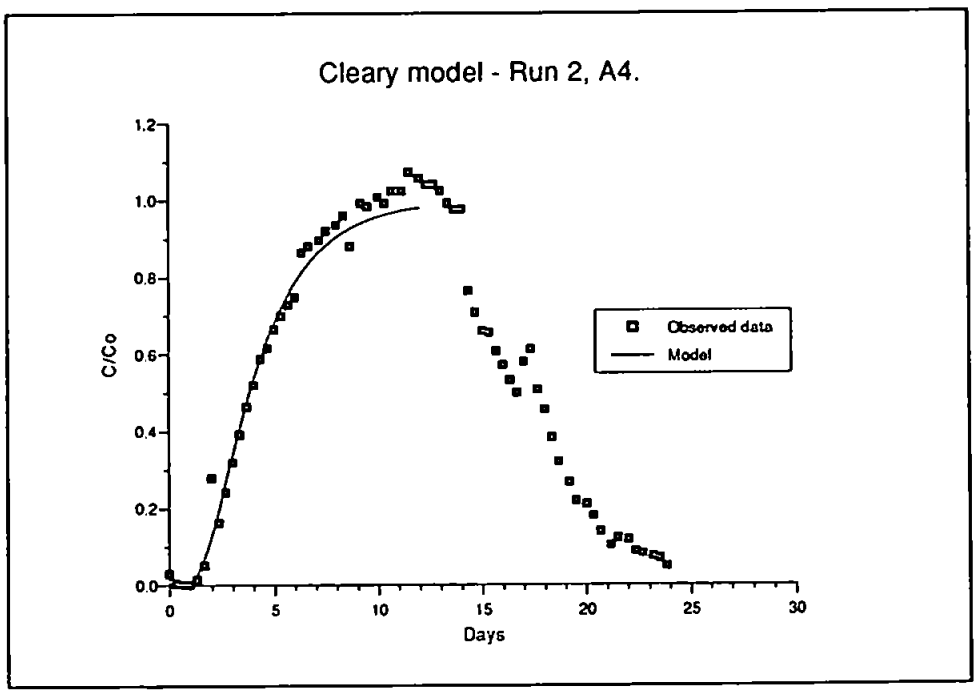

Figure 7.58 - Breakthrough curve A4 (run 2) with CLEARY model fitted.

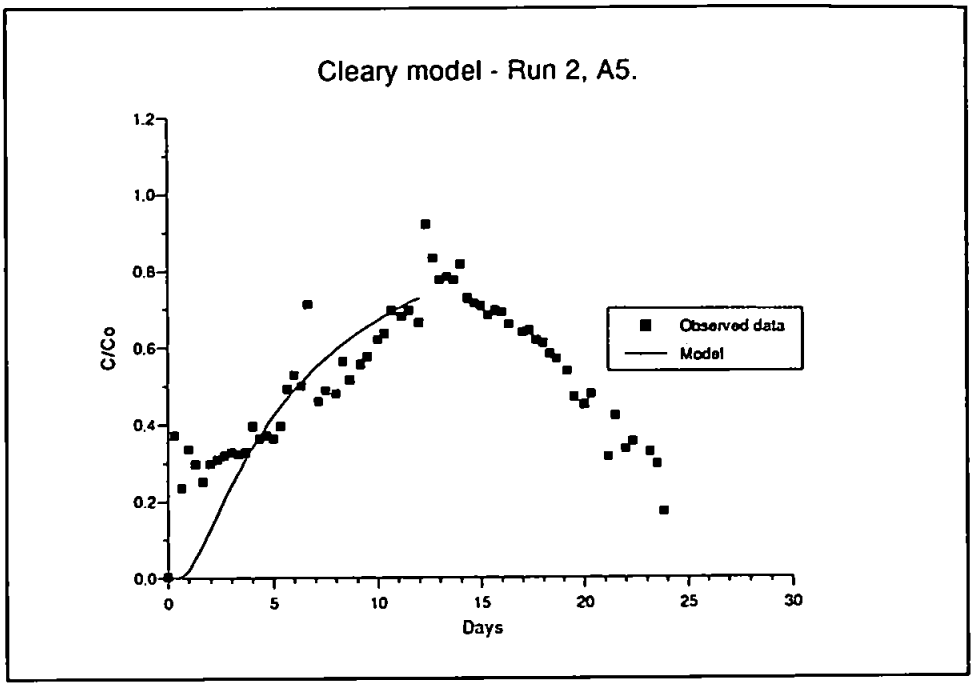

Figure 7.59 - Breakthrough curve A5 (run 2) with CLEARY model fitted.

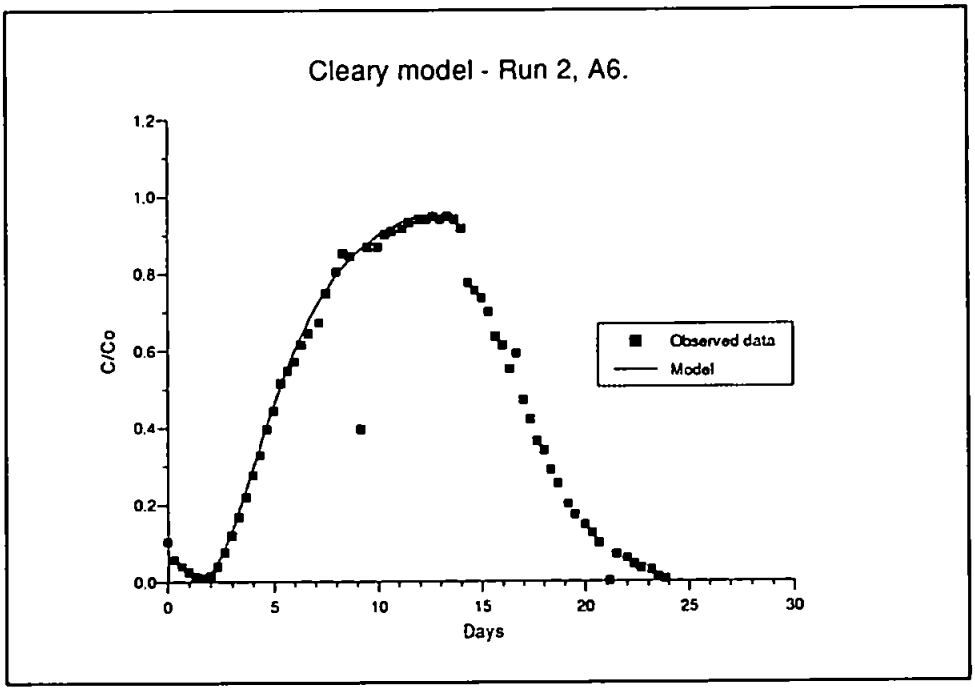

Figure 7.60 - Breakthrough curve A6 (run 2) with CLEARY model fitted.

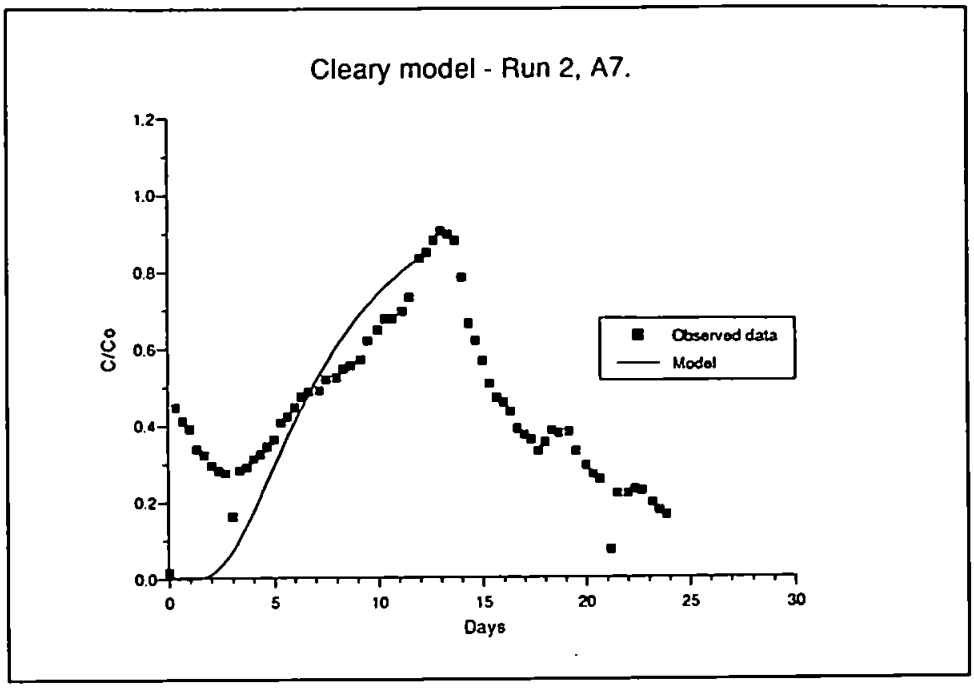

Figure 7.61 - Breakthrough curve A7 (run 2) with CLEARY model fitted.

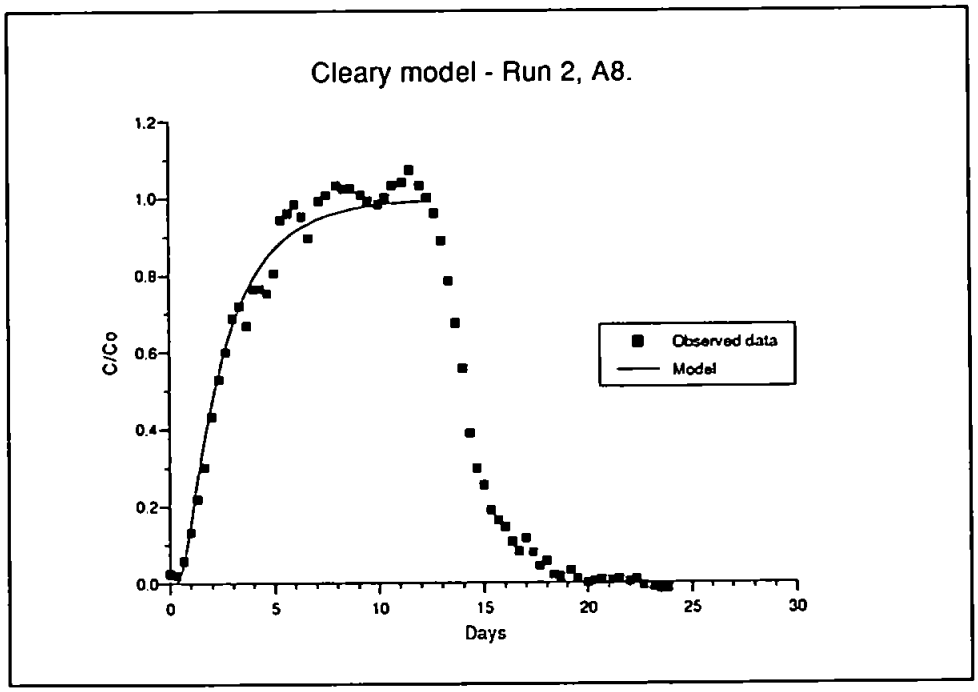

Figure 7.62 - Breakthrough curve A8 (run 2) with CLEARY model fitted.

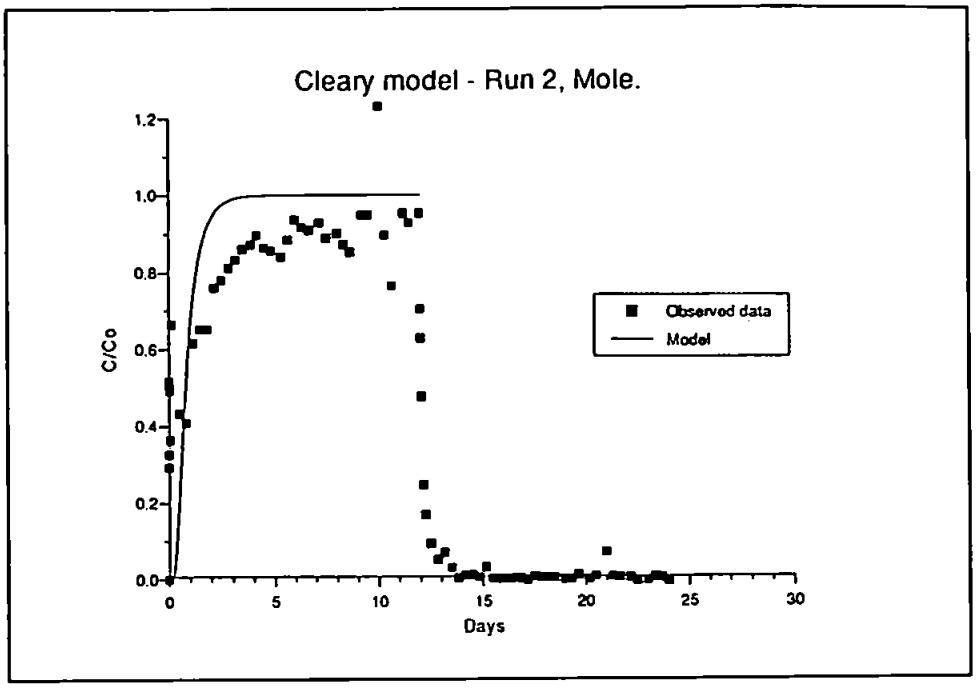

Figure 7.63 - Breakthrough curve for mole drain sample (run 2) with CLEARY model fitted.

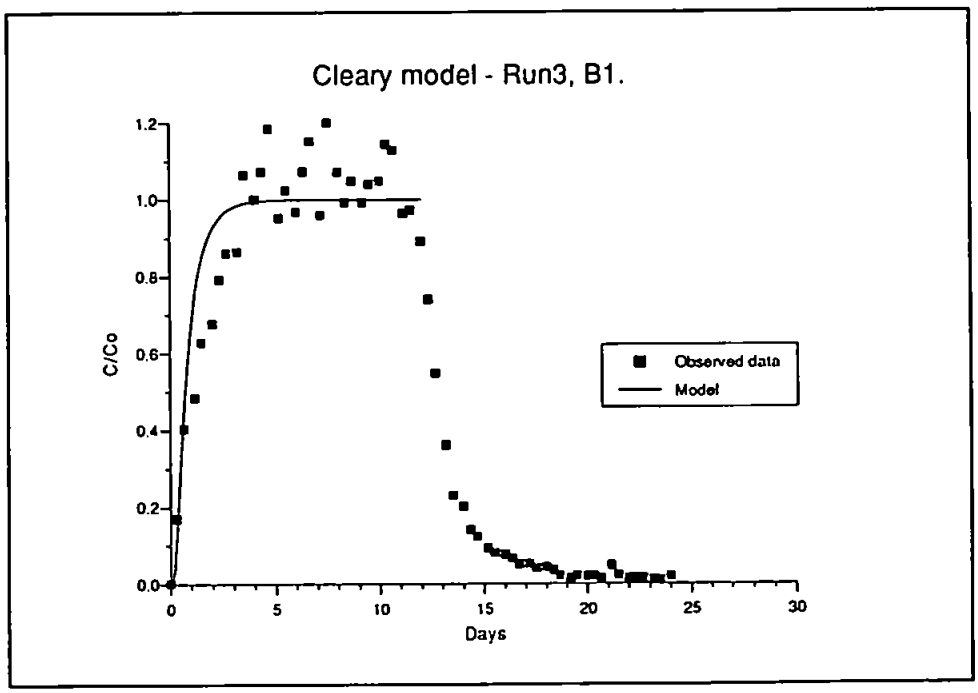

Figure 7.64 - Breakthrough curve B1 (run 3) with CLEARY model fitted.

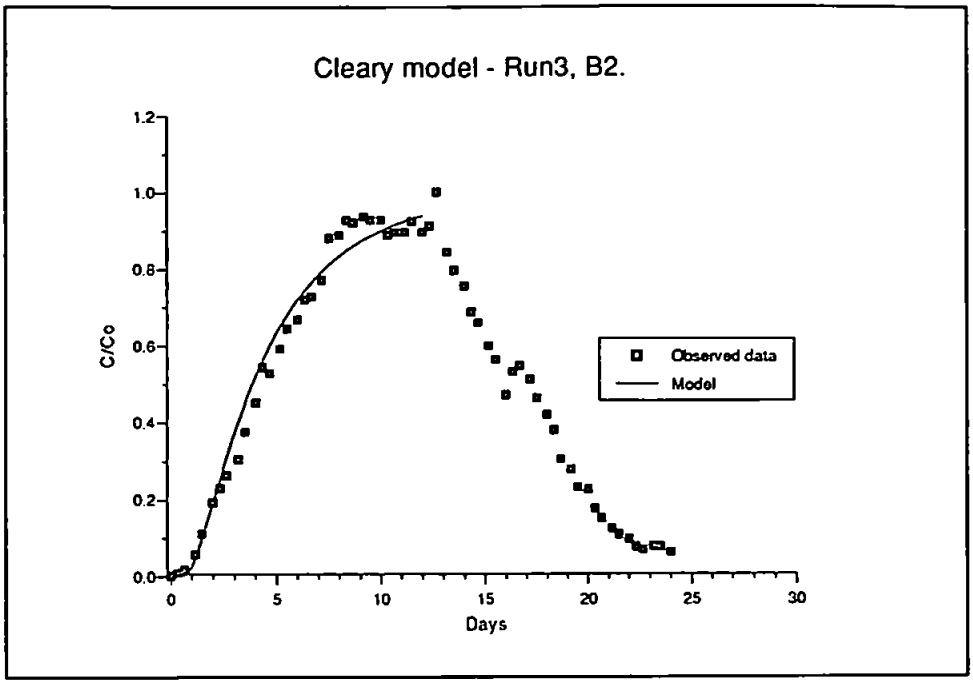

Figure 7.65 - Breakthrough curve B2 (run 3) with CLEARY model fitted.

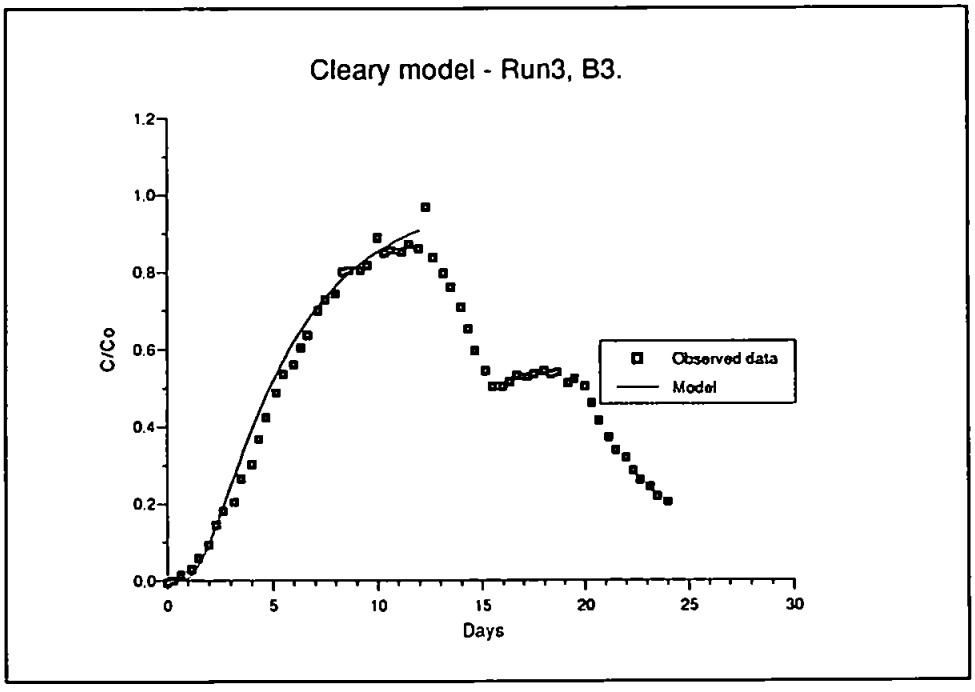

Figure 7.66 - Breakthrough curve B3 (run 3) with CLEARY model fitted.

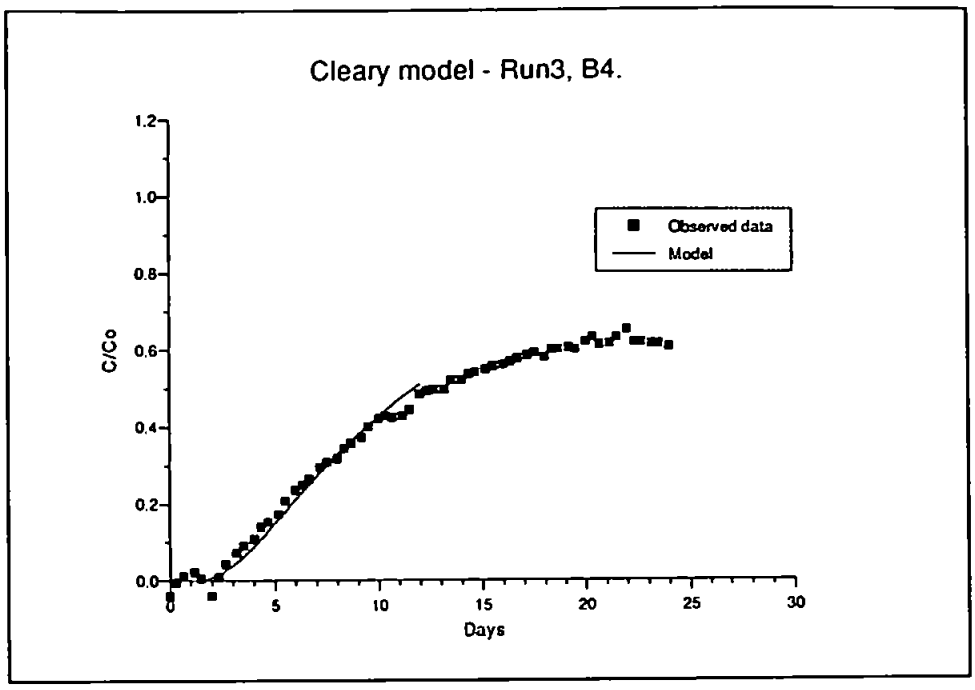

Figure 7.67 - Breakthrough curve B4 (run 3) with CLEARY model fitted.

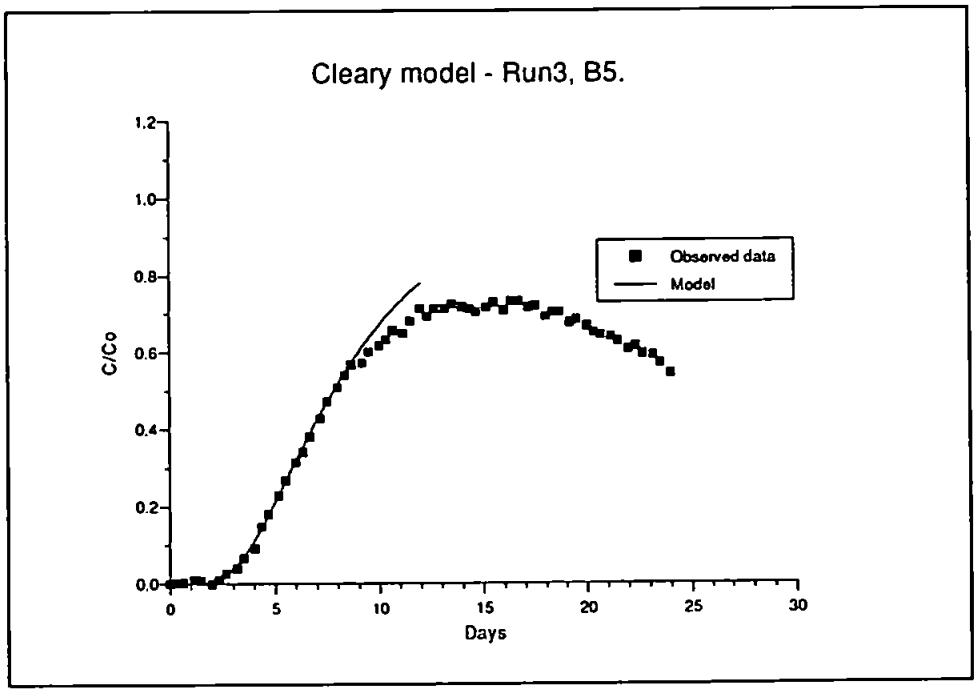

Figure 7.68 - Breakthrough curve B5 (run 3) with CLEARY model fitted.

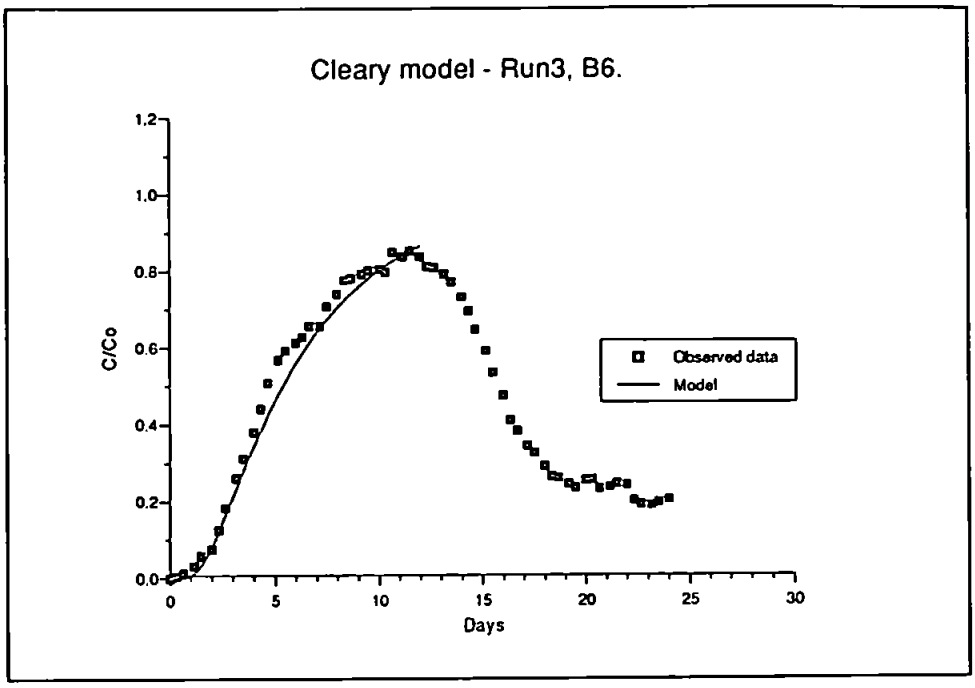

Figure 7.69 - Breakthrough curve B6 (run 3) with CLEARY model fitted.

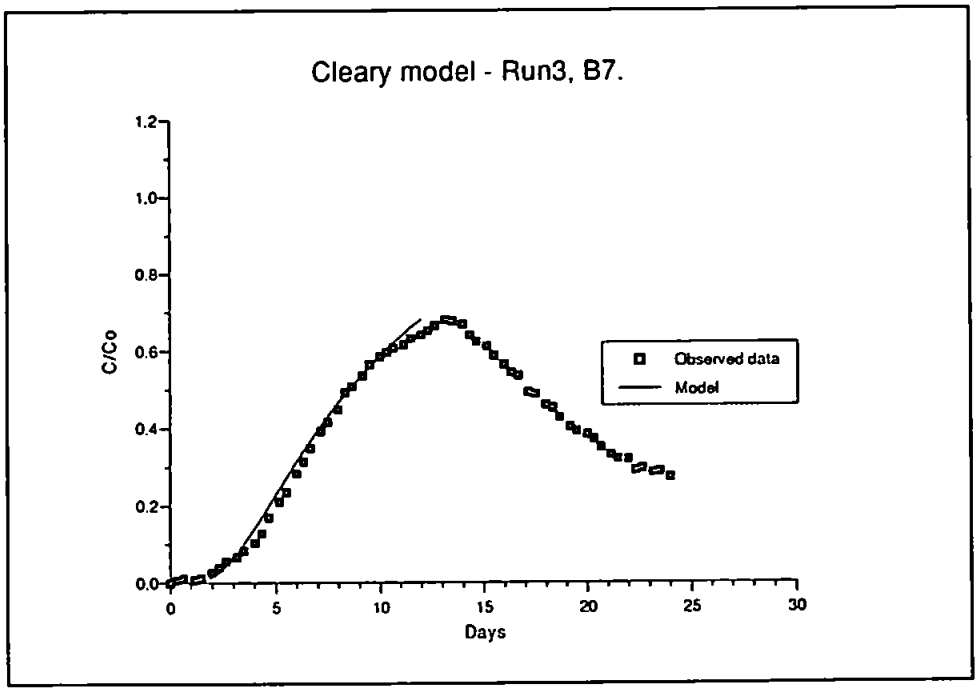

Figure 7.70 - Breakthrough curve B7 (run 3) with CLEARY model fitted.

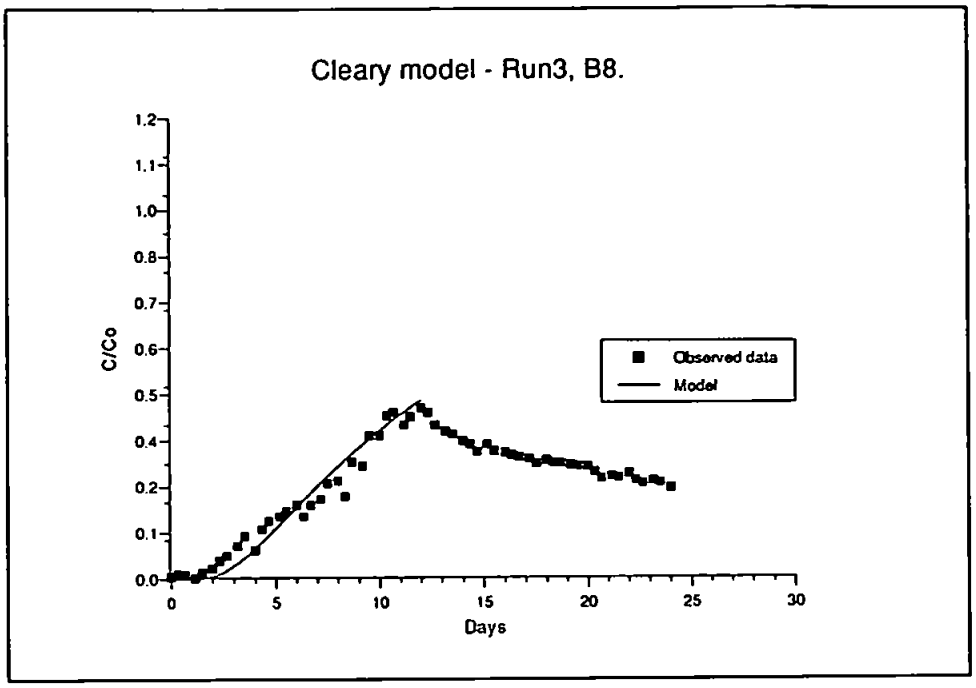

Figure 7.71 - Breakthrough curve B8 (run 3) with CLEARY model fitted.

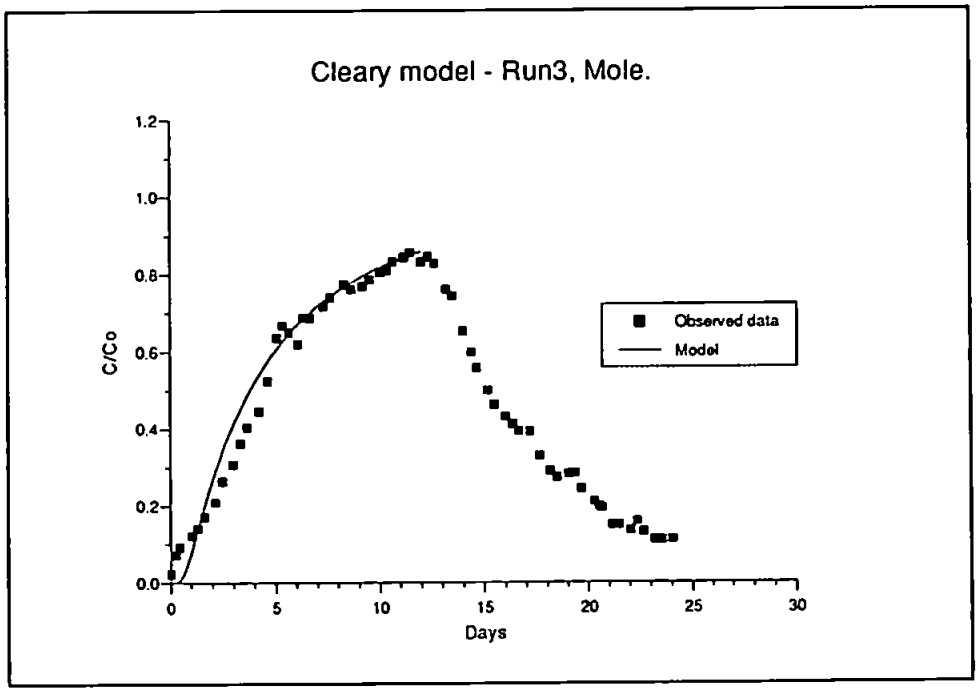

Figure 7.72 - Breakthrough curve for mole drain sample (run 3) with CLEARY model fitted.

7.5.2. Conclusions.

Aggregated Mixing Zone Model:

This model is intended to fit observed curves and to that extent it works well. A fitted curve is produced that mimics the shape of the observed data. However, the parameters estimated by the model to achieve this fit were in most cases unrealistic, for example levels of dispersion that approach the maximum parameter of 2000 $cm^2 h^{-1}$ are not plausible. Only minimal confidence can therefore be placed on the other predicted parameters so little is learnt about soil water movement from the AMZ model.

Advection-Dispersion Model (CLEARY):

In general dispersivity was predicted to increase with depth in the soil in both blocks A and B (Table 7.24 and 7.25). Predicted dispersivity was slightly larger in block A than in block B, as was predicted velocity. The results of the dispersivity and velocity analysis would suggest that solute moved more rapidly through block A than B. The similarity between observed and predicted rates of velocity were closer in block A (Table 7.24) than in block B (Table 7.25). In block B predicted velocity in some cases was less than 1/10 th of the observed velocity. The largest rate of dispersivity was predicted from the mole drain observations as a result of large rates of solute velocity and multi pathway solute transport.

From Figures 7.55 to 7.72 it can be seen that CLEARY managed to produce a reasonable fit for all the observed data locations. The largest differences between observed and fitted data occurred at A5(10 cm) (Figure 7.59), A7(45 cm) (Figure 7.61) and mole(A) (Figure 7.63). As stated previously the advection-dispersion model has difficulty in predicting dual porous pathways in a soil. In Section 7.7 above it was shown, from the interpretation of breakthrough curves, that block A was more influenced by both bypass and matrix flow, while block B was primarily dominated by slow pathways only. Chapter 8 will consider in

greater detail the link between structure and porosity and the models ability to fit the observed data.

7.6. SUMMARY OF SOLUTE MOVEMENT.

Observations of changing solute concentration through time as well as of breakthrough curve analysis suggested that considerable spatial variability in solute movement existed within the individual soil blocks. A comparison of the results of the two blocks, which represented REVs of the same soil, revealed that differences were observed between the two blocks in terms of rate and concentration of solute movement. In general maximum concentration was reached at sampling locations in block A quicker than in block B. From breakthrough curve analysis block A was shown to have a larger proportion of flow dominated by faster flowpaths than block B. This observation must therefore be the consequence of differences in structural heterogeneity and soil water status. 'At a point' solute sampling therefore requires further structural analysis to be conducted.

Variability in order of response was also observed through time. Research undertaken by Quisenberry *et al.* (1994) has suggested that pathways will remain constant through time for a given soil water content. From the observations made in this research temporal variability may be due to slight changes in soil water content through time or change in pathways due to fauna activity. Although confirmation that temporal change was significant would require a larger number of observations based on the same experimental strategy. Solute observations also revealed the potential for rapid movement of concentrated solute to move below field drainage levels.

Double peaks were observed at some sampling locations during the two pulse experiments (runs 4 and 5). A larger concentration peak followed by trough and a second, smaller

concentration peak can be explained by the presence of two distinct pathways (Holden *et al.*, 1995b). The first peak was the result of solute having moved via rapid pathways were minimal mixing and therefore dilution of solute concentration occurred. The second smaller peak represents solute that has moved along slower more tortuous pathways to reach that location. Loss in concentration is due to an increased mixing between mobile and immobile zones.

Some similarities were noticed between the solute concentration responses of the two blocks. During the miscible displacement experiments solute concentrations on the 'right hand side' of each block increased in time to peak with increasing depth while on the 'left hand side' time to peak concentration was more variable. Both mole drains had flow that could be associated with rapid macropore or preferential flowpaths. These patterns of response may be the result of natural structure although towards the mole drain it is more likely to be due to artificially created pathways. These observations would therefore suggest that at the micro-scale solute flow is highly variable but when the entire block is considered (REV) it possess a pattern of response that is repeated in a similar REV of the same soil.

The one-dimensional advection-dispersion model (CLEARY) provided a good 'fit' to the concentration-time results (Figures 7.55 to 7.63) and made good predictions of parameters for block A (Table 7.24). Although the model predictions appeared to fit the observed data curves for block B (Figure 7.64 to 7.72) predicted parameters for velocity were far lower than observed velocities (Table 7.25). From breakthrough curve analysis the observations indicate that the model was more reliable in predicting solute that had travelled quickly through the soil. From a comparison of Tables 7.20 with 7.24, and Tables 7.21 with 7.25 it can be seen that when a relative concentration, C/Co = 0.5, occurs before one pore volume predicted and observed velocities were closer and as pore volume required to reach

C/Co = 0.5 decreased the values become even closer. However, beyond a certain speed of movement the predictions become less accurate, for example towards the mole C/Co = 0.5 was reached in block A at pore volume equal to 0.001 and predicted velocity was extremely overestimated (Table 7.24). Conversely as velocity decreases and C/Co = 0.5 after one pore volume predicted velocity was underestimated compared to observed results. Three categories of flow therefore seem to exist and will be defined as macropore, mesopore and micropore flow. Of the three types of flow the one-dimensional CLEARY model would appear to predict mesopore flow the best.

The following chapter (Chapter 8) brings together observations of soil structure, soil water status and chemical movement to show how each of the individual elements were reliant on other elements.

CHAPTER 8

SOIL STRUCTURE, SOIL MOISTURE AND CHEMICAL TRANSPORT.

8.1. INTRODUCTION.

Two fundamental objectives were identified in this experiment. The primary aim of this investigation was to examine the spatial and temporal factors that affect both water and solute movement. The second aim was to examine the interaction and independence of different sized flowpaths, including bypass flow and matrix flow.

The investigation described in this thesis has progressed from a qualitative description of two 0.85 m^3 soil blocks, in Chapter 2, to a more quantitative assessment of soil physical properties including soil structure (Chapter 5) and soil water status (Chapter 6), and includes a qualitative and quantitative interpretation of solute movement (Chapter 7). This chapter integrates the information on soil structure, soil water status and solute movement to determine the interdependence of soil physical properties on solute movement. Several factors may contribute to variable solute movement through the soil (Biggar and Nielsen, 1976; Saleh *et al.*, 1990; Singh and Kanwar, 1991; Ogden *et al.*, 1992). These factors include both physical soil properties (for example, hydraulic conductivity, soil moisture content and bulk density); chemical properties governing sorption and advection; and nonequilbrium of transport (Brusseau and Rao, 1990).

The second important aspect of the work was the investigation of the interaction between mobile and immobile zones within the soil (Dowd *et al.*, 1991). Restriction to flow, including pore size reduction and dead end pores, together with concentration gradients and residence time will influence the rate of diffusion between mobile and immobile zones (Walker and Trudgill, 1983; Saleh *et al.*, 1990). Solute flow along different pathways can,

however, be inferred from the shape of breakthrough curves (Cassel *et al.*, 1974; Kluitenberg and Horton, 1990; Singh and Kanwar, 1991). The amount of mixing and diffusion that occurred was deduced from breakthrough curves and predicted by modelling observed data (Chapter 7).

The logical progression is to examine in detail the soil structure which is associated with the soil water pathways as discussed above. Soil structure is an important factor controlling water and solute movement through the soil (Brusseau and Rao, 1990; Booltink, 1993). Measurement of soil structural properties, including porosity, bulk density, hydraulic conductivity and soil water release curves, all provide evidence about the pore size distribution through which water and solute can potentially move (Marshall and Holmes, 1979; Rowell, 1994). The abundance of pores in a specific size range determines the quantity of fluid that can physically pass through the soil as defined by Poiseuille's law. The cross-sectional shape, tortuosity and connectivity that these pore spaces make through the soil influence the degree of mechanical dispersion and potential for advection-diffusion to take place (Walker and Trudgill, 1983; Ringrose-Voase and Bullock, 1984), and thus influences solute movement, through the soil and diffusion between mobile and immobile zones.

In this chapter the major soil structural measurements will be described in order to highlight the importance of particular pore sizes for controlling soil water and hence influencing chemical movement. Preliminary investigations of different pore sizes (Chapter 5) will be coupled with hydraulic gradients, as measured in Chapter 6, to determine the most significant flow routes. This measurement will be of great importance in the macropore/matrix flow argument as it will determine which pathways were potentially available to conduct solute and which were not. Variations of soil water content within the

blocks (Chapter 6) and soil structure (Chapter 5) will be linked to solute movement, as described in Chapter 7, to provide an insight into soil solute and water movement processes. Furthermore, residual nitrate in the soil will be examined with regard to porosity, hydraulic conductivity and hydraulic gradient, together with breakthrough curves and model predictions, to explain the interaction between mobile (preferential) and immobile (matrix) water movement. Conclusions will be drawn from these results and the implications that they have for the transport of chemical pollutants through the soil will be discussed.

8.2. FLOW RATES THROUGH DIFFERENT PORE SIZES.

Pore size distributions were examined in the macropore and mesopore size range (Luxmoore, 1981) in Chapter 5 using binary transect method (BTM) and resinated core section method (RCSM). Structure not only influences where water and solute can move but also where it cannot (Kung, 1990b). Furthermore, flow in a given structure is dependent on a second factor: soil water content. A saturated soil is assumed to have all pores occupied by solution and hence all pores can potentially conduct water. As the soil drys the larger pore spaces/cracks empty first (Section 1.8.) such that, movement of water will be restricted to the smaller pores. A measurement of soil water status is, therefore, important in determining which pathways were available for solute movement.

Many authors suggest that the flow through finer pores is essentially limited (Beven and Germann, 1982; Watson and Luxmoore, 1986; Luxmoore *et al.*, 1990) and would not be capable of transmitting observed flow rates of solute. One way to investigate the ability of a pore to conduct water is to use Poiseuille's law. Poiseuille suggested that the ability of a pore/crack to conduct solute is proportional to the radius of a pore (r^4) according to the flow equation (Marshall and Holmes, 1979):

$$Q = \frac{\pi r^4}{8\mu} \times \rho g \frac{\delta H}{\delta L} \qquad (8.1)$$

Where, Q is flow rate ($m^3 s^{-1}$), r is the radius of a pipe (m), μ is the coefficient of viscosity (1.0E-03 kg $m^{-1} s^{-1}$ at 20 °C), ρ is the density of water (998.2 kg m^{-3}), g is the acceleration due to gravity (9.80 m s^{-2}) and δH/δL is the hydraulic gradient.

Figure 8.1 and 8.2 illustrate the extremes of flow rate that occur through a range of pore sizes (4000 to 0.204 μm, diameter) observed in this experiment. These calculations were based on weighted hydraulic gradient values, with depth from surface, calculated from gradients in Chapter 6, for run 2 (block A) and run 3 (block B), respectively. Table 8.1 and 8.2 show the rate of flow for four specific pore size diameters calculated using Poiseuille's flow equation (Equation 8.1), for blocks A(run 2) and B(run 3). Figures 8.1 and 8.2, together with Table 8.1 and 8.2, clearly show that larger diameter pores can conduct a greater flow than smaller pores. Therefore, to achieve an equivalent discharge to that of a larger pore, a greater number of smaller pores would be required, for example approximately 120 pores 300 μm (diameter) would be required to conduct the same flow as one 1000 μm (diameter) pore in Tables 8.1 and 8.2. The ability of different pore sizes to conduct specific flow rates will be examined in Section 8.2.1.

The type of pathways which were involved in the transmission of solutes have an effect on the residence time, tortuosity and the amount of soil surface area encountered by the solute as all these factors will effect the speed and concentration of a solute moving to depth in the soil and therefore the time available for biological and chemical transformation to occur. Fast transport through macropores has been shown by Beven and Germann (1982),

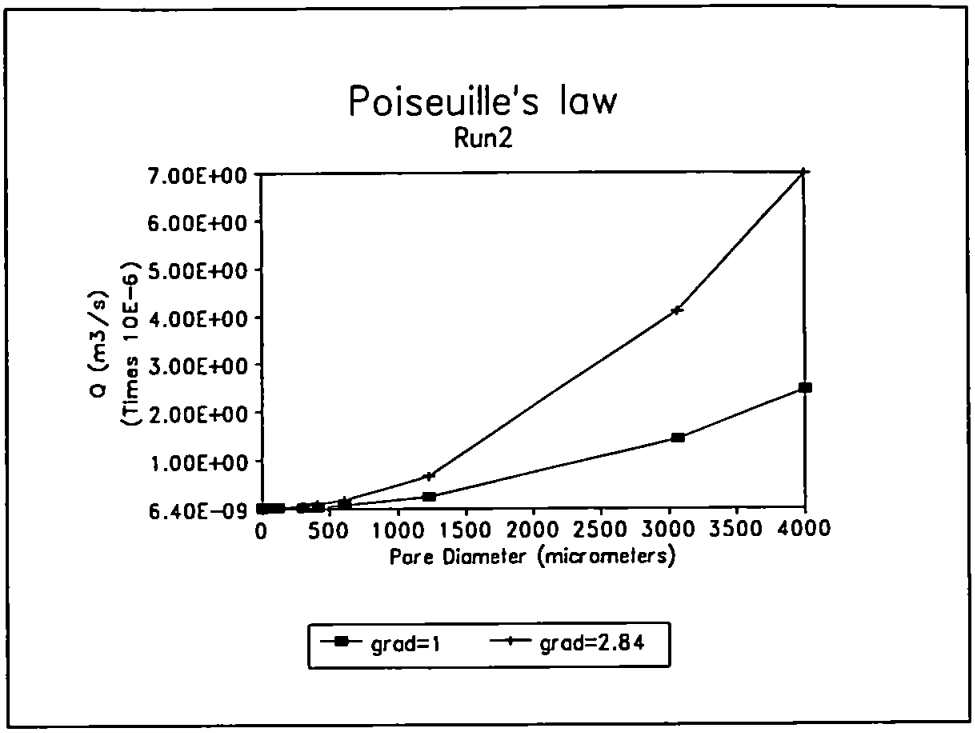

Figure 8.1 - Extremes of flow calculated using Poiseuille's flow equation for hydraulic data in run 2, block A.

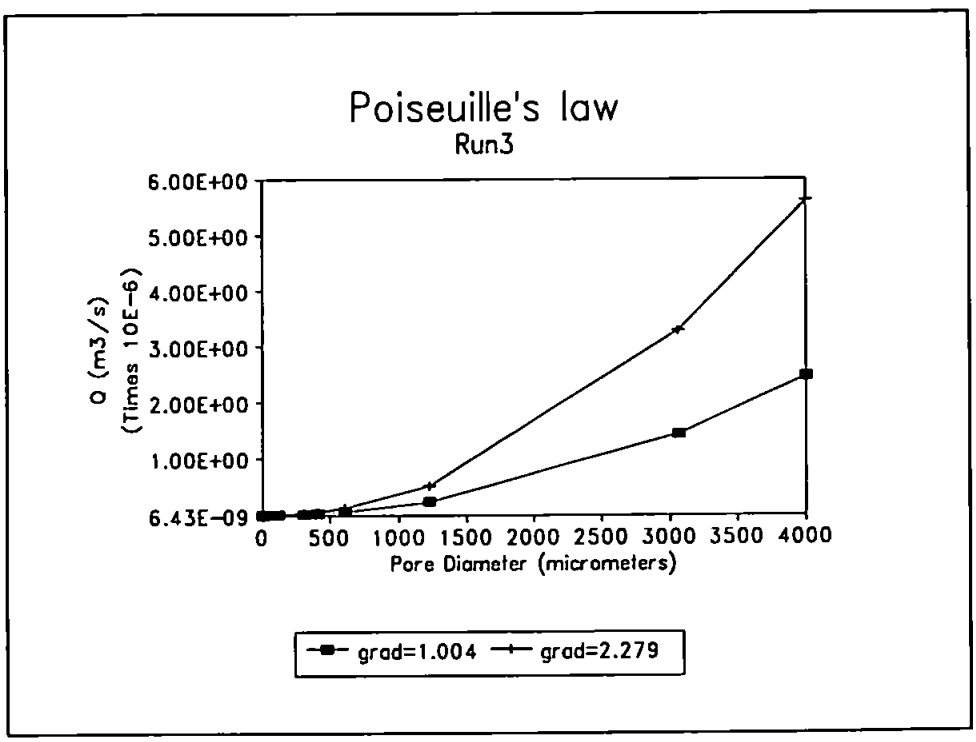

Figure 8.2 - Extremes of flow calculated using Poiseuille's flow equation for hydraulic data in run 3, block B.

Table 8.1 - Rate of flow (Q), for run 2, predicted through pore sizes calculated using Poiseuille's flow equation (Equ. 8.1). Values of Q in l/s. Weighted hydraulic gradient values, with depth from surface.

	Pore Diameter (µm)	4000	1000	300	136
	Suction of water (cm)	0.76	3.06	10.19	22.49
Depth in profile (cm)	Sampler and hydraulic gradient				
10 cm	A1 2.383	1.46E-01	5.72E-04	4.63E-06	1.96E-07
	A5 2.840	1.75E-01	6.82E-04	5.52E-06	2.33E-07
25 cm	A2 1.305	8.02E-02	3.13E-04	2.54E-06	1.07E-07
	A6 1.680	1.03E-01	4.03E-04	3.27E-06	1.38E-07
45 cm	A3 1.049	6.45E-02	2.52E-04	2.04E-06	8.62E-08
	A7 1.000	6.15E-02	2.40E-04	1.94E-06	8.21E-08
50 cm	M 1.000	6.15E-02	2.40E-04	1.94E-06	8.21E-08
60 cm	A4 1.154	7.09E-02	2.77E-04	2.24E-06	9.48E-08
	A8 2.147	7.05E-02	2.75E-04	2.23E-06	9.42E-08

Table 8.2 - Rate of flow (Q), for run 3, predicted through pore sizes calculated using Poiseuille's flow equation (Equ. 8.1). Values of Q in l/s. Weighted hydraulic gradient values, with depth from surface.

	Pore Diameter (µm)	4000	1000	300	136
	Suction of water (cm)	0.76	3.06	10.19	22.49
Depth in profile (cm)	Sampler and hydraulic gradient				
10 cm	B1 1.032	6.34E-02	2.48E-04	2.01E-06	8.48E-08
	B5 2.344	1.44E-01	5.63E-04	4.56E-06	1.93E-07
25 cm	B2 1.852	1.14E-01	4.45E-04	3.60E-06	1.52E-07
	B6 1.676	1.03E-01	4.02E-04	3.26E-06	1.38E-07
45 cm	B3 1.286	7.90E-02	3.09E-04	2.50E-06	1.06E-07
	B7 1.077	6.62E-02	2.59E-04	2.09E-06	8.85E-08
50 cm	M 1.000	6.15E-02	2.40E-04	1.94E-06	8.21E-08
60 cm	B4 1.213	7.46E-02	2.91E-04	2.36E-06	9.96E-08
	B8 1.164	7.15E-02	2.79E-04	2.26E-06	9.56E-08

Andreini and Steenhuis (1990) and Singh and Kanwar (1991), to result in the quick removal of solute to depth with minimal dilution in concentration. In addition, other authors have suggested that rapid flow may be possible even through mesopores (Glass *et al.*, 1989; Selker, 1992a/b; Radulovich *et al.*, 1992).

8.2.1. Results.

Slight structural differences existed between blocks A and B. Tables 5.20 and 5.21 showed block B to have a higher occurrence of pores and cracks with pore sized diameters in the 1 to 4 mm range than block A, using the BTM. The calculated porosity for each block, using these values, was 18.43 % (block B) and 10.17 % (block A). Structural results from the RCSM, which considered pore sizes in the range of 1000 to 136 μm (diameter), indicated that block A had a higher porosity (7.11 %) than block B (4.3 %), in this particular pore size range (Table 5.23 (b)). From these results it may have been expected that an applied tracer would have moved more rapidly through block B, which had a greater proportion of larger pores and cracks (1 - 4 mm, diameter) and, therefore, a greater potential for rapid macropore flow.

However, a comparison between miscible displacement experiments in block A and B, using results from run 2 and run 3 (Tables 7.5 and 7.8) showed that although initial breakthrough times were not dissimilar the time taken to reach a peak concentration was. Block A reached peak concentration quicker than block B. This result suggested that the proportion of smaller pores and cracks played an important roll in determining the speed of tracer movement to the sampling locations. Results from breakthrough curve analysis in Section 7.7.1. also supported the idea that macropore flow was not responsible for tracer movement to most of the sampling locations in this soil.

Tables 8.3 and 8.4 indicate the number of pores required for four different pore diameters to achieve observed and predicted flow rates, in runs 2 and 3. The observed flow rates were calculated from time taken for initial breakthrough (first change in concentration after the start of irrigation) to occur and time to peak concentration from start of irrigation (Chapter 7), both with respect to depth in soil, from which velocity was calculated. Predicted flow rate was calculated from CLEARY model projections of velocity (Section 7.8.1.). Flow (Q) was calculated from velocity for observed and modelled data using the formula:

$$Q = vn \qquad (8.2)$$

Where, v is velocity (cm s^{-1}) and n equals weighted porosity with depth from surface, calculated from bulk density figures using values calculated from soil water release curves determined in Section 2.3.3. Calculated flow rates were then compared with Tables 8.1 and 8.2 to predict how many pores of different diameters would be required to achieve such a flow in the soil (Table 8.3 and 8.4).

In Tables 8.3 and 8.4, where frequency of pores was less than 1, the pores of this diameter were not considered to be actively involved in transmitting water (Beven and Germann, 1981). Tables 8.3 and 8.4 show that to the majority of sampling locations, solute did not flow in pores sized 4000 μm (4 mm) (diameter). This result was only applicable to the column of soil in the vicinity of the soil suction sampler. In contrast, results from initial breakthrough flow to mole drain A (Table 8.3) could only have been achieved by flow occurring through channels with a greater diameter than 4000 μm.

Table 8.3 - Number of pores of different diameters required to achieve observed and predicted flow, from soil surface to depth in the soil. Values refer to calculations made for run 2 block A. InBT (time to initial breakthrough with depth, cm s^{-1}), PEAK (time to peak concentration with depth, cm s^{-1}) and MODEL (value of Q calculated using CLEARY model prediction of velocity).

		Pore diameter (μm)			
Location of sample (cm)	Q	4000	1000	300	136
A1 10 cm	InBT 2.10E-03	0.01	3.67	453.13	10728.92
	PEAK 2.80E-04	0.002	0.49	60.42	1430.52
	MODEL 7.00E-04	0.05	12.23	1510.45	35763.07
A2 25 cm	InBT 5.09E-03	0.06	16.25	2005.57	47486.27
	PEAK 4.84E-04	0.01	1.54	190.71	4515.39
	MODEL 1.22E-03	0.02	3.89	480.71	11381.78
A3 45 cm	InBT 5.51E-03	0.09	21.88	2700.89	63949.47
	PEAK 5.69E-04	0.01	2.26	278.91	6603.86
	MODEL 7.35E-04	0.01	2.92	360.28	8530.46
A4 60 cm	InBT 6.76E-04	0.01	2.44	301.21	7131.84
	PEAK 4.41E-04	0.01	1.59	196.50	4652.58
	MODEL 6.00E-04	0.09	21.66	2673.48	63300.37
A5 10 cm	InBT 1.96E-03	0.01	2.87	354.87	8402.31
	PEAK 5.32E-05	0.0003	0.08	9.63	228.06
	MODEL 6.60E-06	3.78E-05	0.01	1.19	28.29
A6 25 cm	InBT 8.58E-04	0.01	2.13	262.61	6217.83
	PEAK 1.52E-04	0.002	0.38	46.52	1101.53
	MODEL 1.88E-04	0.002	0.47	57.54	1362.42
A7 45 cm	InBT 8.59E-04	0.01	3.58	441.70	10458.13
	PEAK 2.09E-04	0.003	0.87	107.47	2544.53
	MODEL 7.88E-05	0.001	0.33	40.52	959.37
A8 60 cm	InBT 2.05E-02	0.29	74.44	9190.14	217596.20
	PEAK 6.48E-04	0.01	2.35	290.50	6878.16
	MODEL 8.65E-04	0.01	3.14	387.78	9181.50
Mole 50 cm	InBT 3.66	59.55	15243.95	1881969.0	44559664.0
	PEAK 3.32E-04	0.01	1.38	170.71	4042.02
	MODEL 3.05E-03	0.05	12.70	1568.31	37133.05

Table 8.4 - Number of pores of different diameters required to achieve observed and predicted flow, from soil surface to depth in the soil. Values refer to calculations made for run 3 block B. InBT (time to initial breakthrough with depth, cm s^{-1}), PEAK (time to peak concentration with depth, cm s^{-1}) and MODEL (value of Q calculated using CLEARY model prediction of velocity).

		Pore diameter (μm)			
Location of sample (cm)	Q	4000	1000	300	136
B1 10 cm	InBT 3.27E-03	0.05	13.20	1629.29	38577.04
	PEAK 1.63E-03	0.03	6.58	8121.56	19229.53
	MODEL 5.45E-04	0.01	2.20	271.55	6429.51
B2 25 cm	InBT 4.48E-03	0.04	10.08	1243.85	29450.85
	PEAK 1.23E-04	0.001	0.28	34.15	808.58
	MODEL 5.97E-05	0.0005	0.13	16.58	392.46
B3 45 cm	InBT 4.00E-03	0.05	12.95	1599.38	37868.65
	PEAK 2.29E-04	0.003	0.74	91.56	2167.98
	MODEL 2.97E-05	0.0004	0.10	11.88	281.17
B4 60 cm	InBT 5.35E-03	0.71	18.73	2267.90	53697.47
	PEAK 1.62E-04	0.002	0.56	68.67	1625.98
	MODEL 2.08E-04	0.003	0.71	88.17	2087.68
B5 10 cm	InBT 2.82E-04	0.002	0.50	61.86	1464.71
	PEAK 4.17E-05	0.0003	0.07	9.15	216.59
	MODEL 6.60E-06	4.58E-05	0.01	1.45	34.28
B6 25 cm	InBT 3.20E-03	0.03	7.95	981.76	23245.39
	PEAK 1.38E-04	0.001	0.34	42.34	1002.46
	MODEL 6.41E-05	0.001	0.16	19.67	465.63
B7 45 cm	InBT 2.05E-03	0.03	7.93	978.75	23173.89
	PEAK 2.09E-04	0.003	0.81	99.78	2362.61
	MODEL 6.06E-05	0.001	0.23	28.93	685.04
B8 60 cm	InBT 2.67E-03	0.04	9.55	1179.48	27926.67
	PEAK 2.96E-04	0.004	1.06	130.76	3095.99
	MODEL 1.77E-04	0.003	0.63	78.19	1851.32
Mole 50 cm	InBT 7.21E-02	1.17	300.30	37073.77	877801.0
	PEAK 2.65E-04	0.004	1.10	136.26	3226.31
	MODEL 3.00E-04	0.005	1.25	154.26	3652.43

8.2.2. Conclusions.

From Table 8.3 and 8.4 it can be seen that it would have been feasible for pores within the size range 1000 to 136 μm (diameter) to have conducted both observed and predicted flow rates to the majority of the sampling locations providing sufficient pores within this size range were present within the soil. This pore size range falls within Luxmoore's (1981) definition of mesopores. From the total pore count using the RCSM (Chapter 5), there would have been sufficient pores within the mesopore size range (pore size classes 2 and 3) to have achieved such flow in the soil. An important additional factor in achieving such flow rates was that connections existed from the surface of the soil to depth within the specified pore size range.

Flow in pores with diameters between 1000 and 4000 μm (macropores) contributed most notably towards the mole drain observations. Although a steady soil water state was achieved, using a mean irrigation rate of 2.76 mm h^{-1}, the majority of the soil was shown to be unsaturated (Chapter 6). Flow along channels greater than 4000 μm (diameter) was limited in this experiment as indicated by the small volume of mole drain flow collected (0.02 mm h^{-1} and 0.002 mm h^{-1} block A and B respectively). Although flow along macropores was considered to have been limited from the results macropore flow was not totally absent. It is possible that although the whole of the macropore may not have been flooded flow may still have occurred along the edges of the channels. From Tables 6.4 and 6.5, which indicate values of soil water tension in runs 2 and 3, at depths of 10, 25,45 and 60 cm, it was possible to deduce the following: At 10 cm pores >300 μm (diameter), at 25 cm pores >200 μm (diameter), at 45 cm pores >1000 μm (diameter) and at 60 cm pores >300 μm (diameter) would have been drained. Flow was unlikely to have occurred in pores much smaller than 136 μm. From Tables 8.3 and 8.4 the number of pores in the size group 136 μm (diameter) required to achieve the flow rate exceeded the observed number of these

pores (Section 5.3.1., RCSM class 4). Luxmoore (1981) defined pores with a diameter less than 10 μm as micropores containing stagnant water. The majority of flow was, therefore, considered to have occurred, in this soil experiment, in the pore size range of 1000 to 136 μm (diameter). Although block B had a larger calculated porosity than block A, in the pore size range of 1 to 4 mm, it had a lower porosity than block A in the pore size range of 1000 to 136 μm (diameter) (Chapter 5). If as predicted in Table 8.3 and 8.4, pore sizes greater than 1000 μm in diameter were not actively involved in transmitting solute, given the suction calculated in the soil, this would explain why block A peaked before block B. Block A had a larger proportion of pores in the active pore size range than block B.

Flow in this soil could at times be described as rapid. However, a description of such flow as being macropore flow, implying movement through large channels greater than 1000 μm (1 mm) in diameter, was not considered to be an appropriate one for this soil. A better description would be preferential flow, as this does not necessarily imply rapid movement along large channels alone but also includes convergence of flowpaths in the direction of least resistance resulting in finger like flow (Glass *et al.*, 1987; Kung, 1990b; Radulovich *et al.*, 1992).

The effects of flow occurring through the agglomeration of water in mesopores, to chemical movement include: a greater surface area of solids encountered on which chemical absorption could occur and more opportunity for mechanical dispersion as pathways become more tortuous (Luxmoore *et al.*, 1990). The more obstacles water and solute is diverted around the greater the potential for eddys to be developed. Eddying will increase the potential for diffusion to occur between mobile and immobile zones. The implications of this for chemical transport will be discussed in the following section.

8.3. FLOWPATHS AND CHEMICAL MOVEMENT.

The section above concentrated on the ability of individual pore sizes to conduct flow. This section will consider the ability of a range of pore size's to conduct flow. Section 8.2 identified mesopore flowpaths as being the dominant pathways in the soil. It has been suggested by Luxmoore *et al.* (1990) that such pathways will allow a greater opportunity for chemical mixing and interaction between mobile and immobile zones. This section will compare observed flowpaths (Chapter 5) to chemical tracer observations (Chapter 7). Conclusions will be drawn to the effect that pathways had on tracer movement. The interaction between mobile and immobile zones will be considered later in this chapter.

8.3.1. Results.

Tables 8.5 (a and b) show the results of weighted porosity with depth calculated using BTM (calculated for pore size diameters in the range of 4000 to 1000 μm) and RCSM (calculated from pore size diameters in the range of 1000 to 136 μm). Porosity calculated by RCSM is of interest to this experiment as this method is based on mesopore pathways alone, which have been identified as the major active pore size grouping involved in solute and water movement through the two soil blocks. From Tables 8.5 it is evident that porosity at 10 cm, in both blocks, was smaller than at 25 cm. Porosity (calculated from RCSM) in general increased from 10 cm to 25 cm and decreased from 25 cm to 60 cm, with the exception that porosity at A3(45 cm) was greater than at A2(25 cm) and A8(60 cm) had a larger porosity than A7(45 cm).

From Section 8.2 and mean suction values in Tables 6.8 to 6.12 it can be suggested that water flowed only in pores of less than 1000 μm (diameter). Only locations A7/B7(45 cm, left) and B1(10 cm, right) displayed a mean suction that would imply flow could have occurred in pores greater than 1000 μm in diameter. Location B7(45cm, left) displayed a

Table 8.5 - Weighted porosity (%) with depth for block A (a) and block B (b). Porosity calculated using Resinated Core Section Method (RCSM) for pore size range 1000 - 136 µm, and Binary Transect Method (BTM) for pore size range 4000 - 1000 µm.

(a)

	Porosity (%)			Porosity (%)		
Depth cm	Sample location	RCSM	BTM	Sample location	RCSM	BTM
0 - 10	A5	5.85	9.4	A1	5.85	7.9
0 - 25	A6	5.73	10.78	A2	9.18	8.55
0 - 45	A7	5.16	10.8	A3	9.61	10.19
0 - 60	A8	5.33	10.4	A4	9.15	10.57

(b)

	Porosity (%)			Porosity (%)		
Depth cm	Sample location	RCSM	BTM	Sample location	RCSM	BTM
0 - 10	B5	4.5	20.6	B1	1.86	20.15
0 - 25	B6	8.10	20.62	B2	6.14	20.28
0 - 45	B7	5.32	19.88	B3	3.9	19.27
0 - 60	B8	4.99	18.65	B4	3.35	18.25

suction associated with saturated soil water conditions. At locations A7/B7 and B1 cracks >1000 µm were observed intercepting the porous cup, during destructive sampling. Bouma *et al.* (1982) observed suction in a tensiometer to be influenced by the interception of a single macropore.

The results of tracer movement experiments, for both miscible displacement [run 1, 2 (block A) and 3 (block B)] and pulse application [runs 4 and 5 (block B)] were given in Chapter 5. Table 8.6 provides a brief summary of the general observations of results for suction cup lysimeter samples made in Chapter 5. The response of the mole drain in block

Table 8.6 - Summary of results of suction cup lysimeter responses to tracer application from Chapter 5.

Experiment	Location - left of block (A5/B5(10 cm), A6/B6(25 cm), A7/B7(45 cm) and A8/B8(60 cm))	Location - right of block (A1/B1(10 cm), A2/B2(25 cm), A3/B3(45 cm) and A4/B4(60 cm))
Run 1	Initial breakthrough occurred fastest at A8. A6 taking the longest to show initial breakthrough. Peak irrigation concentration reached first at A6 (part I). During flush A8 reached background concentration first, A6 reached the next lowest concentration followed by A7 and A5. (part II) A5 to A8 did not reach applied irrigation concentration. A8 reached the highest concentration followed by A6, A5 and A7.	A1 to A4, increased in time to initial breakthrough and peak irrigation concentration with depth for both tracer and flush.
Run 2	A8 showed initial breakthrough and reached irrigation concentration first. Initial breakthrough (tracer) A5 to A7 occurred in order of depth. A6 was the only other sampling location, apart from A8, to reach irrigation concentration. Initial breakthrough (flush) took longest at A6. A6 reached a lower concentration at the end of the flush than A5 which had a higher residual concentration than A7.	A1 to A4, increased in time to initial breakthrough and peak irrigation concentration with depth for both tracer and flush.
Run 3	B5 took the longest to react to both tracer and flush, retained highest concentration of chloride. Peak irrigation concentration not reached at any sampler location (B5 to B8). B6 reached higher peak concentration than B7 followed by B8. During flushing initial breakthrough B8 responded the fastest. At end of flush residual chloride higher in B7 than B8 followed by B6 and B5.	B1 to B4 showed an increase in time to depth for initial breakthrough. Time to peak B2 took longer than B3, otherwise an increase time to peak irrigation was observed with depth. After flushing there was an increase in residual tracer concentration left with depth.
Run 4	Chloride: Fastest peak B7, highest peak concentration at B8. In general there was an increase in peak concentration with depth. Nitrate: Highest peak concentrations reached at B6 and B7, lowest at B5.	Chloride: B1 to B4 showed a decrease in peak concentration and increase in time to peak with depth. Nitrate: B1 to B4 showed a decrease in peak concentration and increase in time to peak with depth.
Run 5	Chloride: In general there was an increase in peak concentration with depth. B8 peaked the quickest, B7 the slowest. Nitrate: Decrease in peak concentration with depth. B7 slowest to peak.	Chloride: B1 peaked first with highest concentration. B2 to B4 showed an increase in time and concentration of peak with depth. Nitrate: B1 peaked first, B2 peaked last. In general decrease in concentration with depth.

A (miscible displacement) was fast and reached both the peak concentration and returned to background concentration after leaching. The mole drain in block B (miscible displacement) responded quickly and reached a larger concentration during the tracer application although not the largest and reached a low dilution during flushing although not the lowest. The mole drain of block B was less responsive to change in concentrations than block A. During the pulse experiments, run 4 and run 5, it took the mole drain a longer time to reach peak concentration than the peak recorded at the base of the block. For the chloride pulse a larger peak was recorded at the mole than at the base of block. However, for the nitrate pulse a smaller peak concentration was observed at the mole than at the base of the block.

8.3.2. Conclusions.

The increase in time to initial breakthrough with depth (miscible displacement) may be explained by a decrease in porosity (with depth) delaying flow to deeper levels. Increased residual chloride with depth may be linked to lower porosity, restricting leaching. The cause of decrease in nitrate with depth is examined in Section 8.5 where the interaction between mobile and immobile zones is discussed.

The rapid solute breakthrough observed at the mole and sampler location A8 cannot easily be explained by increase of porosity with depth. However, the observed flow rate may only have been achieved by a combination of mesopore and macropore flow (Tables 8.3 and 8.4). Table 8.5(a and b) shows that macropores were present at all sampling locations and may therefore have become active if soil water conditions had permitted. Similarly the response of A6/B6(25 cm) which recorded some of the largest solute concentrations on the left side of the soil block may have been intersected by a macropore. The weak concentration observed at A7(45 cm) in Chapter 7 may be linked to an area, recorded by

tensiometer data in Chapter 6, as being saturated (Tables 6.8 and 6.9). The increased water content at 45 cm depth (left), linked to observed low porosity (Table 8.5), resulted in increased dilution and mixing. The effect of soil water status on solute transport will be discussed in Section 8.4. For sample locations at depth to reach larger concentrations than samplers higher up in the block, for example A8(60 cm) and A6(25 cm), the sample locations must have been receiving solute that moved preferentially through the soil, while higher sample locations were bypassed by the faster flow. The slow response of B5(10 cm) compared to B6(25 cm) (run 3, block B) may be explained by the presence of bypass flow, as well as, the limitation of the sampler size compared to the scale of the phenomena being measured in the heterogeneous soil. The sampler at 10 cm may have been located in an immobile zone, although preferential pathways were known to exist in this horizon because of the quicker response at depth, the location and size of the sampler at 10 cm cloaks the wider scale movement of solute. The larger porosity at B6(25 cm) compared to B5(10 cm) may have caused finger flow at depth (Miyazaki, 1993).

The quicker peak response recorded at the base of block compared to the mole may also have been due to bypass flow occurring through the soil. Macropores were generated in the soil when the mole drain was pulled but when matric potential in the soil water was less than zero, preferential flow along macropores would not have occurred. Water would have drain to the mole however, even when matric potential was less than zero because of the suction gradient. Delay in flow to the mole drain occurred because of the slower pathways involved in the transport of solute and also at the soil air interface were capillary forces had to be overcome. Rapid flow to the base of the block was most likely the result of finger like flow developing in zones of saturation.

The overall effect of flow being restricted mainly to mesopore pathways was reflected in

the shape of the breakthrough curves presented in Section 7.7.1., run 2 (block A) and run 3 (block B). In general, the shape of the breakthrough curves showed that large levels of mixing occurred between added and antecedent solution, which resulted in a gentle and prolonged rise to peak concentration, and on occasions the failure to reach peak irrigation concentration. Such flow reflects a large degree of hydraulic dispersion due to the tortuous nature of the flowpaths as well as large levels of diffusion between mobile and immobile pathways. Dispersivity will be examined later in this chapter.

The effect of mesopore flow on chemicals being introduced into a soil would be the accumulation of chemicals in the matrix as well as rapid flow via zones of saturation. The large concentrations of chemicals monitored below the base of the block suggest that chemicals can be readily leached below the depth of the field drains. Increased residence time will increase the potential for anion exchange between mobile and immobile zones but may also increase the proportion of denitrification and therefore loss of nitrate from the soil especially under anaerobic conditions.

Sections 8.2 and 8.3 have shown that structure determines the pathway through which solutes can move and interact. However, structure alone cannot adequately explain solute movement and other physical soil factors must also be taken into account. These factors are considered below.

8.4. SOIL WATER STATUS.

In Chapter 5 it was shown that a wide size range (macropore to mesopore) of pathways existed in the soil. Section 8.2 showed that although these pathways existed they did not necessarily contribute to solute transport. Soil water content affected which pathways were actively involved in transmitting solute. Two aspects of soil water content will be

considered in this section, namely, driving force (suction) and conductance (K).

Measurements of soil water content were made using TDR probes, by which variability in soil water content was monitored both spatially and temporally. Suction, which was determined from tensiometer data, was used to predict the direction and potential for solute movement through the calculation of hydraulic gradients (Chapter 7). Speed of movement and hence residence time of solute in the soil was calculated from the prediction of hydraulic conductivity (K) based on measurements of soil water content. Hydraulic conductivity being dependent on structure/porosity and indirectly proportional to suction. Conclusions will be drawn about the effects that soil water content had on solute movement through the blocks.

8.4.1. Results.

Suction measurements and calculated hydraulic gradients in the soil were presented in Chapter 6. TDR measurements made over a large sampling volume (1540000 mm^3) showed that soil water content remained stable through time and decreased with depth in the soil, as porosity decreased.

Suction was more variable through time, which suggested that although soil water status may have been regarded as being steady on a large scale, microscopic variations in soil water status were more variable. Tables 6.8 to 6.12 summarised the mean suctions for each experiment and the hydraulic gradients were presented in Tables 6.13 to 6.18 (Chapter 6). In general mean suction decreased with depth from 10 cm to 45 cm and then increased from 45 cm to 60 cm while TDR results showed soil water content to reduce with depth (Tables 6.20 to 6.24)). Locations A7/B7(45 cm, left) recorded some of the lowest mean suctions, as did B1(10 cm, right). Sample location A7(45 cm) recorded saturated conditions

at that position in the soil, probably as a result of porosity reducing at A7(45 cm) compared to A6(25 cm) resulting in an internal catchment. The smallest hydraulic gradient in block A run 1 (I and II) occurred at a depth of between 10 cm and 25 cm (right), in run 2 it occurred between 25 cm and 45 cm (left) and in block B the smallest hydraulic gradient occurred between 25 and 45 cm (left). As hydraulic gradient decreases hydraulic conductivity increases as a result of increasing soil water content. In run 1 (I and II) at sample locations A1(10 cm) and A2(25 cm) (right) the quickest response and largest peak concentrations were observed, similarly at location B6(25 cm) (left) a larger peak concentration was observed than at B5(10 cm), these observations can be linked to zones of reduced hydraulic gradient and therefore rapid hydraulic conductivity. In run 2 samples at A7(45 cm) (left) reached the smallest recorded peak concentration and maintained a elevated background concentration at the end of flushing. From the tensiometer data a saturated zone was observed in the locality of A7(45 cm), mixing and restricted flow would explain the observed weak peak concentration and slow dilution.

Values of saturated hydraulic conductivity (K.sat) for a poorly structured clay soil are normally found within the range of 1E-10 to 1E-07 cm s^{-1} (Freeze and Cherry, 1979). The soil texture of the blocks was described as silty clay loam, increasing in clay sized particles and decreasing in sand and silt with depth (Chapter 2). Hydraulic conductivity (K) in this section was estimated using three different methods of calculating velocity.

1. Initial breakthrough to depth (Chapter 7), which represented an observed measurement of velocity through the soil.
2. Bulk density (Chapter 2), which was an estimate of potential velocity through the total pore space.
3. CLEARY model predictions of velocity (Chapter 7).

Velocity was predicted from bulk density samples using Equation 2.5 to calculate porosity from which velocity was then calculated using the equation:

$$Velocity = \frac{Flux\ input}{\%\ occupied\ by\ paticles} \qquad (8.3)$$

Calculations of velocity were put into Equation 8.2 to predict flow (Q) and into Equation 6.2 to predict hydraulic conductivity (K). The estimates of hydraulic conductivity are shown in Table 8.7. Initial breakthrough (K) represents a laboratory measurement, bulk density/porosity results represent potential values of K and values calculated from the model (CLEARY) represent a predicted value of K. From Table 8.5, K values, predicted by the model were predominantly the slowest, while initial breakthrough either predicts the largest or was very similar to K predicted by bulk density.

In general the estimated values of K were larger than expected for a poorly structured clay soil even though K was not calculated at saturation. Saturation would normally be expected to increase K. Calculated K values fell within the soil classification range of a silt, loess and silty sand soil (1E-07 to 1E-01 cm s^{-1}). Saturated K was calculated for the Hallsworth soil in Chapter 2 and was shown to be 9.60E-03 cm s^{-1} at 0 to 10 cm and 4.35E-06 cm s^{-1} at 50 to 60 cm. These values are larger than those estimated for a poorly structured clay soil. This increase in K must, therefore, be associated with the presence of structure due in part to fracturing induced when the mole was pulled. Indeed values of hydraulic conductivity recorded at the mole showed the largest K values throughout the block which indicate the presence of rapid pathways from surface to the mole. Conductivity below the mole drain was also calculated to be larger than that of a clay soil. Large cracks were

reported in this horizon (60 cm depth, Chapter 5). Rapid pathways may have been induced in the lower soil horizons when the soil block was being transport or may have been due to pressure release and/or disturbance, although it is also likely that these pathways existed in the natural, undisturbed soil.

In general smaller values of K were anticipated using the bulk density method based on total porosity, than from initial breakthrough, because bulk density parameters were only predicted from specific sampling areas. In a heterogeneous soil hydraulic conductivity calculated from bulk density samples may not be representative of the entire environment through which solute and water could have travelled (Beven and Germann, 1981). Even at a fine sampling rate REV may not be sufficient to reflect the entire system. Initial breakthrough, however, is calculated from the time it takes the first solute to reach a sampler, with respect to pathway taken, and was therefore a better indicator of the speed of conductance through the soil block as a whole. The dissimilarity between the three different predictions of K emphasised the problem of non-representative sampling and model prediction to what was in fact occurring in the soil. The most prominent example of disagreement between methods occurred at the mole drain (Table 8.7).

8.4.2. Conclusions:

As soil water content decreased in the profile suction increased and hydraulic conductivity (K) reduced. From bulk density predictions of K (Table 8.7) block A at depths between 10 and 45 cm showed suction decreased (Table 6.9) and conductivity increased, at 45 to 60 cm suction increased (Table 6.9) while conductivity decreased. In block B suction and conductivity were more variable than in block A, however, as suction decreased conductivity was still observed to increase and vis versa.

Table 8.7 - Predicted values of hydraulic conductivity (K) from initial breakthrough (InBT), bulk density (BD) and CLEARY model (MODEL) parameters. Results for block A, run 2 and block B, run 3.

Sample location, block A (depth, cm)	Method	Predicted K (cm s^{-1})	Sample location, block B (depth, cm)	Method	Predicted K (cm s^{-1})
A1(10)	InBT	8.82E-05	B1(10)	InBT	3.17E-04
	BD	5.35E-05		BD	5.52E-05
	MODEL	2.94E-05		MODEL	5.28E-05
A2(25)	InBT	3.90E-04	B2(25)	InBT	2.42E-04
	BD	9.05E-05		BD	3.67E-05
	MODEL	9.36E-05		MODEL	3.22E-06
A3(45)	InBT	5.25E-04	B3(45)	InBT	3.11E-04
	BD	8.93E-05		BD	5.23E-05
	MODEL	7.00E-05		MODEL	2.31E-06
A4(60)	InBT	5.86E-05	B4(60)	InBT	4.41E-04
	BD	7.75E-05		BD	5.56E-05
	MODEL	5.20E-05		MODEL	1.72E-05
A5(10)	InBT	1.63E-04	B5(10)	InBT	1.20E-05
	BD	3.81E-05		BD	3.55E-05
	MODEL	2.32E-07		MODEL	2.81E-07
A6(25)	InBT	5.10E-05	B6(25)	InBT	1.91E-04
	BD	5.87E-05		BD	4.74E-05
	MODEL	1.12E-05		MODEL	3.83E-06
A7(45)	InBT	8.59E-05	B7(45)	InBT	1.91E-04
	BD	9.17E-05		BD	6.52E-05
	MODEL	7.88E-06		MODEL	5.63E-06
A8(60)	InBT	1.81E-03	B8(60)	InBT	2.29E-04
	BD	7.21E-05		BD	5.73E-05
	MODEL	7.54E-05		MODEL	1.52E-05
Mole(50)	InBT	3.70E-01	Mole(50)	InBT	7.21E-03
	BD	9.28E-05		BD	6.89E-05
	MODEL	3.05E-04		MODEL	3.00E-05

Measurements of K determined from initial breakthrough times were faster than those calculated by the bulk density method. For example at sites A2 and A3 the values based on the initial breakthrough method were some five to ten times greater (Table 8.7). The initial breakthrough method was based on tracer movement, monitored in relatively large volumes of soil, whereas the bulk density method was based on relatively small volumes of soil. It would be interesting to explore the link between 'size' of sample,length of pathway and increased conductivity. There may be a link between ped size, sampler size and conductivity which could be explored further.

8.5. INTERACTION BETWEEN MOBILE AND IMMOBILE ZONES.

The sections above have concentrated on the potential for, and recorded movement of, solute and water through the soil. The objective of this section is to address the second aim of this investigation, namely, the extent of interaction between mobile and immobile zones in the soil. Residual nitrate content in the soil will be examined to determine whether porosity or water movement, in turn dependent on hydraulic gradient and hydraulic conductivity were associated with areas of accumulation of nitrate within the soil.

8.5.1. Residual Nitrate in the Soil.

Table 8.8 shows the amount of nitrate (µg TON/g soil) retained in the soil at the end of run 5 (block B). The largest concentration of residual nitrate was observed at 60 cm depth while at 20 cm there was a depleted layer. Some nitrate was retained in the soil above 20 cm. and below this depth nitrate levels began to accumulate progressively with depth.

Weighted porosity values (with depth from surface) were shown in Table 8.5 (b) for block B, taken from calculations in Chapter 5. The RCSM clearly showed a smaller porosity at 10 cm depth which may explain the accumulation of nitrate. The largest porosity was

Table 8.8 - Residual nitrate (µg TON/g soil) in block B at the end of run 5.

1	2	3	4	5	
0.0087	0.1346	0.1755	0.3121	0.2345	10 cm
0.0000	0.0784	0.0403	0.0942	0.0498	20 cm
0.0450	0.1297	0.1458	0.6925	0.0284	30 cm
0.5781	0.3479	0.3110	0.4631	0.1716	40 cm
0.6361	0.6295	0.5844	0.4876	0.5994	50 cm
1.0083	0.7063	0.6748	0.7815	0.4222	60 cm
					Depth

observed at a depth of 25 cm in block B. From the porosity values, as well as flow rates (Table 8.2), nitrate solution would have been potentially able to travel quickly through the 25 cm horizon, which would have allowed less time for diffusion to have occured. Porosity reduced with depth, below 25 cm, increasing the potential for diffusion. The largest nitrate concentrations were recorded at the deepest point (60 cm) because of greater input from above combined with reduced soil porosity.

Porosity calculated using the BTM technique showed that there was a larger porosity in the top 0 - 25 cm of soil followed by a reduction of porosity with depth. This would explain the smaller accumulation of nitrate in the soil at 20 cm followed by an increase in nitrate with depth. Solute at 20 cm was quickly transported to depth via large pores and cracks or preferential finger flow, where a smaller porosity allowed more time for diffusion to take place. However, an increased porosity at 10 cm as calculated by the BTM could not explain why nitrate should have accumulated at 10 cm compared to 20 cm. This could only be accounted for by considering the proportion of less than 1000 µm (diameter) pores calculated by the RCSM. The RCSM showed that porosity between 0 and 10 cm depth was less than the recorded porosity between 0 and 25 cm (depth).

Flow rate (Q) was more rapid at 25 cm than at deeper layers in the soil (Table 8.2). Flow may have been sufficiently rapid, even through finer mesopores (1000 - 136 μm, diameter) at 25 cm depth to have limited diffusion. However, dispersion was more likely to have occurred along mesopore than macropore pathways as mesopores tend to be more tortuous. Rapid movement of water in mesopores can cause leaching. Rapid bypass flow (finger flow) along zones of saturation at 25 cm depth would have limited the volume of soil influenced by the tracer, leading to a less even distribution of solute, with zones of soil that are bypassed by the tracer. Deeper horizons with smaller porosity values may result in a more even redistribution of solute due to the homogeneous nature of the major, active, proportion of soil volume.

8.5.2. Observations of Chemical Tracer Concentration Through Time.

The relationship between concentration gradient and diffusion rate, between mobile and immobile zones, is a positive correlation (Fick's law, Section 1.11.2.). As the concentration gradient increases, potential for diffusion from stronger to weak concentration, increases. Potential for diffusion would be limited by speed of movement of solute through the soil. Diffusion between mobile and immobile zones can be inferred from a comparison of the behaviour of two chloride tracer experiments, in which first the gradient between the mobile and immobile zone was large, and second, where the gradient was reduced.

Run 1 (part II) and run 3 represented experiments in which applied concentration of tracer (in a miscible displacement) was larger in comparison to the background concentration in the soil (immobile zone). The maximum concentration of chloride between the mobile and immobile zones, in runs 1 (II) and 3, being 250 mg l^{-1} and 10 mg l^{-1} respectively. Run 2 in contrast had a reduced concentration gradient between mobile and immobile zones because of incomplete leaching of chloride from the matrix after the end of run 1. A

comparison of the results of runs 1 (II) and 3 with those for run 2 showed that when the gradient between the mobile and immobile zones was reduced the time to initial breakthrough and peak concentration was reduced. At six out of nine sample locations, run 2 showed a quicker initial response time, and time to peak, compared with run 1 (II). A larger peak concentration was observed in run 2 compared with runs 1 (II) and 3. In run 1 (II) 4/9 and run 3 2/9 sample locations reached the peak concentration while in run 2 7/9 sample locations reached the peak concentration. As similar variabilities in response times with depth occurred between run 1 (part II) and run 2 it was believed that similar pathways were active in both cases.

From pulse experiments run 4 and run 5, diffusion of nitrate between mobile and immobile zones was more apparent in run 4 when the nitrate concentration gradient was large resulting in smaller peak concentrations (Table 7.12 and 7.16). By run 5 the nitrate concentration gradient had reduced because of nitrate retained in the matrix, after run 4, stronger concentrations of nitrate were left in solution indicating a reduced amount of dilution by diffusion. Pathways were considered to be identical in both experiments, therefore, dilution due to dispersion was considered to be identical also.

Nitrate concentration in solution, in general, decreased with depth in the profile, while nitrate retained in the soil generally increased with depth. At lower depths porosity reduced, therefore, reducing hydraulic conductivity and increasing residence time. Small concentrations of nitrate in solution were most likely due to loss of nitrate from mobile zones into immobile zones, the amount of which increased as velocity of flow was slowed due to a reduction in porosity.

The amount of diffusion was, therefore, a function of concentration gradient and speed of

flow/residence time. A fertilizer applied to a soil with a small residual chemical concentration would, therefore, be expected to take up by diffusion a large proportion of chemical into immobile zones, reducing losses out of the system as observed at the mole drain.

8.5.3. Dispersivity.

The amount of diffusion and dispersion that takes place can be inferred from breakthrough curves and predicted by modelling. The shape of a breakthrough curve plus other parameters, including initial breakthrough time and proportion of immobile water, can be used to suggest how solute is being transported or retained in the soil (Walker and Trudgill, 1983; Singh and Kanwar, 1991). Walker and Trudgill (1983) identified that positively skewed breakthrough curves, which pass to the left of pore volume (PV) = 1, when C/Co = 0.5 were associated with rapid water and solute movement. A prolonged rise to peak and extended tailing was an indication of dispersion and diffusion causing delay and loss (into sinks) of solute (Kluitenberg and Horton, 1990; Hayot and Lafolie, 1993). The curves for the experiment in this thesis were presented in Chapter 7 (Figures 7.26 to 7.43). Curve parameters were presented in Tables 7.8 and 7.9.

With regard to dispersion, all but A5 and A6, run 2 (block A) reached C/Co = 0.5 before PV = 1, which would imply preferential flow was partially influential in these results. In run 3, block B, except for the mole, C/Co = 0.5 was not reached within 1 PV which suggests slower pathways and/or greater diffusion and dispersion of tracer as it passed through the soil. The small values of immobile pore water and extensive tailing of curves, with the exception of A7 and mole A for both runs 2 and 3 again indicated a dominance of non-macropore flow, which would be linked with large diffusion and dispersion rates.

Dispersivity increases with depth in soil. Diffusion and dispersion increases with distance travelled through soil, therefore at 10 cm a slow rate of dispersivity was recorded because travel distance through the soil was limited. From dispersivity predictions made by the CLEARY model in Chapter 7 (Tables 7.24 and 7.25) an increase in dispersivity occurred with depth in both blocks. The only anomalies to this occurred at A2 and at mole locations which record larger dispersivity values than the next sample location depth.

The large predicted dispersivities at A2, A8 and mole A can be linked to breakthrough curves with early initial breakthrough, immobile pore water fractions >0.5 and extensive tailing to peak concentrations. Features of breakthrough curves which imply the existence of preferential pathways, allowing rapid movement, small rate of diffusion and dispersion, as well as slower pathways which result in an increase in diffusion and dispersion. In block B, mole, a similar observation was made to block A although the proportion of immobile water was smaller. In comparison with the rest of the block the observation at the mole (block B) was the largest recorded value of immobile water fraction.

The large dispersivity at A2 may be linked to an internal catchment which resulted in saturated soil conditions at this point in the soil (Figure 6.3(b)), prohibiting movement of solute and thus allowing solutes that have travelled via different pathways to mix. As with the mole drain results saturated soil conditions developed around the mole but because of capillary forces the air-soil interface was not easily crossed, accumulation of water from different pathways built up around the mole before water had a chance to flow into the mole. The mole drain results also represent solute arriving at this point from a wider area than to the suction cup lysimeters, therefore, it was more likely that the solute moved through a larger variety of pore sizes before reaching the sampling location. The sample collected from the mole may reflect more accurately what was happening in the soil as it

represents a sample collected over a larger area than that supplying the suction cup lysimeters. Samples collected from A8 directly under the mole were influenced by the solute in the mole. A crack was observed that directly linked A8 with the mole.

A combined porosity, of RCSM and BTM (Table 8.7 (a and b)), calculation showed an increase of porosity from 10 cm to 25 cm. At A2 unlike any other sample location, at this depth (25 cm), porosity was smaller than the next deepest location. Small porosity with larger predicted dispersivity, compared to the next deepest location, would suggest that diffusion and dispersion at this location was increased due to a restriction of flow through limited pore space.

Caution must be applied to dispersivity calculations as not all model predictions matched observed values, for example A5(10 cm, left), A7(45 cm, left) and mole A (Figures 7.59, 7.61 and 7.63). Therefore, this value may be slightly misleading in its prediction of dispersivity.

8.6. CONCLUSION

In this chapter it has been shown that the way in which water moves in the soil was controlled by: space available to move through; connectivity between spaces and tortuosity of pathways; hydraulic gradient controlling direction of movement, pore size range available to conduct flow and rate of flow; and freedom of flow where water could have become channelled into areas of flow, or may have been retained in the soil in 'dead zones'.

Smaller pores are potentially capable of conducting equivalent flow rates as larger pores, providing there is a sufficient number of pores available and soil water conditions permit.

However, as flow occurs along an increasing number of channels the flowpaths become more divided and tortuous increasing the potential for mechanical dispersion. Soil surface area encountered also increases, therefore, there is a greater opportunity for chemical absorption. Potential for diffusion was increased due to an increase in eddying caused by disrupted flow, a greater potential for solute to move into a 'dead end' pore or for flow rate to suddenly decrease due to a decrease in the number of available pores, either due to porosity or change in soil water content.

Interaction between flowpaths and soil matrix can be predicted from residual solute left in the soil, observations of solute transport, breakthrough curves and model predictions. Dispersivity values showed that as the distance the solute travelled through the soil increased the rate of dispersivity also increased. Porosity and flow also influence dispersivity. Where flow was reduced, due to low porosity, there was a greater opportunity for mixing of different pore groups and an increase in time for diffusion to occur. The shape of the breakthrough curve would suggest that dispersivity was a dominate process in this soil that allow applied chemicals to linger in the soil and be absorbed into the soil matrix. However, breakthrough curve analysis also implied that the introduction of the mole drain provided pathways, displaying both low and high rate of dispersivity, connecting the soil surface to the drain. These results would imply that a potential existed for rapid movement and drainage of water and solute even when soil conditions were below saturation levels.

CHAPTER 9.

SUMMARY AND FUTURE WORK.

9.1. SOIL BLOCK METHODOLOGY.

Study of matrix-preferential-macropore flow requires intensive spatial and temporal sampling as described in this thesis. However, intensity of sampling and measurement technology available placed a constraint on the volume of soil which could be considered. Inevitably there was a compromise between the scale of the experiment and how representative such a block of soil was: as the volume of soil under consideration became smaller and more unique, in general the results could be said to become less representative.

For this research study the main aim was to examine the preferential flow behaviour in soils. The experiment was set up using a moderately impermeable soil found throughout the Culm Measures of South West England and which is representative of larger tracts of heavy land in Britain. The experiment was set up in such a way that a preferential flow route was induced by moling a heavy clay soil. The individual flow routes in the soil were likely to be of the usual water pathways since mole plough treatment responsible for the major cracks was a typical agricultural grassland management practice.

A spatially and temporally detailed examination of solute movement requires an intensive instrumentation network that is at present impracticable to establish in anything but a small scale block experiment (Holden *et al.*, 1995a). The present study investigated water movement and solute transport within a block of soil 1 m^2 by 0.85 m. The methodology consisted of applying existing field techniques in a laboratory experiment to monitor detailed changes in water and solute movement both spatially and temporally. Observations of soil water status, soil structure and solute movement were made to fulfil the aims as

outlined in Section 1.4. The experiment was carefully designed to ensure that the block was large enough to encompass a large number of aggregates and associated flowpaths. The large volume ensured that only so called natural water pathways functioned and problems associated with smaller cores and blocks were avoided.

In the following sections the sampling methods will be reviewed in more detail and the main findings will be discussed. From these observations a number of important conclusions were made. These included an examination of which pathways were predominantly involved in solute transport, the relative amount of mixing that occurred between mobile and immobile zones within the soil and the number and size of pores involved in much of the solute transfer. Particular attention will be focused on the comparison of soil block results to show that the hydrology of the block was similar to that of the field. Finally, suggestions will be presented about how this research could be developed in the future.

9.2. TECHNIQUES.

9.2.1. Soil Block Collection.

The method of extracting, transporting and emplacing the soil blocks in the laboratory (Chapter 2) worked well and caused no discernable disturbance to the soil. By using a separate wooden framework to support the soil during transport and replacing it with a wax frame once in place prevented any edge effect. Only where the waxed side was exposed to the greatest range of temperatures did the wax start to crack and pull away from the soil. The remedial action taken to repair the edge seal was successful (Section 3.5.). An improved method of sealing the sides of the soil will be discussed later in this chapter.

The use of a sand table to support the soil allowed a positive contact to be made between

the soil such that suction was induced in the soil. This assertion was confirmed by suction measurements at the base of the block, it only became saturated during the high water table experiment. Some loss of suction limited the sand tables capability in this investigation, however, the potential capability of the system was proven.

9.2.2. Irrigation.

An even application of tracer and water was applied by the misting system. Some small areas of surface accumulation were observed but only after prolonged irrigation as the soil surface became sealed. Only slight fluctuations in rate of irrigation were noted between the experiments. The mean irrigation rate for the experiment was 2.76 mm h^{-1}. From TDR results (Section 6.3.) soil water content monitored over 1540000 mm^3 of soil remained stable through time. The stable soil water content would therefore suggest that the misting system applied an even irrigation distribution through time. Pathways actively involved in transmitting solution are dependent on many factors. Using a single irrigation rate had the advantage of eliminating one of the variables that may cause pathways to alter.

9.2.3. Instrumentation.

Detailed monitoring of soil water status and solute movement was made. The 1 cm radius of the tensiometers was perhaps too large compared with the phenomenon of preferential flow. However, the number of tensiometers and their allocation gave good spatial coverage. The size of the lysimeters was such that sample volumes were adequate, although the temporal resolution of the solute collection every four hours may have missed peak solute concentration. The sensitivity of the lysimeter system could be improved by sampling more frequently. A fully automated sampling system such as developed by Holden *et al.* (1995a) could provide an improved sampling resolution. The TDR soil water content results are less spatially sensitive than the tensiometer system. This technique, however, provided a useful

means of observing average soil water conditions from which a comparison between micro-scale and macro-scale observations could be drawn.

The number and location of samplers was considered to be appropriate for the volume of soil. More intensive instrumentation would have caused interference between instrumentation and unacceptable disruption to natural soil water flow patterns. Smaller instruments could be used in the future to limit the effect of disturbance. The positioning of instruments at specific locations rather than randomly proved to be a wise decision that made comparisons between instrumentation easy and an understanding of spatial patterns more straightforward.

9.2.4. Soil Structural Analysis.

Three quantitative methods of soil structural analysis were developed: profile tracing method (PTM), binary transect method (BTM) and resinated core section method (RCSM) (Chapter 5). The various techniques all had advantages and limitations. The PTM proved to be a technique that could produce a visual image of the patten of cracks (>1 mm diameter) within the soil profile. By using a Quantimet system (Section 5.) to analyse the traced image a quantified description of the orientation, tortuosity and porosity of the cracks in the vertical section was possible. The method was limited to cracks that were >1 mm (diameter) with respect to one orientation of vertical section through the soil.

The BTM enable a more detailed survey of crack and pores ≥1 mm (diameter) to be recorded along fixed transect lines. The information gained from each transect line enabled a calculation of pore size distribution (in the range 1, 2, 3, 4 and ≥5 mm) and porosity (both for the whole transect line as well as for 160 mm sections) to be calculated and compared to other locations within the vertical section. The BTM was limited because only

pores ≥1 mm could be recorded, there was no indication of how pores and cracks connected with each other through the profile and the method was more time consuming than the PTM to conduct.

The RCSM allowed detailed quantitative analysis of pore sizes in the range 1000 to 136 μm (diameter). Measurements of pore size distribution, porosity and shape were possible. The RCSM samples represented a smaller total area of the soil than the other two methods and also represented a horizontal rather than vertical section. No indication of pore or crack connectivity through the profile was possible.

The three methods used together complemented each other: the RCSM for example produced detailed observations of pores sizes in the mesopore range which combined with BTM could be used to describe a range of pore sizes in the macropore and mesopore scale.

9.3. SUMMARY OF MAJOR FINDINGS.

9.3.1. Soil Structure.

The structural characteristics of the soil blocks were shown to be dominated by round and intermediate shaped pathways which at a scale of above 1 mm (diameter) were in general vertically orientated. The smaller cracks (≈1 mm diameter) which showed a greater tendency away from the vertical (Section 5.2.1.) may be linked to fracture cracks, created by the cylindrical foot of the mole plough, radiating from the mole drain (Spoor and Ford, 1987). Both vertical and Horizontal fracture cracks would normally be associated with mole drain ploughing (Section 1.2.). The largest total pore count ≥1 mm (diameter) occurred at 5 cm depth in the soil (Table 5.12) with the smallest recorded observation in this size group occurring below 40 cm depth. The abundance of macropores above 40 cm may be a reflection of artificially generated cracks produced by the mole plough. In the pore size

range 1000 to 136 μm (diameter) the largest total pore count was observed at 25 cm depth. Porosity calculated with respect to depth from soil surface from a combination of pore sizes (>1 mm to 136 μm diameter) (Table 8.5) showed that porosity increased from 10 to 25 cm depth and subsequently decreased below 25 cm depth. Only 5% of the soil porosity was considered to be attributable to mesopore pathways, although the total number of pores in that size range was greater than in the macropore range. In general block A had a lower porosity than block B in the macro-scale pore size range (≥1 mm diameter) 10.17% compared to 18.43% respectively. However, in the meso-scale pore size range (1000 to 136 μm diameter) block A was shown to have a higher porosity than block B, 7.11% compared to 4.3% respectively. Structural observations revealed that macropore pathways were connected from the soil surface to depth in the soil which implied that rapid transport to depth through macropores was possible.

9.3.2. Soil Water Status.

A stable bulk water content was achieved in both soil blocks. Observations of soil water content within a volume of soil 1540000 mm^3, at fifteen locations in each block, revealed that soil water content decreased with depth in soil but between experiments the values remained stable (Section 6.3). At a more detailed scale slight fluctuations related to changes in soil water content were observed. The fluctuations observed at the detailed scale can be attributed to preferential flow intercepted by the porous cup of the tensiometer and to diurnal temperature fluctuations (Section 6.2).

Observations of soil suction showed that in general the soil blocks dried slightly and tensions increased by about +3 (cm H_2O) with a maximum increase in suction of +10 (cm H_2O) (Section 6.2.1. and Table 6.2).

The suction results suggest that only pores in the mesopore size range (1000 to 10 μm diameter) were saturated and therefore involved in transmitting water (Section 8.2.2.). Although macropore pathways may still have conducted solute there is less evidence to suggest that macropores were fully saturated. The volume of flow lost via the mole drain was minimal (mean flow rate from mole drain block A 0.02 mm h^{-1} from block B 0.002 mm h^{-1}) the major volume of the water passed by the drain to a deeper depth in the soil.

9.3.3. Solute Movement.

The transport of solute through the soil was shown to be highly variable (Sections 7.4. and 7.5.). Initial solute concentration in the soil had a marked effect on the time to peak concentration. When residual solute concentration was small the time to reach peak concentration in the miscible displacement experiment took longer (Section 7.4.3). A pulse of nitrate was observed to reach a larger peak concentration in a quicker time after residual nitrate in the soil had been increased (Section 7.5.2.).

9.3.4. Controlling Factors of Water and Solute Movement.

Water and solute movement through the soil was controlled by structure and soil water content. Structural analysis revealed that a continually variable range of pore sizes existed in the soil. In order to simplify the definition of which structural pathways were actively involved in transmitting water and solute the range of pathways was divided into three categories according to Luxmoore's (1981) definition, macropore, mesopore and micropore (Section 1.10). Soil water content controlled the range of pore sizes that could actively transmit solution. The active pathways during the experiments were considered to be limited to mesopore sized channels (Section 8.2.2.). Breakthrough curve analysis of runs 2 and 3 revealed that although concentration had risen quickly at sample locations with respect to increasing depth in soil (Section 7.4. and 7.5.) only at a few locations was

macropore type flow quantified. The most consistent location at which macropore type flow was identified was the mole drain. Block A was observed to have had a greater proportion of flow attributable to rapid macropore type flow than block B. Structural analysis of the soil revealed that block A had a larger proportion of pores in the mesopore size range than block B. As soil water content restricted flow to the mesopore channels rapid flow in block A cannot have been attributable to macropore flow but rather preferential flow along a saturated zone of mesopore pathways (Sections 1.10. and 8.2.). Although movement to depth was rapid along the mesopore pathways the increased tortuosity and reactive surface area reduced the speed at which peak concentration was reached at depth.

9.3.5. Interaction Between Mobile and Immobile Flowpaths.

An indirect observation of the interaction between flowpaths was achieved by comparing the results of the five experiments (Sections 7.3. and 7.4.), by breakthrough curve analysis (Section 7.7.1.) and by measurement of residual nitrate concentration in the soil at the end of run 5 (Section 8.5.1.).

Comparing the results of weak initial residual soil concentration to those of the greater residual solute concentrations revealed that more interaction between mobile and immobile zones occurred when the concentration gradient between the two solutions was larger, as the gradient reduced peak concentrations at depth were reached more quickly and pulse tracers were observed to reach a higher peak concentration.

Breakthrough curve and model predictions showed that a large rate of dispersivity and therefore reaction and mixing occurred between the mobile and immobile zones. The largest accumulation of residual nitrate occurred in areas of lower porosity. Although mesopore flow has been shown to conduct solute rapidly to depth (Section 8.2.) mixing and therefore

dilution in concentration of mobile solute is related to speed of flow.

9.3.6. Conclusions and Field Scale Implications.

Previous work on Rowden Moor has shown that mole drainage systems alter the dominant hydrological pathway of the soil from overland flow to lateral subsurface flow (Hallard, 1988; Addison, 1995). Rapid movement of water towards the mole, that exceeds the predicted rate associated with piston type flow, has been explained by the existence of artificially created macropores (McDonnell, 1990; Beven, 1991) combined with the presence of a naturally fractured soil that link soil surface to drainage channel. Although not all lateral subsurface flow is directed towards the mole drain (Addison, 1995). Hallard's (1988) observation of macropore flow in a mole drained soil suggested that flowpaths were discrete with little mixing occurring between matrix and irrigation water. The observation, at the field scale, of increased leaching of nitrate after mole ploughing has helped substantiate discrete pathway theory (Hallard, 1988; Scholefield *et al.*, 1995). However, the results of both the block experiments conducted in this investigation as well as observations made by Addison (1995) at field (1 Ha), plot (10 m^2) and lysimeter (10 m^2) scales would suggest that flowpaths far from being discrete are rather a continuum of pore sizes.

Addison (1995) identified two main runoff generation mechanisms: macropore flow which allowed rapid transport of water to depth and preferential finger-like flow through zones of saturation in the soil. Although describing rapid flow as macropore flow Addison argued that 'classical' bypass macropore flow (in which macropore flow does not interact with the soil matrix solution) could not be used to explain all cases of rapid movement. These observations concur with the results of the block experiment presented in this thesis. Addison also observed that rapid transport was associated with mixing of matrix water and irrigation water with a high residual concentration of tracer left in the matrix. Such

observations were observed at both 10 m^2 and 1 Ha scale (Addison, 1995). The 0.85 m^3 block experiment produced similar results that also suggested a high degree of dispersion and mixing between *in situ* soil water and irrigation solution. The more detailed investigation showed that not only macropores were capable of rapid flow but also smaller pores. The smaller pores being more tortuous in nature would explain the degree of mixing observed.

Variations in soil water content surrounding the mole drain were noted in a lysimeter and plot (Addison, 1995). Discrete zones of saturated soil gave rise to a form of discontinuous translatory flow. The distribution of these zones was linked to hydraulic variability within the profile. Water accumulated within these zones until storage capacity was exceeded. Observations of saturated zones within the soil blocks were noticed and could also be connected to zones of different hydraulic properties.

The results of this investigation have shown that even at the limited volume of 0.85 m^3 the soil conditions are highly variable. The most important implication of micro-scale variability in a structured soil at the field scale include; uneven distribution of fertilizers and pesticides, the rapid contamination of soil matrix by pollutants but with a reduced concentration of pollutants in drainage water and indeed rapid delivery of pollutants to drainage water.

Observations would suggest that a large proportion of water and solute is transported to a depth below field drainage. Accumulation of solutes in the water table could lead to the contamination of drinking water supplies. Accumulation may also contribute to seasonal peaks in chemical loss as the water table rises above the level of field drainage.

9.4. FUTURE WORK.

Detailed measurement of soil structure, soil water status and solute movement, for a naturally poorly structured soil of the Hallsworth series were made. The dominant soil water pathway was determined. A detailed data base should be established for a number of other soil types observed at the 0.85 m^3 scale. A comparison of a variety of different soil structures, such as the De Bathe (Credition series) which represents a well structured soil with few macropores, could be used to identify any similar patterns of cause and effect. The data base could then be used to assess the suitability of land for agricultural use, waste disposal or the consequence of accidental spillage of toxic waste.

9.4.1. Improvement to the Approach Taken.

Further investigation of how pathways were interconnected in the soil is required. Research by Booltink *et al.* (1993) suggested that staining actively transmitting macropores with blue dye was a good method by which macropore flowpaths could be quantified. Ringrose-Voase (1987) used ultra violet dye to define pores that had transmitted solute. However, dyes are not so successful when trying to quantify mesopore and micropore flow. The main disadvantage of dyes is their inability to mimic water flow because of molecular size and chemical attractiveness.

In this investigation tracer was applied evenly to the surface of the soil. An uneven application of tracer could be applied to examine what impact this had to solute distribution within the soil, as a simulation of accidental spillage. Similarly different methods of irrigation could be investigated, including rain like simulation, to explore how water droplet size may influence surface ponding, soil capping and subsequent absorption into the soil. Timing of the irrigation could be altered for example between application of a pulse of tracer and timing of rainfall event or duration of rainfall.

The method used to seal the edge of the soil to prevent flow occurring along the side of the block may be improved by strengthening the external support so that stress due to volume changes does not lead to a loss of contact between the soil and the edge seal. Other materials such as puddling clay and expanding water tight foam (Holden *et al.*, 1995a) have been used successfully as a sealant. Ideally a compound that has both strength but flexibility would be the most suitable so that a permanent edge seal could be maintained even if soil volume varied.

Model predictions were based on a one-dimensional model (CLEARY, Cleary and Ungs, 1979). The one-dimensional model had problems in predicting solute concentration changes at the mole drain. Ideally a two-dimensional model would be better suited to predicting mole drain output.

Improved observations of spatial variation of solute exiting the base of the block may be achieved by dividing the base of the block into separate sampling zones. Techniques including isolated ceramic plates (Buchter *et al.*, 1995), free draining grid lysimeters (Andreini and Steenhuis, 1990; Ogden *et al.*, 1992) and wick samplers (Poletika and Jury, 1994) have been used to improve the spatial observations from the base of soil blocks.

9.4.2. Improvements to Instrumentation.

At present the measurement of soil suction is taken at a different locality from where the solute sample is collected. The heterogeneous nature of the soil means that although the two different instruments may be located in the same horizontal plain the surrounding soil structure will not be identical. A method is needed whereby both a measurement of soil water status and solute sample can be obtained at the same location.

The variability of solute and water movement at the micro-scale is such that to improve both the spatial and temporal resolution of sampling would require a fully automated system. Research conducted by Marshall (1994) and Holden *et al.* (1995a) has shown how solute samples can be collected and analysed in real time using a flow-injection system and field spectrophotometer. TDR systems have also been automated (Baker and Allmaras, 1990; Heimovaara and Boulten, 1990) and it is possible to capture and store TDR traces which both increases the speed and accuracy of interpretation (Dowd *et al.* pers. comm).

APPENDIX A

Timetable of experimental events.

	1991	1992	1993	1994	1995
	O N D	J F M A M J J A S O N D	J F M A M J J A S O N D	J F M A M J J A S O N D	J F M A M
Construction of sand tables		----------			
Mole drain pulled and soil block cut		-			
Blocks extracted and placed on sand table		--			
Preparation and instrumentation of blocks			----------		
Irrigation of blocks				----------	
Grass died off			--		
Run 1 (I) - miscible displacement of 100 mg l^{-1} Cl (block A)				--	
Run 1 (II) - miscible displacement of 250 mg l^{-1} Cl (block A)				-	
Run 2 - miscible displacement of 250 mg l^{-1} Cl (block A)				--	
Run 3 - miscible displacement of 250 mg l^{-1} Cl (block B)				--	
Run 4 - pulse of 2500 mg l^{-1} Cl and 500 mg l^{-1} TON (block B)				-	
Run 5 - pulse of 2500 mg l^{-1} Cl and 500 mg l^{-1} TON (block B)				-	
Destructive sampling of block A				---	
Destructive sampling of block B				- --	
Analysis of soil samples (i.e. SMRC, BD, resination and Quantimet analysis)				----------	
Interpretation of data (tensiometer, TDR, lysimeter, etc)				----------	

APPENDIX B

Campbell 21X Data Logger Programs.

Transducer Program.

```
*1

00:   5

01P:  92    0     5     1

02P:  31    1     2     30    1     0


*3

01P:  85    1

02P:  20    1     1

03P:  87    0     20

04P:  22    1     200   0     5000

05P:  2     1     3     1     1C    0

06P:  95

07P:  20    0     1

08P:  86    10

09P:  77    110

10P:  70    31    1

11P:  95
```

Spray System Program.

```
*2

00:   1

01P:  92    0     120   30

02P:  20    1     3

03P:  87    1     3

04P:  95

05P:  20    0     3

06P:  20    1     2

07P:  87    1     3

08P:  95

09P:  20    0     2

10P:  95
```

Tipping Bucket Program.

```
*1

60

01P:  3     1     2     2     3     0.2   0

02P:  92    0     1     10

03P:  80    3     4

04P:  72    1     3

05P:  89    4     2     0     30

06P:  80    1     26

07P:  77    220

08P:  70    1     4

09P:  95
```

APPENDIX C.

TENSIOMETER CALIBRATION EQUATIONS.

The calibration equations for each individual tensiometer is given in Table 1 for block A and Table 2 for block B. The calibration is presented as an equation for a straight line

$$Y = mx + c$$

Where m is the gradient of the line, y is the y-axis coordinate (cm H_2O suction), x is the x-axis coordinate (mV response) and c is the location at which the line intersects the y-axis (constant). These equations were used to convert mV responses, recorded by the transducers as a result of change in pressure in the tensiometer, to suction (cm H_2O suction) in Chapter 6.

Depth in profile	Left of block		Right of block	
10 cm	T5	-24.58x + 0.20	T1	-24.73x + 4.13
25 cm	T6	-24.71x + -2.19	T2	-24.28x + -0.19
45 cm	T7	-26.56x + -3.52	T3	-24.59x + 2.91
60 cm	T8	-25.81x + 7.25	T4	-24.77x + -2.47

Table 1 - Calibration equations for tensiometers in block A.

Depth in profile	Left of block		Right of block	
10 cm	T5	-24.57x + -3.30	T1	-26.57x + 4.40
25 cm	T6	-24.63x + 8.27	T2	-26.36x + 4.62
45 cm	T7	-24.63x + 8.27	T3	-25.46x + 2.05
60 cm	T8	-24.66x + 2.01	T4	-26.41x + 3.58

Table 2 - Calibration equations for tensiometers in block B.

APPENDIX D.

TRACINGS OF SOIL PROFILES PRODUCED DURING PROFILE TRACING METHOD.

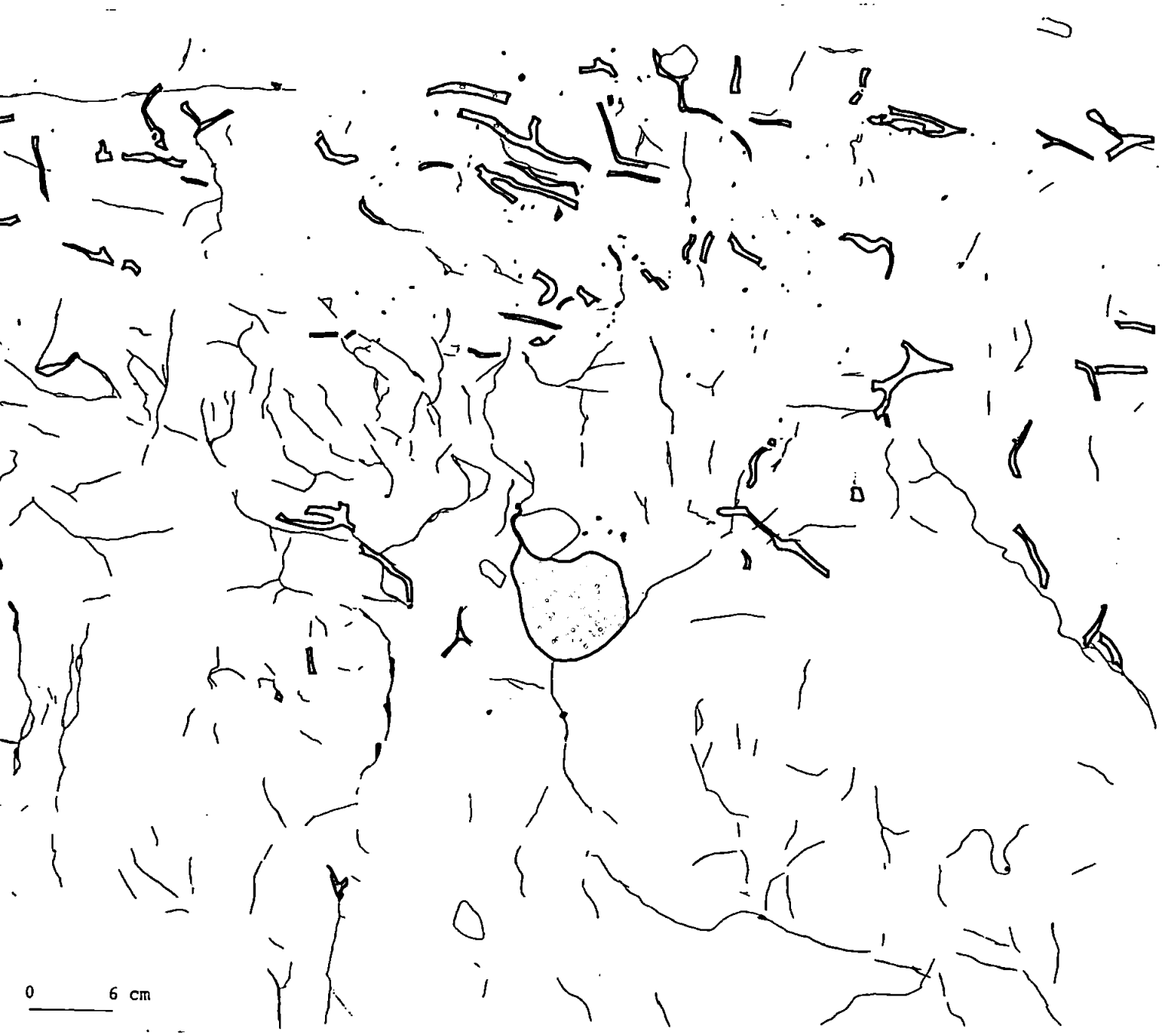

Figure D1 - Tracing 0 cm into block A.

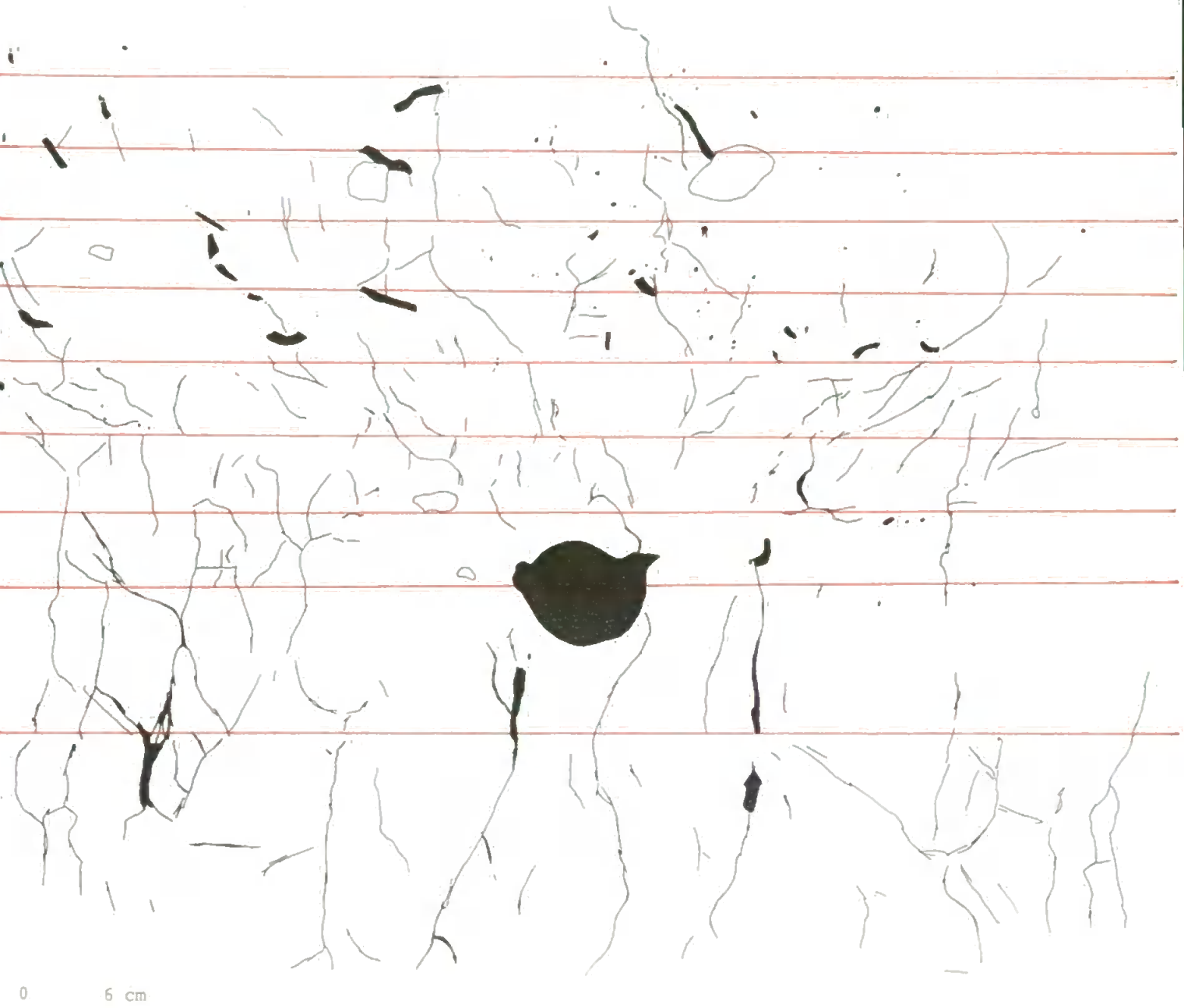

Figure D2 - Tracing 10 cm into block A, showing locations of binary transect lines (—).

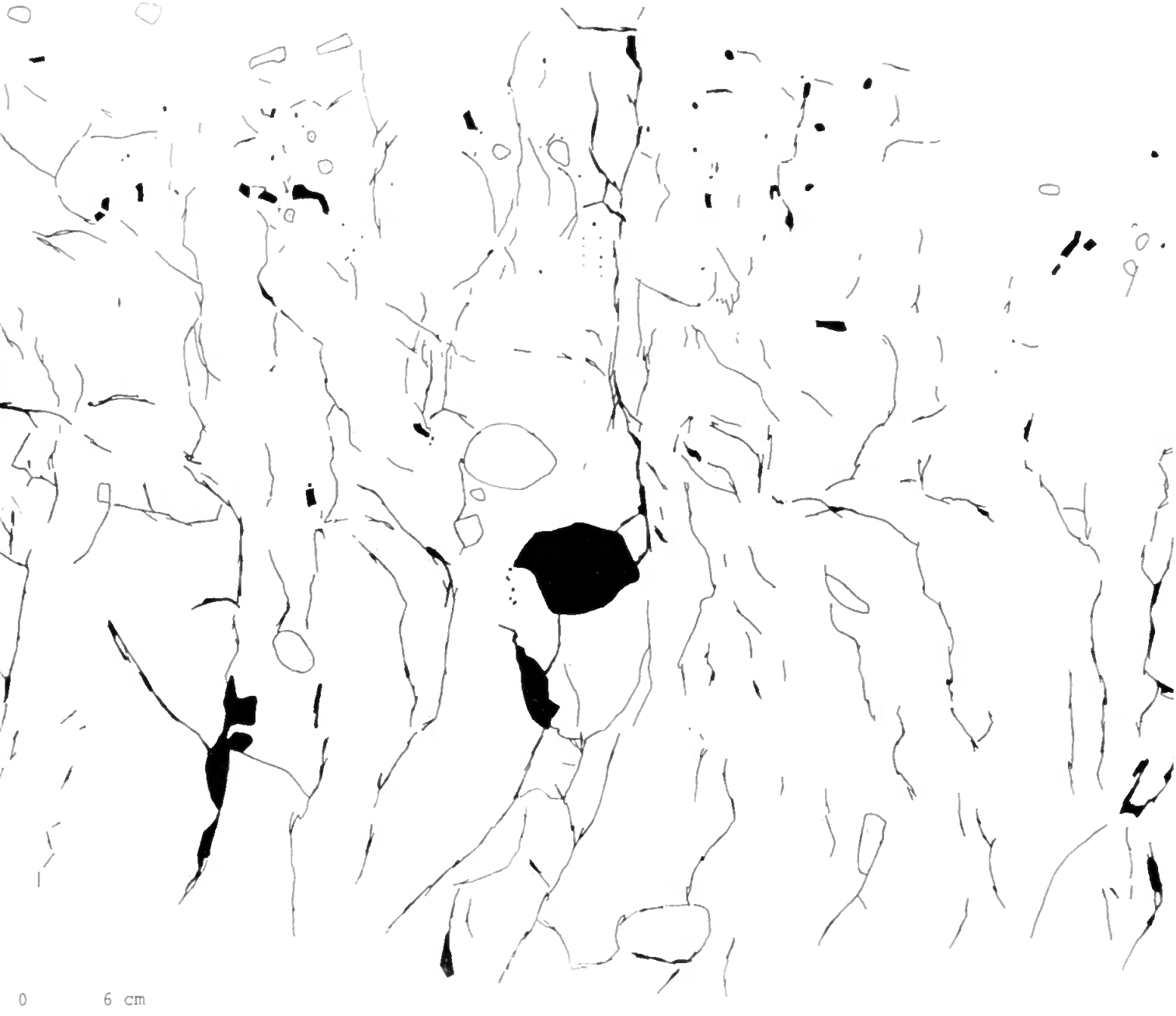

Figure D3 -Tracing 20 cm into block A.

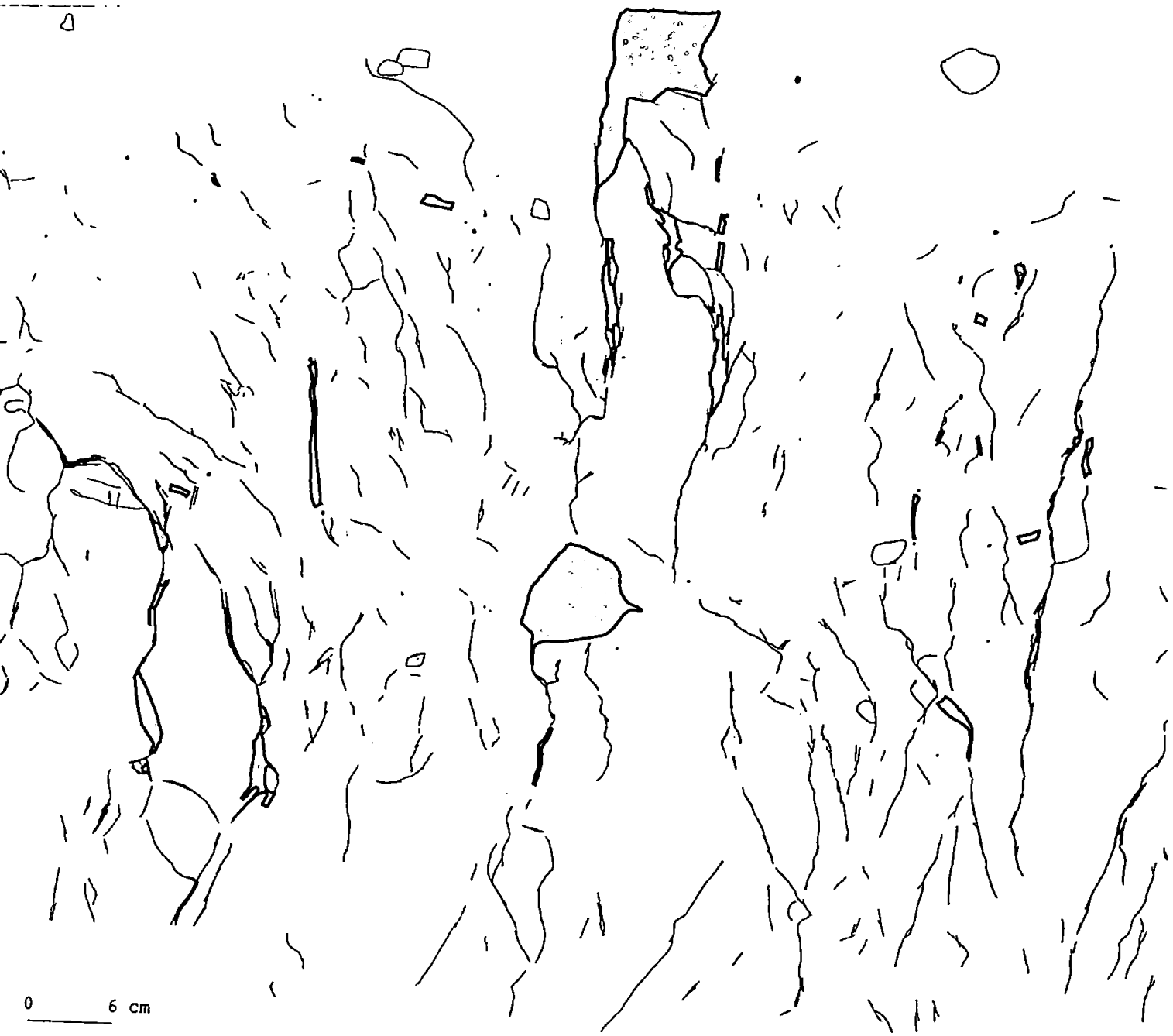

Figure D4 - Tracing 40 cm into block A.

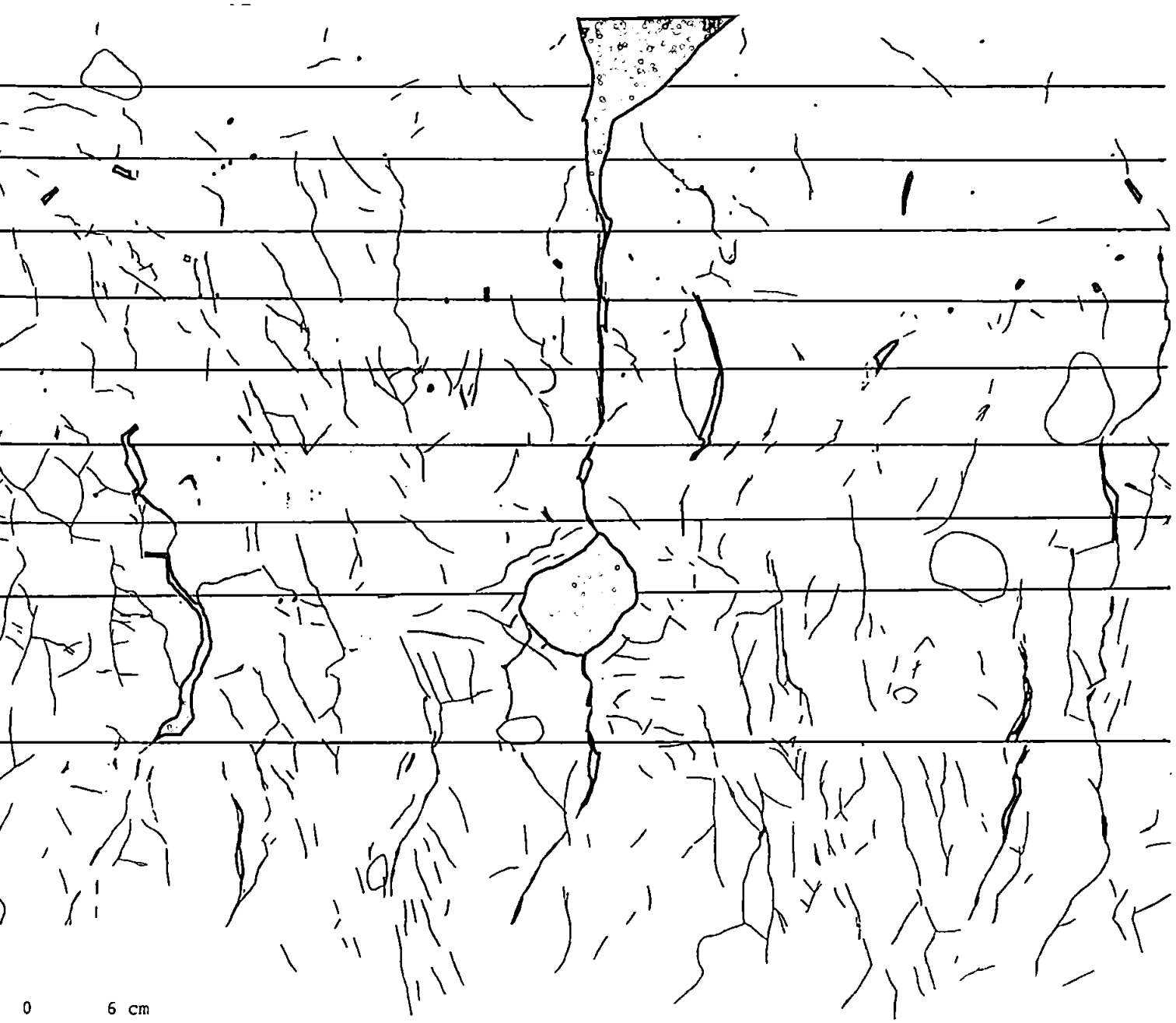

Figure D5 - Tracing 50 cm into block A, showing locations of the binary transect lines (—).

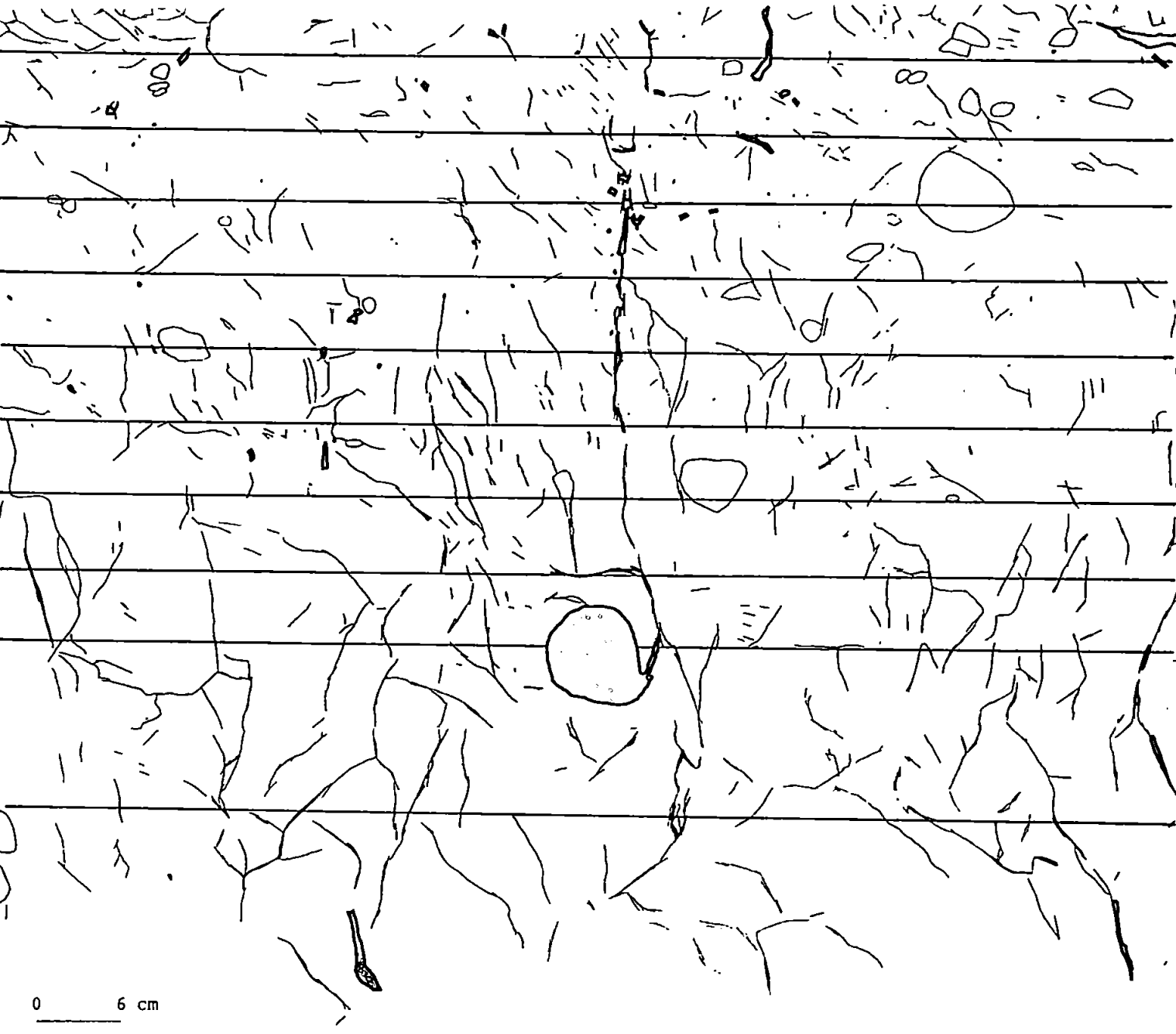

Figure D6 - Tracing 10 cm into block B, showing locations of binary transect lines (—).

Figure D7 - Tracing 20 cm into block B.

Figure D8 - Tracing 40 cm into block B.

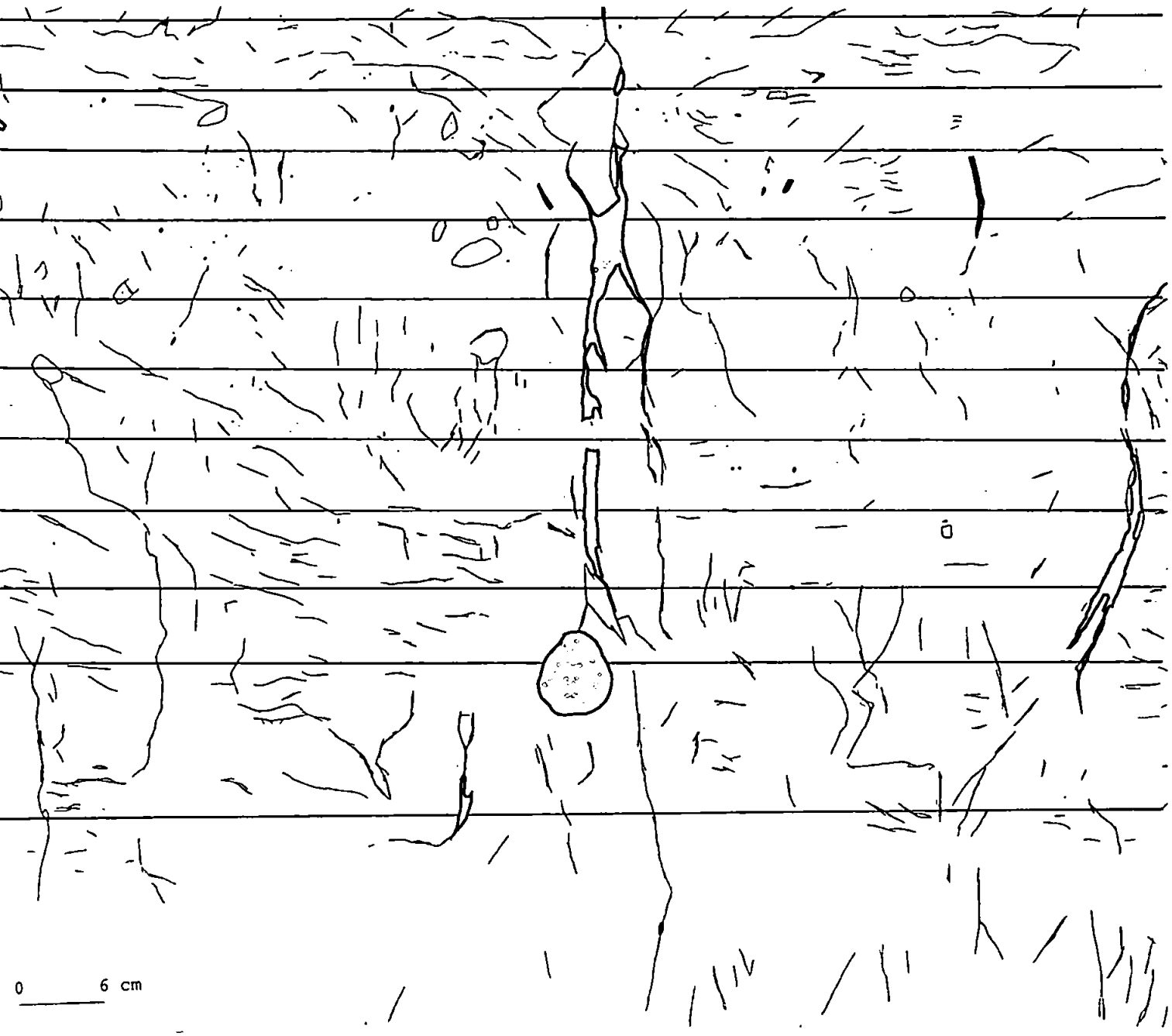

Figure D9 - Tracing 50 cm into block B, showing locations of binary transect lines (—).

APPENDIX E.

Regresion equations for curves shown in Figures 6.1 to 6.6 of tensiometer results through time. Tensiometers positioned in the soil profile at 10, 25, 45 and 60 cm, on both the left and right hand side of the block.

Run 1 (I)

Left:		Right:	
10 cm	Y = 0.05X + 11.18	10 cm	Y = 0.25X + 9.54
25 cm	Y = 0.16X - 3.31	25 cm	Y = 0.24X + 2.10
45 cm	Y = 0.24X + 12.29	45 cm	Y = -0.08X + 10.10
60 cm	Y = 0.12X + 16.99	60 cm	Y = 0.39X + 12.93

Run 1 (II)

Left:		Right:	
10 cm	Y = 0.31X + 5.76	10 cm	Y = 0.23X + 8.45
25 cm	Y = -0.04X + 1.56	25 cm	Y = 0.27X - 4.09
45 cm	Y = 0.06X + 16.15	45 cm	Y = 0.21X + 2.41
60 cm	Y = 0.28X + 12.76	60 cm	Y = 0.24X + 14.59

Run 2

Left:		Right:	
10 cm	Y = 0.03X + 8.44	10 cm	Y = 0.07X + 8.37
25 cm	Y = 0.09X - 1.12	25 cm	Y = 0.08X + 1.25
45 cm	Y = 0.07X + 16.13	45 cm	Y = 0.002X + 7.62
60 cm	Y = 0.05X + 17.77	60 cm	Y = 0.03X + 13.46

Run 3

Left:		Right:	
10 cm	Y = 0.06X + 9.08	10 cm	Y = 0.003X + 12.73
25 cm	Y = -0.22X + 6.08	25 cm	Y = 0.24X + 9.99
45 cm	Y = 0.04X + 16.37	45 cm	Y = 0.27X + 18.06
60 cm	Y = 0.20X + 11.07	60 cm	Y = 0.07X - 0.49

Run 4

Left:		Right:	
10 cm	Y = -0.18X + 9.50	10 cm	Y = 0.07X + 12.15
25 cm	Y = 0.66X - 1.83	25 cm	Y = 0.19X + 11.15
45 cm	Y = -0.18X + 14.32	45 cm	Y = 0.43X + 11.64
60 cm	Y = 0.32X + 8.32	60 cm	Y = 0.27X + 0.75

Run 5

Left:		Right:	
10 cm	Y = 0.07X + 7.55	10 cm	Y = 0.02X + 14.35
25 cm	Y = -0.74X + 5.07	25 cm	Y = -0.25X + 13.60
45 cm	Y = -0.06X + 14.93	45 cm	Y = -0.02X + 12.87
60 cm	Y = 0.05X + 8.22	60 cm	Y = -0.09X + 2.74

REFERENCES.

Addiscott, T. M., Whitmore, A. P. and Powlson, D. S., 1991. *Farming, fertilizers and the nitrate probloem.* CAB International, Wallingford, U.K. 170 p.

Addison, P. J., 1995. *An investigation of soil water movement on drained and undrained clsy grassland in South West Devon.* unpubl. Ph.D Thesis, Univeristy of Plymouth, U.K.

Ahuja, L. R., Wendroth, O. and Nielsen, D. R., 1993. Relationship between initial drainage of surface soil and average profile saturated conductivity. *Soil Sci. Soc. Am. J.* 57:19-25.

Anderson, J. L. and Bouma, J., 1977. Water movement through pedal soils: I. Saturated flow. *Soil Sci. Soc. Am. J.* 41: 413-418.

Andreini, M. S. and Steenhuis, T. S., 1990. Preferential paths of flow under conventional and conservation tillage. *Geoderma.* 46: 85-102.

Armstrong, A. C., Atkinson, J. L. and Garwood, E. A., 1984. Grassland drainage economics experiment, North Wyke, Devon. ADAS LWS R & D Report No. RD/FE/23, MAFF, London.

Armstrong, A. C. and Garwood, E. A., 1991. Hydrological consequences of artificial drainage of grassland. *Hydrological Processes.* 5: 157-174.

Aubertin, G. M., 1971. *Nature and extent of macropores in forest soils and their influence on subsurface water movement.* USDA Forest Service Research Paper NE-192.

Baker, J. M. and Allmaras, R. R., 1990. System for automating and multiplexing soil moisture measurement by time-domain reflectometry. *Soil Sci. Soc. Am. J.* 54: 1-6.

Baker, J. M. and Lascano, R. J., 1989. The spatial sensitivity of time-domain reflectometry. *Soil Sci.* 147: 378-384

Bear, J., 1972. *Dynamics of fluids in porous media.* Elsevier, New York.

Beer, T. and Young, P. C., 1983. Longitudinal dispersion in catural streams. *J. Environ. Eng.*, ASCE, 109:1049-1067.

Beven, K. and Germann, P., 1981. Water flow in soil macropores II. A combined flow model. *J. Soil Sci.* 32: 15-29.

Beven, K. and Germann, P., 1982. Macropores and water flow in soils. *Water Resour. Res.* 18: 1311-1325.

Beven, K. J. and Young, P. C., 1988. An aggregated mixing zone model of solute transport through porous media. *J. Contam. Hydrol.* 3: 129-143.

Biggar, J. W. and Nielsen, D. R., 1962. Miscible displacement. II. Behavior of tracers. *Soil Sci. Soc. Am. Proc.* 26: 125-132.

Biggar, J. W. and Nielsen, D. R., 1976. Spatial variability of the leaching characteristics of a field soil. *Water Resour. Res.* 12: 78-84.

Birkland, P. W., 1984. *Soil and geomorphology.* Oxford univ. Press, New York, N.Y., p.372.

Booltink, H. W. G., 1993. *Morphometric methods for simulation of water flow.* Thesis Wageningen, Grafisch, Netherlands.

Booltink, H. W. G. and Bouma, J., 1991. Physical and morphological characterization of bypass flow in a well-structured clay soil. *Soil Sci. Soc. Am. J.* 55: 1249-1254.

Booltink, H. W. G., Hatano, R. and Bouma, J., 1993. Measurement and simulation of bypass flow in a structured clay soil: a physico-morphological approach. *J. Hydrol.* 148: 149-168.

Bouma, J., 1981. Comment on "micro-, meso-, and macroporosity of soil". *Soil Sci. Soc. Am. J.* 45: 1244-1245.

Bouma, J., 1989. Using soil survey data for quantitative land evaluation. In. B. A. Stewart (ed.), *Advances in Soil Science,* Springer, Berlin. 9: 117-123.

Bouma, J., 1990. Using morphometric expressions for macropores to improve soil physical analyses of field soils. *Geoderma.* 46: 3-11.

Bouma, J. and Anderson, J. L., 1971. Relationships between soil structure characteristics and hydraulic conductivity. p. 77-105. Field soil water regime. SSSA Spec. Publ. no. 5. Am. Soc. of Agronomy, Madison, Wis.

Bouma, J., Belmans, C. F. M. and Dekker, L. W., 1982. Water infiltration and redistribution in a silt loam subsoil with vertical worm channels. *Soil Sci. Soc. Am. J.* 46: 917-921.

Bouma, J., Jongerius, A., Boersma, O., Jager, A. and Schoonderbeek, D., 1977. The function of different types of macropores during saturated flow through four swelling soil horizons. *Soil Sci. Soc. Am. J.,* 41: 945-950.

Bouma, J. and Wösten, J. H. M., 1979. Flow patterns during extended saturated flow in two, undisturbed swelling clay soils with different macrostructures. *Soil Sci. Soc. Am. J.* 43: 16-22.

Brewer, R., 1964. *Fabric and mineral analysis of soils.* John Wiley and Sons Inc. New York.

Briggs, L. J., 1897. The mechanics of soil moisture. *U.S.D.A. Division of Soils Bulletin No. 10.* Government Printing Office, Washington, USA.

Briggs, L. J. and McCall, A. G., 1904. An artificial rootway for inducing capillary movement of soil moisture. *Science.* 20: 566-569.

Brülhart, A., 1969. Jahreszeitliche Veränderungen der Wasserbindung und der Wasserbewegung in Waldböden des schweizerischen Mittellandes. *Mitt. Schweiz.*

Anst. Forstl. Versuchsw. 45: 127-232.

Brusseau, M. L., 1993. The influence of solute size, pore water velocity, and intraparticle porosity on solute dispersion and transport in soil. *Water Resour. Res.* 29: 1071-1080.

Brusseau, M. L. and Rao, P. S. C., 1990. Modeling solute transport in structured soils: a review. *Geoderma.* 46: 169-192.

Buchter, B., Hinz, C., Flury, M. and Flühler, H., 1995. Heterogeneous flow and solute transport in an unsaturated stony soil monolith. *Soil Sci. Am. J.* 59: 14-21.

Bullock, P. and Thomasson, A. J., 1979. Rothamsted studies of soil structure II. measurement and characterisation of macroporosity by image analysis and comparison with data from water retention measurements. *J. Soil Sci.* 30: 391-413.

Burt, T. P., Heathwaite, A. L. and Trudgill, S. T., 1993. *Catchment sensitivity to land use controls. Landscape sensitivity.* Wiley. 229-240.

Burt, T. P. and Haycock, N. E., 1992. Catchment planning and the nitrate issue: a UK perspective. *Prog. Phy. Geog.* 16: 379-404.

Cameron, K. C., Smith, N. P., McLay, C. D. A., Fraser, P. M., McPherson, R. J., Harrison, D. F. and Harbottle, P., 1992. Lysimeters without edge flow: an improved design and sampling procedure. *Soil Sci. Soc. Am. J.* 56: 1625-1628.

Cassel, D. K. and Klute, A., 1986. Water potential: Tensiometry. *In.* A. Klute (ed.) *Methods of soil analysis.* 2nd ed. Agronomy. 9: 563-596.

Cassel, D. K., Krueger, T. H., Schroer, F. W. and Norum, E. B., 1974. Solute movement through disturbed and undisturbed soil cores. *Soil Sci. Soc. Am. Proc.*, 37: 36-38.

Chappell, N. A., 1990. *The characterization and modelling of soil water pathways beneath a coniferous hillslope in Mid Wales.* Unpubl. Ph.D. Thesis, Polytechnic South West, Plymouth, UK.

Chen, C., Thomas, D. M., Green, R. E. and Wagenet, R. J., 1993. Two-domain estimation of hydraulic properties in macropore soils. *Soil Sci. Soc. Am. J.* 57: 680-686.

Chow, T. L., 1977. A porous cup soil-water sampler with volume control. *Soil Sci.* 124: 173-176.

Cleary, U. and Ungs, M. 1979. *Princeton analytical models 7 mass transport and 3 flow models.*

Curtis, A. A., Watson, K. K. and Jones, M. J., 1987. The numerical analysis of water and solute movement in scale heterogeneous profiles. *Transp. Porous Media.* 2: 479-496.

Danckwerts, P. V., 1953. Continuous flow systems (distribution of residence time). *Chem. Eng. Sci.* 2: 1-13.

Darcy, H., 1856. *Les fontaines publiques de la ville de Dijon.* Victor Dalmont, Paris.

Davies, B., Eagle, D. and Ginney, B., 1972. *Soil management.* Farming Press Limited, Ipswich, Suffolk.

Debyle, N. V., Hennes, R. W. and Hart, G. E. 1988. Evaluation of ceramic cups for determining soil solution chemistry. *Soil Sci.* 146: 30-36.

De Smedt, F. and Wierenga, P. J., 1979. A generalized solution for solute flow in soils with mobile and immobile water. *Water Resour. Res.* 15: 1137-1141.

Dirksen, C. and Matula, S., 1994. Automatic atomized water spray system for soil hydraulic conductivity measurements. *Soil Sci. Soc. Am. J.* 58: 319-325.

Dowd, J. F. and Williams, A. G., 1989. Calibration and use of pressure transducers in soil hydrology. *Hydrol. Processes.* 3: 43-49.

Dowd, J. F., Williams, A. G. and Bush, P., 1991. Preferential and matrix flow in a structured soil in Georgia, Southeast U.S.A. Extended abstract of the poster paper presented at IAHS symposium H4 held during the XX general assembly of IUGG in Vienna 11-24 August.

Ela, S. D., Gupta, S. C. and Rawls, W. J., 1992. Macropore and surface seal interactions affecting water infiltration into soil. *Soil Sci. Soc. Am. J.* 56: 714-721.

England, C. B., 1974. Comments on a 'technique using porous cups for water sampling of any depth in the unsaturated zone' by W. W. Wood. *Water Resour. Res.* 10: 1049.

Foth, H. D., 1990. *Fundamentals of soil science.* Eighth edition. John Wiley & Sons, New York.

Freeze, R. A. and Cherry, J. A., 1979. *Groundwater.* Prentice-Hall, Englewood Cliffs, New Jersey.

Fellner-Feldegg, H., 1969. The measurement of dielectrics in the time domain. *J. Physical Chem.* 73: 616-623.

Findlay, D. C., Colborne, G. J. N., Cope, D. W., Harrod, T. R., Hogan, D. V. and Staines, S. J., 1984. *Soils and their use in South West England.* Harpenden, Kent.

Gardner, W., Israelson, O. W., Edlefsen, N. E. and Clyde, H. S., 1922. The capillary potential function and its relation to irrigation practice. *Physics Review* (series 2). 20: 196.

Garwood, E. A. *et al.*, 1986. Nitrogen losses from drained grassland. In Cooper, J.P. and Raymond, W. F. (Eds.) *Grassland Manuring.* B. G. S. Occ. Symposium (20) pp 94-96. British Grassland Society, Hurley.

Germann, P., 1976. Wasserhaushalt und Elektrolytverlagerung in einem mit Wald und einem mit Wiese bestockten Boden in ebener Lage. Mitteilungen der eidgen. Anstalt fur das forstliche Versuchswesen. 52: 163-309.

Germann, P. and Beven, K., 1981a. Water flow in soil macropores I. An experimental approach. *J. Soil Sci.* 32: 1-13.

Germann, P. and Beven, K., 1981b. Water flow in soil macropores III. A statistical approach. *J. Soil Sci.* 32: 31-39.

Glass, R. J., Parlange, J-Y. and Steenhuis, T. S., 1987. Water infiltration in layered soils where a fine textured layer overlays a coarse sand. In. *Proc. Int. Conf Infiltration Development Application,* 5-9 January. Honolulu, Hawaii. 66-81.

Glass, R. J., Parlange, J-Y. and Steenhuis, T. S., 1989. Wetting front instability I. Theoretical discussion and dimensional analysis. *Water Resour. Res.* 25: 1187-1194.

Godwin, R. J., 1981. An experimental investigation into the force mechanics and resulting soil disturbance of mole ploughs. *J. of Agric. Eng. Res.* 26: 477-497.

Goss, M. J., Harris, G. L. and Howse, K. R., 1983. Functioning of mole drains in a clay soil. *Agric. Water Management.* 6: 27-30.

Goss, M. J., Howse, K. R., Lane, P. W., Christian, D. G. and Harris, G. L., 1993. Losses of nitrate-nitrogen in water draining from under autumn-sown crops established by direct drilling or mouldboard ploughing. *J. Soil Sci.* 44: 35-48.

Greenland, D. J. and Hayes, M. H. B. (Ed) 1981. *The chemistry of soil processes.* Chichester, Wiley.

Grossmann, J. and Udluft, P., 1991. The extraction of soil water by the suction-cup method: a review. *J. Soil Sci.* 42: 83-93.

Hall, D. G. M., Reeve, M. J., Thomasson, A. J. and Wright, V. F., 1977. Water retention, porosity and density of field soils. *Soil Survey Technical Monograph No. 9.* Soil Survey of England and Wales, Harpenden, UK. 25-29.

Hallard, M., 1988. *The effects of agricultural drainage on the hydrology of a grassland site in South West England.* Unpubd. Thesis, University Exeter.

Haise, H. R. and Kelley, O. J., 1950. Causes of diurnal fluctuations of tensiometers. *Soil Sci.* 70: 301-313.

Hansen, E. A. and Harris, A. R., 1975. Validity of soil-water samples collected with porous ceramic cups. *Soil Sci. Soc. Am. Proc. 39: 528-536.*

Harris, G. L., Goss, M. J., Dowdell, R. J., Howse, K. R. and Morgan, P., 1984. A study of mole drainage with simplified cultivation for autumn sown crops on a clay soil. 2. Soil water regimes, water balances and nutrient loss in drain water 1978-80. *J. Agricultural Sci. Cambridge.* 102: 561-581.

Harrod, T. R., 1981. *The soils of North Wyke and Rowden.* Soil Survey of England and Wales. Harpenden, Herts.

Harvey, J. W., 1993. Measurement of variation in soil solute tracer concentration across a range of effective pore sizes. *Water Resour. Res.* 29: 1831-1837.

Hayot, Ch. and Lafolie, F., 1993. One-dimensional solute transport modelling in aggregated porous media Part 2. effects of aggregate size distribution. *J. Hydrol.* 143: 85-107.

Heimovaara, T. J. and Boulten, W., 1990. A computer-controlled 36-channel time domain reflectometry system for monitoring soil water contents. *Water Resour. Res.*, 26: 2311-2316.

Hemmen, K. J., 1990. Comparison of tracer concentrations from suction lysimeters and soil water extrations for a structured piedmont soil. Unpubl. Msc. Thesis, University of Georgia, Athens, Georgia, USA.

Hendrickx, J. M., Nieber, J. L. and Siccama, P. D., 1994. Effect of tensiometer cup size on field soil water tension variability. *Soil Sci. Soc. Am. J.* 58: 309-315.

Hodgson, J. M., ed. 1976. *Soil survey field handbook,* Tech. Monog. No. 5., Soil Survey, Rothamsted Exp. Sta., Harpenden, England.

Holden, N. M., 1993. A two-dimensional quantification of soil ped shape. *J. Soil Sci.* 44: 209-219.

Holden, N. M., Scholefield, D., Williams, A. G. and Dowd, J. F., 1995a. A large soil block for conduction soil hydrology and multitracer experiments. (Submitted to) *Soil Sci. Soc. Am. J.*

Holden, N. M., Scholefield, D., Williams, A. G. and Dowd, J. F., 1995b. Near real-time determination of nitrate leaching as an integrated component of a large soil block experiment for fine resolution investigation of preferential flow. 8 th Nitogen Workshop, University of Gent, Sept 5-8, Gent, Belgium.

Hornberger, G. M., Beven, K. J. and Germann, P. F., 1990. Inferences about solute transport in macroporous forest soils from time series models. *Geoderma.* 46: 249-262.

Hornberger, G. M., Germann, P. F. and Beven, K. J., 1991. Throughflow and solute transport in an isolated sloping soil block in a forested catchment. *J. Hydol.* 124: 81-99.

Hu, Q. and Brusseau, M. L., 1994. The effect of solute size on diffusive-dispersive transport in porous media. *J. Hydrol.* 158: 305-317.

Hutson, J. L. and Wagenet, R. J., 1992. *Leaching Estimation And Chemistry Model - a process-based model of water and solute movement, transformations, plant uptake and chemical reactions in the unsaturated zone.* Department of soil, crop and Atmospheric Sciences. 92-3.

Jardine, P. M., Wilson, G. V. and Luxmoore, R. J., 1990. Unsaturated solute transport through a forest soil during rain storm events. *Geoderma.* 46: 103-118.

Jarvis, S. C., 1993. Nitrogen cycling and losses from dairy farms. *Soil Use and Management.* 9: 99-105.

Jarvis, N. J., Jansson, P-E., Dik, P. E. and Messing, I., 1991. Modelling water and solute

transport in macroporous soil. I. Model description and sensitivity analysis. *J. Soil Sci.* 42: 59-70.

Jarvis, N. J., Bergström, L. and Dik, P. E., 1991. Modelling water and solute transport in macroporous soil. II. Chloride breakthrough under non-steady flow. *J. Soil Sci.* 42: 71-81.

Jarvis, N. J. and Leeds-Harrison, P. B., 1987. Modelling water movement in drained clay soil. I. Description of the model, sample output and sensitivity analysis. *J. Soil Sci.* 38: 487-498.

Jensen, K. H. and Refsgaard, J. C., 1991a. Spatial variability of physical parameters and processes in two field soils. Part I: Water flow and solute transport at local scale. *Nordic Hydrology.* 22: 275-302.

Jensen, K. H. and Refsgaard, J. C., 1991b. Spatial variability of physical parameters and processes in two field soils. Part II: Water flow at field scale. *Nordic Hydrology.* 22: 303-326.

Jensen, K. H. and Refsgaard, J. C., 1991c. Spatial variability of physical parameters and processes in two field soils. Part III: Solute transport at field scale. *Nordic Hydrology.* 22: 327-340.

Jongerius, A., 1957. Morphologic investigations of soil structure. Meded. Sticht. Bodemkartering. Wageningen, The Netherlands, Bodem Stud.

Jongerius, A., Schoonderbeek, D., Jager, A. and Kowalinski, St., 1972. Electro-optical soil porosity investigation by means of quantimet-B equipment. *Geoderma.* 7: 177-198.

Jury, W. A., Sposito, G. and White, R. E., 1986. A transfer function model of solute transport through soil. I. Fundamental concepts. *Water Resour. Res.* 22: 243-247.

Kluitenberg, G. J. and Horton, R., 1990. Effect of solute application method on preferential transport of solutes in soil. *Geoderma.* 46: 283-297.

Klute, A. and Gardner, W. R., 1962. Tensiometer response time. *Soil Sci.* 93: 204-207.

Knight, J. H., 1991. Discussion of 'The spatial sensitivity of time-domain reflectometry' by J. M. Baker & R. J. lascano. *Soil Sci.* 151: 254-255.

Knight, J. H., 1992. Sensitivity of time domain reflectometry measurements to lateral variations in soil water content. *Water Resour. Res.* 28: 2345-2352.

Kung, K-J. S., 1990a. Preferential flow in a sandy vadose zone: 1. Field observation. *Geoderma.* 46: 51-58.

Kung, K-J. S., 1990b. Preferential flow in a sandy vadose zone: 2. Mechanism and implications. *Geoderma.* 46: 59-71.

Lapidus, L. and Amundson, N. R., 1952. Mathematics of adsorption in beds: 6. The effect of longitudinal diffusion in ion exchange and chromatographic columns. *J. Phys. Chem.* 56: 984-988.

Lawrence, G. P., 1977. Measurement of pore sizes in fine-textured soils: a review of existing techniques. *J. Soil Sci.* 28: 527-540.

Ledieu, J., Ridder, P. De., Clerck, P, De. and Dautrebande, S., 1986. A method of measuring soil moisture by time-domain reflectometry. *J. Hydrol.* 88: 319-328.

Leeds-Harrison, P., Spoor, G. and Godwin, R. J., 1982. Water flow to mole drains. *J. Agric. Engng. Res.* 27: 81-91.

Leij, F. J. and Dane, J. H., 1989. *Solution of the one-dimensional advection and two-dimensional dispersion equation.* Alabama Agricultural Experiment Station Aubun University, Alabama.

Linden, D. R. and Dixon, R. M., 1973. Infiltration and water table effects of soil air pressure under border irrigation. *Soil Sci. Soc. Am. Proc.* 37: 94-98.

Litaor, M. I., 1988. Review of soil solution samplers. *Water Resour. Res.* 24: 727-733.

Lord, E. I. and Shepherd, M. A., 1993. Developments in the use of porous ceramic cups for measuring nitrate leaching. *J. Soil Sci.* 44: 435-449.

Luxmoore, R. J., 1981. Micro-, meso-, and macroporosity of soil. *Soil Sci. Soc. Am. J.*, 45: 671-672.

Luxmoore, R. J., Jardine, P. M., Wilson, G. V., Jones, J. R. and Zelazny, L. W., 1990. Physical and chemical controls of preferred path flow through a forested hillslope. *Geoderma.* 46: 139-154.

Marshall, J. E., 1994. *Comparison of tracer movement through disturbed vs intact cores taken from a structured piedmount soil.* Unpul. Msc. Thesis, University of Georgia, Athens, Georgia, USA.

Marshall, T. J. and Holmes, J. W., 1979. *Soil physics.* 2nd ed. Cambridge University Press, Cambridge.

McBratney, A. B. and Moran, C. J., 1990. A rapid method of analysis for soil macropore structure: II. Stereological model, statistical analysis, and interpretation. *Soil Sci. Soc. Am. J.* 54: 509-515.

Meybeck, M., Chapman, D. and Helman, P., 1989. *Global freshwater quality: a first assessment.* Global Environment Monitoring System/UNEP/WHO.

Miyazaki, T., 1993. *Water flow in soils.* Marcel Dekker, New York.

Moran, C. J., 1990. A morphological transformation for sharpening edges of features before segmentation. *Compter-Vision, Graphics and Image Processing.* 49: 84-94.

Moran, C. J., McBratney, A. B. and Koppi, A. J., 1989. A rapid method for analysis of soil macropore structure. I. Specimen preparation and digital binary image production. *Soil Sci. Soc. Am. J.* 53: 921-928.

Murphy, C. P., Bullock, P. and Turner, R. H., 1977. The measurement and charcterisation

of voids in soil thin sections by image anslysis. I. Principles and techniques. *J. Soil Sci.* 28: 498-508.

Newman, A. C. D. and Thomasson, A. J. 1979. Rothamsted studies of soil structure III pore size distribution and shrinkage processes. *J. Soil Sci.* 30: 415-439.

Nielsen, D. R., Biggar, J. W. and Erh, K. T., 1973. Spatial variability of field-measured soil-water properties. *Hilgardia.* 42: 215-260.

Nyhan, J. W. and Drennon, B. J., 1990. Tensiometer data acquisition system for hydrologic studies requiring high temporal resolution. *Soil Sci. Soc. Am. J.* 54: 293-296.

Ogden, C. B., Wagenet, R. J., van Es and Hutson, J. L., 1992. Quantification and modeling of macropore drainage. *Geoderma.* 55: 17-35.

Parker, J. C. and Van Genuchten, M. Th., 1984. Flux-averaged and volume-averaged concentrations in continuum approaches to solute transport. *Water Resour. Res.* 20: 866-872.

Parlange, J. -Y., Steenhuis, T.S., Glass, R. J., Richard, T. L., Pickering, N. B., Waltman, W. J., Bailey, N. O., Andreini, M. S. and Throop, J. A., 1988. The flow of pesticides through preferential paths in soils. *NY Food Life Sci. Q.* 18: 20-23.

Peteson, A. E. and Dixon, R. M., 1971. Water movement in large soil pores: Validity and utility of the channel system concept. Res. Rep. 75. Res. Div., College of Agric. and Life Sci., Univ. of Wisconsin, Madison.

Phillips, R. E., Quisenberry, V. L., Zeleznik, J. M. and Dunn, G. H. 1989. Mechanism of water entry into simulated macropores. *Soil Sci. Soc. Am. J.* 53: 1629-1635.

Poletika, N. N. and Jury, W. A., 1994. Effects of soil surface management on water flow distribution and solute dispersion. *Soil Sci. Soc. Am. J.* 58: 999-1006.

Powlson, D. S., 1993. Understanding the soil nitrogen cycle. *Soil Use and Management.* 9: 86-94.

Quisenberry, V. L. and Phillips, R. E., 1976. Percolation of simulated rainfall under field conditions. *Soil Sci. Soc. Am. J.* 40: 484-489.

Quisenberry, V. L., Phillips, R. E. and Zeleznik, J. M., 1994. Spatial distribution of water and chloride macropore flow in a well-structured soil. *Soil Sci. Soc. Am. J.* 58: 1294-1300.

Quisenberry, V. L., Smith, B. R., Phillips, R. E., Scott, H. D. and Nortcliff, S., 1993. A soil classification system for describing water and chemical transport. *Soil Sci.* 156: 306-315.

Radulovich, R. and Sollins, P., 1987. Improved performance of zero-tension lysimeters.*Soil Sci. Soc. Am. J.* 51: 1386-1388.

Radulovich, R., Sollins, P., Baveye, P. and Solórzano, E., 1992. Bypass water flow through unsaturated microaggregated tropical soils. *Soil Sci. Soc. Am. J.* 56: 721-726.

Rao, P. S. C., Jessup, R. E., Rolston, D. E., Davidson, J. M. and Kilcrease, D. P., 1980a. Experimental and mathematical description of nonadsorbed solute transfer by diffusion in spherical aggregates. *Soil Sci. Soc. Am. J.* 44: 684-688.

Rao, P.S. C., Rolston, D. E., Jessup, R. E. and Davidson, J. M., 1980b. Solute transport in aggregated porous media: Theoretical and experimental evaluation. *Soil Sci. Soc. Am. J.* 44: 1139-1146.

Reeves, A. D. and Beven, K. J., 1990. The use of tracer techniques in the study of soil water flows and contaminant transport. NSS/R213

Reid, I. and Parkinson, R. J., 1984. The nature of the tile drain outfall hydrograph in heavy clay soils. *J. Hydrol.* 72: 289-305.

Richards, L. A., 1931. Capillary conduction of liquids through porous mediu. *Physics.* 1: 318-333.

Ringrose-Voase, A. J., 1987. A scheme for the quantitative description of soil macrostructure by image analysis. *J. Soil Sci.* 38: 343-356.

Ringrose-Voase, A. J. and Bullock, P., 1984. The automatic recognition and measurement of soil pore types by image analysis and computer programs. *J. Soil Sci.* 35: 673-684.

Robinson, M. and Beven, K. J. 1983. The effect of mole drainage on the hydrological response of a swelling clay soil. *J. Hydrol.* 64: 205-233.

Ross, P. J., 1993. A method of deriving soil hydraulic properties from field water contents for application in water balance studies. *J. Hydrol.* 144: 143-153.

Rowell, D. L., 1994. *Soil science methods and applications*.Longman, Singapore.

Russell, A. E. and Ewel, J. J., 1985. Leaching from a tropical Andept during big storms: A comparison of three methods. *Soil Sci.* 139: 181-189.

Russo, D. and Bresler, E., 1981. Soil hydraulic properties as stochastic processes I. An analysis of field spatial variability. *Soil Sci. Soc. Am. J.* 45: 682-687.

Russo, D., Jury, W. A. and Butters, G. L., 1989. Numerical analysis of solute transport during transient irrigation 1. The effect of hysteresis and profile heterogeneity. *Water Resour. Res.* 25: 2109-2118.

Ryden, J. C., Ball, P. R. and Garwood, E. A., 1984. Nitrate leaching from grassland. *Nature.* 311: 50-53.

Saleh, F. M. A., Bishop, D. J., Dietrich, S. F., Knezovich, J. P. and Harrison, F. L., 1990. Transport of nonsorbed chemicals in the subsurface environment: proposed model with experimental verification. *Soil Sci.* 149: 23-34.

Sassner, M., Jensen, K. H. and Destouni, G., 1994. Chloride migration in heterogeneous soil 1. experimental methodology and results. Water Resour. Res. 30: 735-745.

Scholefield, D. and Jarvis, S. C., 1995. UK/Japan Workshop- controlling methane and the nitrogen cycle on farms

Scholefield, D., Lord, E. I., Rodda, H. J. E. and Webb, B., 1995. Estimating peak nitrate concentration from annual nitrate loads. (in press) *J. Hydrol.*

Scholefield, D., Tyson, K. C., Garwood, E. A., Armstrong, A. C., Hawkins, J. and Stone, A. C., 1993. Nitrate leaching from grazed grassland lysimeters: effects of fertilizer input, field drainage, age of sward and patterns of weather. *J. Soil Sci.* 44: 601-613.

Schubert, H., 1982. *Kapillarität in Porösen Feststoff-systemen.* Springer Verlag, Berlin.

Schuh, W. M. and Cline, R. L., 1990. Effect of soil properties on unsaturated hydraulic conductivity pore-interaction factors. *Soil Sci. Soc. Am. J.* 54: 1509-1519.

Schweigh, D. and Sardin, M., 1981. Adsorption, partition, ion-exchange and chemical-reaction in bach reactors or in colums - a review. *J. Hydrology.* 50: 1-33.

Scotter, D. R., Heng, L. K., Horne, D. J. and White, R. E., 1990. A simplified analysis of soil water flow to a mole drain. *J. soil Sci.* 41: 189-198.

Selker, J., Leclerq, P., Parlange, J. -Y. and Steenhuis, T., 1992a. Fingered flow in two dimensions 1. measurement of matric potential. *Water Resour. Res.* 28: 2513-2521.

Selker, J., Parlange, J. -Y. and Steenhuis, T., 1992b. Fingered flow in two dimensions 2. predicting finger moisture profile. *Water Resour. Res.* 28: 2523-2528.

Setiawan, B. I. and Nakano, M., 1993. On the determination of unsaturated hydraulic conductivity from soil moisture profiles and from water retention curves. *Soil Sci.* 156: 389-395.

Severson, R.C. and Grigal, D. F.,1976. Soil solution concentration: Effect of extraction time using porous ceramic cups under constant tension. *Water Resour. Bulletin.* 12: 1161-1170.

Seyfried, M. S. and Rao, P. S. C., 1987. Solute transport in undisturbed columns of an aggregated tropical soil: Preferential flow effects. *Soil Sci. Soc. Am. J.* 51: 1434-1444.

Shaffer, K. A., Fritton, D. D. and Baker, D. E., 1979. Drainage water sampling in a wet, dual-pore soil system. *J. Environ. Qual.* 8: 241-246.

Shuford, J. W., Fritton, D. D. and Baker, D. E., 1977. Nitrate-nitrogen and chloride movement through undisturbed field soil. *J. Environ. Qual.* 6: 255-259.

Singh, P. and Kanwar, R. S., 1991. Preferential solute transport through macropores in large undisturbed saturated soil columns. *J. Environ. Qual.* 20: 295-300.

Skopp, J., 1981. 'Comment on "Micro-, meso-, and macroporosity of soil"', *Soil Sci. Soc. Am. J.* 45: 1246.

Smedt, F. De. and Wierenga, P. J., 1979. A generalized solution for solute flow in soils with mobile and immobile water. *Water Resour. Res.* 15: 1137-1141.

Smith, M. W. and Patterson, D. E., 1980. *Investigation of frozen soils using time domain reflectometry*. Final Rep. Dept. Energy, Mines and Resources, Canada. Geotecn. Sci. Lab., Carleton Univ,. Ottawa, Canada, 64 pp.

Soil Suvey Staff. 1975. *Soil taxonomy*. Agric. Handb. No. 436, Soil Cons. Ser., US Dept. Agr. Washington, D.C.

Sollins, P. and Radulovich, R., 1988. Effects of soil physical structure on solute transport in a weathered tropical soil. *Soil Sci. Soc. Am. J.* 52: 1168-1173.

Spaans, E. J. A. and Baker, J. M., 1993. Simple baluns in parallel probes for time domain reflectometry. *Soil Sci. Soc. Am. J.* 57: 668-673.

Spoor, G. and Ford, R. A., 1987. Mechanics of mole drainage channel deterioration. *J. Soil Sci.* 38: 369-382.

Spoor, G., Leeds-Harrison, P. B. and Godwin, R. J., 1982. Some fundamental aspects of the formation, stability and failure of mole drainage channels. *J. Soil Sci.* 33: 411-425.

Steenhuis, T. S., Parlange, J. -Y. and Andreini, M. S., 1990. A numerical model for preferential solute movement in structured soils. *Geoderma.* 46: 193-208.

Sudicky, E. A., 1990. The Laplace Transform Galerkin technique for efficient time-continuous solution of solute transport in double-porosity media. *Geoderma.* 46: 209-232.

Tindall, J. A., Hemmen, K. and Dowd, J. F., 1992. An improved method for field extration and laboratory analysis of large, intact soil cores. *J. Environ. Qual.* 21: 259-263.

Topp, G. C. and Davis, J. L., 1981. Detecting infiltration of water through soil cracks by time-domain reflectometry. *Geoderma.* 26: 13-23.

Topp, G. C. and Davis, J. L., 1985. Time-domain reflectometry (TDR) and its application to irrigation scheduling. *In. Advances in irrigation*, vol. 3., D. Hillel (ed.). Academic, New York. 107-127.

Topp, G. C., Davis, J. L. and Annan, A. P., 1980. Electromagnetic determination of soil water content: measurements in coaxial transmission lines. *Water Resour. Res.* 16: 574-582.

Towner, G. D., 1980. Theory of time response of tensiometers. *J. Soil Sci.* 31: 607-621.

Towner, G. D., 1989. The application of classical physics transport theory to water movement in soil: development and deficiencies. *J. Soil Sci.* 40: 251-260.

Trafford, B. D., 1971. The langabeare drainage experiment. *Agriculture.* 78: 305-311.

Tyler, D. D. and Thomas, G. W., 1981. Chloride movement in undisturbed soil columns.

Soil Sci. Soc. Am. J. 45: 459-461.

Tyson, K. C., Garwood, E. A., Armstrong, A. C. and Scolefield, D. 1992. Effects of field drainage on the growth of herbage and the liveweight gain of grazing beef cattle. *Grass and Forage Science.* 47: 290-301.

Tyson, K. C., Hawkins, J. M. B. and Stone, A. C., 1993. *Final report on the AFRC-ADAS drainage experiment.* 1982-1993, IGER, North Wyke.

Van Genuchten, M. Th. and Dalton, F. N., 1986. Models for simulating salt movement in aggregated field soils. *Geoderma.* 38: 165-183.

Van Stiphout, T. P. J., Van Lanen, H. A. J., Boersma, O. H. and Bouma, J., 1987. The effect of bypass flow and internal catchment of rain on the water regime in a clay loam grassland soil. *J. Hydrol.* 95: 1-11.

Wagenet, R. J., 1992. *Quantitative prediction of the leaching of organic and inorganic solutes in soil.* Dept. Agronomy, Cornell University, Ithaca, NY USA 14853.

Walker, P. J. C. and Trudgill, S. T., 1983. Quantimet image analysis of soil pore geometry: comparison with tracer breakthrough curves. *Earth Surfaces Processes and Landforms.* 8: 465-472.

Watson, K. W. and Luxmoore, R. J., 1986. Estimating macroporosity in a forest watershed by use of a tension infiltrometer. *Soil Sci. Soc. Am. J.* 50: 578-582.

Whalley, W. R., 1993. Considerations on the use of time-domain reflectometry (TDR) for measuring soil water content. *J. Soil Sci.* 44: 1-9.

White, R. E., 1985. The influence of macropores on transport of dissolved and suspended matter through soil. In: B. A. Stewart (Ed.), *Advances in Soil Science,* Vol. 3. Springer, New York, N. Y. Vol. 3. 95-120.

Wood, W. W., 1973. A technique using porous cups for water sampling at any depth in the unsaturated zone. *Water Resour. Res.* 9: 486-488.

Wraith, J.M., Comfort, S. D., Woodbury, B. L. and Inskeep, W. P., 1993. A simplified wave-form analysis approach for monitoring solute transport using time-domain reflectometry. *Soil Sci. Soc. Am. J.* 57: 637-642.

Wu, L., Vomocil, J. A. and Childs, S. W., 1990. Pore size, particle size, aggregate size, and water retention. *Soil Sci. Soc. Am. J.* 54: 952-956.

Youngs, E. G. and Leeds-Harrison, P. B., 1990. Aspects of transport processes in aggregated soils. *J. Soil Sci.* 41: 665-675.

Zegelin, S. J., White, I. and Jenkins, D. R., 1989. Improved field probes for soil water content and electrical conductivity measurment using time domain reflectometry. *Water Resour. Res.* 25: 2367-2376.